Attachment D

DRAFT COPY

AN ABSTRACT OF THE THESIS OF Michael Curtis Hagood for the Master of Science in Geology presented February 21, 1985.

Title: Structure and Evolution of the Horse Heaven Hills in South-Central Washington.

APPROVED BY MEMBERS OF THE THESIS COMMITTEE:

Marvin H. Beeson, Chairman

Michael L. Cummings

Gilbert T. Benson

Stephen P. Reidel

The Horse Heaven Hills uplift in south-central Washington consists of distinct northwest and northeast trends which merge in the lower Yakima Valley. The northwest trend is adjacent to and parallels the Rattlesnake-Wallula alignment (RAW; a part of the Olympic-Wallowa lineament). The northwest trend and northeast trend consist of aligned or en echelon anticlines and monoclines whose axes are generally oriented in the direction of the trend. At the intersection,

folds in the northeast trend plunge onto and are terminated by folds of the northwest trend.

The crest of the Horse Heaven Hills uplift within both trends is composed of a series of asymmetric, north vergent, eroded, usually double-hinged anticlines or monoclines. Some of these "major" anticlines and monoclines are paralleled to the immediate north by lower-relief anticlines or monoclines. All anticlines approach monoclines in geometry and often change to a monoclinal geometry along their length.

In both trends, reverse faults commonly parallel the axes of folds within the tightly folded hinge zones. Tear faults cut across the northern limbs of the anticlines and monoclines and are coincident with marked changes in the wavelength of a fold or a change in the trend of a fold. Layer-parallel faults commonly exist along steeply-dipping stratigraphic contacts or zones of preferred weakness in intraflow structures. Most of these faults appear to reflect strain from folding.

Isopach maps of Columbia River basalt (CRB) flows/Ellensburg Formation interbeds and paleodrainage maps of the ancestral Columbia River system indicate that deformation occurred simultaneously and coincident with both trends of the Horse Heaven Hills uplift, the lower Yakima Valley syncline, the Piening syncline (within the Horse Heaven Plateau), and the Hog Ranch-Naneum Ridge anticline (within the lower Yakima Valley) since at least Roza time. Data are not available for determining the timing and location of deformation prior to Roza time, nor does the geologic record allow for a detailed description of

the growth history after CRB time, except that the observed present structural relief along the Horse Heaven Hills uplift developed after Elephant Mountain time (10.5 m.y.B.P.).

Relief between the Horse Heaven Hills uplift and the lower Yakima Valley syncline developed at a rate of less than approximately 70 m/m.y., during Wanapum and Saddle Mountains time (combined rate of vertical uplift and subsidence). Growth rates appear to decrease during Wanapum and Saddle Mountains time. Growth rates extrapolated to the present approximate the cumulative relief developed since Wanapum time indicating the possibility that folds developed at a uniform rate since CRB time to the present. However, the data from this study do not preclude the variability of growth rates in post CRB time.

Data from this study suggest that tectonic models which directly or indirectly pertain to the origin of the Horse Heaven Hills uplift might be constrained by: (1) the predominance of monoclinal or near-monoclinal fold geometries and reverse faults along both the northwest and northeast trends; (2) preliminary data which suggest clockwise rotation has occurred along folds of both trends; (3) folds along both trends were developing simultaneously and at similar rates (at least during Wanapum and Saddle Mountains time); (4) folds along the northwest trend of the Horse Heaven Hills uplift are genetically related to and formed simultaneously with at least some folds along the RAW; (5) the uplift was developing simultaneously with the north-northwest-trending Hog Ranch-Naneum Ridge anticline as well as other Yakima folds during at least CRB time. It is proposed that folds of both

trends of the Horse Heaven Hills uplift were generated by the same tectonic processes.

STRUCTURE AND EVOLUTION OF THE HORSE HEAVEN HILLS IN SOUTH-CENTRAL WASHINGTON

by

MICHAEL CURTIS HAGOOD

A thesis submitted in partial fulfillment of
the requirements for the degree of

MASTER OF SCIENCE
in
GEOLOGY

Portland State University

1985

TO THE OFFICE OF GRADUATE STUDIES AND RESEARCH:

The members of the Committee approve the thesis of Michael Curtis Hagood presented February 21, 1985.

Marvin H. Beeson, Chairman

Michael L. Cummings

Gilbert T. Benson

Stephen P. Reidel

APPROVED:

Paul E. Hammond, Head, Department of Geology

Jim F. Heath, Dean of Graduate Studies and Research

ACKNOWLEDGEMENTS

I would like to thank Dr. Stephen Reidel for introducing me to the many geologic aspects of the Columbia Plateau. His enthusiastic support, insight, and guidance were drawn upon frequently. Many discussions with Stephen Reidel, Terry Tolan, and Karl Fecht generated several ideas that were incorporated into this study. These three also provided very thorough reviews of the thesis which greatly improved it. As my thesis advisor, Dr. Marvin Beeson provided timely advice, support, and beneficial reviews of the thesis, and deserves my sincere thanks. I would also like to thank Drs. Michael Cummings and Tom Benson for their constructive reviews of the thesis.

This study was funded by a grant from the Northwest College and University Association for Science (NORCUS), with additional support from Rockwell Hanford Operations. I wish to express my thanks to Dr. Brian Valett of NORCUS for his assistance.

I would like to thank the staff and management of Rockwell Hanford Operations for their support of this study. Drs. Stephen Reidel, Ann Tallman, and Terry Tolan took time out from their busy schedules to make sure support for various aspects of the study were there. Bill Crowely aided immensely in the drafting of many of the figures and maps. Dale Landon provided some unpublished mapping, chemical analyses, and an initial orientation to the study area. Don Saul, Donna Starr, and Dave Thiede patiently instructed me in the use

of the computers and computer programs. Steve Strait provided helpful information and support for borehole geophysical logging.

Several other people and organizations contributed technical support to the study. Bill Myer of the Department of Ecology first introduced me to the utility of borehole geophysical logs, and freely and enthusiastically discussed aspects of the area geology. In addition, discussions with Frank Packard of the U.S. Geological Survey have been most beneficial. The U.S. Geological Survey in Tacoma, Washington allowed the use of several unpublished borehole geophysical logs. Washington State University College of Engineering provided me with borehole geophysical logs. Randy Brown of Richland, Washington provided useful information for interpreting driller's logs. Drs. Bob Simpson and Ray Wells allowed me the use of their unpublished paleomagnetic data. Jim, Dan, and Christine Dilts provided me with drill cuttings from the Moon #1 well.

I would like to thank landowners Pete Sharpe, Milo Bauder, Bill Phelps, and Paul Drake for allowing me access to their property.

I also wish to say thank you to my parents, Mel and Pat Hagood, for their support during this study.

Lastly, but of no less importance, I wish to thank my wife, Mary Jean, for her patience and understanding through the duration of this study; and for putting up with the lost weekends and evenings, as well as my absences during field seasons.

TABLE OF CONTENTS

LIST OF TABLES

TABLE PAGE

LIST OF FIGURES

FIGURE PAGE

FIGURE PAGE

FIGURE PAGE

FIGURE PAGE

FIGURE PAGE

FIGURE PAGE

INTRODUCTION

Purpose

Several generally narrow, east-west-trending Yakima folds extend eastward from the Cascade Range into the central Columbia Basin. Two of these folds, the Rattlesnake Hills uplift and the Horse Heaven Hills uplift, abruptly change trend near the western margin of the Pasco Basin and continue southeast towards the Blue Mountains (Fig. 1). The northwest-trending portions of the Horse Heaven Hills and Rattlesnake Hills uplifts are coincident with and parallel, respectively, a portion of the Rattlesnake-Wallula structural alignment (RAW, Bingham and others 1970; Fig. 1) which is part of the Olympic-Wallowa topographic lineament (OWL) of Raisz (1945, Fig. 2). The northwest trend of the Horse Heaven Hills uplift is itself part of another structural alignment, the Anderson Ranch-Wallula alignment (ARW; Fig. 1). The structural and evolutionary relationships of these two northwest- and two northeast-trending structural trends at their intersections is poorly understood but is important to understanding the development of the Yakima folds. It is the purpose of this study to describe the structure and evolution of one of these uplifts, the Horse Heaven Hills, at its abrupt structural transition. In this study, this was achieved by (1) delineating the structure within the two trends as they approach the intersection, (2) determining the timing and location of uplift within each trend, (3) comparing and

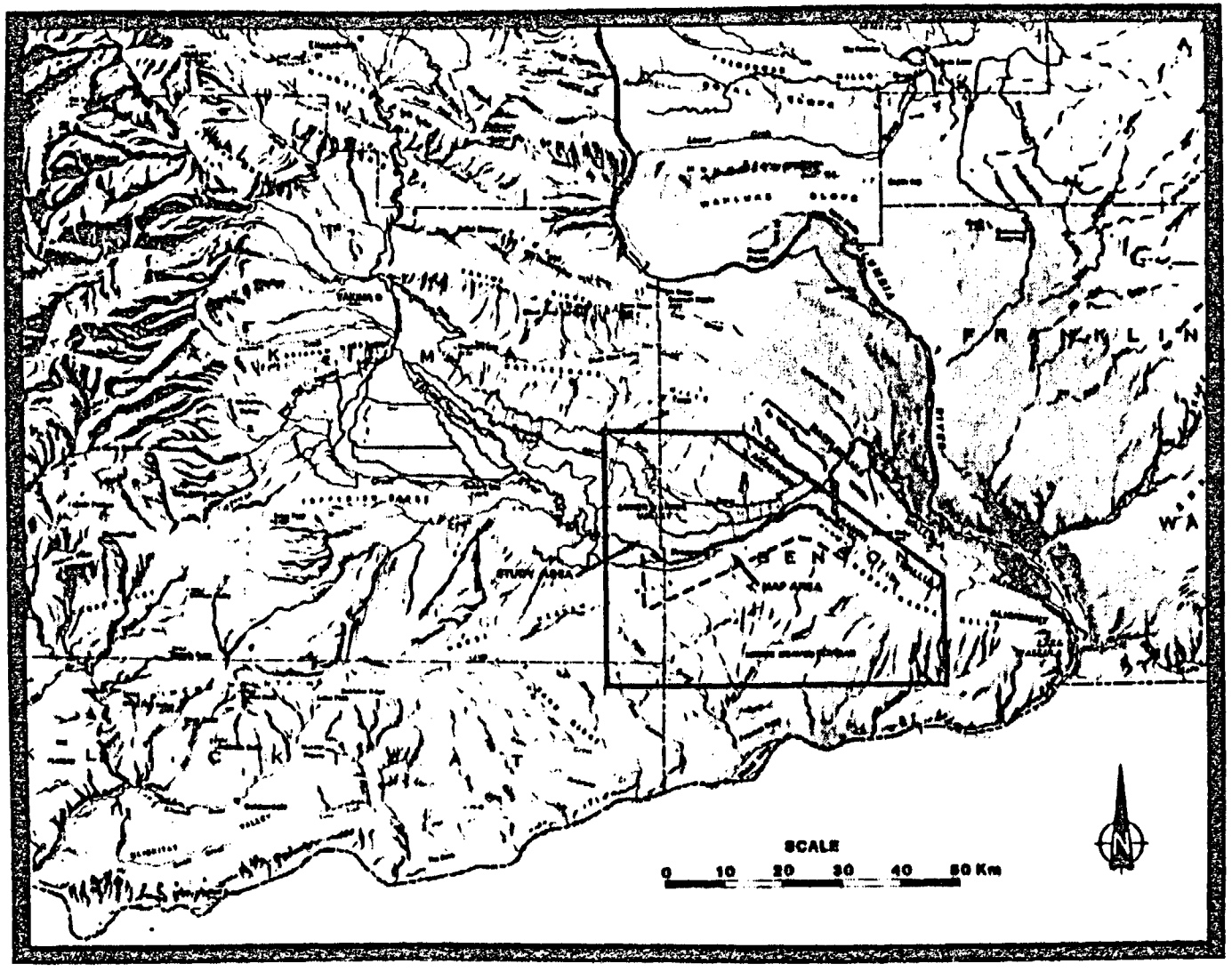

Figure 1. Location of study area and map area.

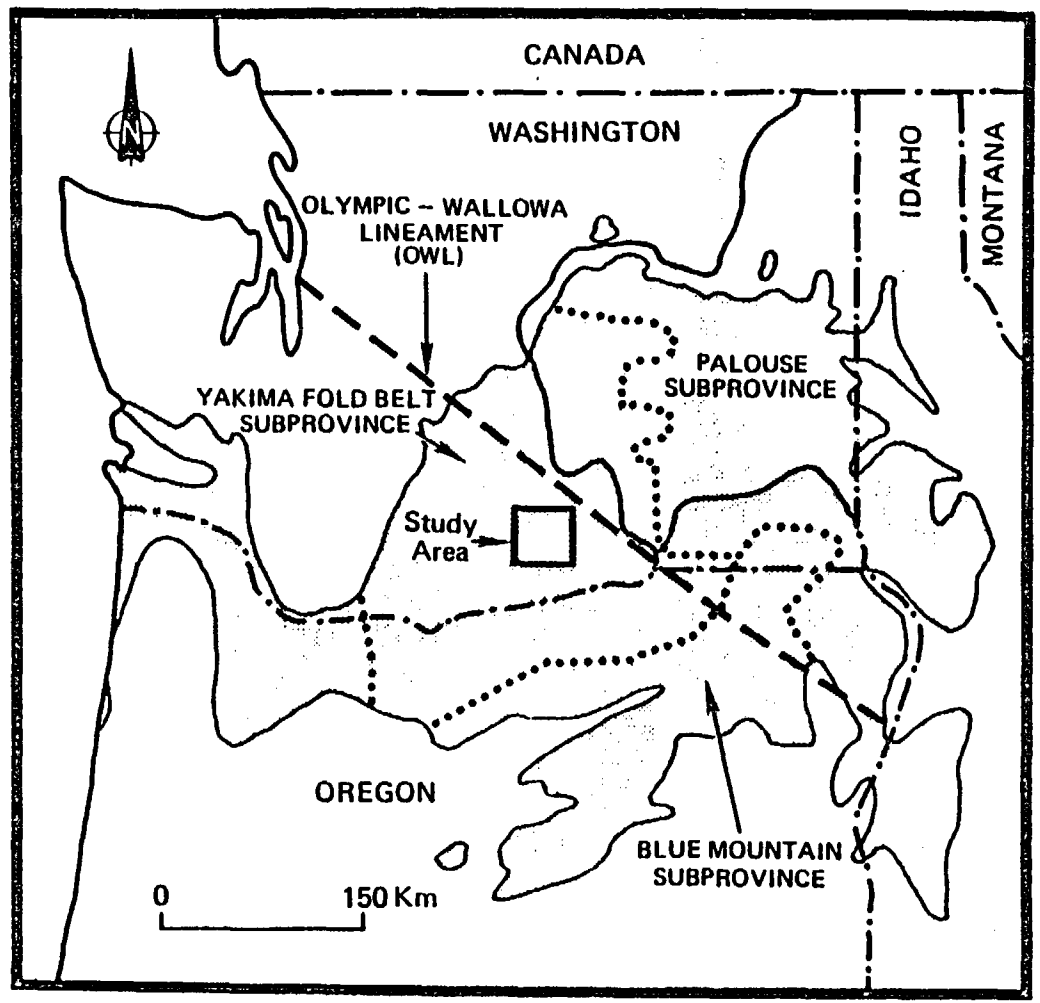

Figure 2. Structural subprovinces of the Columbia Plateau (Myers and others 1979) shown in relationship to the extent of the CRBG (stippled area).

contrasting Miocene vertical growth rates along folds within both trends, and (4) suggesting constraints for tectonic models that pertain to the genesis of the Horse Heaven Hills uplift. These objectives can only be fulfilled if the stratigraphy of the area is first delineated.

Regional Geologic Setting

The Horse Heaven Hills uplift lies within the Columbia Plateau geologic province, which is an intermontaine basin between the Cascade Range to the west and the Rocky Mountains to the east. The Columbia Plateau can be divided into three informal structural subprovinces (Myers and others 1979; Fig. 2): (1) the Blue Mountains subprovince characterized by the northeast-trending Blue Mountains uplift, (2) the Palouse subprovince characterized by a generally undeformed, westward-tilting paleoslope, and (3) the Yakima Fold Belt subprovince characterized by generally east-west and northwest-southeast-trending folds of which the Horse Heaven Hills uplift is one.

Three of the five formations that make up the Miocene tholeiitic flood basalts of the Columbia River Basalt Group (CRBG) are known to underlie the Yakima Fold Belt subprovince: (1) the Grande Ronde Basalt, (2) the Wanapum Basalt, and (3) the Saddle Mountains Basalt. Basalt flows of these three formations were erupted during a period of time spanning 17 to 6 m.y.B.P. (McKee and others 1977; Long and Duncan 1982) from northwest-trending linear vent systems in the eastern portion of the Columbia Plateau (Waters 1961; Taubeneck 1970; Swanson and others 1975; Price 1975; Swanson and others 1975). Intercalated

with and overlying the Columbia River basalt (CRB) in western and central portions of the Columbia Plateau are epiclastic and volcaniclastic sediments of the Ellensburg Formation that were derived from both within and outside the Columbia Plateau (Waters 1955; Mackin 1961; Schmincke 1964, 1967c; Swanson and others 1979c). Overlying the CRB and Ellensburg Formation to the east of the lower Yakima Valley are remnants of Miocene and Pliocene fluvial/lacustrine sediments of the Ringold Formation (Myers and others 1979; Tallman and others 1981), and to the northwest of the lower Yakima Valley are Pliocene Thorp or Thorp-equivalent sediments (Waitt 1979; Campbell 1983). Pleistocene glaciofluvial deposits from catastrophic floods mantle portions of many of the basins within the Yakima Fold Belt (Baker and Nummendal 1978). Loess and dune sand of Pleistocene and Holocene age blanket much of the area as well.

Location and Physical Description

The study area covers portions of the lower Yakima Valley, Horse Heaven Hills, Horse Heaven Plateau, and Badger Coulee (Fig. 1). The Horse Heaven Hills are a series of ridges averaging 600 m in elevation. Approximately 450 m of topographic relief exists between these ridge crests and the lower Yakima Valley. The Horse Heaven Hills uplift is bordered to the north by the eastward-flowing Yakima River.

Any portion of the study area is accessible to within a few kilometers of any road. The Horse Heaven Hills uplift can be reached from major arterials such as Interstate 82 between Benton City and

Prosser, Washington; State Highway 22 between Prosser and Mabton, Washington; and State Highway 221 between Prosser and Paterson, Washington. Secondary roads such as Webber Canyon Road, McBee Grade, Lincoln Grade, Ward Gap Road, and Byron Road all cross the ridge crest of the Horse Heaven Hills. Dirt roads along portions of the crest are usable with permission from the landowner. Irrigation ditch roads also provide good access to the northern base of the Horse Heaven Hills uplift, but permission for access is required from the appropriate irrigation districts.

Methodology

To delineate the structure and stratigraphy exposed along the Horse Heaven Hills uplift, a bedrock outcrop map (scale 1:24,000) and a geologic map (scale 1:62,500) were constructed (map area, Fig. 1; Plate 1). Stratigraphic units were identified using their characteristic properties: (1) basalt lithology, (2) stratigraphic position, (3) basalt paleomagnetic polarity (using a fluxgate magnetometer), and (4) major oxide chemistry (as determined by x-ray fluorescence analysis? (XRF)). In addition, subsurface stratigraphic units within the study area (generally located in the area adjacent to the Horse Heaven Hills uplift) were identified using borehole geophysical logs, driller's logs, lithology of drill cuttings, and XRF analyses of drill cuttings.

To determine the timing and location of deformation in the study area, computer-generated isopach maps were constructed of individual CRB members and Ellensburg Formation interbeds using section-thickness

data gathered from borehole geophysical logs, driller's logs, and field sections. These isopach maps were later modified by the author to be more representative of the geology of the area.

Growth rates were calculated for the Horse Heaven Hills uplift by plotting cumulative paleorelief (determined from isopach maps) against radiometric age dates of certain CRB flows.

More background on some of these methods is presented in the appendices.

Previous Work

Several geologic studies have encompassed portions, or all, of the study area, both in reconnaissance and in detail. Table I generally summarizes the various studies that include aspects of the structure of the Horse Heaven Hills uplift (and immediate area) and stratigraphy of the CRB and Ellensburg Formation within the study area. A major advancement in the study of the structure and stratigraphy of the CRB occurred when major oxide chemistry, paleomagnetics, and borehole geophysical logging were found useful in identifying basalt flow.

TABLE I

PREVIOUS WORK PERTINENT TO THIS STUDY WHICH ENCOMPASSES ALL OR PORTIONS OF THE STUDY AREA

REFERENCE	REGION OF STUDY	MAJOR SUBJECT(S)	SPECIAL METHOD(S) EMPLOYED	MAPS PRODUCED
Russell, 1893	central Washington	-water resources -stratigraphy -structure		
Waring, 1913	south-central Washington	-water resources -stratigraphy -structure		-reconnaissance map showing location of water wells, springs and approximate extent of geologic formations. scale, 1"= 13 mi.
Rhodd, 1923	Prosser and Pasco quadrangles	-stratigraphy		-geologic map. scale, 1:125,000
Warren, 1941b	south-central Washington	-Hood River conglomerate		
Dennis, 1938	Horse Heaven Hills	-structure		
Mason, 1953	south-central Washington	-structure -lithology		
Laval, 1956	south-central Washington	-stratigraphy -structure		-geologic maps, scale, 1:62,500
Schmincke, 1964	south-central Washington	-stratigraphy -petrography	-major oxide analyses	
Schmincke, 1967a	south-central Washington	-fused tuffs -peperites	-major oxide analyses	
Schmincke, 1967c	south-central Washington	-stratigraphy -petrography -chemistry	-major oxide analyses	
Schmincke, 1967d	south-central Washington	-flow paths of the CRB -paleodrainage -paleoslopes	-basalt intraflow structures -sedimentary structures	
Newcomb, 1970	Columbia Plateau	-structure		-tectonic structure maps scale, 1:500,000
Crosby and others, 1972	Horse Heaven Plateau	-groundwater hydrology -subsurface stratigraphy -structure	-borehole geophysical logs	
Lobdal and Brown, 1977	lower Yakima Valley	-groundwater hydrology -subsurface stratigraphy -structure	-borehole geophysical logs	
Bond and others, 1978	southwest Pasco Basin	-stratigraphy -structure	-major oxide analyses -paleomagnetics	-structure contour map -distribution map of limited CRB flows -geologic maps, scale 1:24,000
Brown, 1978	Horse Heaven Plateau	-groundwater hydrology -subsurface stratigraphy -structure	-borehole geophysical logs	
Brown, 1979	eastern and southern parts of the Pasco Basin	-groundwater hydrology -subsurface stratigraphy -structure		-structure contour map on top of the CRB
Myers and others, 1979	Pasco Basin	-surface stratigraphy -subsurface stratigraphy -structure -tectonics	-major oxide analyses -paleomagnetics -borehole geophysical logs -geophysical methods	-isopach maps of CRB and Ellensburg Fm. -structure contour maps on top of CRB units. -geologic maps, scale 1:62,500
Swanson and others, 1979a	eastern Washington and northern Idaho	-stratigraphy -structure	-major oxide analyses -paleomagnetics	-geologic maps, scale 1:250,000
Swanson and others, 1979b	eastern Washington and northern Idaho	-subsurface stratigraphy -structure	-borehole geophysical logs	-structure contour maps on top of CRB units.

STRATIGRAPHY

This chapter focuses on the surface and subsurface stratigraphy of the CRBG and Ellensburg Formation in the study area that are important to delineating structures and reconstructing the evolution of the Horse Heaven Hills uplift. The stratigraphy of the study area is shown in Figure 3. Pliocene sediments are absent from the study area such that the CRB or Ellensburg Formation is unconformably overlain by Pleistocene or Holocene deposits. The surface stratigraphy was generally determined from field mapping along the Horse Heaven Hills uplift (Plate 1), while the subsurface stratigraphy was determined from borehole data (see Appendix B). The stratigraphic nomenclature for the study area generally follows the usage of Swanson and others (1979c) as well as that of Myers and others (1979). Radiometric age dates for the CRBG (Fig. 3) are from McKee and others (1977), Watkins and Baksi (1974), Long and Duncan (1982), and unpublished data from Rockwell Hanford Operations and Duncan (1982). The magnetostratigraphy was compiled from several studies (Fig. 3; Reitman 1966; Van Alstine and Gillett 1981; Sheriff 1984; Beeson and others, in prep.).

Grande Ronde Basalt

The Grande Ronde Basalt (Swanson and others 1979c) composes up to 85% by volume of the CRBG, approximately 275,000 km^3 (Reidel and

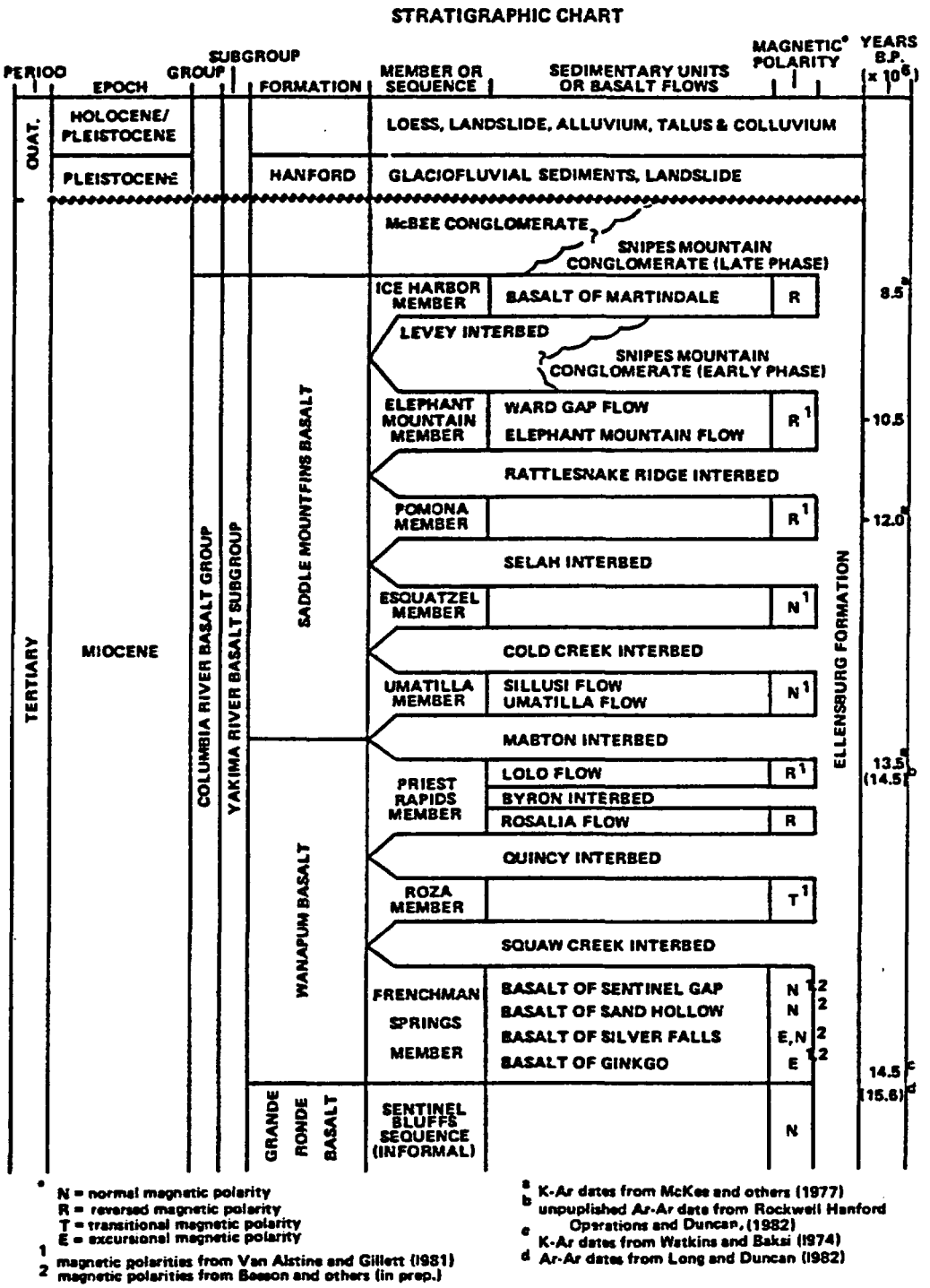

Figure 3. Stratigraphy of the study area, after Swanson and others (1979c) and Myers and others (1979).

others 1982). The upper portion of the Grande Ronde Basalt was penetrated in two boreholes within the study area, the Horse Heaven Test well (see Fig. 59) and the Moon #1 well (see Fig. 58), which are both located on the Horse Heaven Plateau (Fig. 4). Chemical analyses (see Appendix A, Table II) and borehole geophysical logs indicate that the boreholes penetrated part of the Sentinel Bluffs sequence of Myers and others (1979). From other studies, it has been shown that the Sentinel Bluffs sequence consists entirely of high MgO flows (Long and Landon 1981). From inspection of drill cuttings from the Moon #1 well and interpretations of the borehole geophysical logs, it appears that the Vantage Member of the Ellensburg Formation does not overlie the Grande Ronde Basalt at these two sites, or the interbed is too thin to identify.

Wanapum Basalt

The Wanapum Basalt (Swanson and other 1979c) consists of three members within the study area. These are (from oldest to youngest) the Frenchmen Springs, Roza, and Priest Rapids Members. The Wanapum Basalt is separated from the overlying Saddle Mountains Basalt by the Mabton interbed and from the underlying Grande Ronde Basalt by the Vantage Member where present. Distinct lithologic, chemical, and paleomagnetic differences occur between the members, aiding in their identification. However, a lack of a significant variation in the K_2O content of these members (Fig. 5) makes their identification on natural gamma geophysical logs very difficult.

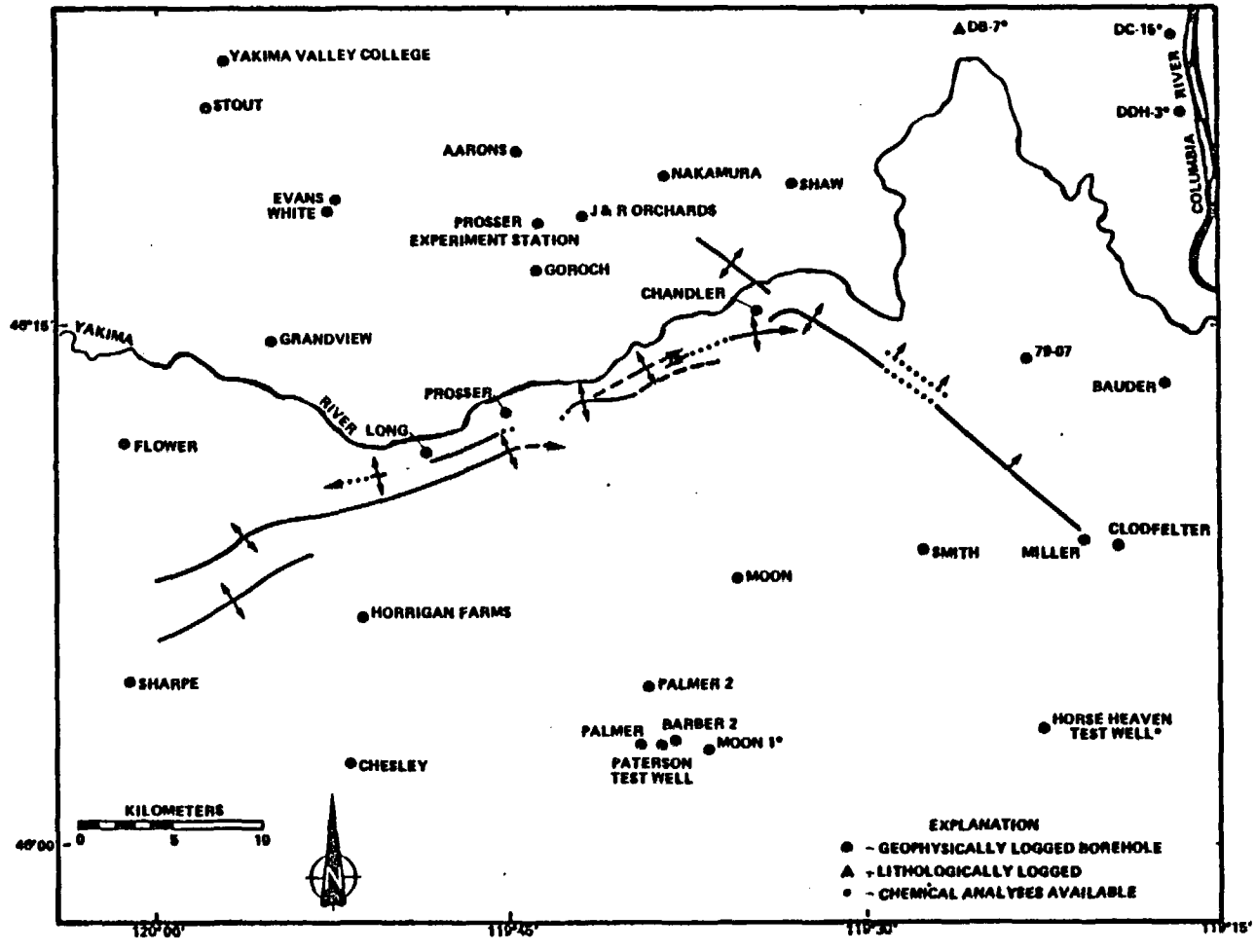

Figure 4. Names and locations of geophysically logged and lithologically logged boreholes used in this study.

TABLE II

AVERAGE MAJOR OXIDE COMPOSITION OF COLUMBIA RIVER BASALT GROUP FLOWS FOUND IN THE STUDY AREA

MEMBER	GRANDE RONDE		FRENCHMAN SPRINGS								ROZA[2]		PRIEST RAPIDS	
FLOW			BASALT OF GINKGO		BASALT OF SILVER FALLS		BASALT OF SAND HOLLOW		BASALT OF SENTINEL GAP				ROSALIA	
	N=3		N=3		N=2		N=7		N=8		N=13		N=4	
	$\bar{X}$	1σ	$\bar{X}$	1σ	$\bar{X}$	1σ	$\bar{X}$	1σ	$\bar{X}$	1σ	$\bar{X}$	1σ	$\bar{X}$	1σ
SiO_2	53.34	.68	50.66	1.02	51.80	.49	51.42	.69	51.36	.66	50.60	.35	50.39	.61
Al_2O_3	15.26	.34	14.30	.13	13.98	.13	14.49	.46	14.62	.53	14.35	.37	14.88	1.10
TiO_2	1.86	.12	3.07	.04	3.06	.03	2.89	.07	3.05	.10	3.01	.11	3.66	.19
FeO[3]	11.57	.50	14.43	.36	14.09	.13	13.42	.83	13.56	.71	12.44	.54	13.83	.52
MnO	.20	.01	.23	.02	.22	.01	.21	.02	.21	.02	.23	.01	.22	.02
CaO	8.66	.04	8.17	.22	8.46	.11	8.30	.30	8.23	.46	8.65	.20	8.34	.99
MgO	4.81	.22	4.32	.10	4.06	.59	4.43	.19	4.22	.17	4.59	.31	4.15	.23
K_2O	1.17	.16	1.29	.05	1.13	.11	1.34	.12	1.32	.17	1.17	.13	.85	.30
Na_2O	2.62	.05	2.72	.30	2.43	.13	2.51	.18	2.68	.29	2.43	.20	2.82	.36
P_2O_5	.31	.02	.61	.01	.54	.01	.56	.02	.55	.03	.54	.03	.69	.03

MEMBER	PRIEST RAPIDS		UMATILLA				ESQUATZEL		POMONA		ELEPHANT MOUNTAIN		ICE HARBOR[2]	
FLOW	LOLO		UMATILLA		SILLUSI								BASALT OF MARTINDALE	
	N=7		N=12		N=6		N=6		N=29		N=7		N=14	
	$\bar{X}$	1σ	$\bar{X}$	1σ	$\bar{X}$	1σ	$\bar{X}$	1σ	$\bar{X}$	1σ	$\bar{X}$	1σ	$\bar{X}$	1σ
SiO_2	50.04	.73	53.29	.72	54.06	.28	51.66	1.82	51.57	.63	50.30	.49	48.44	.49
Al_2O_3	14.62	.34	15.09	.32	15.29	.19	14.90	.54	15.76	.34	14.41	.27	14.18	.36
TiO_2	3.17	.06	3.04	.10	2.65	.03	3.23	.16	1.69	.08	3.58	.06	3.26	.13
FeO	13.64	.67	12.42	.86	12.27	.46	13.04	1.10	9.97	1.24	14.40	.65	12.38	.87
MnO	.22	.01	.20	.04	.20	.01	.20	.02	.18	.02	.21	.01	.23	.01
CaO	8.77	.53	6.47	.49	6.04	.28	8.22	1.47	10.44	.54	8.41	.18	10.20	.59
MgO	4.89	.30	3.06	.22	2.78	.13	3.78	.12	6.54	.39	4.29	.25	5.65	.36
K_2O	1.07	.14	2.57	.16	2.86	.25	1.73	.31	.48	.14	1.16	.14	.68	.17
Na_2O	2.72	.31	2.92	.25	2.89	.28	2.63	.24	2.56	.34	2.45	.19	2.30	.13
P_2O_5	.67	.02	.74	.02	.86	.04	.43	.04	.24	.02	.50	.02	.68	.04

[1]N = number of samples used in average

[2]Results taken from Reidel and Fecht, 1981

[3]FeO = FeO + .9(Fe_2O_3)

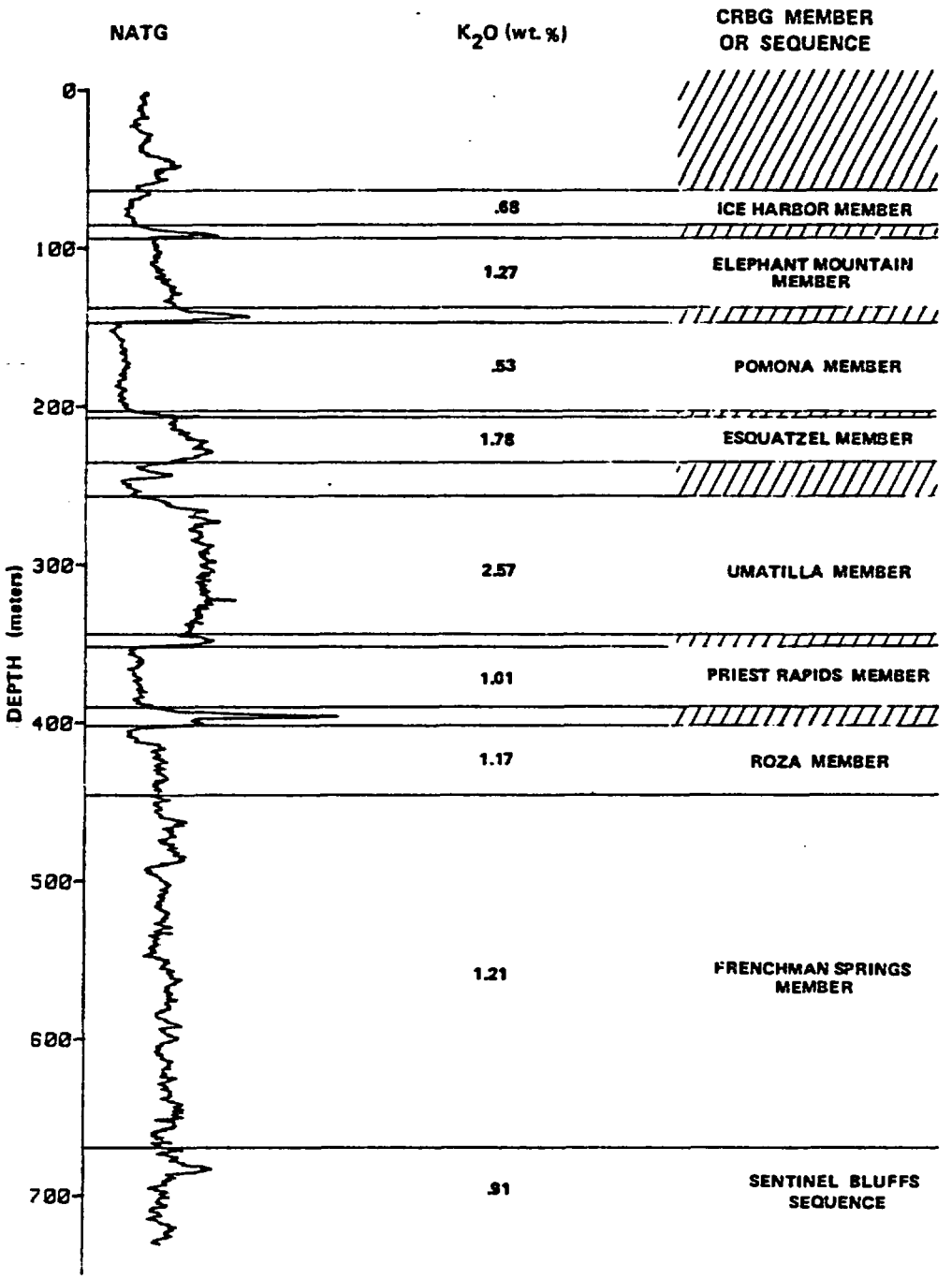

Figure 5. Natural gamma geophysical log of borehole DDH-3 shown alongside the average concentration of K_2O for CRB members. Hachured intervals represent sedimentary interbeds. The log is from the files of Rockwell Hanford Operations, Richland, Washington. The mean concentrations of K_2O were taken from Reidel and Fecht (1981) and Long and Landon (1981). Stratigraphic contacts were taken from Rockwell Hanford Operations document SD-BWI-DP-035 Rev. B-0.

Frenchman Springs Member. In the study area, the Frenchman Springs Member has been subdivided using criteria developed by Beeson and others (in prep.) in which they use major oxide and trace element compositions, paleomagnetics, and physical characteristics to divide this member into six stratigraphic units.

In the study area, only the upper stratigraphic units of the Frenchman Springs Member (i.e., basalts of Sand Hollow and Sentinel Gap) are exposed along the Horse Heaven Hills uplift. However, the Moon #1 and Horse Heaven Test wells on the Horse Heaven Plateau penetrated the entire Frenchman Springs section (see Fig. 58 and 59) from which flows belonging to the basalt of Ginkgo, Silver Falls, Sand Hollow, and Sentinel Gap are present. Along the Horse Heaven Hills, the uppermost Frenchman Springs flows are either directly overlain by the Roza Member or the Squaw Creek interbed. The upper exposed Frenchman Springs flows are not separated by sedimentary interbeds, although an hyaloclastite is observed at the base of the uppermost Frenchman Springs flow along the Chandler anticline (NE1/4 SW1/4 sec. 20, T.9N., R.26E.). In the Moon #1 and Horse Heaven Test wells, the Frenchman Springs Member is overlain by either the Priest Rapids Member or the Quincy interbed and underlain by the Grande Ronde Basalt.

The upper Frenchman Springs flows exposed along the Horse Heaven Hills uplift all have entablature-dominated jointing patterns with some flows having a flow top breccia up to 7 m thick. The flow top breccias contain basalt of a pahoehoe texture meshed with massive, angular clasts of basalt. The hackly entablature flows of the

Sentinel Gap and Sand Hollow form talus slopes of angular clasts that weather to a distinctive rust brown color. The basalt colonnade is very thin and is more gray in color relative to the entablature. Drill cuttings and borehole geophysical logs from the Moon #1 well indicate the presence of up to 13 m of flow top breccia in individual Sentinel Gap flows and up to 10 m in some Sand Hollow flows.

In hand sample, the Sentinel Gap and Sand Hollow flows have a black, fine-grained to glassy, and usually aphyric groundmass. An unknown black filling (possibly a mineraloid) is found locally in small circular vesicles in samples from the entablature. Sparse tabular plagioclase phenocrysts up to a centimeter in length were found in these upper flows.

Data from the chemically analyzed Frenchman Springs Member fall within expected ranges of major oxide concentrations for the Frenchman Springs chemical type of Wright and others (1973). Generally, the Frenchman Springs Member has distinctive P_2O_5 and TiO_2 concentrations that help differentiate it from other CRBG flows (Table II). Small variations in P_2O_5, TiO_2, and chromium concentrations, as well as stratigraphic position, help differentiate Frenchman Springs flows from each other (Table II). The Ginkgo flows have relatively higher P_2O_5 concentrations and lower chromium concentrations. The basalt of Sand Hollow has a lower P_2O_5 and TiO_2 concentration and a higher chromium concentration. Finally, the basalt of Sentinel Gap has a intermediate P_2O_5 value and a lower chromium value similar to the basalt of Silver Falls, but can be differentiated from the basalt of Silver Falls on the basis of stratigraphic position.

Roza Member. Along the Horse Heaven Hills uplift, the Roza Member is composed of one, or two flows or flow lobes. The occurrence of the two flows appears to be more common in the western portion of the Horse Heaven Hills uplift. The Roza Member commonly has a pillowed base, especially in the Byron Road area (center SW1/4 sec. 23, T.8N., R.23E.) where it is thickest (approximately 5 m) and overlies thin sediments that contain fragments of petrified wood. The Roza Member is overlain by either a thin sedimentary interbed or a flow of the Priest Rapids Member.

Outcrops of the Roza Member are commonly spheroidally weathered. The blocky basal colonnade of the Roza is locally platy jointed, with sheet fractures oriented perpendicular to the columns.

Fresh samples of the Roza Member have a medium-grained groundmass, are a dark gray color, and contain large (approximately 1 to 2 cm), abundant, colorless to orange-yellow phenocrysts and glomerocrysts of plagioclase. The presence of these phenocrysts make the Roza Member an excellent stratigraphic marker in the field, although local occurrences have been found elsewhere where phenocrysts are absent (Myers 1973). The groundmass, where weathered, has the appearance of being coarse grained.

The major oxide composition of the Roza Member (Table II) lies within the Frenchman Springs Member chemical type of Wright and others (1973). The Roza Member cannot be distinguished from flows of the Frenchmen Springs Member solely on the basis of its major oxide composition.

Priest Rapids Member. The Priest Rapids Member (Mackin 1961) is dated at approximately 14.5 m.y.B.P. (unpub. data from Rockwell Hanford Operations and Duncan 1982). In the Horse Heaven Hills, the Priest Rapids Member is overlain by the Mabton interbed and underlain by either the Quincy interbed or Roza Member. Within the study area, the Priest Rapids Member contains two distinct chemical types, an older Rosalia chemical type (Swanson and others 1979c) and a younger Lolo chemical type (Wright and others 1973). Although both chemical types are found within the study area, the flow of the Rosalia chemical type may be locally absent along the Horse Heaven Plateau as interpreted from borehole geophysical logs (see Fig. 58 and 59). Multiple flow units of Rosalia composition were found along the Horse Heaven Hills uplift, but only a single Lolo flow was found. However, on the Horse Heaven Plateau, it is interpreted from borehole geophysical logs and major oxide chemistry (see Fig. 58 and 59; Table II) that the Moon #1 and Horse Heaven Test wells penetrated two flow units of the Lolo chemical type. Locally, a discontinuous sedimentary interbed of the Ellensburg Formation, the Byron interbed, is present between the Rosalia and Lolo flows.

Outcrops of the flows of the Priest Rapids Member along the Horse Heaven Hills uplift are usually characterized by spheroidal weathering. Less weathered outcrops reveal a hackly entablature overlying a well-developed basal colonnade. The basal colonnade is often characterized by platy jointing oriented subparallel to the dip of the flows.

Fresh hand samples of the Priest Rapids Member are medium-grained to glassy. However, a highly weathered groundmass appears coarse. The Lolo flow contains sparse plagioclase phenocrysts and glomerocrysts.

Both flows are chemically distinct from each other (Table II). The Rosalia chemical type has higher TiO_2 and lower MgO concentrations than the Lolo chemical type.

Saddle Mountains Basalt

Within the study area, the Saddle Mountains Basalt is represented by five members (Fig. 3). They are from oldest to youngest, the Umatilla, Esquatzel, Pomona, Elephant Mountain, and Ice Harbor Members. Members of the Saddle Mountains Basalt have diverse lithologies, major oxide concentrations, and paleomagnetic polarities that easily distinguish them from each other and from other CRBG flows found within the study area. In addition, variations in K_2O between the flows of the Saddle Mountains Basalt members make natural gamma geophysical logs a useful tool in identifying these flows in the subsurface (Fig. 5).

Umatilla Member. In the study area, the Umatilla Member (Laval 1956) consists of the older Umatilla flow and the younger Sillusi flow (ARHCO 1976). The member directly overlies the Mabton interbed and underlies either the Cold Creek or Selah interbeds (Fig. 3).

Along the Horse Heaven Hills uplift, outcrops of the flows of the Umatilla Member are entablature dominated. The hackly entablatures commonly weather to a reddish brown color and form talus

composed of angular clasts. The basal portion of the flows are blocky jointed with thin, slabby to prismatic plates, and contain large almond-shaped vesicles near the lower contact. The basal portion is locally oxidized to a dark red. A highly distinctive, thick, rubbly flow top that is composed of scoriaceous and massive basalt clasts locally accompanies the flows (Fig. 6). Outcrops of the Umatilla Member are similar in appearance to the flows of Sand Hollow and Sentinel Gap of the Frenchman Springs Member.

Fresh hand samples from the entablature of the Umatilla Member flows are black, fine-grained, aphyric, and fracture conchoidally. Small plagioclase crystals (less than 1 mm in length) are locally present along with widely spaced vesicles filled with a black to gray mineraloid(?). Towards the base of the flows, samples appear to be medium grained, bluish gray, and contain small plagioclase crystals approximately 1 mm in length.

The major oxide composition of both flows of the Umatilla Member (Table II) is quite distinctive from other CRBG flows in the study area as it contains relatively higher P_2O_5, SiO_2, K_2O, and lower MgO, and both flows fall within the Umatilla chemical type of Wright and others (1973). The Sillusi flow can be distinguished from the Umatilla flow by the relatively lower TiO_2 and MgO, and higher P_2O_5 concentrations (Table II; Reidel and Fecht 1981). The high K_2O concentration of both flows provides an excellent signal in the natural gamma geophysical logs (Fig. 5) aiding in the member's identification in boreholes.

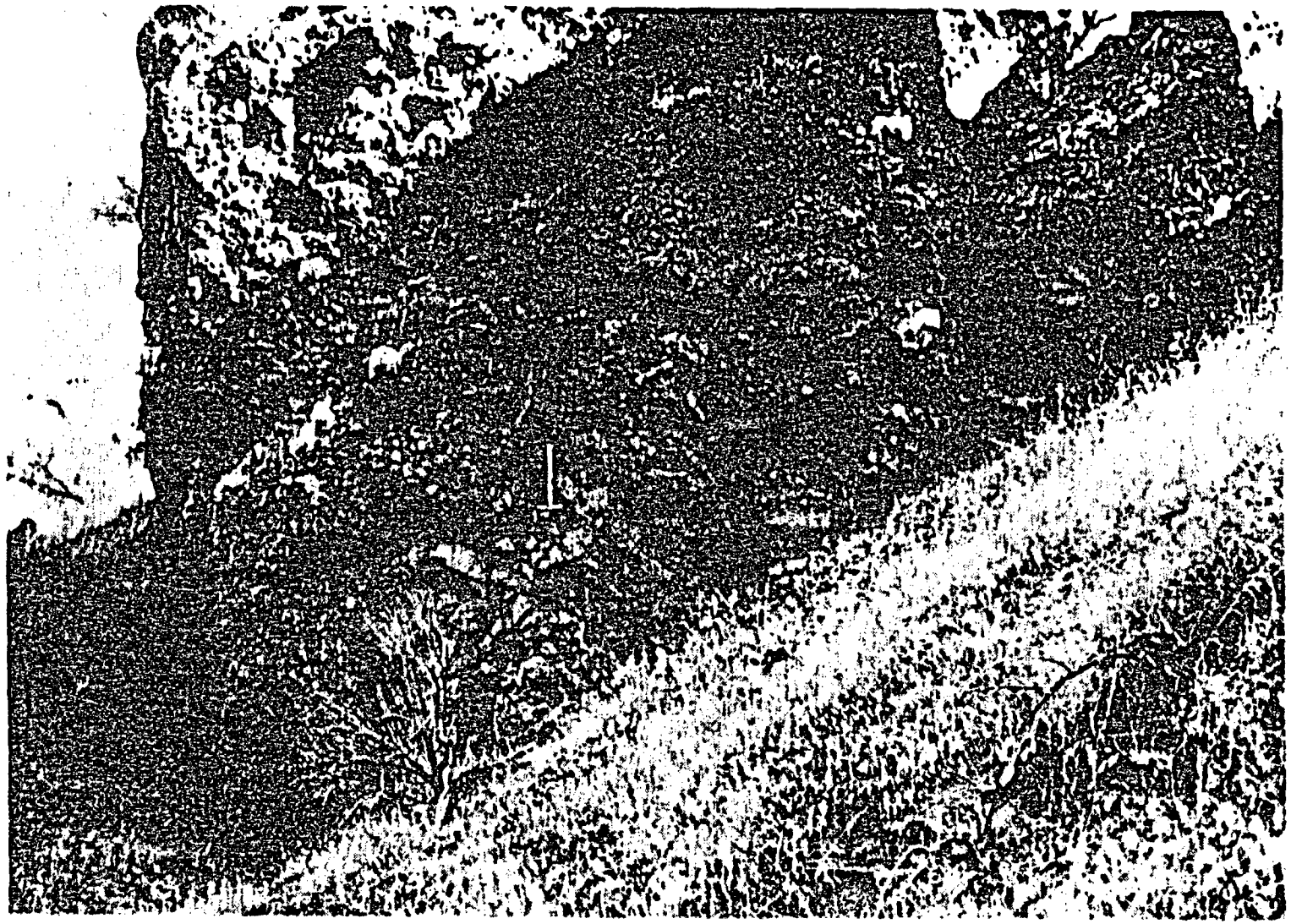

Figure 6. Flow top breccia of the Umatilla Member.

Esquatzel Member. Within the study area, the Esquatzel Member consists of one flow that lies beneath the Pomona Member or Selah interbed and above the Cold Creek interbed of the Ellensburg Formation (Fig. 3).

Exposures of the Esquatzel Member are rare, but where exposed, the basalt colonnade displays platy jointing and vesicles oriented parallel to the dip of the flow. Hackly entablature overlies the columns and grades into an oxidized pahoehoe flow top. Esquatzel Member outcrops weather to a distinctive brown color.

Fresh hand samples of the Esquatzel Member gathered from either the colonnade or entablature are gray-black to black in color (darker in the entablature) and microphyric with sparse lath-shaped plagioclase phenocrysts found in the entablature (less than 3 mm in length). The groundmass of the entablature has a more glassy texture than the colonnade; it commonly fractures conchoidally and contains local diktytaxitic zones.

The major oxide composition of the Esquatzel Member (Table II) lies within the Esquatzel chemical type defined by Swanson and others (1979c). The flow is distinguished by its intermediate P_2O_5 and TiO_2. The K_2O concentration of the Esquatzel Member lies between that of the Pomona and Umatilla Members aiding in its identification in natural gamma geophysical logs (Fig. 5).

Pomona Member. The Pomona Member (Schmincke 1967c) is overlain by the Rattlesnake Ridge interbed and usually is underlain by the Selah interbed (Fig. 3), but also directly overlies the Umatilla

Member where the Selah interbed, Esquatzel Member, and Cold Creek interbed are absent (e.g., Sunnyside-Grandview area).

The Pomona Member consists of one to three flow units. Two flows or flow lobes of the Pomona Member have been previously mapped and described in the Pasco Basin and eastern portion of the study area (Bond and others 1978; Myers and others 1979). Bond and others (1978) named the upper flow unit the "Chandler flow" and proposed a source vent for it along the Badlands anticline (sec. 8, T.9N., R.26E.) based on the presence of pumice and pyroclastic material at this location. This interpretation was dismissed by Myers and others (1979) because, based on its distribution, the "Chandler flow" would have flowed upslope. Further investigation of the Badlands "vent" area indicates it is a linear, low-amplitude anticline, and the pumicious and pyroclastic material is more likely formed from steam-generated spiracles derived from the interaction of the Pomona lava and water (S. P. Reidel and K. R. Fecht pers. comm., 1982). No evidence was found to support the existence of two separate Pomona flows within the study area.

Outcrops of the Pomona Member along the Horse Heaven Hills uplift display a distinctive jointing style. Overlying the thin basal colonnade are straight to curved, narrow prismatic columns (Fig. 7). These narrow columns of the entablature are locally tiered and may be separated by vesicular zones. At Chandler Butte (SE1/4 sec. 21, T.9N., R.26E.) the Pomona Member is interpreted to form invasive dikes in the Selah interbed. These dikes are composed of curved and slender columns (such as the entablature) that are oriented horizontally and

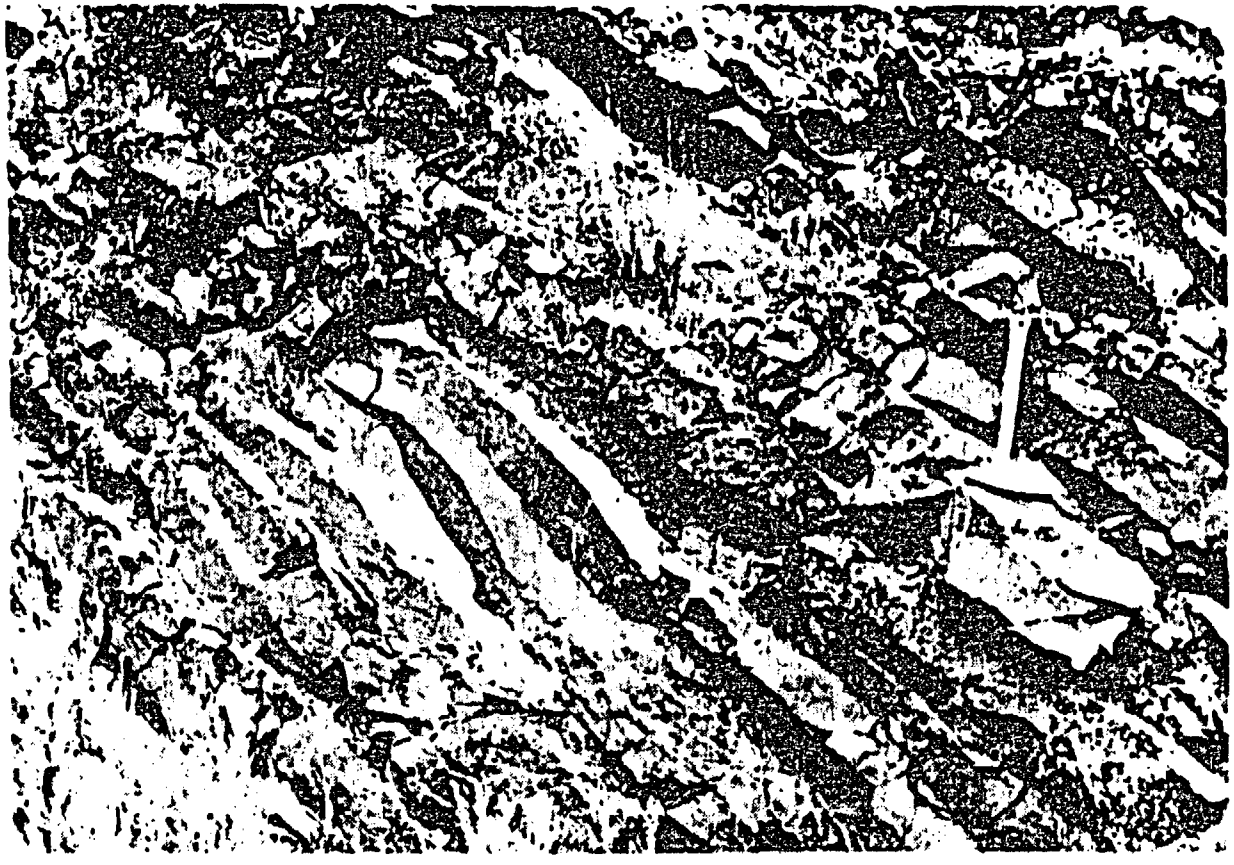

Figure 7. Entablature of the Pomona Member (loc. SE1/4 SW1/4 sec. 16, T.9N., R.26E.).

here interpreted to have formed perpendicular to the basalt/sediment contact. Locally emanating from the dikes are smaller, sinuous, chilled "dikelets" that merge and mix with the sediment forming pepperites similar to those described by Schmincke (1967a). Talus derived from the Pomona entablature is very distinctive since it tends to be uniform in both angularity and size. Locally, a fused tuff of the Selah interbed directly underlies the Pomona Member. In poorly exposed areas, float from the bluish-gray and black fused tuff helps approximate the Pomona/Selah contact.

In hand sample, the groundmass of the Pomona Member is a distinctive grayish black and varies from medium to fine grained. The Pomona Member is phyric, containing small plagioclase phenocrysts which display equant to slender tabular habits.

The chemical composition of the Pomona Member (Table II) falls within the Pomona chemical type of Wright and others (1973). The Pomona Member is marked by a lower P_2O_5 and TiO_2, and higher MgO and CaO content relative to other CRBG flows in the study area. In addition, the Pomona Member's low, uniform K_2O content produces a distinctive signal on natural gamma geophysical logs (Fig. 5).

Elephant Mountain Member. The Elephant Mountain Member consists of two separate flows, the older Elephant Mountain flow of Waters (1955) and the younger Ward Gap flow of Schmincke (1967c). In the study area, the Elephant Mountain Member is commonly the uppermost CRB unit in field sections and is usually directly overlain by either Ellensburg Formation sediments, glaciofluvial deposits, or the Ice

Harbor Member, and is directly underlain by the Rattlesnake Ridge interbed (Fig. 3).

Weathered outcrops of the Elephant Mountain Member are commonly gray to reddish brown in color. Spheroidal weathering also occurs in the blocky basal colonnade, which produces large rounded remnant boulders. Locally, pipe vesicles are found at the base of the flows.

Fresh hand samples of the Elephant Mountain Member are black, fine grained, and locally diktytaxitic. The rocks are abundantly microphyric which is readily apparent in direct sunlight. Larger-sized plagioclase phenocrysts are rare.

The two flows of the Elephant Mountain Member are readily distinguished from other CRBG flows in the study area by their characteristically lower SiO_2, intermediate P_2O_5, and higher TiO_2 concentrations (Table II). On the basis of these major oxide compositions, the two flows of the Elephant Mountain Member are indistinguishable from each other. Thus, they are recognized only by stratigraphic position and not delineated in the mapping. The Elephant Mountain Member has an intermediate K_2O concentration which is reflected in natural gamma geophysical log signatures (Fig. 5), and distinguishes it from the other CRBG flows.

Ice Harbor Member. The Ice Harbor Member consists of three flows (Swanson and others 1979c). These are (from oldest to youngest) the basalts of Basin City, Martindale, and Goose Island. No outcrops of the Ice Harbor are found along the Horse Heaven Hills uplift within the field mapping area, but other mapping in the vicinity of the uplift (Bond and others 1978; Myers and others 1979; Jones and Landon

1978; Gardner and others 1981; Hagood, in prep.) and borehole data from this study indicate that only the Martindale flow is present within the study area (outside of the Horse Heaven Hills uplift). The Martindale flow directly overlies the Elephant Mountain Member or the Levey interbed.

The Martindale flow of the Ice Harbor Member can be distinguished from the Elephant Mountain Member on natural gamma geophysical logs as a direct reflection of their differing K_2O contents (Fig. 5).

Ellensburg Formation

The Ellensburg Formation (Russel 1893) consists of sediments interbedded with, and overlying, the CRBG in the western and central Columbia Plateau (Rigby and Othberg 1979; Swanson and others 1979c). Although the upper and lower boundaries of the Ellensburg Formation are not well defined, it is generally considered that the lower portion of the Ellensburg Formation includes sediments interbedded with and conformably underlying the CRBG in the western part of the Columbia Plateau (Bentley and others 1980a; Waitt 1979). The upper boundary in the Toppenish Basin is considered to be the sediment conformably overlying the CRBG and unconformably underlying Pliocene and Quaternary rocks (Bentley and others 1980a). In the Pasco Basin, the upper section of the Ellensburg Formation is bounded by the Ice Harbor Member (Myers and others 1979) but also at the top of the late phase of the Snipes Mountain conglomerate (Fecht and others, in press). Farooqui and others (1981) designated coeval sediments above

the CRBG in Oregon as belonging to the Dalles Group and sediments interbedded with the CRBG as belonging in the Ellensburg Formation. Since the base of the CRBG is inaccessible in the study area, for the purposes of this study the Ellensburg Formation is defined as including all sedimentary rocks interbedded and conformably overlying the CRBG (but does not preclude sediments underlying the CRBG).

The Ellensburg Formation within the study area consists of one formal member, the Squaw Creek Member (Swanson and others 1979c), and ten informal members: Quincy interbed, Byron interbed, Mabton interbed, Cold Creek interbed, Selah interbed, Rattlesnake Ridge interbed, Levey interbed, early and late phase of the Snipes Mountain conglomerate, and the McBee conglomerate (Fig. 3). The Vantage Member of the Ellensburg Formation was formalized by Swanson and others (1979c) as well, but has not been found within the study area. The Ellensburg Formation interbeds are defined and identified on the basis of the identities of bounding CRBG flows (Schmincke 1967c; ARHCO 1976; Myers and others 1979; Swanson and others 1979c) and not on the basis of their lithologic characteristics. However, both lithology as well as stratigraphic position are used to identify the Snipes Mountain conglomerate and McBee conglomerate. Borehole geophysical logs can be used to identify the sedimentary interbeds of the Ellensburg Formation in the subsurface since the basalt flows can be identified; therefore, interbeds that are intercalated with the Saddle Mountains Basalt are more easily identified than those intercalated with the Wanapum Basalt.

The Squaw Creek Member. The Squaw Creek "Diatomite Bed" was assigned to lie beneath the Roza Member and designated as part of the Frenchman Springs Member by Grolier and Bingham (1966), but was later reassigned to the Ellensburg Formation as the Squaw Creek Member (Swanson and others 1979c)

In the study area, the Squaw Creek Member is a discontinuous interbed which lies between the Roza Member and Frenchman Springs Member (Fig. 3), locally exposed west of Prosser along the Horse Heaven Hills uplift. Near Byron Road (center SW1/4 sec. 23, T.8N., R.23E.) the interbed is composed of tuffaceous silts containing fragments of petrified wood and is overlain by approximately 5 m of Roza Member pillow basalts.

Quincy Interbed. The Quincy interbed, as defined by ARHCO (1976), lies between the Priest Rapids Member and the Roza Member, but for the purposes of this study, includes sediment between the Priest Rapids Member and the next older basalt flow. Along the Horse Heaven Hills uplift, only one outcrop of the Quincy interbed was found (SW1/4 NW1/4 sec. 14, T.8N., R.24E.). At this location, it is composed of opalized material, petrified wood, and some tuffaceous sediment. The interbed here is less than several meters thick. In the Horse Heaven Test well (see Fig. 59) on the Horse Heaven Plateau (Fig. 4), no Roza Member and possibly no Rosalia chemical type flows of the Priest Rapids Member are present based on chemical analyses. Here, nearly 20 m of sediment is interpreted to lie between the Lolo flow of the Priest Rapids Member and the Frenchman Springs Member, and by definition is considered to be the Quincy interbed.

Byron Interbed. Along the Horse Heaven Hills uplift near Prosser, a discontinuous, thin interbed is found between the Rosalia and Lolo flows of the Priest Rapids Member. The interbed variably consists of a baked tuff, opalized material embedded with petrified wood, or tuffaceous sediment that contains fragments of petrified wood. This interbed has been noted elsewhere in the central Columbia Plateau (Reidel 1978; Taylor 1976; Jones and Landon 1978; Bentley and others 1980a) and is here informally named the Byron interbed for a 0.5-m-thick section exposed along Byron Road (SE1/4 SE1/4 sec. 23, T.8N., R.23E.) south of the old town site of Byron.

Mabton Interbed. Sediment directly underlying the Umatilla Member and found along the Horse Heaven Hills south of Mabton, south-central Washington, was named the Mabton interbed by Laval (1956), was renamed the Mabton Member by Schmincke (1967c), and was later reduced to informal status by Swanson and others (1979c). Within the study area, the Mabton interbed lies between the Umatilla Member and the Priest Rapids Member (Fig. 3). Near the upper contact with the Umatilla Member, the Mabton interbed is baked and is a distinctive brick-red color with alternating bluish-gray colored bands that parallel the contact (Fig. 8). The baked zone is relatively erosionally resistant and contains a network of closely spaced columnar joints aligned perpendicular to the banding (Fig. 8). The interbed usually forms erosional saddles along the north dip slopes of anticlines within the Horse Heaven Hills uplift.

The Mabton interbed is composed of tuffaceous clays, silts, and sands. Fluvially deposited sands and pebbly sands of the interbed are

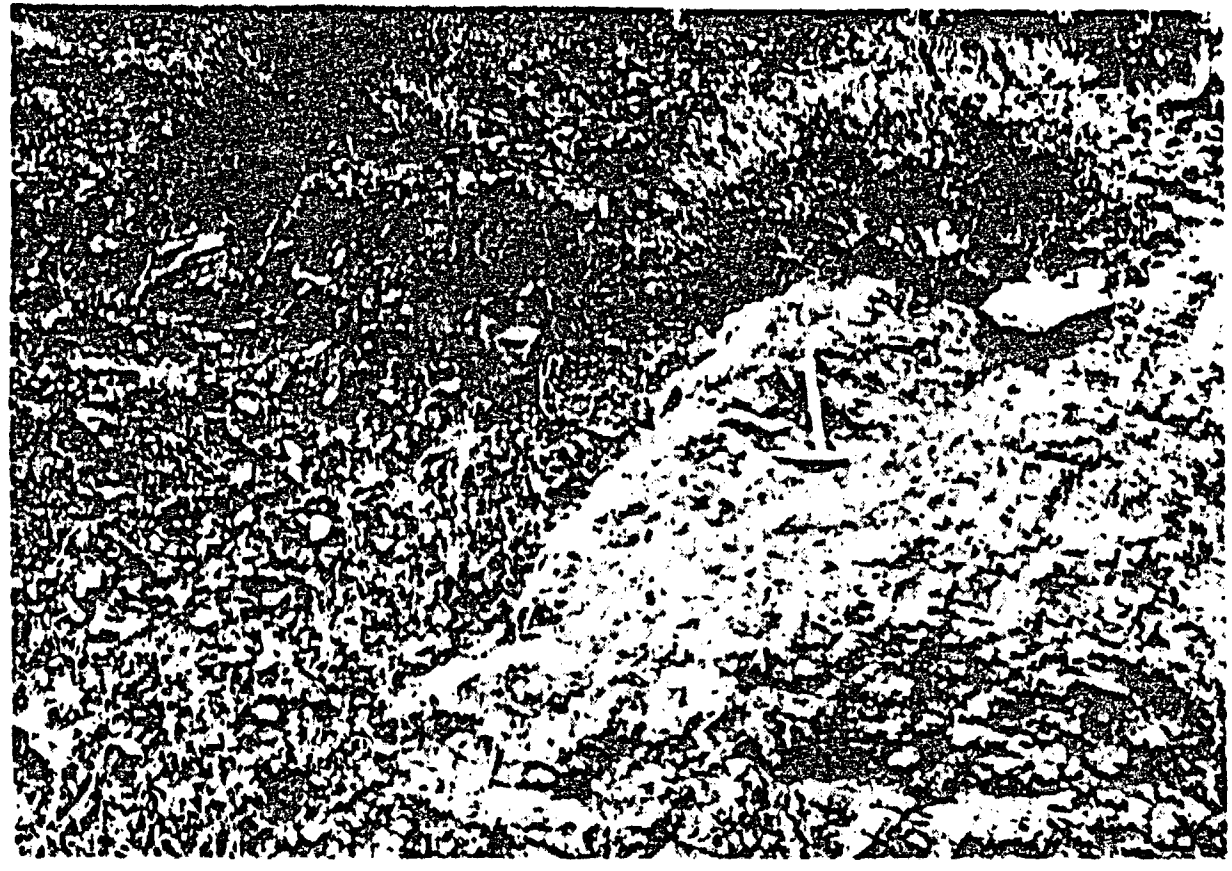

Figure 8. Near-vertical contact between the Umatilla Member and the Mabton interbed (loc. SE1/4 SW1/4 sec. 16, T.9N., R.26E.). The upper portion of the interbed has been baked.

commonly found along the Horse Heaven Hills west of Prosser. These sands contain quartzite, feldspar, and mica, (identifications using hand lens) which were probably derived from outside the Columbia Plateau.

Cold Creek Interbed. The Cold Creek interbed was informally named for sediments found in the Pasco Basin directly underlying the Esquatzel Member (ARHCO 1976; Myers and others 1979). In the study area, the Cold Creek interbed lies between the Esquatzel Member and the Umatilla Member (Fig. 3).

The Cold Creek interbed is poorly exposed along the Horse Heaven Hills uplift, but where exposed it is composed of unconsolidated silt. Natural gamma geophysical logs through the Cold Creek interbed (DNR 79-07 well, see Fig. 70; Shaw well, see Fig. 79; DDH-3 well, see Fig. 5) suggest the interbed lacks a significant amount of potassium-rich sediments.

Selah Interbed. Mackin (1961) named the sediments found between the Pomona Member and Roza Member the "Selah Member" of the Ellensburg Formation. Schmincke (1967c) later redefined the "Selah Member" to be the sediments directly underlying the Pomona Member and overlying the next older basalt flow. This interbed was later informalized by Swanson and others (1979c).

Following the definition of Schmincke (1967c), the Selah interbed within the study area lies between the Esquatzel and Pomona Members (Fig. 3), or between the Umatilla and Pomona Members where the Esquatzel flow is absent.

The Selah interbed consists of sands, silts, tuffs, and conglomerates. A blue-black to gray, banded, fused vitric tuff (Schmincke 1967a), up to several centimeters thick, is often found at the contact between the Selah interbed and the Pomona Member. Float from the fused tuff layer can often be found on hillsides aiding in locating the upper boundary of the Selah interbed. A fluvial facies is recognized within the Selah interbed which consists of a generally poorly indurated conglomerate (Fig. 9). The sand matrix is quartzose and mica rich. The majority of clasts within the conglomerate are Columbia River basalt (Table III), but the conglomerate also contains a significant fraction of plutonic and metamorphic clasts (approximately 40%). As the clast size increases, the CRB comprises a higher percentage of the clasts, while the plutonic and metamorphic rocks (derived from outside the plateau) increase in abundance as clast size diminishes (Table III). The size change, along with the composition of the clasts and sand, reflect distant provenance of the exotics and local derivation of the basalt. The conglomerate is rarely cemented by an iron-bearing mineral. At Chandler Butte (SE1/4 sec. 21, T.9N., R.26E.) the conglomerate is found adjacent to invasive Pomona dikes and exposures of hyaloclastite. The hyaloclastite is interpreted to have formed from the interaction of the fluid Pomona lava with the water-saturated Selah interbed. Fecht and others (in press) interpret the Selah conglomerate to represent the westward extension of the ancestral Clearwater-Salmon River (ancestral Snake River of Swanson and Wright 1976; see Chapter 3). The exposures at Chandler Butte suggest that a paleoriver was present here just prior

Figure 9. Conglomerate within the Selah interbed (loc. NE1/4 SW1/4 sec. 29, T.9N., R.27E.).

TABLE III

PEBBLE COUNTS OF GRAVELS FROM VARIOUS ELLENSBURG FORMATION OUTCROPS

SEDIMENTARY UNIT	LOCATION			COUNT (INTERMEDIATE AXIS SIZE)	BASALT (CRBG) %	QUARTZITE %	OTHER[1] %
	TOWNSHIP	RANGE	SECTION				
McBEE CONGLOMERATE	9N	26E	SE SE 23	100	100.0	0.0	0.0
SNIPES MTN.[2] CONGLOMERATE	8N	24E	SE SE 9	50 OR 100	16.0	10.0	74.0
RATTLESNAKE RIDGE	8N	24E	SW NE 18	194	18.0	15.0	67.0
SELAH	9N	26E	SW SE 21	42 (6-25 cm)	78.6	0.0	21.4
				164 (3-6 cm)	72.6	6.1	21.3
				139 (1-3 cm)	48.2	15.8	36.0
SELAH	9N	26E	SE NE 25	218	60.6	11.9	27.5

1. Generally consists of metamorphic and plutonic lithologies
2. Recalculated from Schmincke (1964). Correlated with the late phase of the Snipes Mountain conglomerate of Fecht (in press)

to the incursion of the Pomona Member. Both the fused tuff and conglomerate within the study area were deposited during the Esquatzel-Pomona interval (see Chapter 3).

A "kick" in the natural gamma log signature is found at the top of the Selah interbed section in several of the boreholes (see Fig. 50 through 79). Observations from this study support Brown's (1978) idea that this kick represents the vitric tuff found regionally at the upper contact of the interbed (Schmincke 1967a).

Rattlesnake Ridge Interbed. Thick sediments separating the Pomona and Elephant Mountain Members, or the upper vitric tuff of the Selah "Member", were named the Rattlesnake Ridge Member by Schmincke (1967c), but the interbed was later informalized by Swanson and others (1979c).

Outcrops of the Rattlesnake Ridge interbed are rare along the northern flanks of the Horse Heaven Hills uplift, since the steeply dipping interbed acts as a slip plane facilitating slumping. Exposures are more commonly found along the ridge crests of the Horse Heaven Hills and along cliffs created by the down-cutting of the Yakima River. Where exposed, the interbed is light tan, light gray, or off-white in color.

The Rattlesnake Ridge interbed consists of laminated silts and clays, cross-bedded, ripple-marked, or massively bedded sandstone, or massive tuffs. The sandstones are locally micaceous and mixed with other heavy minerals of exotic derivation (from outside the Columbia Plateau). Along Ward Gap Road (Fig. 10; NW1/4 NE1/4 sec. 17, T.8N., R.24E.) a 2-m thick conglomerate, containing nearly 15% quartzitic

Figure 10. Conglomerate within the Rattlesnake Ridge interbed.

pebbles and cobbles (Table III), conformably overlies the flow top of the Pomona Member and is itself overlain by a thicker section of laminated siltstone. Based on the gravel lithologies (Table III), stratigraphic position, and geographic location, the conglomerate is here interpreted to have been deposited by the ancestral Columbia River whose channel is found farther to the north (Schmincke 1964, 1967c, 1967d; see Chapter 3). Absence of a major component of CRB clasts in the conglomerate indicates that the ancestral Columbia River was not influenced by the ancestral Clearwater-Salmon River at this time at this location (or to the north of this location).

Levey Interbed. The Levey interbed consists of those sediments between the Ice Harbor and Elephant Mountain Members (ARHCO 1976; Fig. 3). The Levey interbed is not found along the Horse Heaven Hills uplift in the study area, but is found in two of the geophysically logged boreholes (DC-15, DDH-3). The Levey interbed gives a high natural gamma response in these two boreholes. The Levey interbed has been described as being composed of tuffaceous silt or siltstone (Bond and others 1978; Myers and others 1979).

Snipes Mountain Conglomerate. The Snipes Mountain conglomerate was informally introduced by Schmincke (1967c) for an areally extensive conglomerate deposit which directly overlies the Elephant Mountain Member in south-central Washington. The Snipes Mountain conglomerate is characterized by an abundance of quartzite and other metamorphic rocks. Schmincke (1967c) attributed the source of the conglomerate to a sheet deposit of the ancestral Columbia River. Fecht and others (in press) divide the Snipes Mountain conglomerate

into an early and late phase (Fig. 3) based on lithology and distribution. The early phase was deposited between the emplacement of the Elephant Mountain Member and the Ice Harbor Member (between 8.5 and 10.5 m.y.B.P.) and is coeval with the deposition of the Levey interbed. The late phase of the Snipes Mountain conglomerate was deposited after the emplacement of the Ice Harbor Member and is thought to be coeval with the basal unit of the Ringold Formation of the Pasco Basin (Fecht and others, in press). The two phases both contain deposits from the ancestral Columbia River, but they were deposited during slightly different time intervals and in different geographic locations, reflecting a diversion of the ancestral Columbia River (see Chapter 3).

Outcrops of both the early and late phases of the Snipes Mountain conglomerate are identified in the study area based on clast lithology and stratigraphic position, but are tentatively differentiated solely on the geographic distribution of the conglomerates in accordance with the distribution specified by Fecht and others (in press). The early phase of the Snipes Mountain conglomerate is not found along the portion of the Horse Heaven Hills uplift that was in the field mapping area, but is found along the Horse Heaven Hills uplift to the immediate west (Schmincke 1964, 1967c, 1967d; Swanson and others 1979a; Bentley and others 1980a; Bentley and others in press; Hagood, in prep.) and within the lower Yakima Valley in the vicinity of Sunnyside, Washington (Campbell 1977; Rigby and Othberg 1979). Two outcrops of the late phase of the Snipes Mountain conglomerate are tentatively identified along the Horse

Heaven Hills uplift. One occurrence is found along Richards Road (SE1/4 SE1/4 sec. 9, T.8N., R.24E.). Here, Snipes Mountain conglomerate is found conformably overlying the steeply dipping Elephant Mountain Member along the northern flank of the Drake anticline. The conglomerate occurs in lenses surrounded by silts and sands. The outcrop was first identified by Schmincke (1964) who described the lithology of the clasts (Table III). The other occurrence is found along the cliffs at the Gibbon railroad siding (center NE1/4 sec. 26, T.9N., R.25E.). Here, the flat-lying Elephant Mountain Member is overlain by a thin conglomerate (less than 30 cm thick). No pebble counts were conducted on this exposure, but the conglomerate appears to contain a high percentage of plutonic and metamorphic clasts. This conglomerate is overlain by approximately 1 m of siltstone. This exposure was assigned to the Levey interbed by Bond and others (1978).

McBee Conglomerate. Another conglomerate, informally named the McBee conglomerate in this study, was found in two locations along the crest of the Horse Heaven Hills within the northwest trend. Alongside McBee grade (SE1/4 SE1/4 sec. 23, T.9N., R.26E.), the conglomerate is exposed in a gravel pit (Fig. 11) where it appears to overlie the Pomona Member. Laval (1956) described these gravels at this location to be forset-bedded with a northwesterly dip, although this foreset bedding is not apparent today. Near Webber Canyon (SE1/4 SE1/4 sec. 32, T.9N., R.22E.), gravels of the McBee conglomerate appear to overlie the Elephant Mountain Member. The clasts within the conglomerate at both locations consist mostly of rounded to subrounded

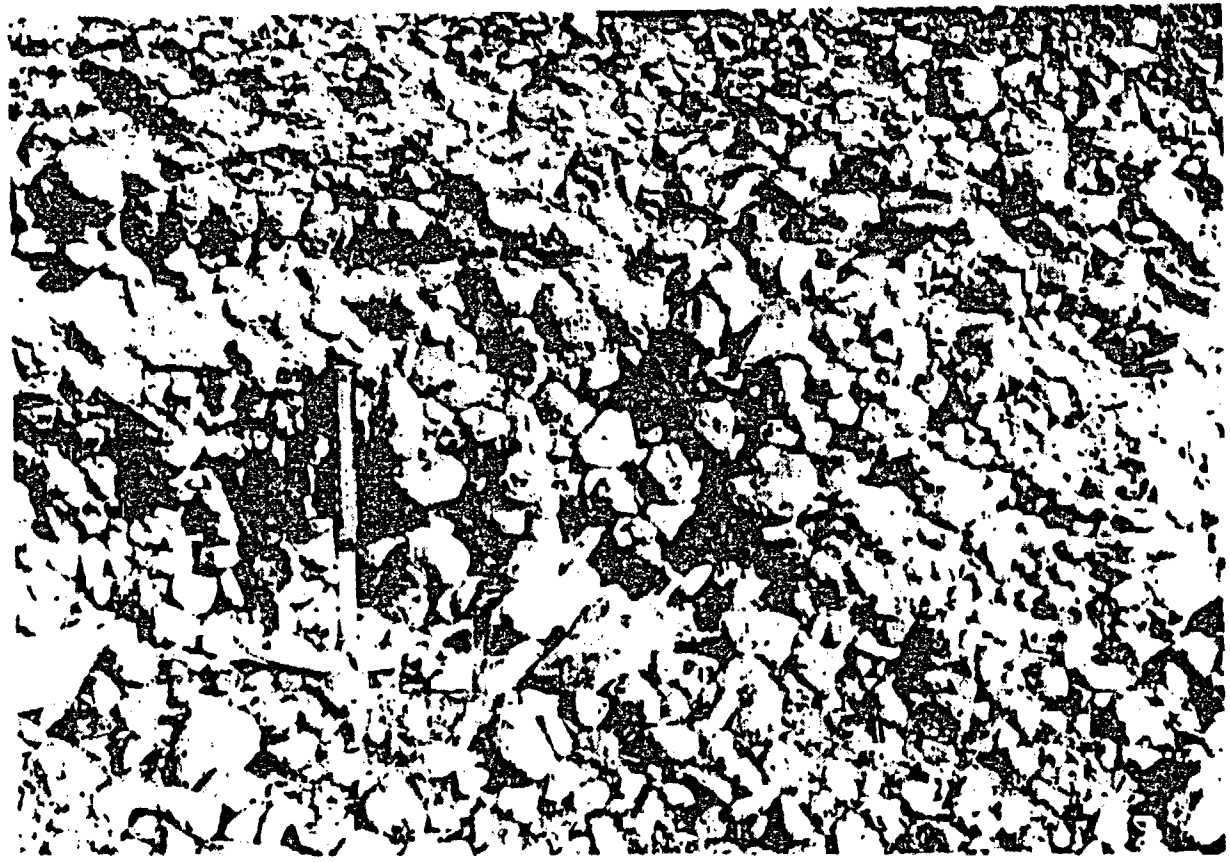

Figure 11. The McBee conglomerate (loc. SE1/4 SE1/4 sec. 23, T.9N., R.26E.).

CRB and are considered here to be locally derived (from within the Columbia Plateau). Further, a majority of the CRB clasts appear to be Pomona basalt. The exact age of the deposit is unknown, but the McBee conglomerate is tentatively thought to be coeval with the late phase of the Snipes Mountain conglomerate based on its distribution (see Chapter 3).

Undifferentiated Ellensburg Formation Sediments. Rarely, poorly exposed sediments outcrop along the Horse Heaven Hills uplift that conformably overlie the Elephant Mountain flow and consist of bedded and laminated silts and clays (e.g., along the northern flank of the Prosser anticline, SW1/4 sec. 13, T.8N., R.23E.), or tuffaceous silts (e.g., along the southern limb of the Chandler anticline, NW1/4 NW1/4 sec. 30, T.9N., R.26E.). The exact age of these sediments is unknown (except that they are post-Elephant Mountain in age), but because of their conformable relationship to the Elephant Mountain Member and their lithologies, they are included in the Ellensburg Formation.

STRUCTURE

This chapter describes the structure of the portion of the Horse Heaven Hills uplift which encompasses the intersection of the northwest and northeast structural trends of the uplift. Because of their proximity and intrinsic relationship with the Horse Heaven Hills uplift, the structure of portions of the lower Yakima Valley, Horse Heaven Plateau, Badger Coulee, and Hog Ranch-Naneum anticline are also described, but more generally, in the beginning of this chapter.

Structure of the Immediate Area

Lying between the RAW and the Toppenish Basin, and between Rattlesnake Ridge and the Horse Heaven Hills (Fig. 12) is a broad east-west-trending syncline called here the lower Yakima Valley syncline. The syncline broadens and abruptly plunges westward towards the Toppenish Basin west of Sunnyside. The lower Yakima Valley syncline is structurally higher than, and separates the Toppenish and Pasco Basins as indicated by top-of-basalt elevations from this and other studies (for the Toppenish Basin - Robbins and others 1975; Bentley and others 1980a; Biggane 1982; for the Pasco Basin - Myers 1981). Low-relief, generally east-west- and northwest-trending anticlines and monoclines are superimposed upon the broad syncline (Fig. 12).

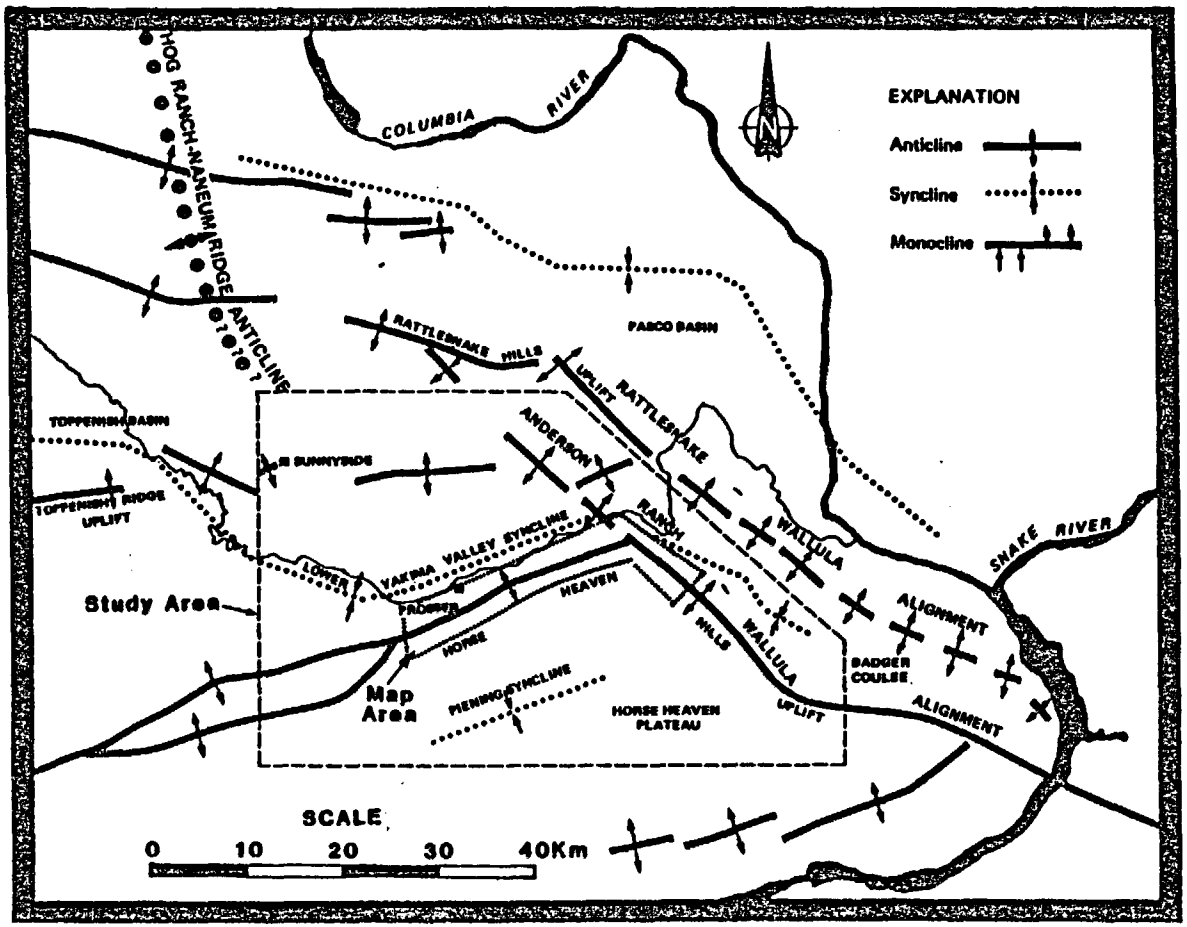

Figure 12. Generalized map showing structures in and adjacent to the study area.

Trending approximately north-northwest across the Yakima folds (Fig. 12) is a broad structural arch which generally separates the Yakima River and Columbia River drainages. The fold system has been referred to in whole or in part as the Table Mountain anticline (Barrash and others 1983), the Naneum Ridge anticline.(Campbell 1984), the Naneum High (a coincident subsurface high, Campbell 1984), the Hog Ranch Axis (Mackin 1961; Bentley 1977; Waitt 1979), the Hog Ranch anticline (Bentley 1977), and the Hog Ranch-Naneum Ridge anticline (Reidel 1984; used in this study). The Hog Ranch-Naneum Ridge anticline has been traced north into the Wenatchee Mountains (Swanson and others 1979a, Tabor and others 1982) where basement structure is involved with the uplift (Campbell 1984; Tabor and others 1982).

The southern extension of this structure has been depicted as extending as far as the Rattlesnake Hills on maps (Mackin 1961; Bentley 1977) but has also been shown extending to the immediate south of Rattlesnake Hills into the lower Yakima Valley syncline (Bentley 1977; Waitt 1979; Barrash and others 1983; Campbell 1984). Although data from this study are not sufficient for determining the presence of the anticline at the surface now, within the lower Yakima Valley, data do suggest that the fold may at least exist as a buried structure in the lower Yakima Valley (see Chapter 3).

The portion of the Horse Heaven Plateau (Fig. 12) which lies within the study area is composed of gentle dips from the south flanks of folds along the northwest and northeast trends of the Horse Heaven Hills uplift. A low-relief syncline, here named the Piening syncline (Fig. 12), can be defined on the structure contour map (Fig. 13). The

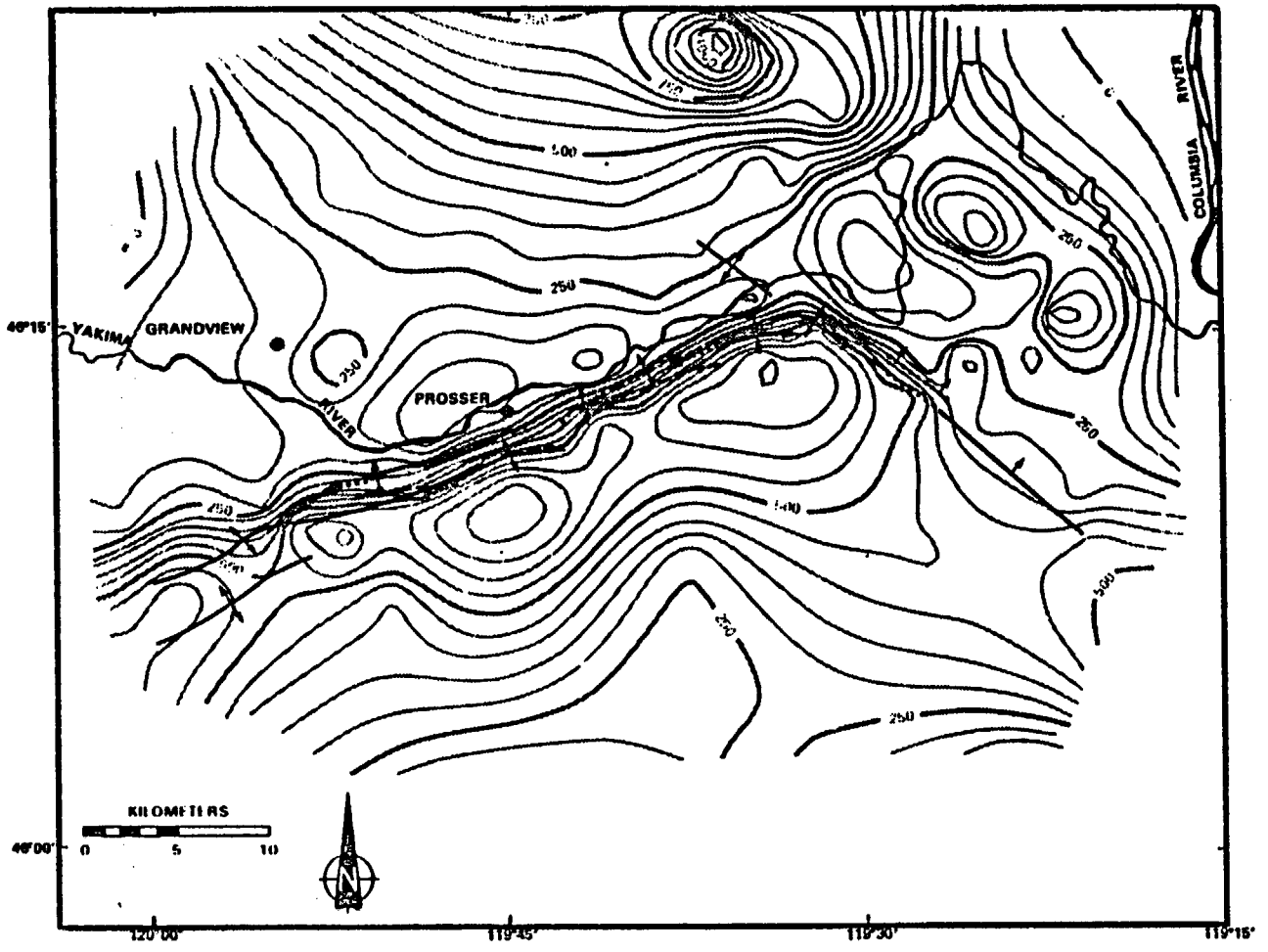

Figure 13. Structure contour map on top of the Pomona Member within the study area and immediate vicinity. Contour interval is 50 m.

southwestern extent of the syncline is unknown, but may continue to the southwest of the study area (Frank Packard, pers. comm. 1984).

Badger Coulee (Fig. 12) is a narrow valley which lies between the RAW and the northwest trend of the Horse Heaven Hills anticline. Brown (1979) mapped the valley as a syncline based on borehole data.

Horse Heaven Hills Uplift

The two structural trends of the Horse Heaven Hills uplift (N50° -55° W and N65°-70°E) are only generally shown in the structure contour map (Fig. 13), but reflect a superimposed en echelon fold pattern along the two trends (Fig. 14). The folds within the northeast trend are oriented in a left-stepping sense to the trend while the folds along the northwest trend are aligned or oriented in a slight right-stepping sense to this trend (Fig. 14). The asymmetry of the uplift is well displayed in the structure contour map indicating northward vergence of the folds in both trends.

Based on geometric distinctions between folds, the Horse Heaven Hills uplift within the study area has been subdivided into six segments (Fig. 15). I have applied the names (1) Byron, (2) Gibbon, and (3) Chandler to segments in the northeast trend, and (4) Webber and (5) Kiona to segments in the northwest trend. Another segment, called the Junction segment, covers the intersection of the two trends. Two types of cross sections have been constructed to display the fold and fault geometry along the Horse Heaven Hills uplift, descriptive cross sections which display structure as observed in the

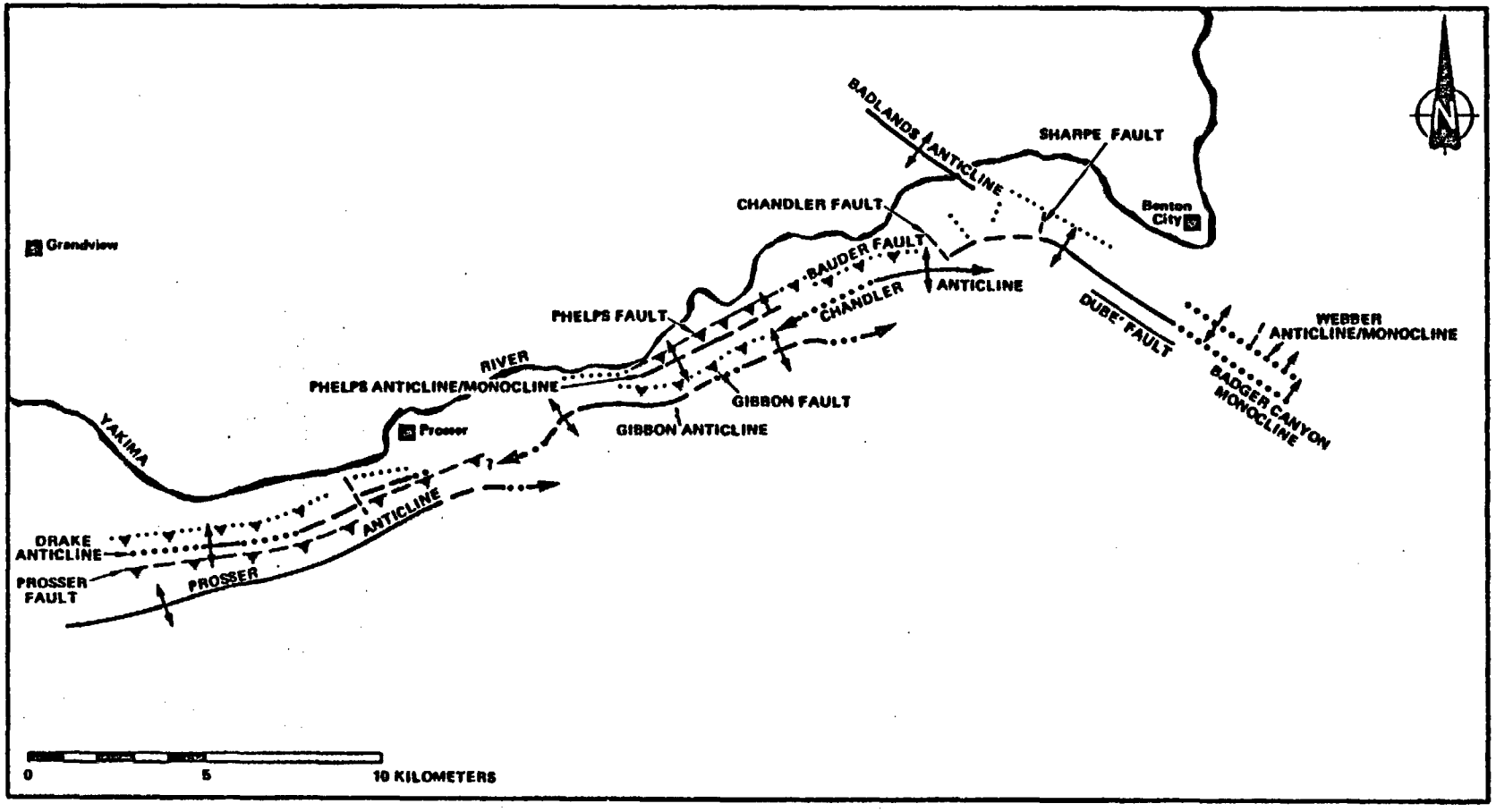

Figure 14. Generalized structure map of the Horse Heaven Hills uplift within the study area.

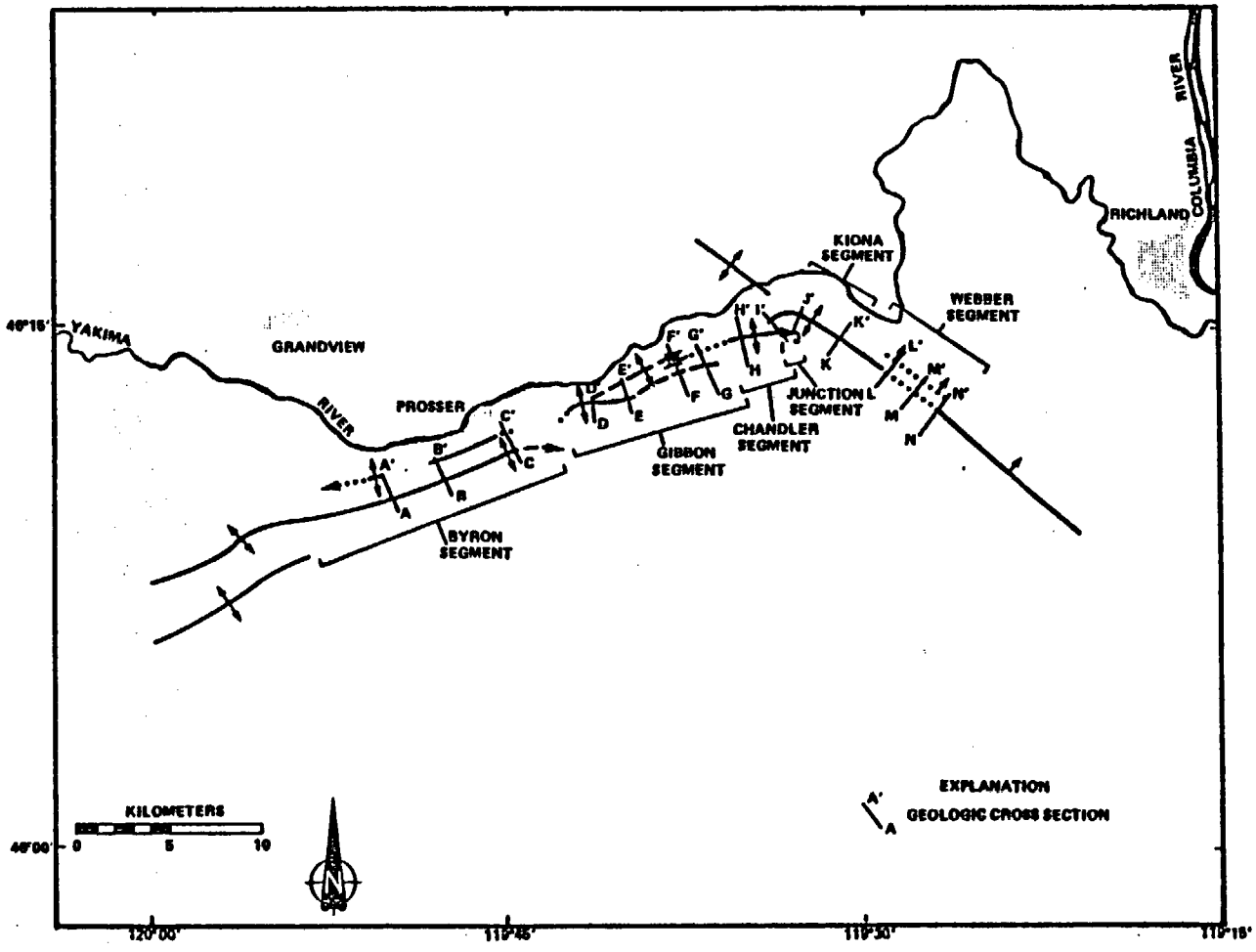

Figure 15. Map showing locations of the segments of the Horse Heaven Hills uplift and geologic cross sections within the study area.

field (see Fig. 79-80, Appendix C) and interpretive geologic cross sections (Fig. 17, 19, 21, 23, 25, 27).

Byron Segment. The Horse Heaven Hills uplift within the Byron segment consists of two parallel folds: the Prosser anticline and the Drake anticline (Fig. 14, 16).

The Prosser anticline is an erosional remnant of a double-hinged, asymmetric fold (north vergence) with a N70°-80°E trending axial trace. East of Prosser, the anticline locally plunges to the northeast, at its northeast end.

The northern limb of the Prosser anticline is offset over the southern limb of the Drake anticline along the Prosser fault, a high-angle reverse or thrust fault (Fig. 17a,b,c). In another location (NW1/4 sec. 12, T.8N., R.24E.), the northern hinge of the Prosser anticline is cut by a high angle reverse fault (Fig. 17c). Within the "interhinge limb", that portion of the fold which lies between the northern and southern hinge of a double-hinged fold, a minor thrust fault offsets the upper portion of the Frenchman Springs section to the north over itself less than a few meters (NW1/4 SW1/4 sec. 7 T.8N., R.25E.). Layer-parallel faulting, indicated by the presence of slickenside striae and fault breccia, are found along stratigraphic contacts of steeply dipping strata such as observed along the Umatilla/Selah contact of the southern limb at Ward Gap (NW1/4 SE1/4 sec. 20, T.8N., R.24E.).

The Drake anticline (Fig. 17a,b,c) is a subtle, low-relief, asymmetric (north vergence), double-hinged fold which parallels the Prosser anticline. Strikes of strata are dichotomous, with the

Figure 16. The Horse Heaven Hills uplift within the Byron segment.

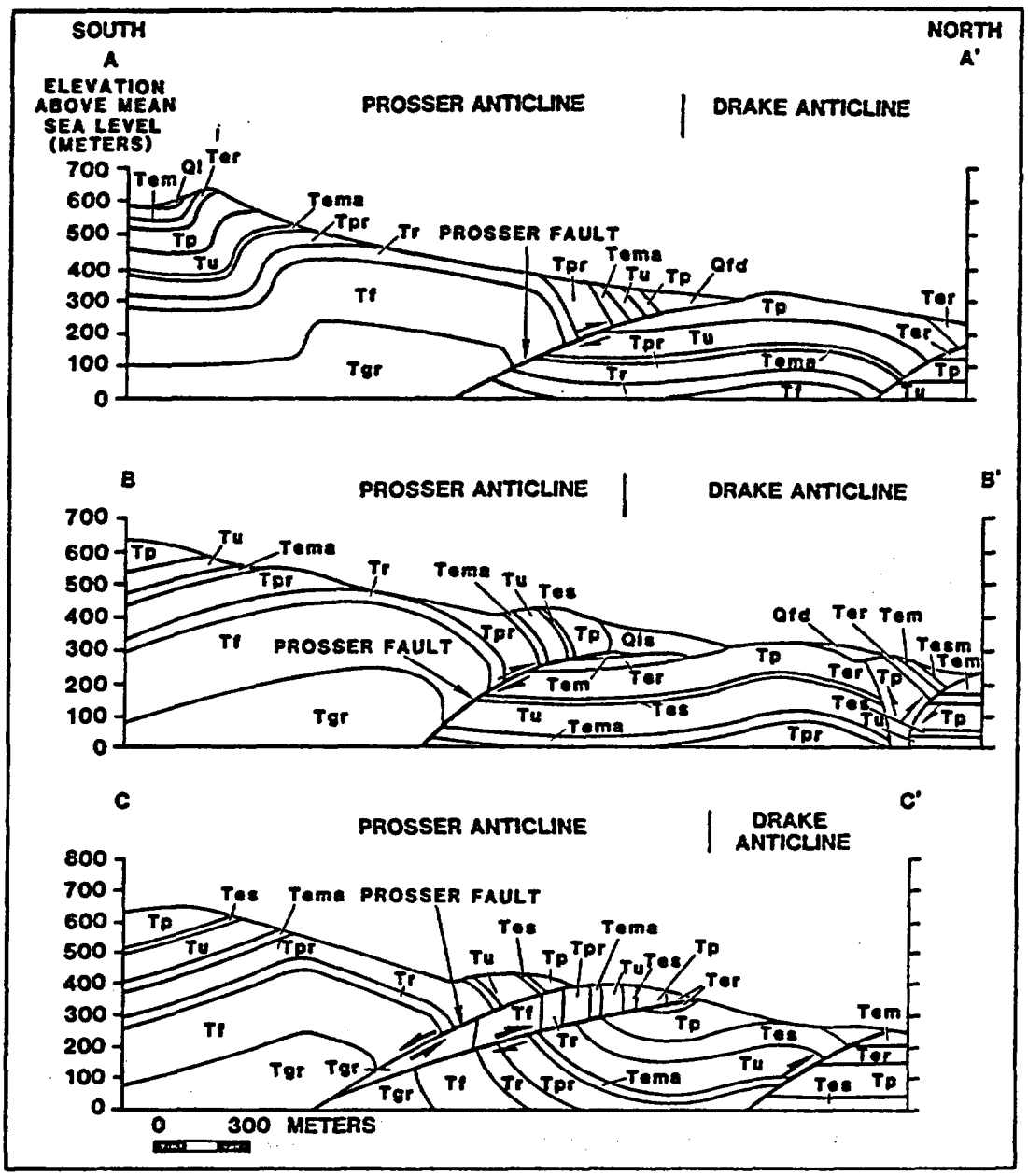

Figure 17. Interpretive geologic cross sections through the Horse Heaven Hills uplift within the Byron segment (see Fig. 80, Appendix C, for corresponding descriptive cross sections).

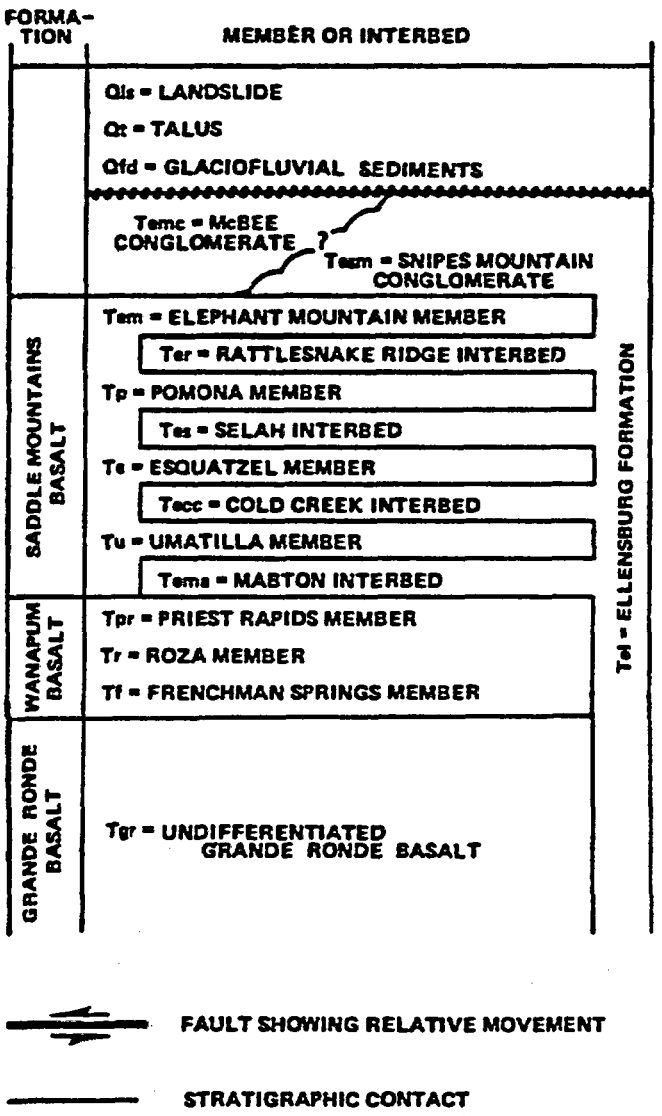

Figure 18. Legend for interpretive geologic cross sections.

southern limb oriented approximately 70° west (counterclockwise) to the axis of the fold while the northern limb parallels the axis (related to movement along the Prosser fault or local plunging of the anticline?). The Drake anticline either dies out or is buried beneath surficial sediment both east of Prosser and west of Byron road.

At one location (NE1/4 NE1/4 sec. 16, T.8N., R.24E.) a high-angle reverse fault can be traced through the northern hinge of the Drake anticline (Fig. 17b). In another location (NW1/4 SW1/4 sec. 11, T.8N., R.24E.) a tear fault with right lateral offset strikes perpendicular to the axis of the Drake anticline (Fig. 14). The attitude of layering and the presence of tectonically shattered basalt along the northern front of the Drake anticline suggests a thrust or high-angle reverse fault may offset the northern limb of the anticline to the north.

Gibbon Segment. The Horse Heaven Hills uplift within the Gibbon segment consists of two subparallel folds, the Gibbon anticline and the Phelps anticline/monocline (Fig. 14, 19).

The Gibbon anticline is an eroded, asymmetric fold (north vergence) which may be locally double hinged. The trace of the anticlinal axis generally trends N.70°E., but locally deviates from this trend. The crestal area of the Gibbon anticline is marked by a local structural dip in the center of the segment which is interpreted to coincide with a less deformed portion of the Gibbon anticline. To the east the anticline dies out onto the south flank of the Chandler anticline. The western end of the anticline plunges beneath landslide debris to the south of Prosser obscuring its structural relationship

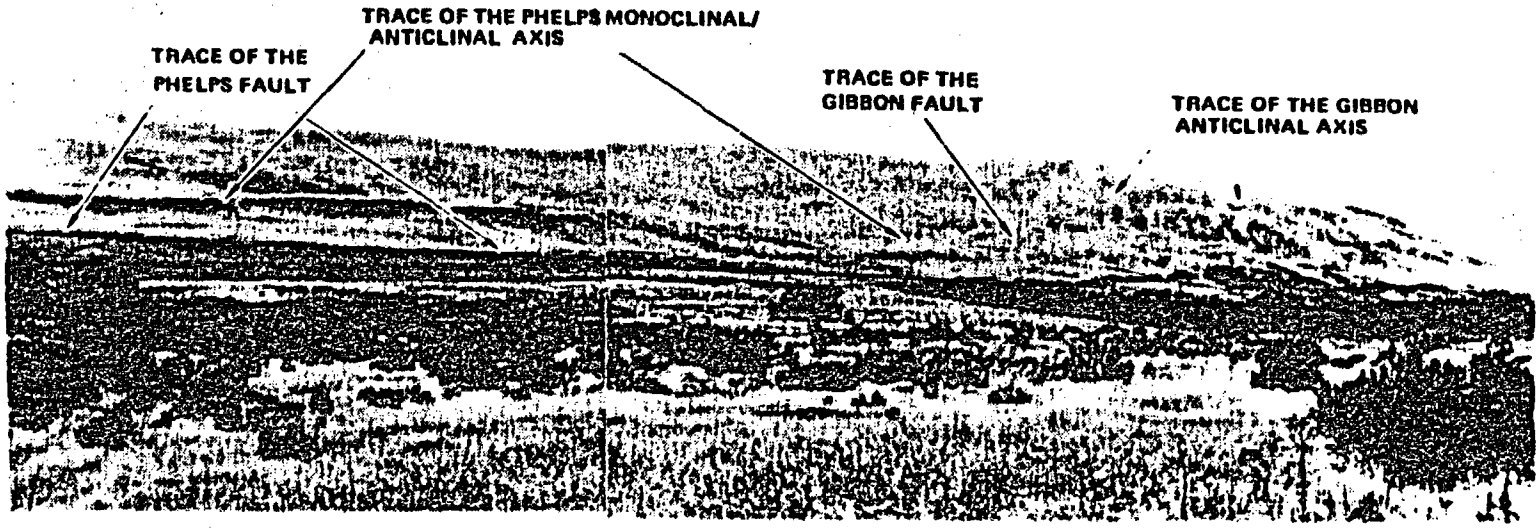

Figure 19. The Horse Heaven Hills uplift within the western portion of the Gibbon segment.

with the Gibbon anticline. However, the Gibbon anticline may be en echelon with the Prosser anticline based on the last traceable portions of the Gibbon and Prosser anticlines.

A thrust or high-angle fault (the Gibbon fault, Fig. 20d,e,f) is interpreted to lie below the northern limb of the Gibbon anticline and is locally manifested by tectonically shattered basalt along the northern limb of the anticline. At one location (NE1/4 SW1/4 sec. 33, T.9N., R.25E.) the hinge zone was cut by a thrust fault (Fig. 20d). At another location (Fig. 20g), a high-angle fault has been mapped by Bond and others (1978) along and parallel to the crest of the Gibbon anticline at its extreme northeastern end. No tear faults across the uplift were observed directly, but such faults may be present between the areas represented by the cross sections F-F' and G-G' (Fig. 20) due to the difference in degree of fold development between these two areas.

To the immediate north of the Gibbon anticline is a subparallel fold which is an anticline on the west end but changes to a monocline at its east end. Thus the fold is named the Phelps anticline and Phelps monocline respectively. The Phelps anticline is an erosional remnant of a low-relief, asymmetrical anticline (north vergence; Fig. 20d,e,f). Both the monocline and anticline have near-vertical northern limbs and a hinge zone which is reflected in a subtle topographic bench along their length (Fig. 19) The western extension of the fold is lost in complex faulting and landslide debris while the eastern end of the fold either dies out or merges with the Chandler anticline.

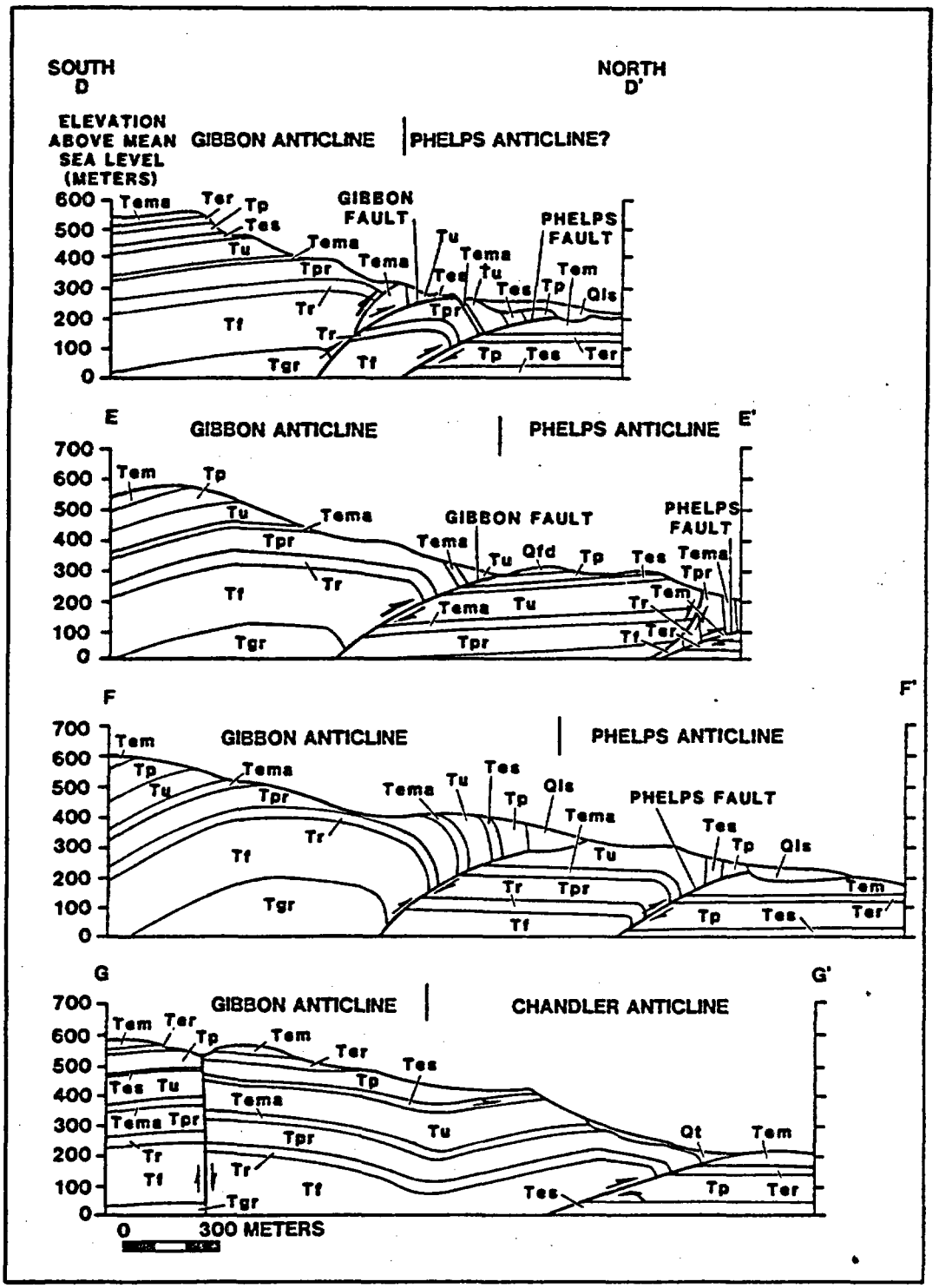

Figure 20. Interpretive geologic cross sections through the Horse Heaven Hills uplift within the Gibbon segment (see Fig. 82, Appendix C, for corresponding descriptive geologic cross sections).

The hinge zone of the Phelps anticline and monocline has locally been obliterated by a fault which offsets the southern limb over the northern limb. A thrust or reverse fault, the Phelps fault (Fig, 20e,f,g), is thought to offset the steep northern limb to the north as well. These two faults have produced a zone of fault breccia, which, along with the presence of thick sedimentary interbeds on the steeply dipping northern limb, facilitates landsliding. A fault was mapped along the Gibbon railroad siding by Bond and others (1978) which they interpreted as offsetting a sequence consisting of the Pomona Member and Selah interbed overlying the Elephant Mountain Member. Reexamination of this area leads this writer to interpret the Pomona Member and Selah interbed as composing a local landslide block which originated from along the northern limb of the Phelps monocline.

Chandler Segment. The Horse Heaven Hills uplift within the Chandler segment consists of one fold, the Chandler anticline (Fig. 14, 21).

The Chandler anticline is an eroded, asymmetric (north vergence), subtly double-hinged fold, which trends N70°E for most of its length, but changes to approximately N85°W at its eastern end. To the east, the anticline plunges onto the southern limb of the Kiona anticline (Fig. 14) and to the west the anticline dies out, possibly onto the back of the Phelps monocline.

The Bauder fault (Fig. 22h) is a reverse fault which is inferred to offset the northern limb of the anticline to the north based on the proximity and attitudes of strata observed between the Chandler well and the northern limb of the anticline. Layer-parallel faults are

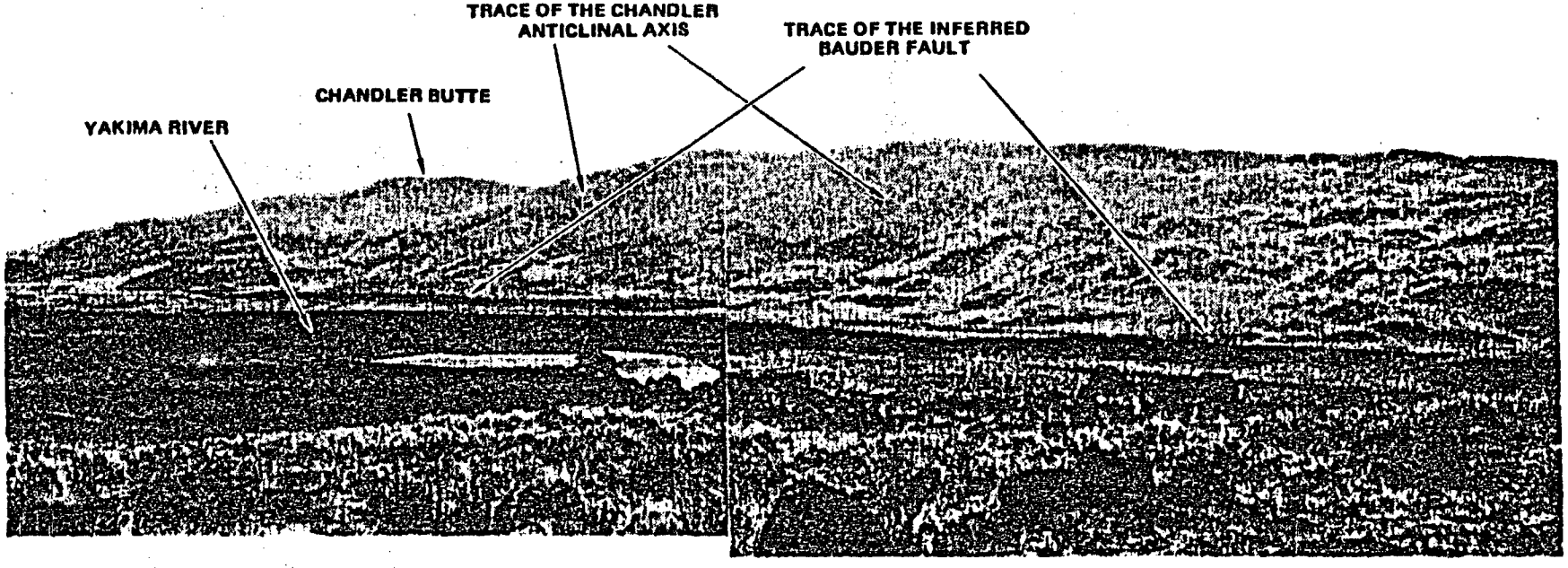

Figure 21. The Horse Heaven Hills uplift within the eastern portion of the Chandler segment.

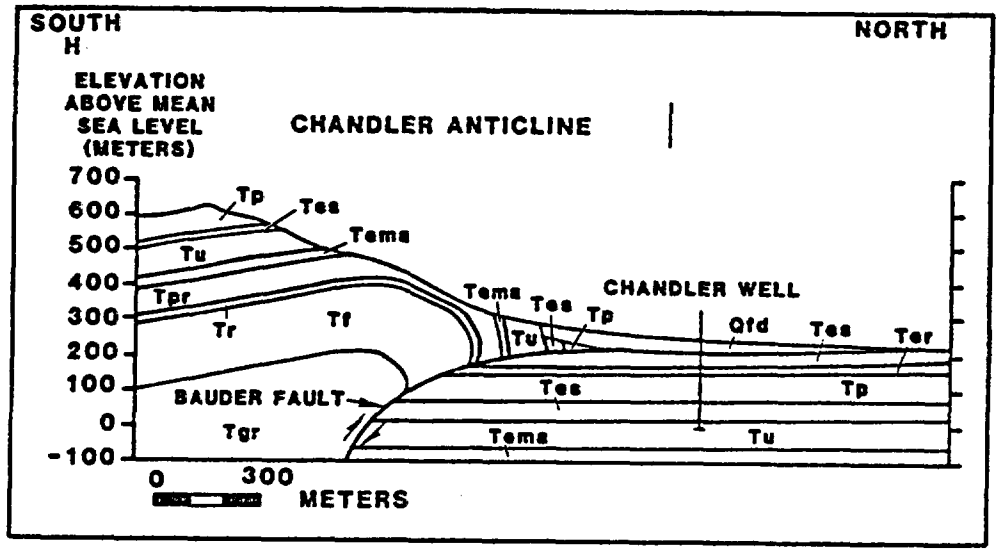

Figure 22. Interpretive geologic cross section through the Horse Heaven Hills uplift within the Chandler segment (see Fig. 83, Appendix C, for corresponding descriptive geologic cross sections).

found along the near-vertical northern limb of the anticline in a hyaloclastite at the base of the Roza Member (NW1/4 SE1/4 sec. 20, T.9N., R.26E.) and within a flow top of the upper Frenchman Springs flow (NW1/4 SE1/4 sec. 20, T.9N. R.26E.). Another layer-parallel fault is observed within the Umatilla Member along the southern limb and is characterized by a 5-m-thick zone of tectonic breccia surrounding more coherent basalt blocks in an anastomosing pattern (Fig. 20g; SE1/4 NE1/4 sec. 25, T.9N., R.25E.).

Webber Segment. The Webber segment contains two parallel folds; one fold which composes the topographic ridge crest of the Horse Heaven Hills, and the other, a lower-relief anticline which is found to the immediate northeast (Fig. 14, 23). Both folds change geometry from monoclines at the southeast end of the segment to anticlines at the northwest end of the segment (Fig. 14).

The fold which composes the topographic ridge crest of the Horse Heaven Hills uplift at the southeastern end of the segment is the Badger Canyon monocline of Myers and others (1979) and the Kiona anticline at the northwestern end of the segment. The Badger Canyon monocline and Kiona anticline have northeast vergence. The Kiona anticline is interpreted to be a double-hinged, asymmetric anticline with a southwestern hinge exposed near the ridge crest but the northeastern hinge obscured by surficial deposits (Fig. 23).

A high-angle reverse fault which parallels the ridge crest (Fig. 14), the Dube' fault, cuts the southeastern hinge of the Kiona anticline (Fig. 24l) juxtaposing the Priest Rapids Member of the southwestern hinge against the Elephant Mountain Member of the

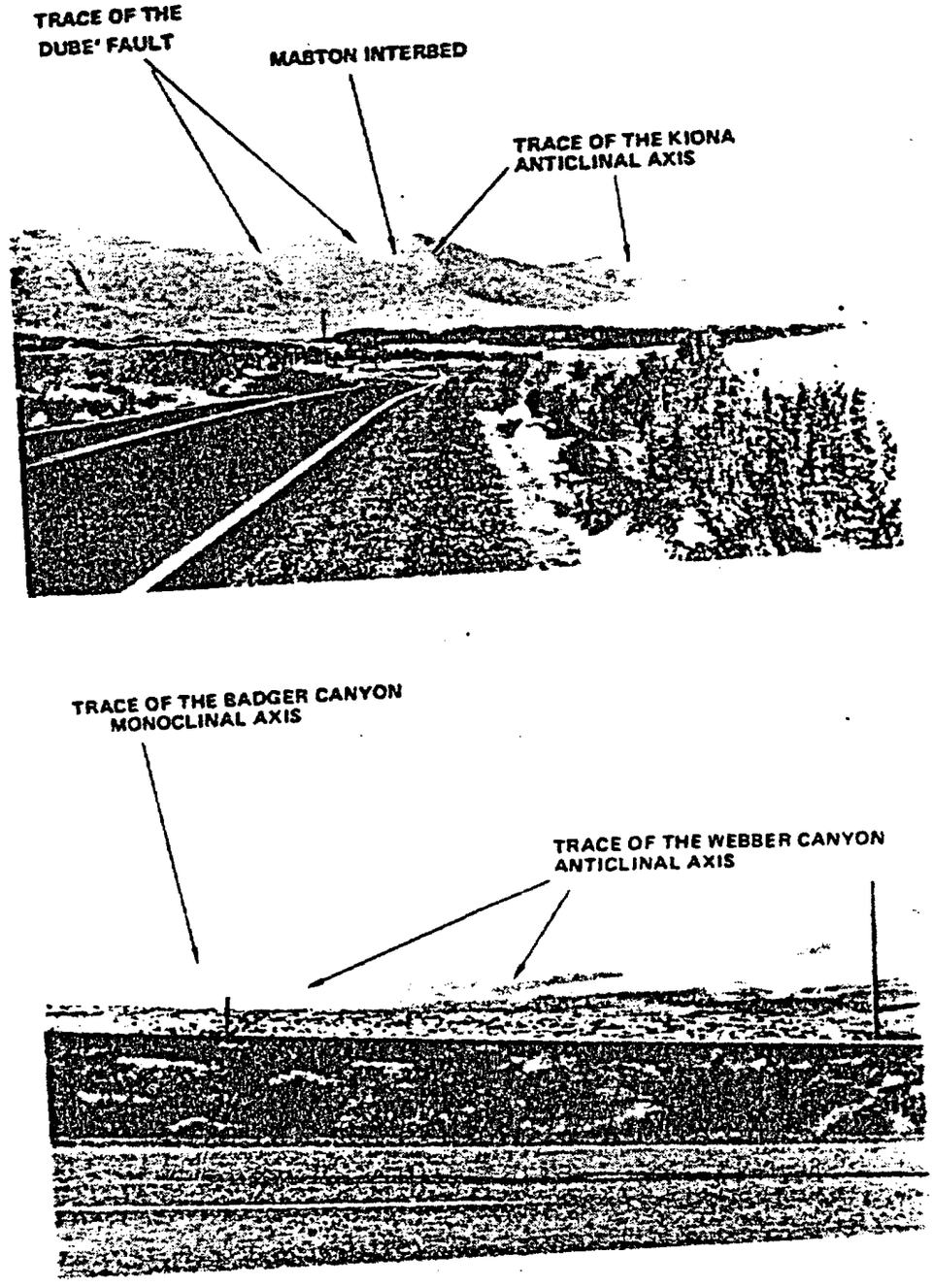

Figure 23. The Horse Heaven Hills uplift within the northwestern portion (top) and southeastern portion (bottom) of the Webber segment.

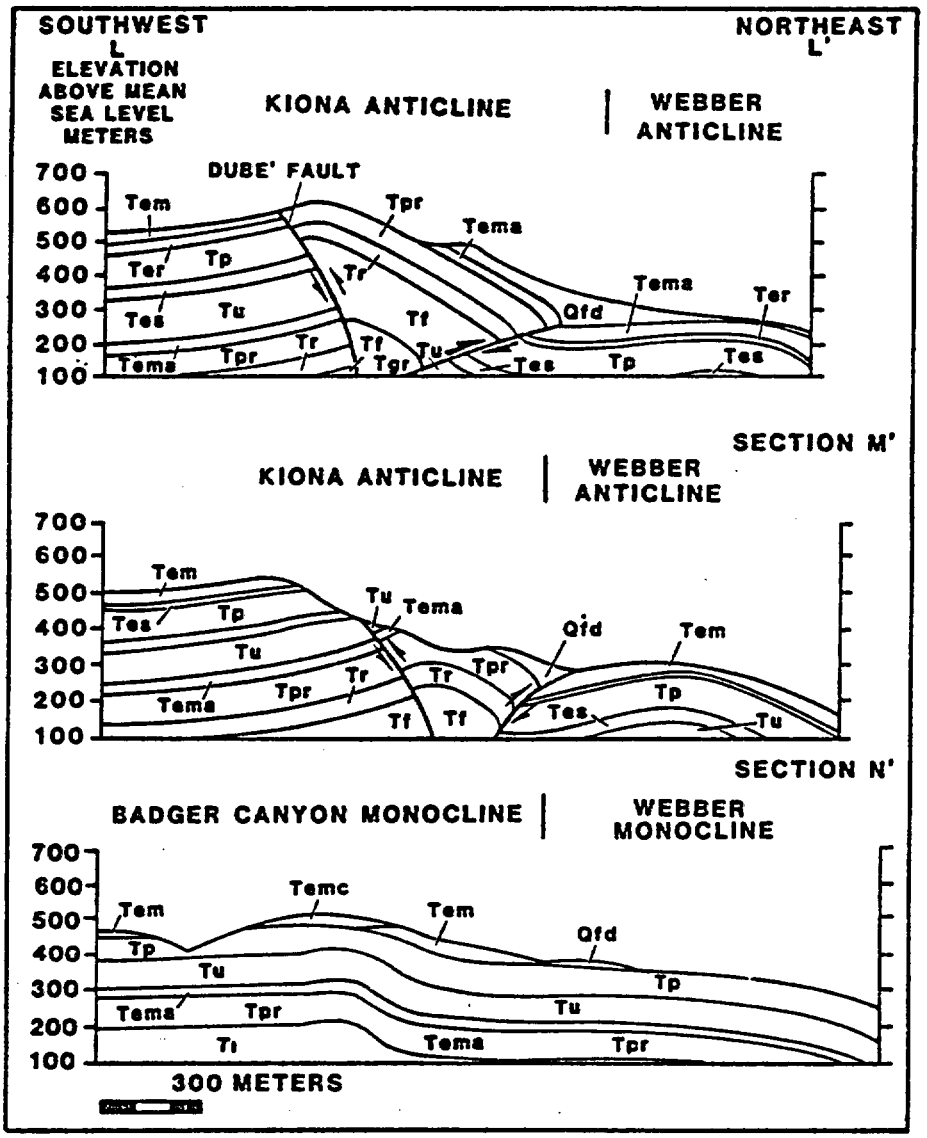

Figure 24. Interpretive geologic cross sections through the Horse Heaven Hills uplift within the Webber segment (see Fig. 83, Appendix C, for corresponding descriptive geologic cross sections).

southwestern limb. Offset decreases along the trace of the fault to the northwest as indicated by the progressive juxtaposition of younger stratigraphic units (Priest Rapids Member, Umatilla Member, Pomona Member) on the northeast side of the fault against the Elephant Mountain Member of the southwestern side of the fault. Although no fault was observed at the base of the northern limb of the Badger Canyon Monocline, one may be present along the base of the Kiona anticline.

The subtle, low-relief fold which parallels the Badger Monocline/Kiona anticline is referred to here as the Webber monocline at its southeastern end and the Webber anticline at its northwestern end (Fig. 14). Both folds have northeast vergence. The Webber monocline extends southeast past Webber Canyon and out of the study area (Hagood, in prep.). The northwest extension of the Webber anticline is lost approximately 4 km northwest of Webber Canyon but is thought to continue buried beneath surficial deposits as indicated by a subtle topographic bench in the topography.

A tear fault is interpreted to cut the Webber anticline (SE1/4 SW1/4 sec. 29, T.9N., R.27E.) based on a marked change in the attitude of layering in two adjacent gullies which cut across the anticline. The more-northern gully exposes a vertically dipping sequence composed of the Pomona Member, Selah interbed, and Umatilla Member (southwest to northeast) which is penetrated by numerous faults generally oriented subparallel to the layering. The more southern gully exposes gently dipping layering as shown in Figure 24n.

Overall there is a progressive southeast to northwest increase in deformation (increase in strain) within the Webber segment. Both folds tighten considerably from southeast to northwest; buckling occurs in the transition from monoclines to anticlines; and the elevation of the crest of the fold increases from the Badger Canyon Monocline to the Kiona anticline.

Kiona Segment. The portion of the northwest-trending Horse Heaven Hills uplift that lies within the Kiona segment consists of a single fold, the Kiona anticline (Fig. 14, 25).

The cross-sectional geometry of the Kiona anticline displays a distinct change between the northwest and southeast ends of the fold. The Kiona anticline within the northwest portion of the segment is an eroded, faulted, broad, double-hinged fold; while the fold in the southeastern portion of the segment is an eroded, tightly folded, asymmetric anticline. Both folds have northeast vergence. The anticlinal axis trends N60°W, but at the northwest end of the segment the northern limb appears to plunge northwest near Interstate I-82 while the crestal portion of the anticline appears to be continuous with the Kiona anticline in the Junction segment.

The two geometrically distinct portions of the Kiona anticline are separated by the northeast-trending Sharpe fault which cuts across the northeastern limb of the anticline (Fig. 14). In the northwest portion of the Kiona segment the northern hinge of the Kiona anticline contains several high-angle reverse and thrust faults (Fig. 26j). Fault breccia was also encountered within the core of the anticline in the southeast portion of the segment (in the Frenchman Springs Member,

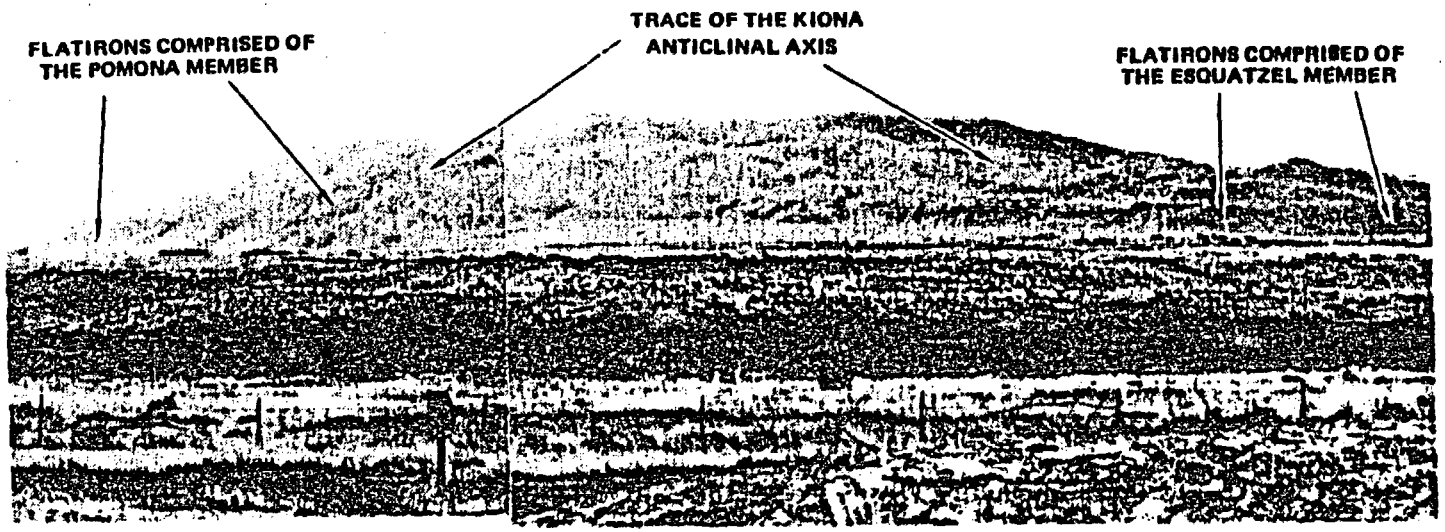

Figure 25. The Horse Heaven Hills uplift within the Kiona segment.

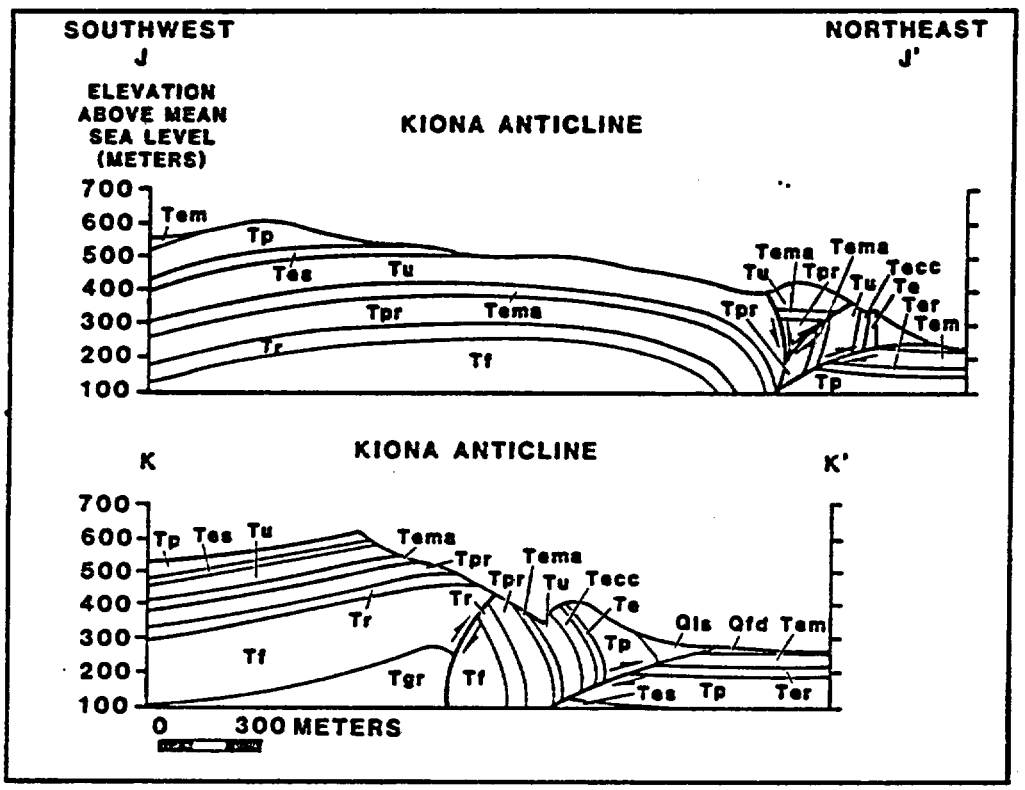

Figure 26. Interpretive geologic cross sections through the Horse Heaven Hills uplift within the Kiona segment (see Fig. 84, Appendix C, for corresponding descriptive geologic cross sections).

SW1/4 NE1/4 sec. 23, T.9N., R.26E.), but it is unknown whether the breccia represents local thrust faulting within the core of the fold or whether it is caused by layer-parallel faulting. However, a thrust fault in the same area is tentatively proposed here based on the tightness of the fold (Fig. 26k). A reverse fault is inferred at the northern base of the fold as well.

Junction Segment. The Junction segment consists of the mergence of the northwestern end of the Kiona anticline and the northeastern end of the Chandler anticline (Fig. 14). The Chandler anticline plunges onto the southern limb of the Kiona anticline within this segment. The strike of the Kiona anticline in the Kiona segment markedly changes from a northwest strike to a nearly east-west strike. A representation of the cross-sectional geometry of the Horse Heaven Hills uplift is shown in Figure 27. The figure shows the broad asymmetric (north vergence) geometry of the Kiona anticline.

Several tear faults cut across the northern flank of the Kiona anticline coincident with a marked change in geometry or trend of the anticline. One left-lateral tear fault, the Chandler fault (Fig. 14), was inferred by Bond and others (1978) as crossing the crest of the ridge here (the Chandler anticline). Mapping for this study, however, indicates that this fault is probably limited to the northern flank.

One explanation for the change in trend of the Kiona anticline is that the east-west striking portion of the Kiona anticline may represent the broad northwest plunging end of the Kiona anticline. Another explanation may be that the oddly oriented fold resulted from

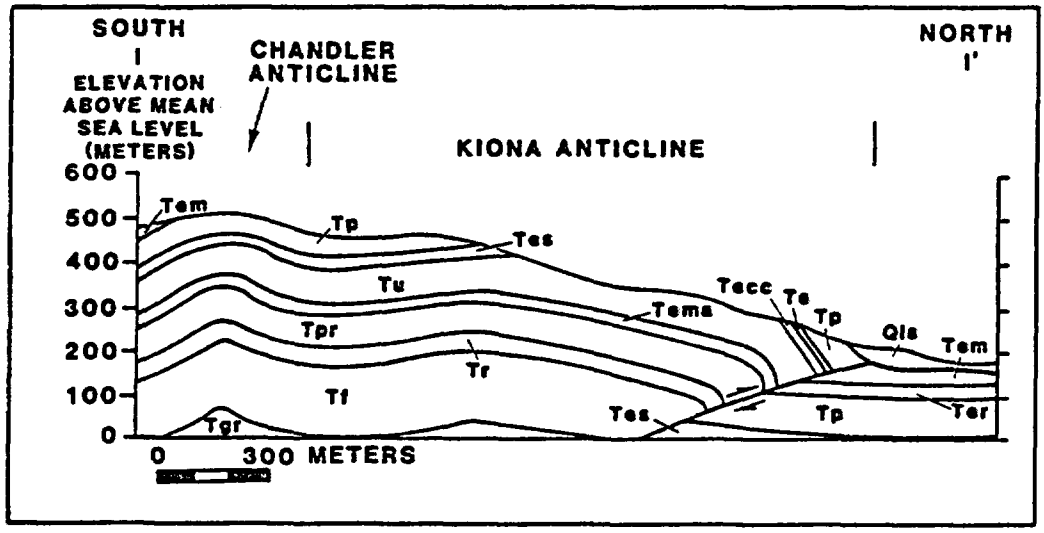

Figure 27. Interpretive geologic cross section through the Horse Heaven Hills uplift within the Junction segment (see Fig. 85, Appendix C, for corresponding descriptive geologic cross section).

the interaction of stresses caused by uplift along the northwest and northeast trend.

It remains unclear as to how the Badlands anticline (Fig. 14) relates structurally with the Kiona anticline. It is aligned with and is proximal to the northwest-trending portion of the Kiona anticline, but its possible connection with the Kiona anticline is obscured by landslide debris.

TIMING AND LOCATION OF DEFORMATION

Several proposals have been made by previous workers as to when, and in what sequence, the Yakima folds developed. This also directly or indirectly implies when folding occurred along the Horse Heaven Hills uplift (Table XII). These proposals imply when the Horse Heaven Hills uplift developed in relation to other Yakima folds. Several workers have proposed that most of the uplift along the Yakima folds developed after 10.5 m.y.B.P. - during late Miocene time and Pliocene time (Barrash and others 1983; Bentley 1977; Brown 1970; Kienle and others 1978; Swanson and others 1979a). Other studies (Reidel 1984) have proposed that deformation along the Yakima folds has been continuous since at least middle Miocene time. It has also been suggested that the Yakima folds originated time sequentially, from south to north, across the Columbia Plateau (Laubscher 1981). Other workers have proposed that growth is currently occurring along the Yakima Folds (Campbell and Bentley 1981; Reidel 1984).

It is the purpose of this chapter to ascertain the timing of uplift along portions of both the northwest and northeast trends of the Horse Heaven Hills uplift. This was accomplished principally by using isopach maps of individual CRB members and Ellensburg interbeds, along with paleodrainage maps of the ancestral Columbia River system to define developing folds at specific times or time intervals. Because of the absence of a sedimentary record for a portion of the

late Miocene and the Pliocene, the timing and location of growth along the Horse Heaven Hills uplift can only be inferred from observations of the present structure. The results will help reconstruct the evolution of the Horse Heaven Hills uplift as well as provide a detailed example of the timing of uplift along a set of intersecting northwest-and northeast-trending Yakima folds. In addition, the timing of development of the Horse Heaven Hills uplift can then be compared to the timing and development of other Yakima folds. The timing and location of deformation found within portions of the lower Yakima Valley syncline and the Horse Heaven Plateau are also evaluated as a consequence of their intrinsic structural relationship with the Horse Heaven Hills uplift.

Isopach Study

Distribution patterns and thickness trends of CRBG flows and sedimentary deposits of the Ellensburg Formation have been recently outlined for the Pasco Basin and some of the bordering Yakima Folds (Long and Landon 1982; Myers and others 1979; Price 1981; Reidel 1984; Reidel and Fecht 1981, 1982; Reidel and others 1980, 1983a,b). Variations in thicknesses of these stratigraphic units are thought to be controlled by the interplay of four factors (Reidel and others 1980; Reidel and Fecht 1981). These factors are (1) the volume of each basalt flow; (2) constructional topography created by previous basalt flow margins; (3) the effect of uplift and subsidence; and (4) the influence of regional paleoslopes. Reidel and Fecht (1981)

argue that the lateral extent and thicknesses of the basalt flows in the Pasco Basin are controlled primarily by uplift and subsidence and secondarily by flow volume, constructional topography, and/or regional paleoslopes.

Flows of the CRBG generally entered the study area from the east (Schmincke 1964, 1967d) repeatedly inundating the paleotopography. Since these basalt flows were fluid and traversed the Columbia Plateau within a few weeks (Shaw and Swanson 1970), they formed a cast of the paleotopography at instances of time. Thickness variations of the interbeds of the Ellensburg Formation in the study area also record the presence of paleotopography but over longer intervals of time. Isopach maps of individual members of the Wanapum and Saddle Mountains Basalts and individual interbeds of the Ellensburg Formation were constructed for this study (Fig. 28-38) to delineate paleostructures present in the study area. The isopach maps constructed for Wanapum Basalt members are less defined due to the presence of fewer measurable exposures along the Horse Heaven Hills uplift and the difficulty in identifying individual members from borehole data (Appendix B).

From the isopach maps several structures appeared recurrently in the paleotopography: (1) the northwest and northeast trend of the Horse Heaven Hills uplift; (2) the lower Yakima Valley syncline; (3) the Piening syncline; and (4) the southern extension of the Hog Ranch-Naneum Ridge anticline.

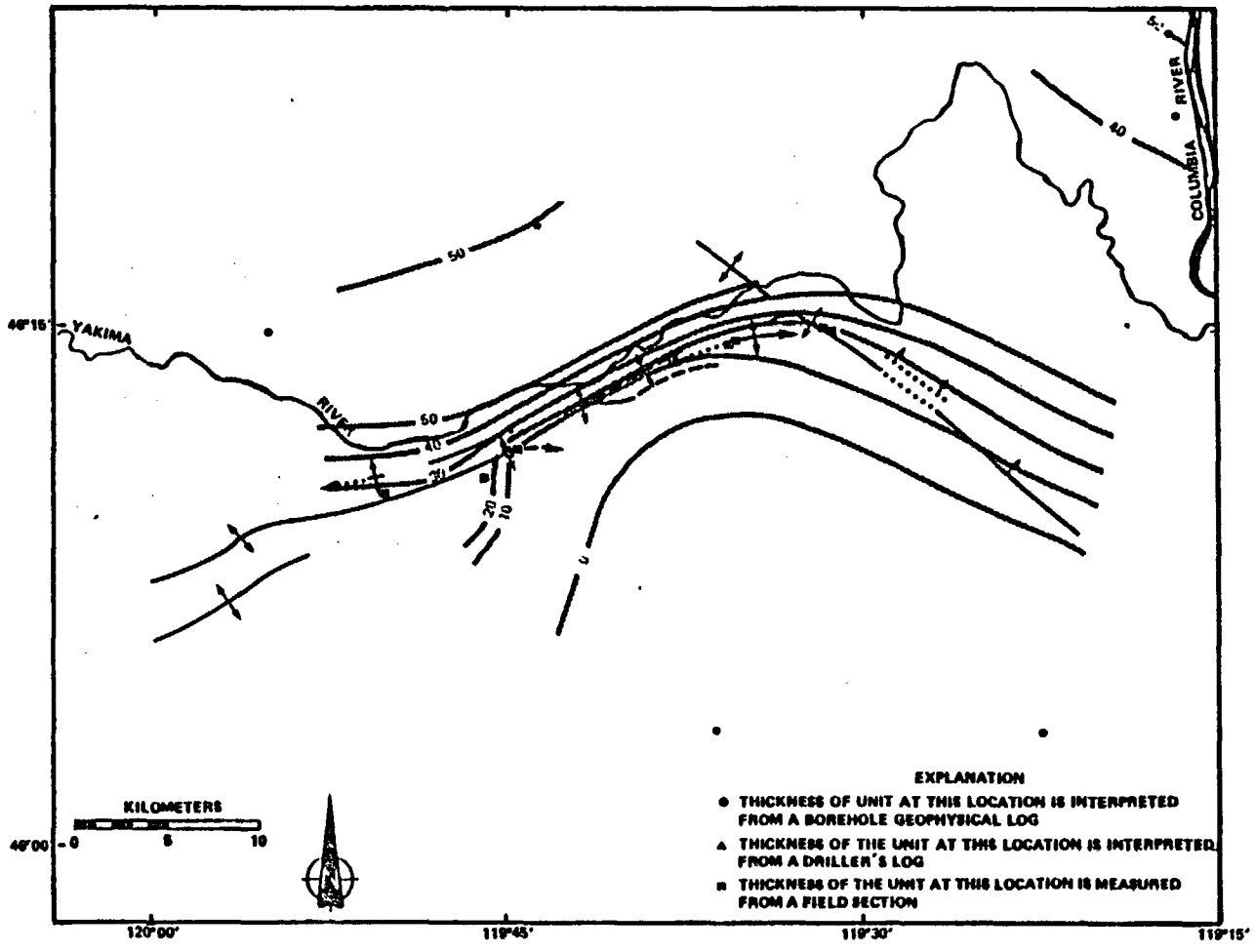

Figure 28. Isopach map of the Roza Member within the study area. Contour interval is 10 m.

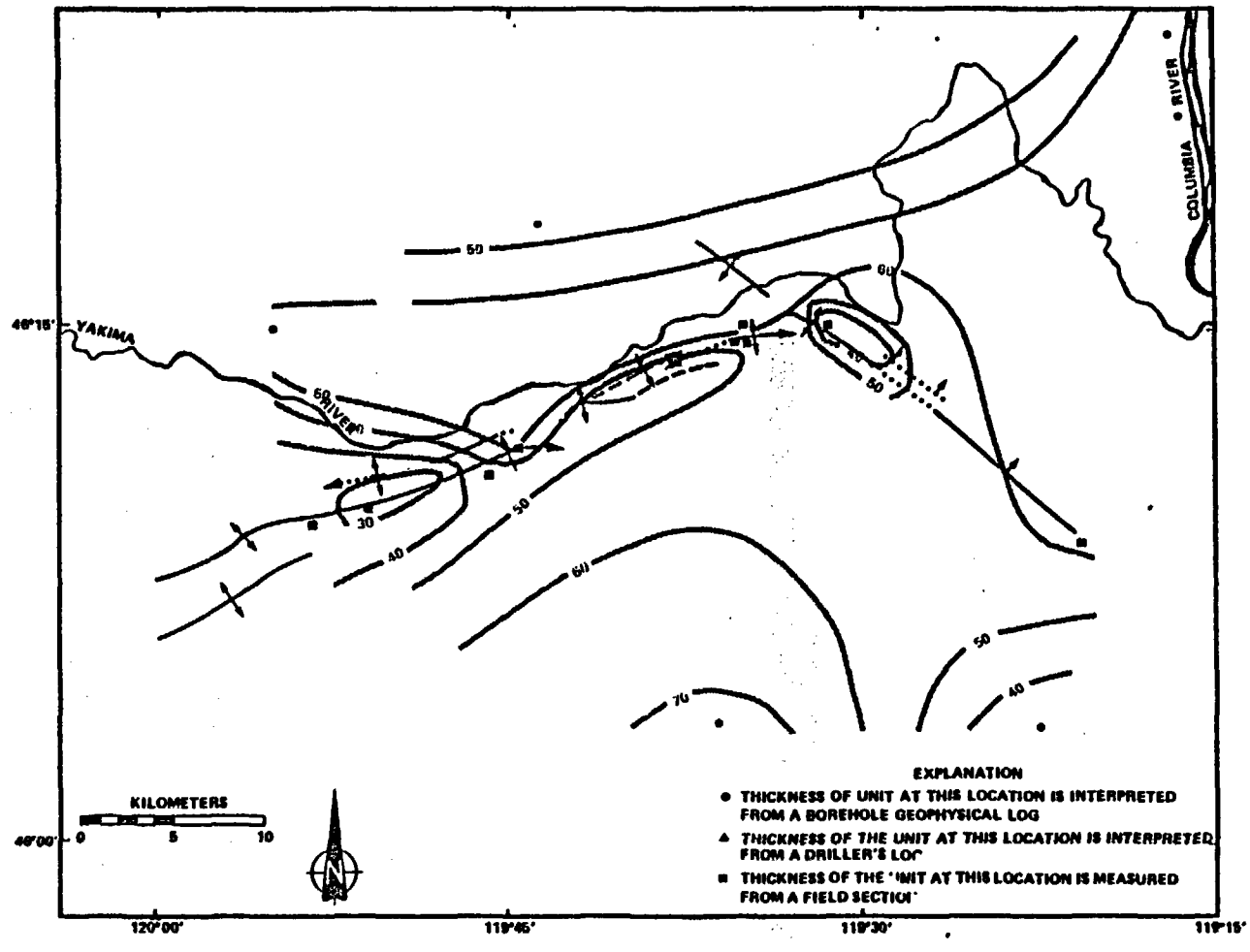

Figure 29. Isopach map of the Priest Rapids Member within the study area. Contour interval is 10 m.

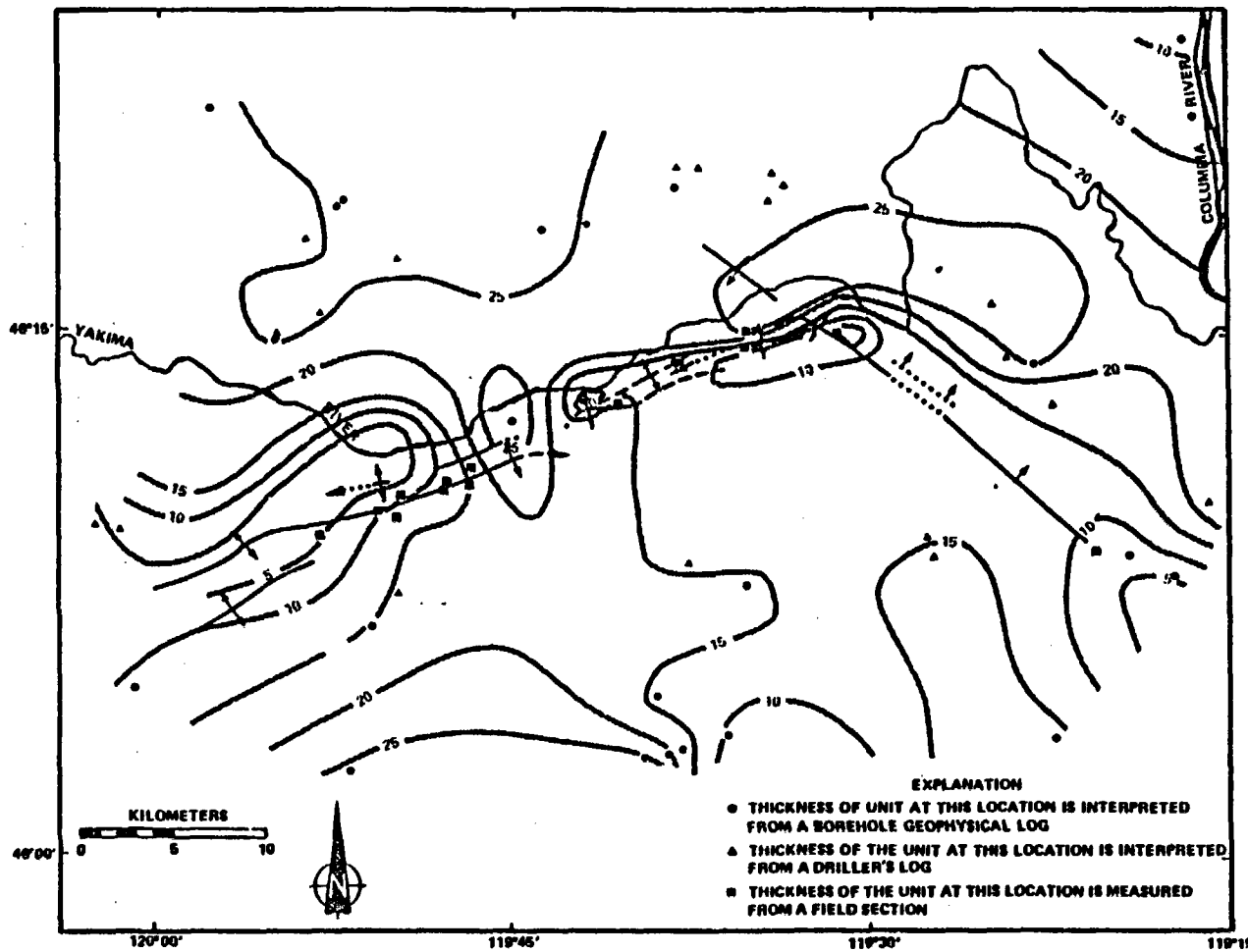

Figure 30. Isopach map of the Mabton interbed within the study area. Contour interval is 5 m.

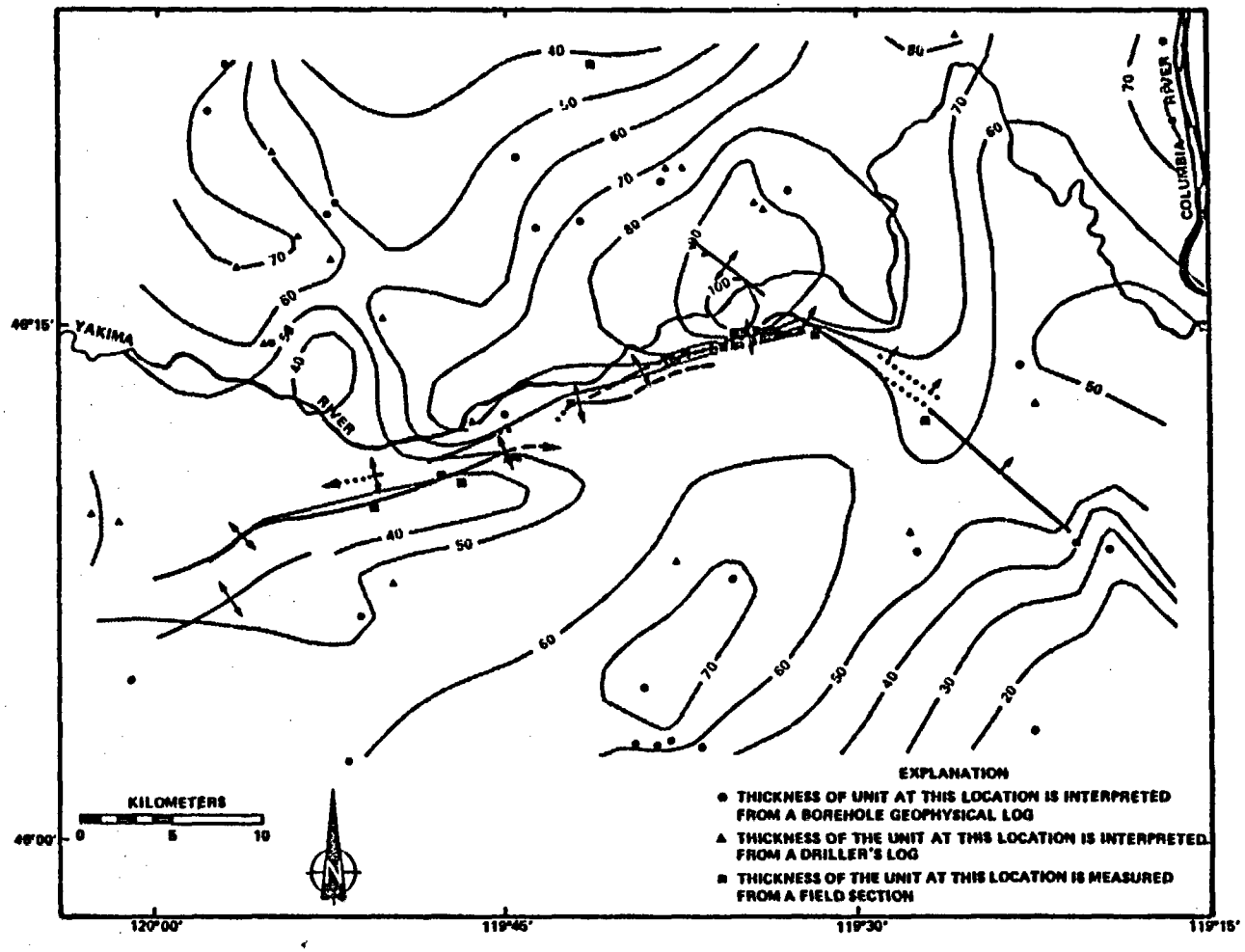

Figure 31. Isopach map of the Umatilla Member within the study area. Contour interval is 10 m.

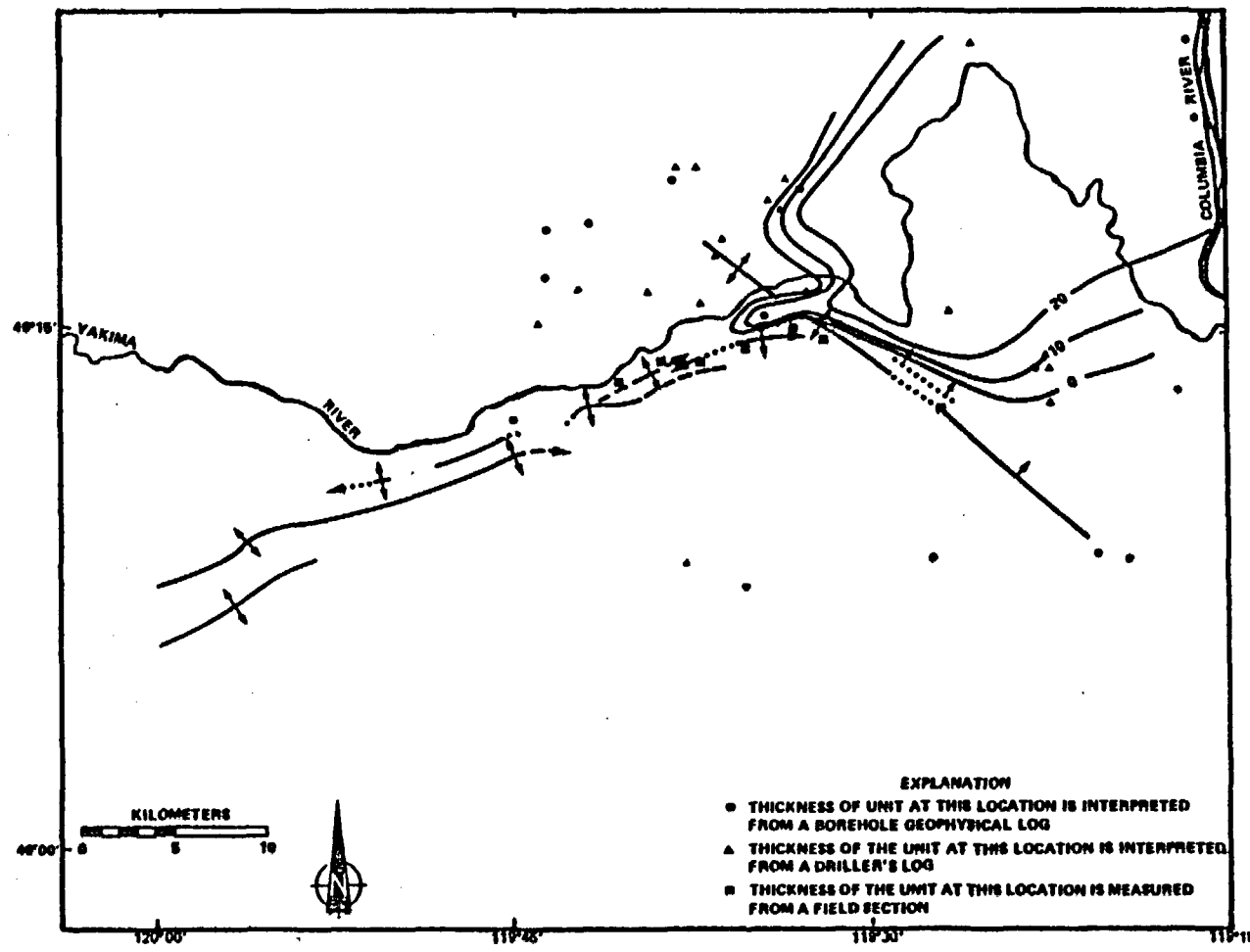

Figure 32. Isopach map of the Esquatzel Member within the study area. Contour interval is 10 m.

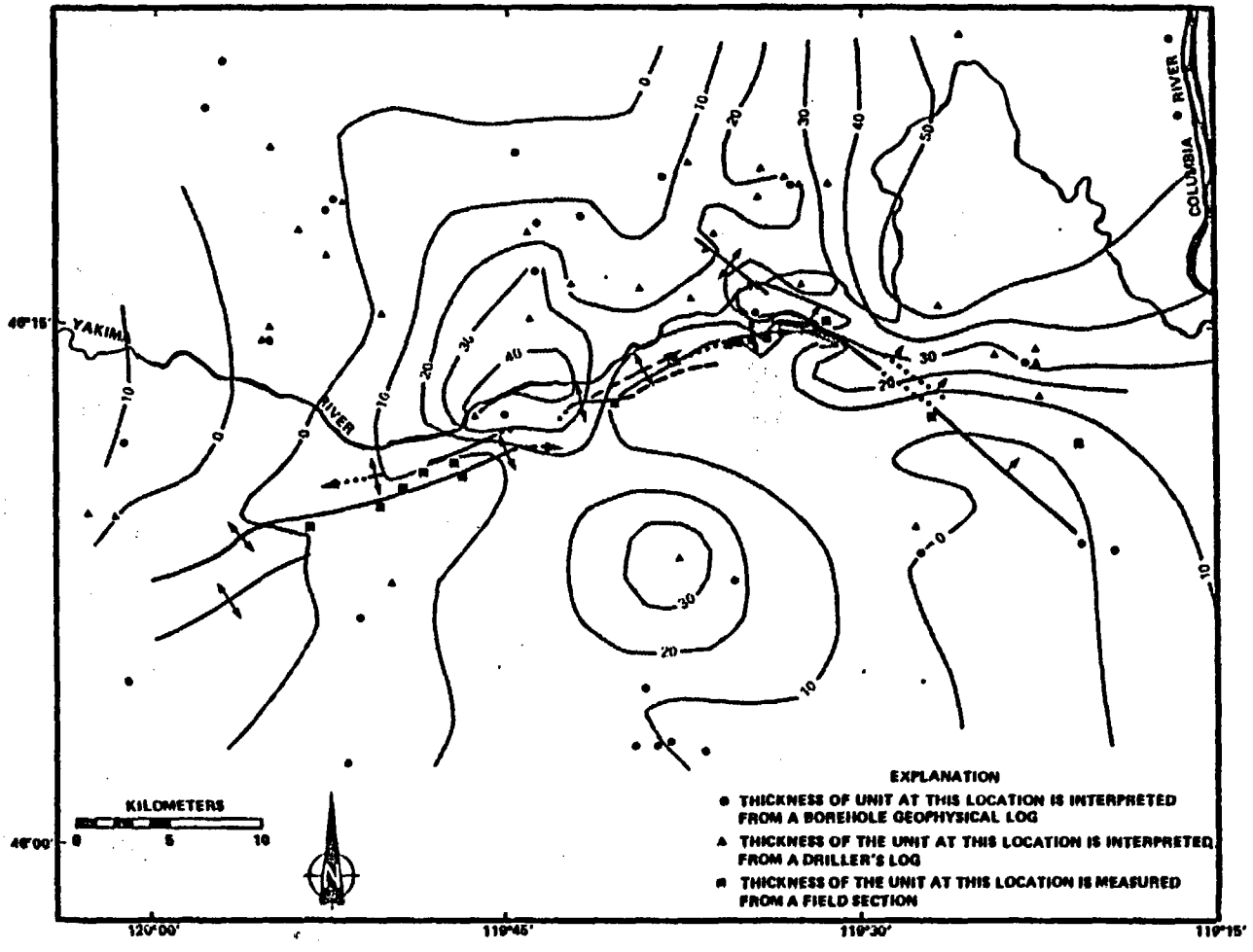

Figure 33. Isopach map of the Cold Creek interbed, Esquatzel Member, and Selah interbed within the study area. Contour interval is 10 m.

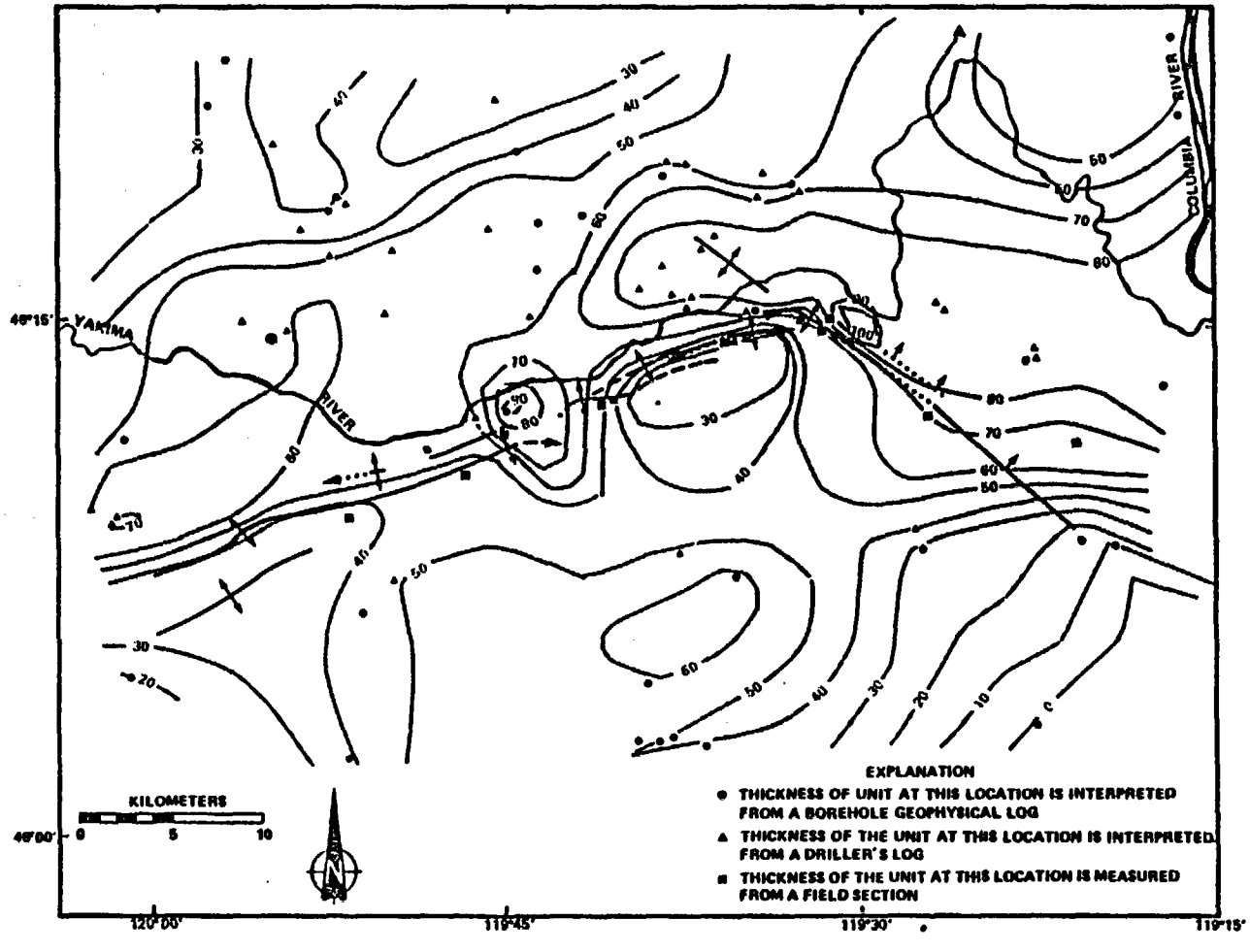

Figure 34. Isopach map of the Pomona Member within the study area. Contour interval is 10 m.

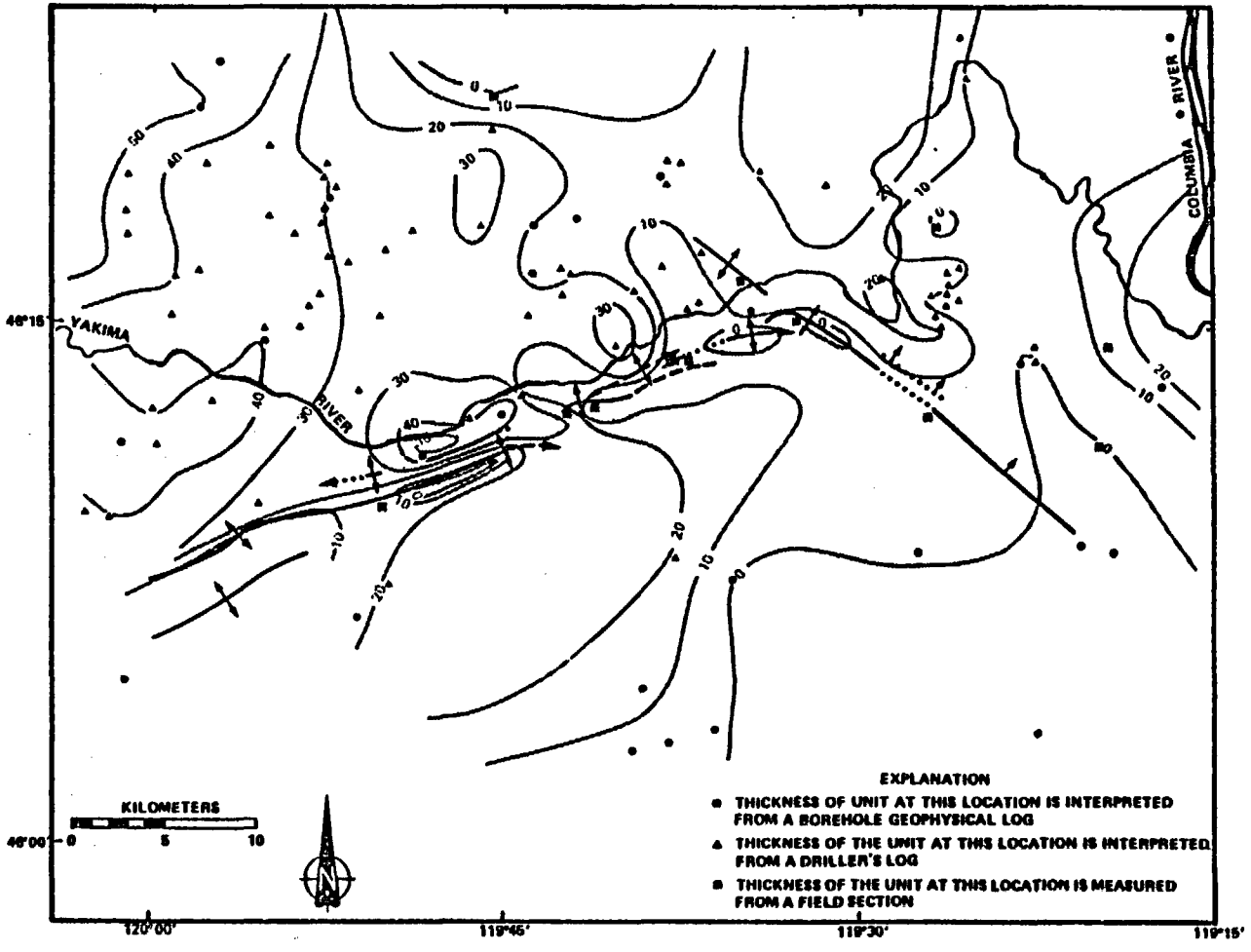

Figure 35. Isopach map of the Rattlesnake Ridge interbed within the study area. Contour interval is 10 m.

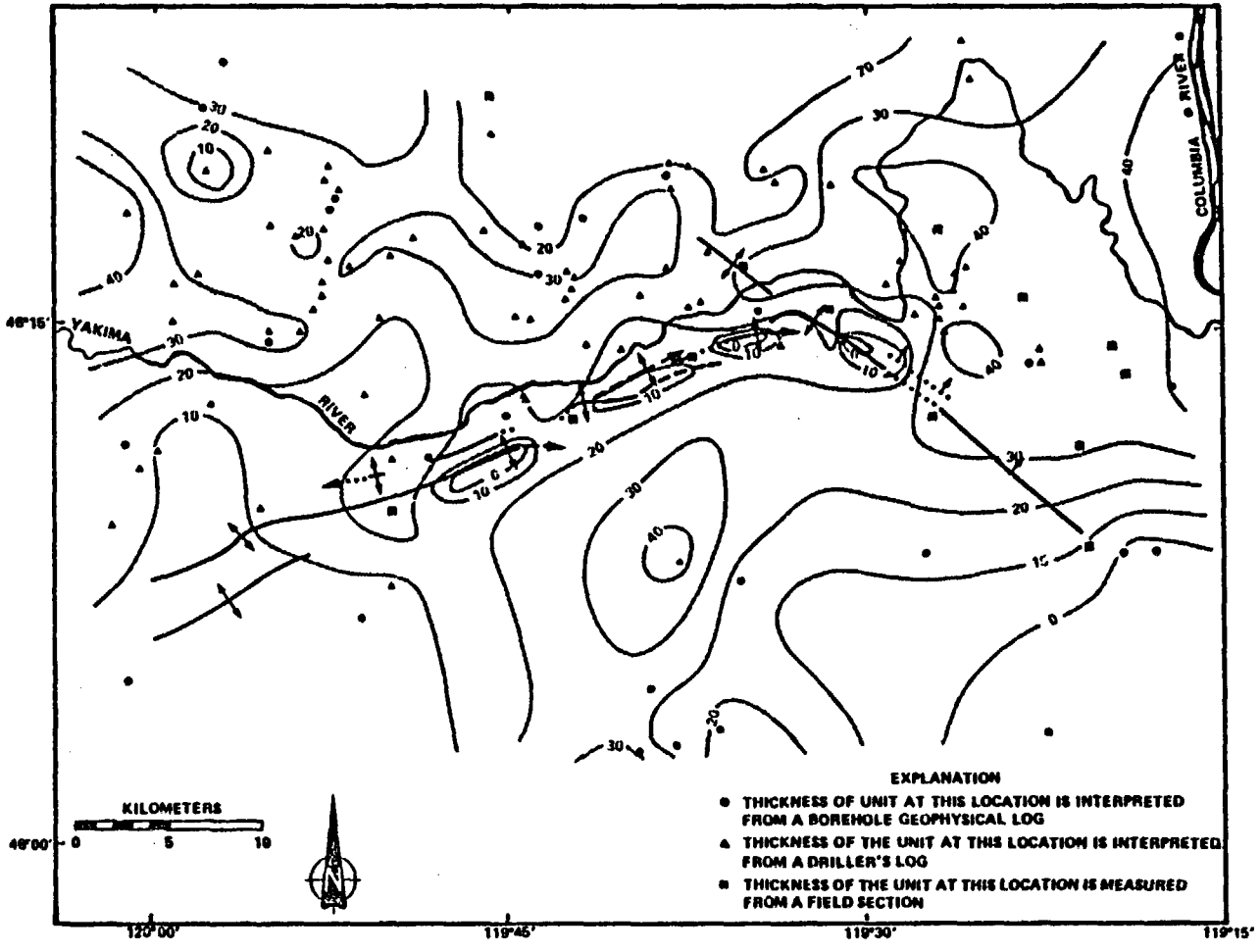

Figure 36. Isopach map of the Elephant Mountain Member within the study area. Contour interval is 10 m.

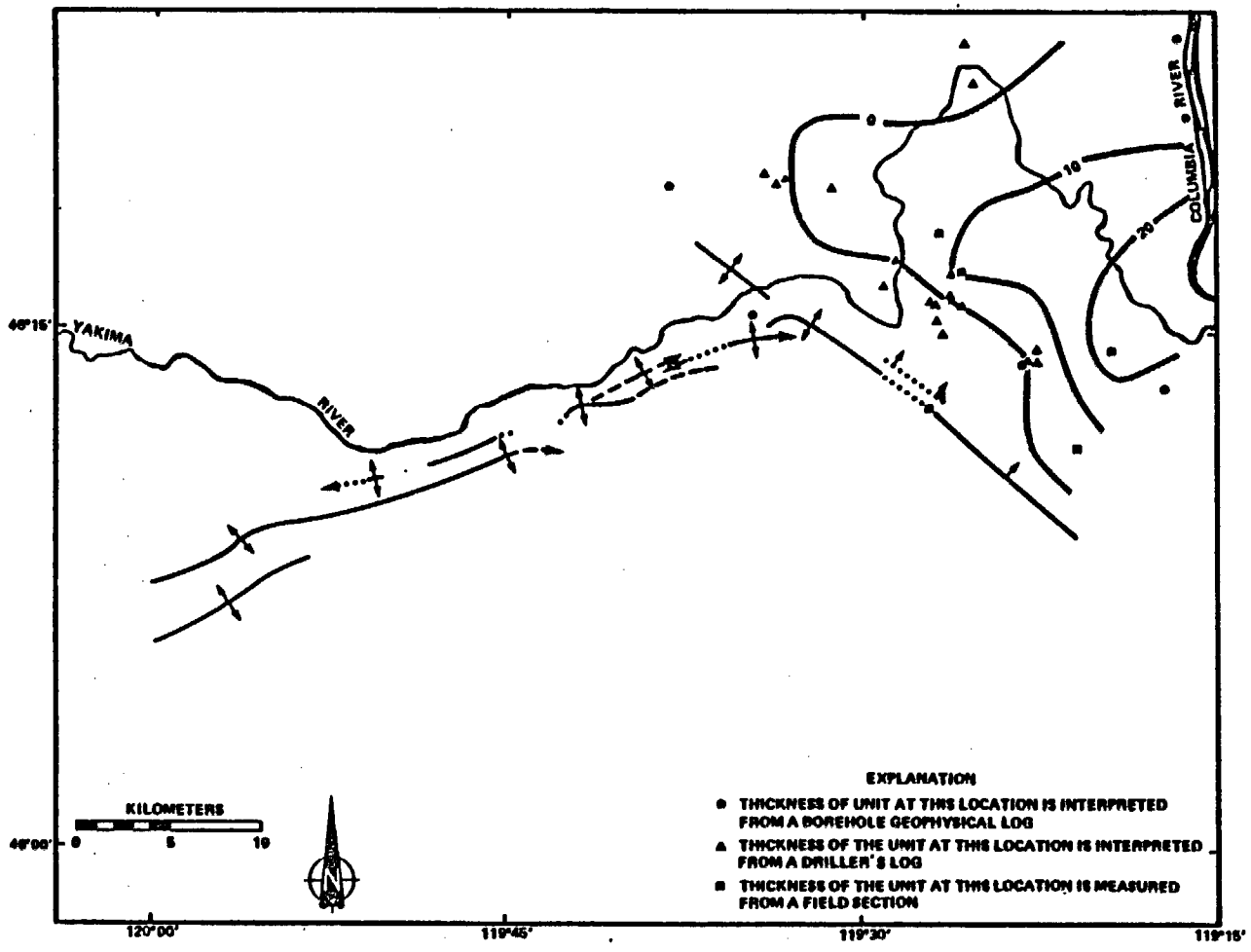

Figure 37. Isopach map of the Levey interbed within the study area. Contour interval is 10 m.

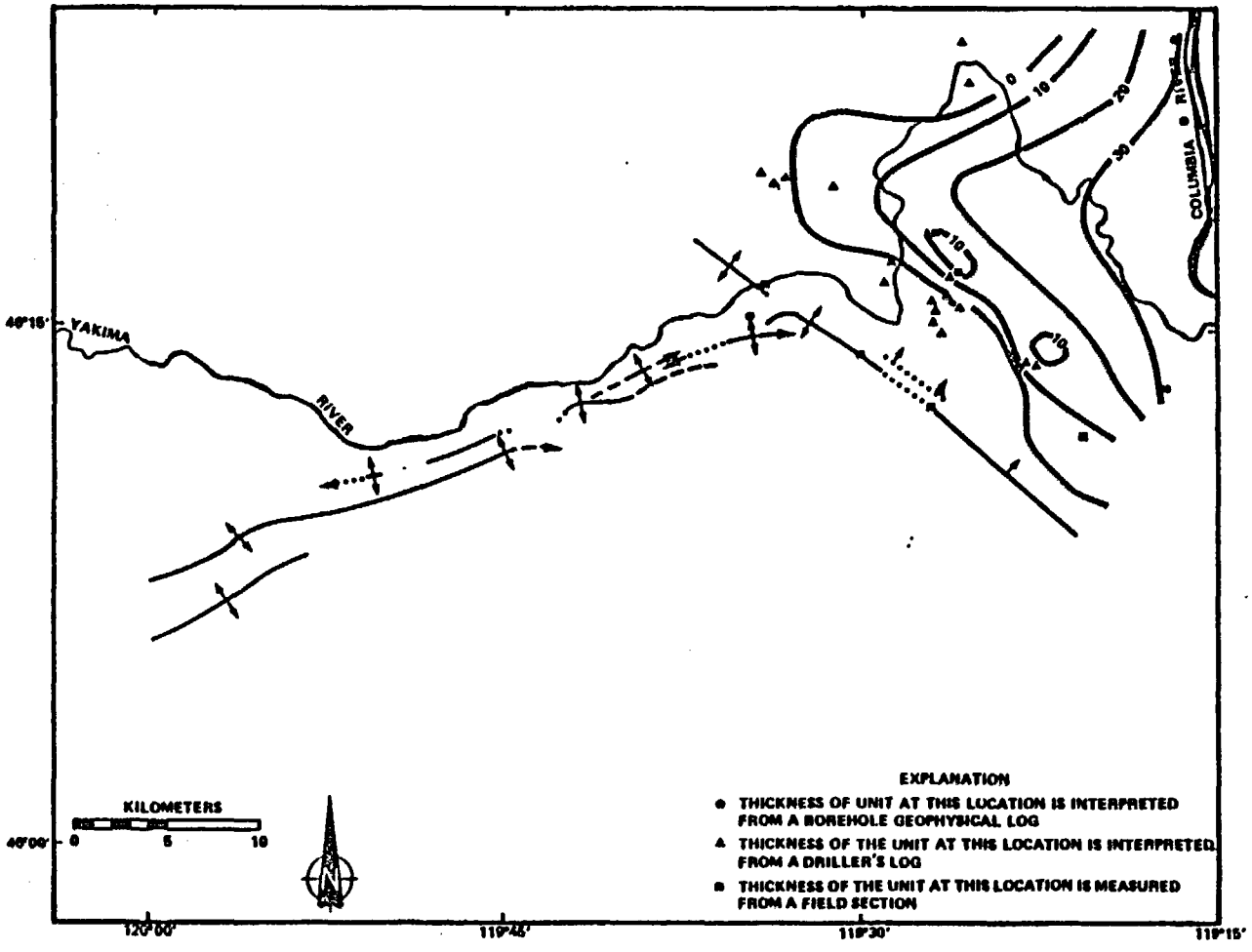

Figure 38. Isopach map of the Ice Harbor Member within the study area. Contour interval is 10 m.

Uplift along folds of both trends of the Horse Heaven Hills uplift (the Prosser, Gibbon, Chandler, and Kiona anticlines and the Badger Canyon monocline) were growing simultaneously since at least Roza time (Fig. 28-38). However, the portions of the Badger Canyon monocline and the Kiona anticline which lie within the Webber segment were not present through at least Pomona time. Topographic relief along the Horse Heaven Hills uplift was extremely low during the emplacement of the Wanapum Basalt and deposition of the Mabton interbed (Fig. 28-30) but was better expressed during Saddle Mountains time (Fig. 30-38) due to the longer time intervals separating basalt flow incursions. A local structural low separated the Chandler and Kiona anticlines during at least Pomona time (Fig. 34). Another structural low is also indicated to have existed along the western portion of the Chandler anticline since at least Umatilla time. Its location is now marked by the overlap of the the Gibbon and Chandler anticlines. Yet another structural low is interpreted to have existed between the Prosser and Gibbon anticlines since at least Priest Rapids time. Growth along the Drake anticline, the Phelps anticline/monocline, and the Webber anticline/monocline cannot be evaluated from the isopach maps since no strategic section thicknesses could be measured along these low-relief folds.

The present structural relief observed along the Horse Heaven Hills uplift developed after Elephant Mountain time. But because of a gap in the late Miocene and Pliocene geologic record in the study area, it is not known whether the uplift developed in a relatively uniform process as suggested for CRB time (in this study) or whether

growth occurred more intermittently. Presently, however, relief along both trends are very similar.

Recurrent thickening trends in the isopachs point to the presence of the lower Yakima Valley syncline since at least Roza time. However, the syncline is not well defined until Saddle Mountains time (Fig. 31-38). The syncline generally is aligned parallel with the northeast trend of the Horse Heaven Hills uplift, with the trace of its axis located near the present-day Yakima River. The eastern end of the syncline is interpreted to have been connected with the Pasco Basin, probably south of the emerging Rattlesnake Mountain (Reidel and Fecht 1981), however the data are too sparse to indicate whether during this time other folds along the RAW were present to separate the Pasco Basin and the lower Yakima Valley syncline.

From the isopach maps of the Umatilla, Esquatzel, and Pomona Members, and the combined sections of the Cold Creek interbed, Esquatzel Member, and Selah interbed (Fig. 31-34), it is apparent that the western extension of the lower Yakima Valley syncline was interrupted by a local eastward-dipping slope located a few miles west of Prosser in the Grandview-Sunnyside area. This slope probably represents the presence of the southern extension of the north-northwest-trending Hog Ranch-Naneum Ridge anticline. However, there is some question as to whether the limited westward extent of the Esquatzel Member (Fig. 32) was caused by the presence of the Hog Ranch-Naneum Ridge anticline or folds developing along the RAW. The low volume of the Esquatzel Member cannot be the sole cause of the flow's limited westward progression, since the member reached as far

west as 120° west longitude in the next valley to the north via an ancestral river canyon (Myers and others 1979). The definition of the Hog Ranch-Naneum anticline can be further refined for Pomona time by combining section measurements from Biggane's (1982) study with those of this study. The east slope of the the Hog Ranch-Naneum Ridge anticline is less clearly defined in isopach maps of both the Rattlesnake Ridge interbed and Elephant Mountain Member (Fig. 35, 36), but the west slope of the anticline is delineated by a marked increase in thickness of the Rattlesnake Ridge interbed and Elephant Mountain Member. The distribution of the Ice Harbor Member suggests the west slope of Hog Ranch-Naneum Ridge anticline was still present during its incursion, preventing the Martindale flow from entering the lower Yakima Valley, but this again could have been influenced by the presence of folds along the RAW. Why the eastern margin of the Hog Ranch-Naneum Ridge anticline loses its definition after Pomona time is unclear but it is possible that the slope developed eastward forming a broad slope through the lower Yakima Valley or simply, the growth along the Hog Ranch-Naneum anticline slowed such that it was a less prominent topographic feature across the lower Yakima Valley, eventually becoming buried.

It is apparent that two components of uplift have occurred since Ice Harbor time within the lower Yakima Valley. The first was the uplift of the lower Yakima Valley syncline relative to the Toppenish and Pasco Basins (or subsidence occurred in the two basins relative to the lower Yakima Valley syncline) as indicated by the elevation of the top of basalt (usually the Elephant Mountain Member) in these three

areas (lower Yakima Valley-this study; Toppenish Basin-Robbins and others 1975, Biggane 1982; Pasco Basin-Myers 1981). The second is that the lower Yakima Valley syncline was tilted westward into its present position. This is indicated on the structure contour map of the Pomona Member (Fig. 13) and by the progressively eastward downcutting through the basalt by the Yakima River. This westward-plunge is in an opposite sense to that present during portions of the middle and late Miocene time. The cause of this tilting can be hypothesized to be a result of continued subsidence of the Toppenish basin and/or uplift along the RAW. The role of the Hog Ranch-Naneum Ridge anticline in the development of the syncline is not understood but could be intricately involved.

A local trough appears recurrently in the isopach maps covering the Horse Heaven Plateau which is coincident with the Piening syncline. The Piening syncline is not well defined in the isopach maps until the emplacement of the Umatilla Member (Fig. 31, 33-36). However, this in part, is probably due to less data available for Wanapum time. The syncline may be elongated in a northeast direction, however the extent of the syncline along its length in either direction is unknown. From patterns observed in certain isopach maps (Fig. 31, 33-35), it is possible that the Piening syncline was continuous with the Badger Coulee area (recall the late development of portions of the Kiona anticline and Badger monocline within the Webber segment). The Piening syncline may have also been continuous with the lower Yakima Valley syncline via a structural low in the Horse Heaven Hills uplift just south of Prosser (Fig. 33, 34). Of special

interest, is the alignment of the Piening syncline with the zone of thickening in the lower Yakima Valley syncline in the Prosser area (Fig. 31, 33-35). This alignment is probably coincidental, however there may also be a relationship between this alignment and the Hog Ranch-Naneum Ridge anticline trending through both of these areas. That is, the Piening syncline, may actually represent a local basin formed against the southern extension of the Hog Ranch-Naneum Ridge anticline.

The north-dipping slope composing the southern limb of the Piening syncline can roughly be delineated from Priest Rapids time through Elephant Mountain time from the isopach maps. The slope may be indicative of uplift to the south which may be related to development of the Paterson Ridge uplift or the southeastern extension of the Horse Heaven Hills uplift.

The thinning of the Priest Rapids Member southward between the Moon #1 well and Horse Heaven Test Well (Fig. 29) provides the first evidence of deformation on the Horse Heaven Plateau. These two boreholes are the only boreholes on the Horse Heaven Plateau in which section thicknesses were interpreted for members of the Wanapum Basalt. The thickness of the Frenchman Springs Member does not change between these two boreholes, while the Roza Member is not present in either of the boreholes. In addition, the Rosalia flow of the Priest Rapids Member is not present in the Horse Heaven Test well, but is present in the Moon #1 well and is less than a few meters thick. It is interpreted that both the Rosalia flow and the Roza Member were

prevented from entering the Horse Heaven Plateau by the presence of the northwest trend of the Horse Heaven Hills uplift southeast of Webber Canyon, but the constructional topography which they created in the Badger Coulee area, allowed the Lolo flow to enter the Horse Heaven Plateau after their emplacement.

Paleodrainage

At least three major ancestral rivers are interpreted to have deposited clastic sediments into the central Columbia Plateau during the Miocene and Pliocene: the Columbia, Clearwater-Salmon (ancestral Snake River of Swanson and Wright 1976) and the Yakima Rivers (Warren 1941a,b; Waters 1955; Laval 1956; Mackin 1961; Schmincke 1964, 1967d, Tallman and others 1981; Fecht and others, in press). Conglomerates deposited by two of these ancestral rivers, the Columbia and the Clearwater-Salmon rivers, are found within the study area in the Selah and Rattlesnake Ridge interbeds and in the early and late phase Snipes Mountain conglomerate. By tracing outcrops of these conglomerates through the study area (and using data adjacent to the study area), paleodrainage patterns were reconstructed (Fig. 40-43) for specific time intervals (i.e., the time between the emplacement of two basalt flows) which can then be used to infer the presence and location of regional paleoslopes, local structure, and basalt flow margins. In this study, the paleodrainage patterns, in conjunction with uplift patterns from the isopach data, were primarily used to delineate areas of structural uplift or subsidence which affected the courses of the ancestral rivers.

Before discussing the structural implications of the paleodrainage patterns, it is necessary to briefly reconstruct the general paleodrainage patterns in the vicinity of the study area since just prior to Esquatzel time through the time of deposition of the late phase of the Snipes Mountain conglomerate.

Just prior to Esquatzel time, the ancestral Clearwater-Salmon River was flowing westward across the northern Pasco Basin (Fig. 39a). The river exited to the west of the Pasco Basin via a channel located north of Rattlesnake Hills on Yakima Ridge (Goff and Myers 1978). When the Esquatzel basalt flowed into the Pasco Basin, the ancestral Clearwater-Salmon River was displaced to the southern edge of the flow and "guided" into the lower Yakima Valley syncline (Fig. 39a). The river then flowed westward, possibly flowing into the Toppenish Basin where it met the ancestral Columbia River. Upon the emplacement of the Pomona Member, the ancestral Clearwater-Salmon River was forced out of the lower Yakima Valley, while the ancestral Columbia River established a course south across the Yakima Valley (Fig. 39b). The ancestral Columbia River did not progress laterally to the east past the present-day location of Grandview, but deposited gravels in a great swath to the west (Schmincke 1964, 1967d). It is speculated that at this same time the ancestral Clearwater-Salmon River was diverted to along the southern flow margin of the Pomona flow. This idea is based on the observation that there is a lack of Clearwater-Salmon River lithologies in the Rattlesnake Ridge conglomerate and only clasts characteristic of the ancestral Columbia River are present

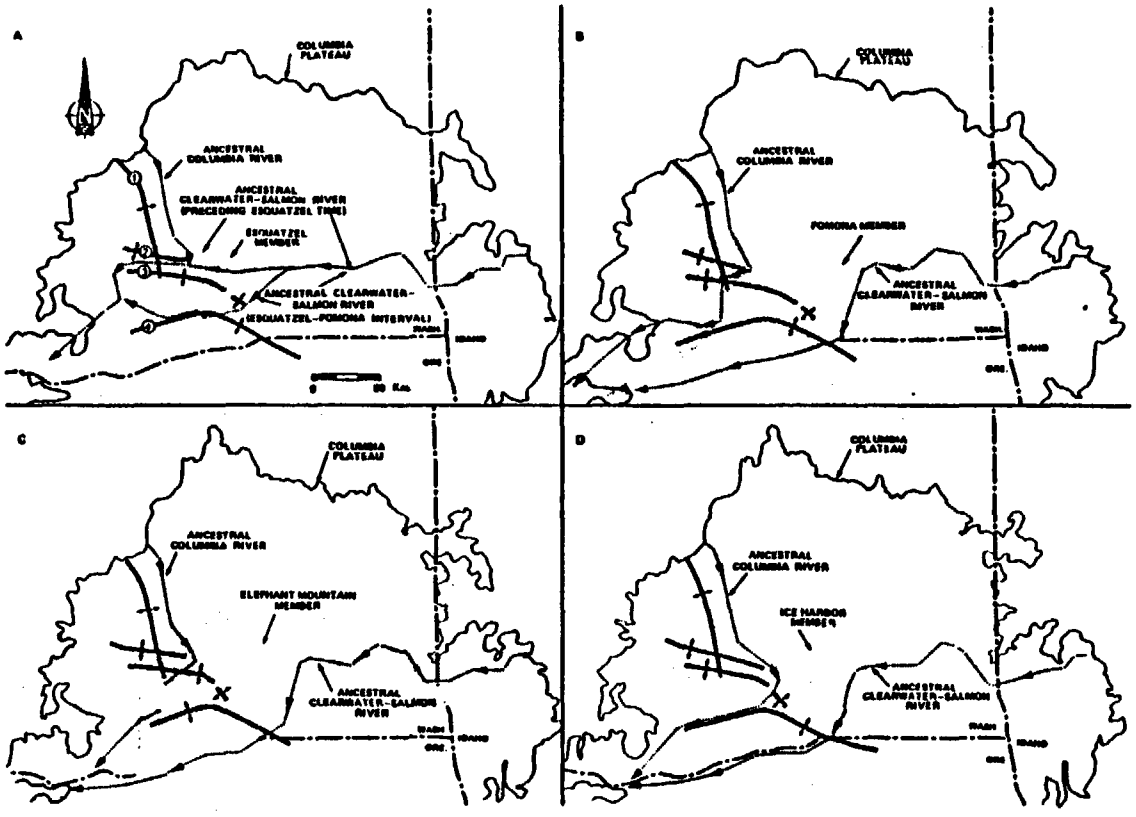

Figure 39. Summary of the paleodrainage of the ancestral Columbia and Clearwater-Salmon Rivers through the Columbia Plateau, after Fecht and others (in press), from just prior to Esquatzel time to the late phase of the Snipes Mountain conglomerate time. A. Paleodrainage prior to Esquatzel time and during Esquatzel-Pomona time. B. Paleodrainage during Pomona-Elephant Mountain time. C. Paleodrainage during deposition of the early phase of the Snipes Mountain conglomerate (Elephant Mountain-Ice Harbor time). D. Paleodrainage during deposition of the late phase of the Snipes Mountain conglomerate (post-Ice Harbor time). Anticlines 1 through 4 represent the Hog Ranch-Naneum Ridge anticline, Yakima Ridge, Rattlesnake Hills, and Horse Heaven Hills, respectively.

(see Chapter 2). Thus, the two rivers did not meet in or to the north of the Yakima Valley. During the Elephant Mountain-Ice Harbor interval, the ancestral Columbia River reestablished itself in approximately the same course as during the Pomona-Elephant Mountain interval. Again, the ancestral Columbia River did not laterally progress to the east past the present-day Grandview area (Fig. 39c), but deposited gravels over a wide area to the west. Sometime between Elephant Mountain and Ice Harbor time, the ancestral Columbia River was diverted into the Pasco Basin north of the lower Yakima Valley. It has been proposed that this diversion was caused by (1) the combined uplift and subsidence of the Hog Ranch-Naneum Ridge anticline and Pasco Basin, respectively (Goff and Myers 1978; Fecht and others, in press); (2) the rise of the Horse Heaven Hills (Warren 1941b); (3) volcaniclastic fans emanating from the Cascades (Waters 1955); (4) rise of Umtanum Ridge (Schminicke 1964). Regardless, the ancestral Columbia River upon entering the Pasco Basin was diverted back into the lower Yakima Valley along the northern flow edge of the Ice Harbor Member and along the rising Horse Heaven Hills uplift (Fig. 39d) for a short period of time, before finally establishing itself within the Pasco Basin (Fecht and others, in press).

It is not known when the ancestral Yakima River established itself in the Yakima Valley, but it is speculated by Fecht and others (in press) that this occurred at nearly the same time the ancestral Columbia River reestablished itself in to the Pasco Basin.

Three major structures were delineated within the study area using the paleodrainage patterns: (1) the Horse Heaven Hills uplift;

(2) the lower Yakima Valley syncline; (3) the Hog Ranch-Naneum Ridge anticline.

The northeast-trending portion of the Horse Heaven Hills uplift was a topographic barrier which controlled both the ancestral Clearwater-Salmon and ancestral Columbia Rivers within the lower Yakima Valley syncline during the Esquatzel-Pomona time interval and during deposition of the late phase of the Snipes Mountain conglomerate, respectively (Fig. 40, 43). The ancestral Clearwater-Salmon River was controlled by the northern edge of the Horse Heaven Hills uplift over an area which is presently occupied by the Phelps anticline/monocline and the Drake anticline (Fig. 40), indicating either the absence or the low relief of these folds during this time. The uplift also diverted the ancestral Columbia River westward from its southward course across the lower Yakima Valley during both the Pomona-Elephant Mountain interval and the Elephant Mountain-Ice Harbor interval (Fig. 41, 42).

The northwest trend of the Horse Heaven Hills uplift affected both the course of the ancestral Clearwater-Salmon River during the Esquatzel-Pomona interval and an intraplateau tributary stream (to the ancestral Columbia River) of post Ice Harbor time (Fig. 40, 43). A fold coincident with a portion of the Kiona anticline (within the Kiona segment), in coordination with the Esquatzel flow, diverted the ancestral Clearwater-Salmon river into a local structural low in the uplift around its southwestern flank (Fig. 40). The tributary stream of the ancestral Columbia River was probably pinched between the western flow edge of the Ice Harbor Member and the northwest trend of

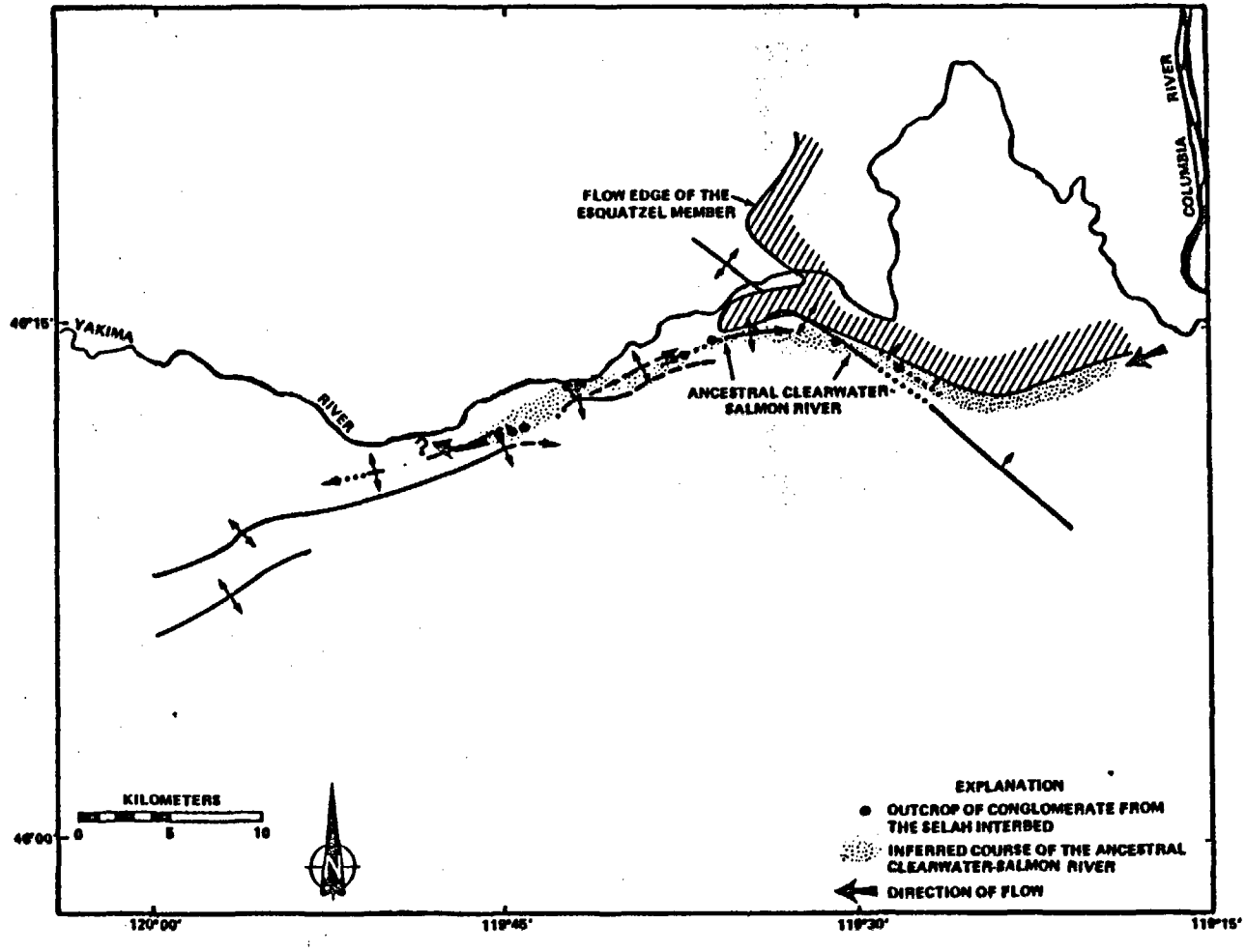

Figure 40. Inferred course of the ancestral Clearwater-Salmon River through the study area during the Esquatzel-Pomona time interval.

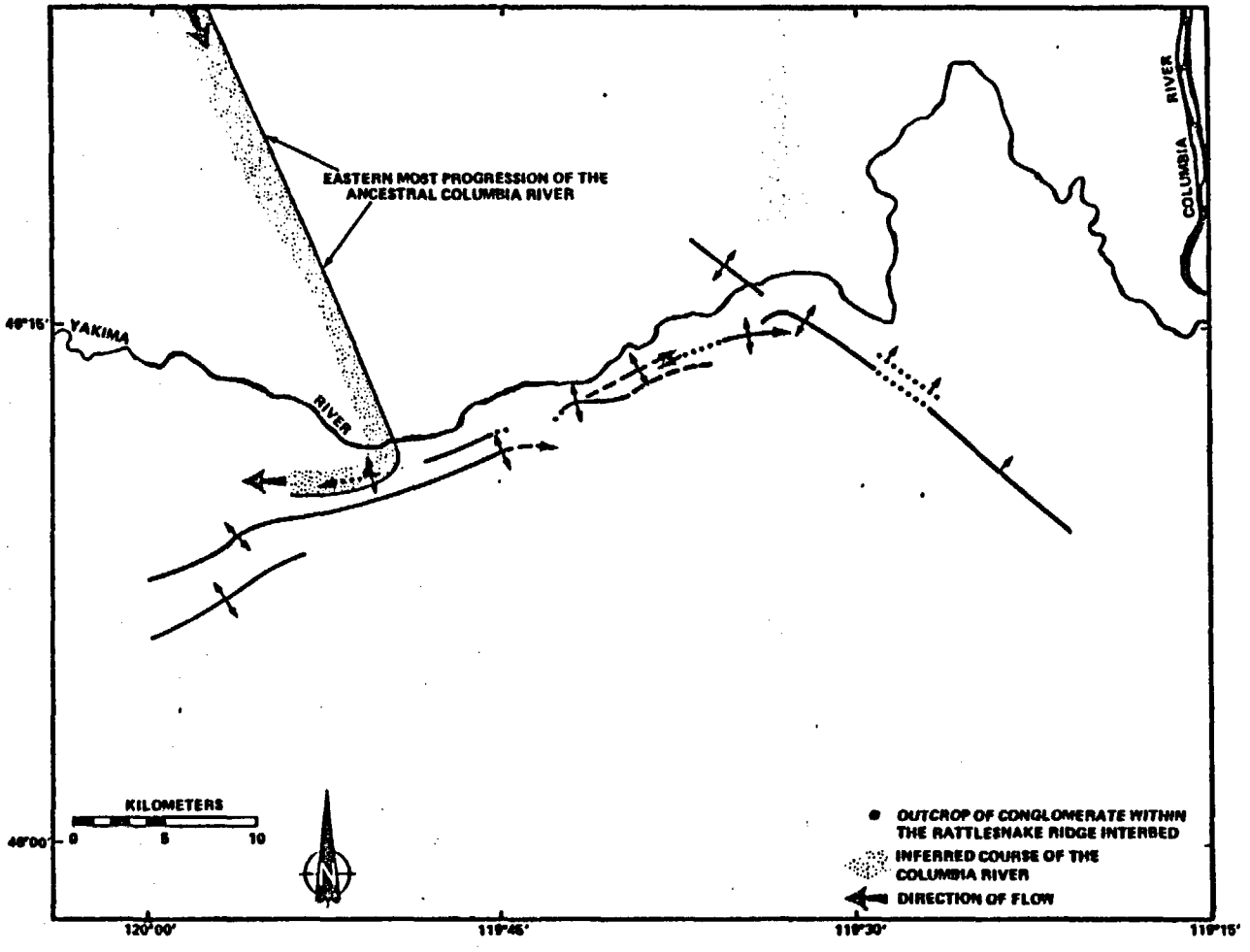

Figure 41. Inferred course of the ancestral Columbia River through the study area during the Pomona-Elephant Mountain time interval.

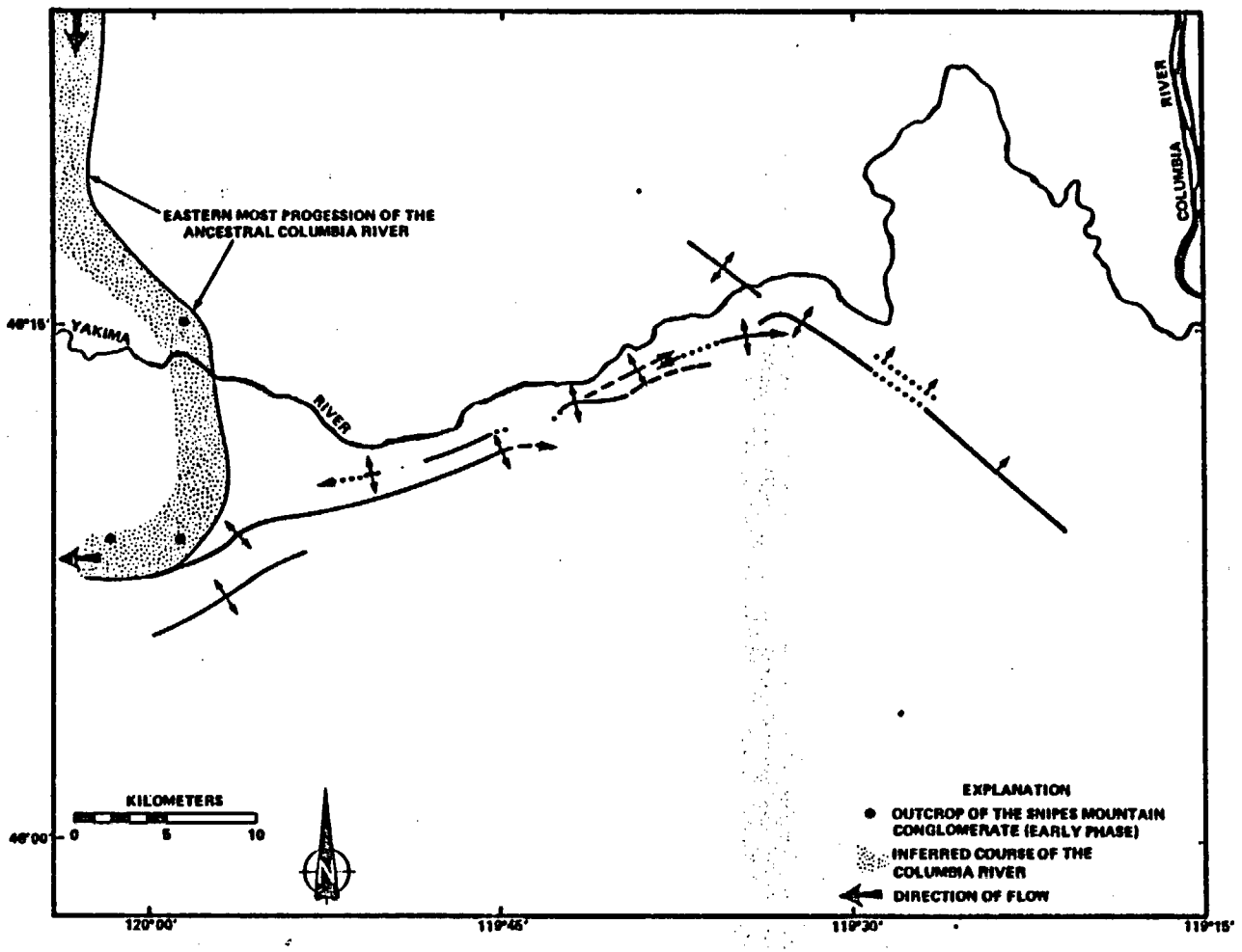

Figure 42. Inferred eastern lateral extent of the ancestral Columbia River through the study area during the Elephant Mountain-Ice Harbor time interval.

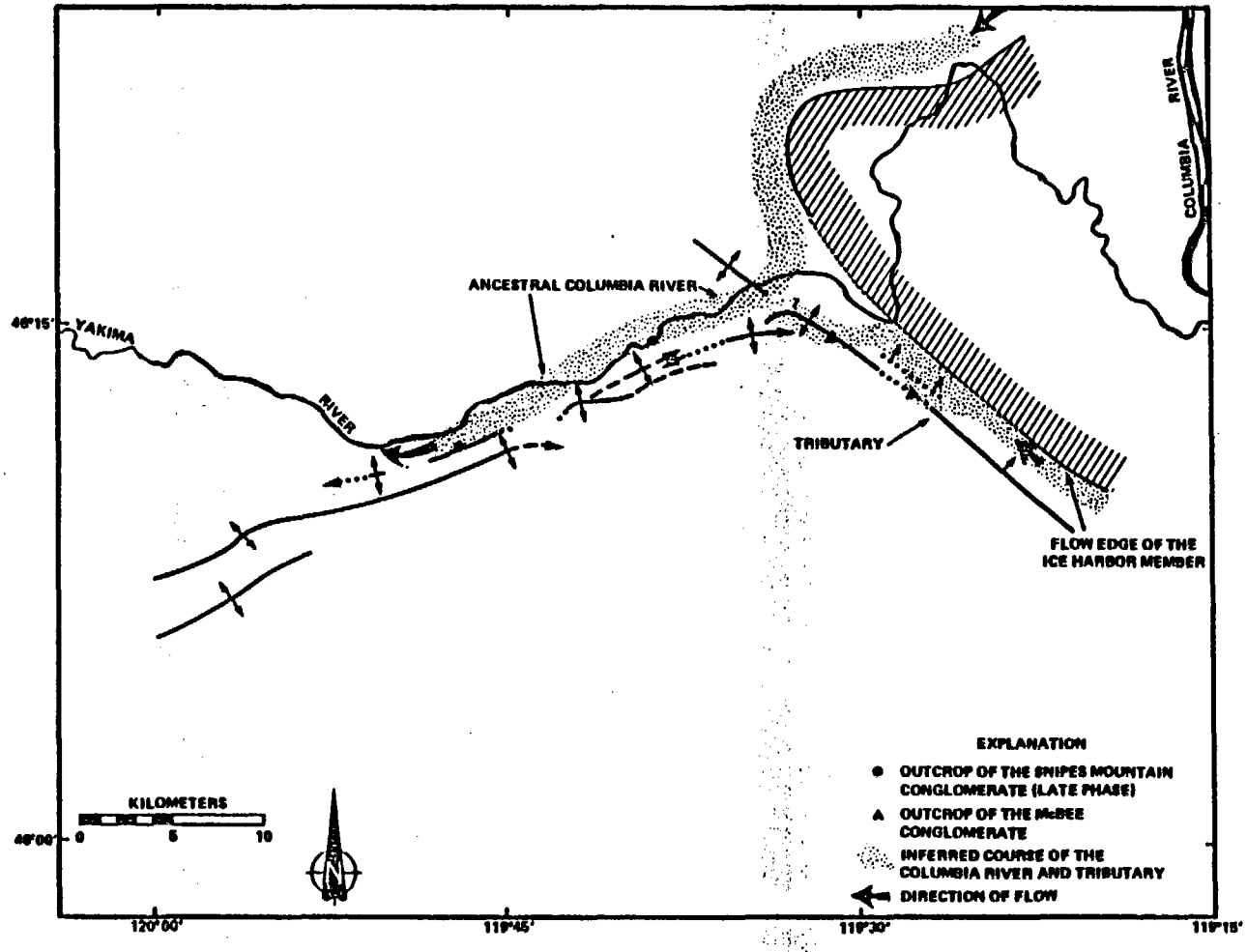

Figure 43. Inferred course of the ancestral Columbia River and a tributary stream through the study area following the emplacement of the Ice Harbor Member.

the uplift (Fig. 43). The location of the conglomerate deposited by this stream (along the crest of the Kiona anticline and Badger Canyon monocline) suggests they were located along undeveloped portions of the uplift.

Two structural lows within the Horse Heaven Hills uplift during the Esquatzel-Pomona interval have been delineated from the paleodrainage pattern of the ancestral Clearwater-Salmon River (Fig. 40). One, mentioned above, was a former structural low found locally along the northwest trend of the uplift approximately where the folds in the Webber segment are now located. The other local structural low separated the northwest and northeast trends of the uplift (now occupied by Chandler Butte). These former structural lows are now located at the ridge crests of the Horse Heaven Hills uplift.

The southern extension of the Hog Ranch-Naneum Ridge anticline in the lower Yakima Valley was a controlling factor for the course of both the ancestral Clearwater-Salmon River and the ancestral Columbia River. The trace of the ancestral Clearwater-Salmon River (Esquatzel-Pomona interval) deposits are not found west of Prosser (Fig. 40); this area also coincides with a marked decrease in thickness of the Selah interbed (see Fig. 33). One explanation is that the river may have encountered the east slope of the Hog Ranch-Naneum Ridge anticline and eventually cut across the anticline, entering the Toppenish Basin via a channel. An alternative to this hypothesis is that the river was diverted south across the Horse Heaven Hills uplift near Prosser, but this idea is dismissed because of the absence of any fluvial deposits or eroded channels along the crest of the uplift.

Evidence is also found for the presence of the Hog Ranch-Naneum Ridge anticline during the Pomona-Elephant Mountain and Elephant Mountain-Ice Harbor intervals. During both intervals, the ancestral Columbia River was flowing south across the lower Yakima Valley (Fig. 41, 42). The eastward migration limit of the ancestral Columbia River during these two time periods was approximately 119°50' west longitude, suggesting the Hog Ranch-Naneum Ridge anticline may have confined the river to the west of the 119°50' west longitude. The Hog Ranch-Naneum Ridge anticline may have controlled this river in coordination with the subsidence of the Toppenish Basin.

The presence of conglomerates along or near the present ridge crest of the Horse Heaven Hills uplift (e.g., conglomerates of the Selah interbed and the McBee conglomerate, Fig. 40, 43) on first impression would seem to indicate that the area was a low. This is locally true (e.g., between Chandler anticline and the Kiona anticline), however in other areas (e.g., Chandler anticline), it is apparent from the trace of the gravel trains and isopach maps, that these crestal outcrops were controlled by structural highs associated with present structures but whose topographic crests were located slightly to the south of their present position. Thus, it is possible that the crestal portions of the folds have migrated with time to their present position and elevated the conglomerate.

GROWTH RATES

In the past, various growth rates of between 100-1500 m/m.y. have been roughly estimated for specific Yakima folds or the Yakima folds as a whole during post CRB time (see Table XIII). Other studies in the vicinity of the Pasco Basin used variations in CRB flows and interbed thicknesses at "instances in time" to calculate vertical growth rates of between 40-600 m/m.y. from CRB time to the present (see Table XIII). These more detailed studies have outlined a pattern of decreasing growth rates from Grande Ronde time to the present (Reidel and others 1983b; Reidel 1984).

Using the approach described by Reidel (1984), it is possible to calculate vertical growth rates for portions of the Horse Heaven Hills uplift relative to the lower Yakima Valley syncline and the Piening syncline. Basically, the cumulative relief which has developed across a fold (calculated using data from Chapter 3; see Tables VI through IX) can be plotted against absolute age dates of individual CRB members (see Table X) which give a rate of combined vertical uplift and subsidence for Wanapum and Saddle Mountains time. Because of the hiatus between the deposition of the Ellensburg Formation sediments and the Pleistocene sediments there are no stratigraphic units for this period to gauge growth rates, thus growth rates were extrapolated to the present time. In addition, no reference line was

confidently delineated from which subsidence and uplift could be differentiated. Several assumptions are necessary when using thickness data and age dates when calculating the growth rates. These assumptions are reviewed in Appendix D.

Results of the growth rate calculations are shown in Figures 44-47. In all four traverses, the rate of development of the relief is less than 70 m/m.y. Additionally, all four curves indicate a decrease in the growth rate with decrease in age during the Wanapum and Saddle Mountains time. Extrapolation of the growth rates to the present approximates the cumulative relief developed since at least Wanapum time suggesting a uniform growth rate of the folds since CRB time to present. However, it is emphasized that at present there is no concrete evidence in the study area to indicate whether this growth occurred at higher or lower rates than the shown extrapolated rates. The three curves which represent development between the Horse Heaven Hills uplift and the lower Yakima Valley syncline all have approximately the same growth rates, with a slightly higher rate determined for the Kiona anticline-Lower Yakima Valley syncline traverse. It is indicated from Figure 47 that relief developed at a slower rate between the Prosser anticline and the Piening syncline.

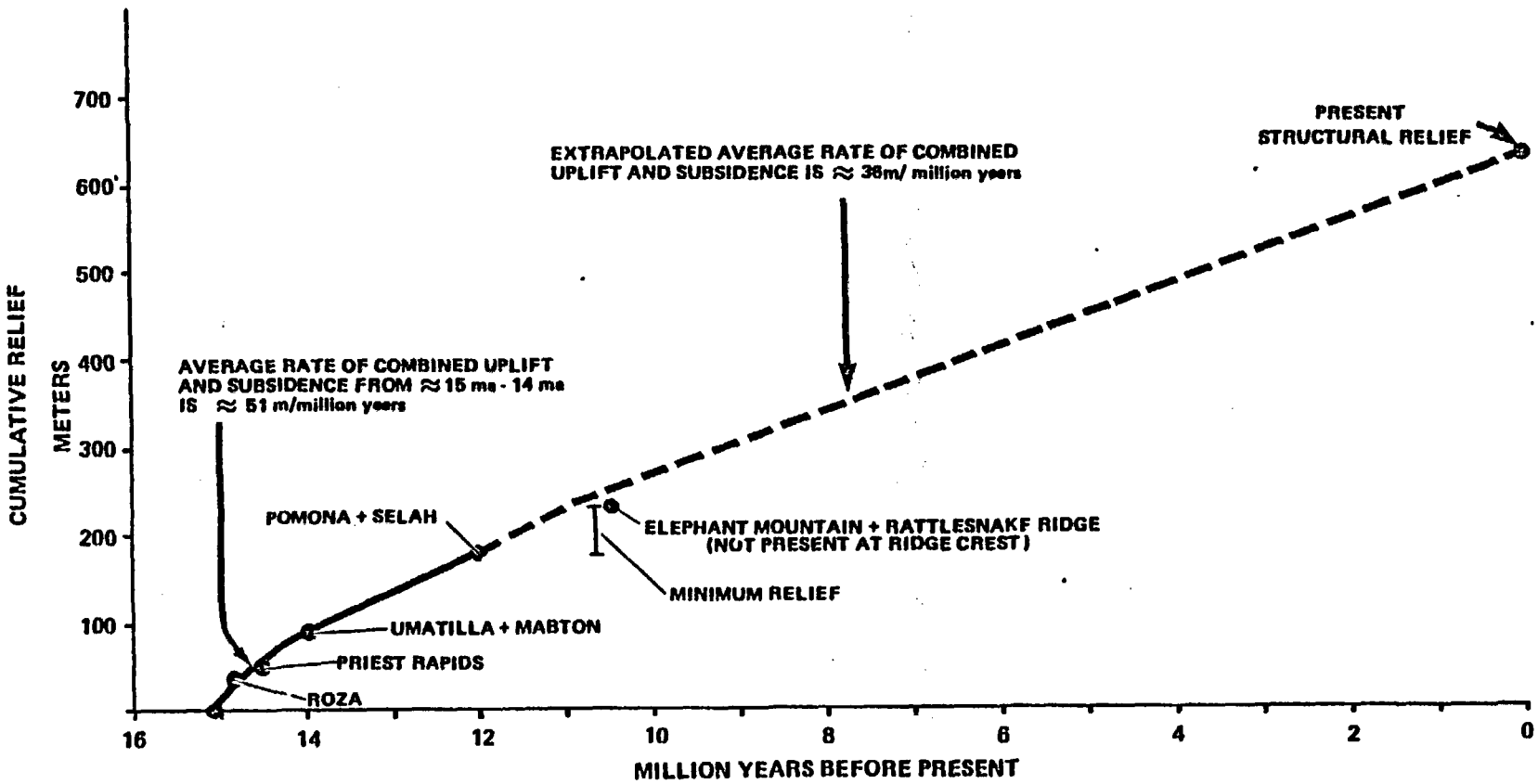

Figure 44. Curve showing rate of relief development between the Prosser anticline and the lower Yakima Valley syncline during a portion of CRB time and extrapolation to the present. Age dates used in constructing the curves are subject to error ranges that could alter the shape of the curve locally, but not the general trend.

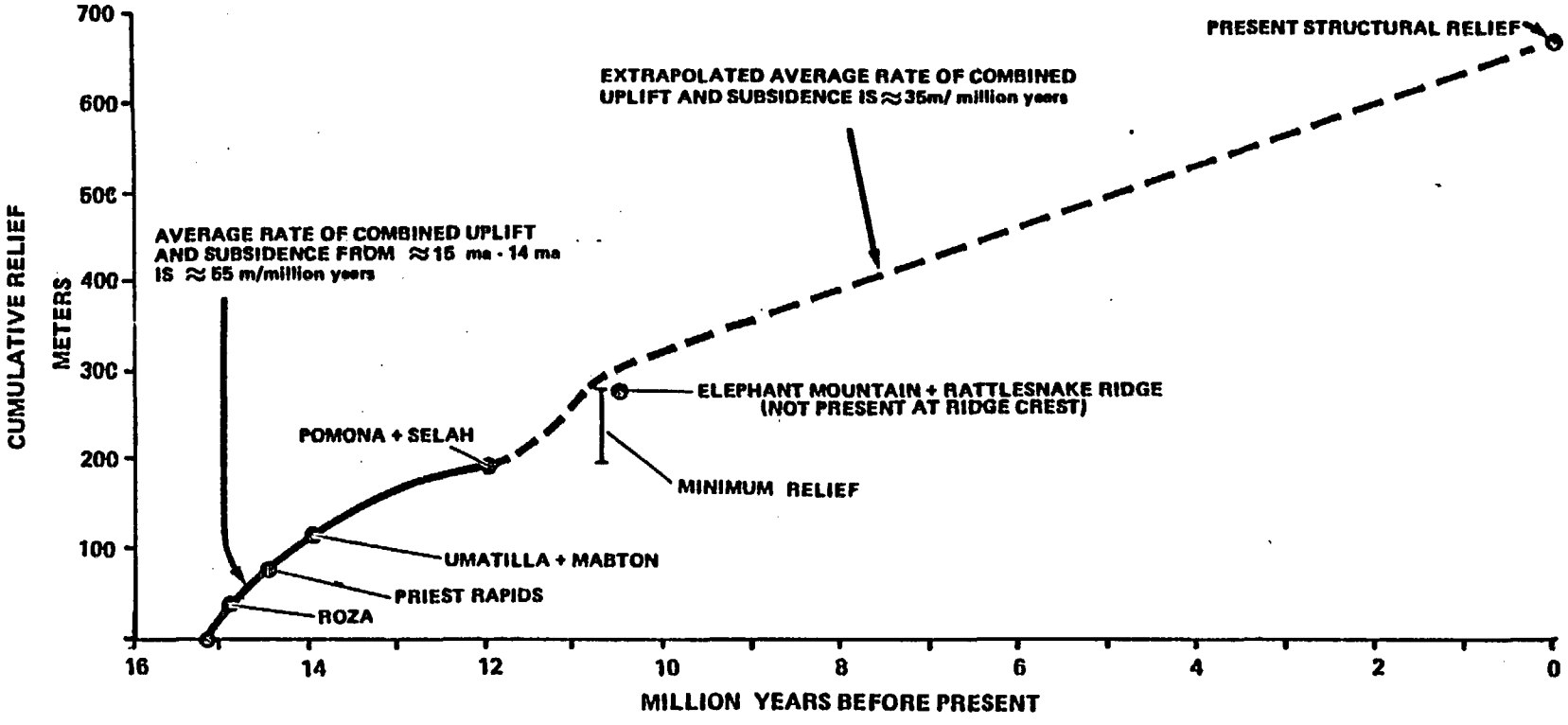

Figure 45. Curve showing the rate of relief development between the Chandler anticline and the lower Yakima Valley syncline during a portion of CRB time and extrapolation to the present. Age dates used in constructing the curves are subject to error ranges which could alter the shape of the curve locally, but not the general trend.

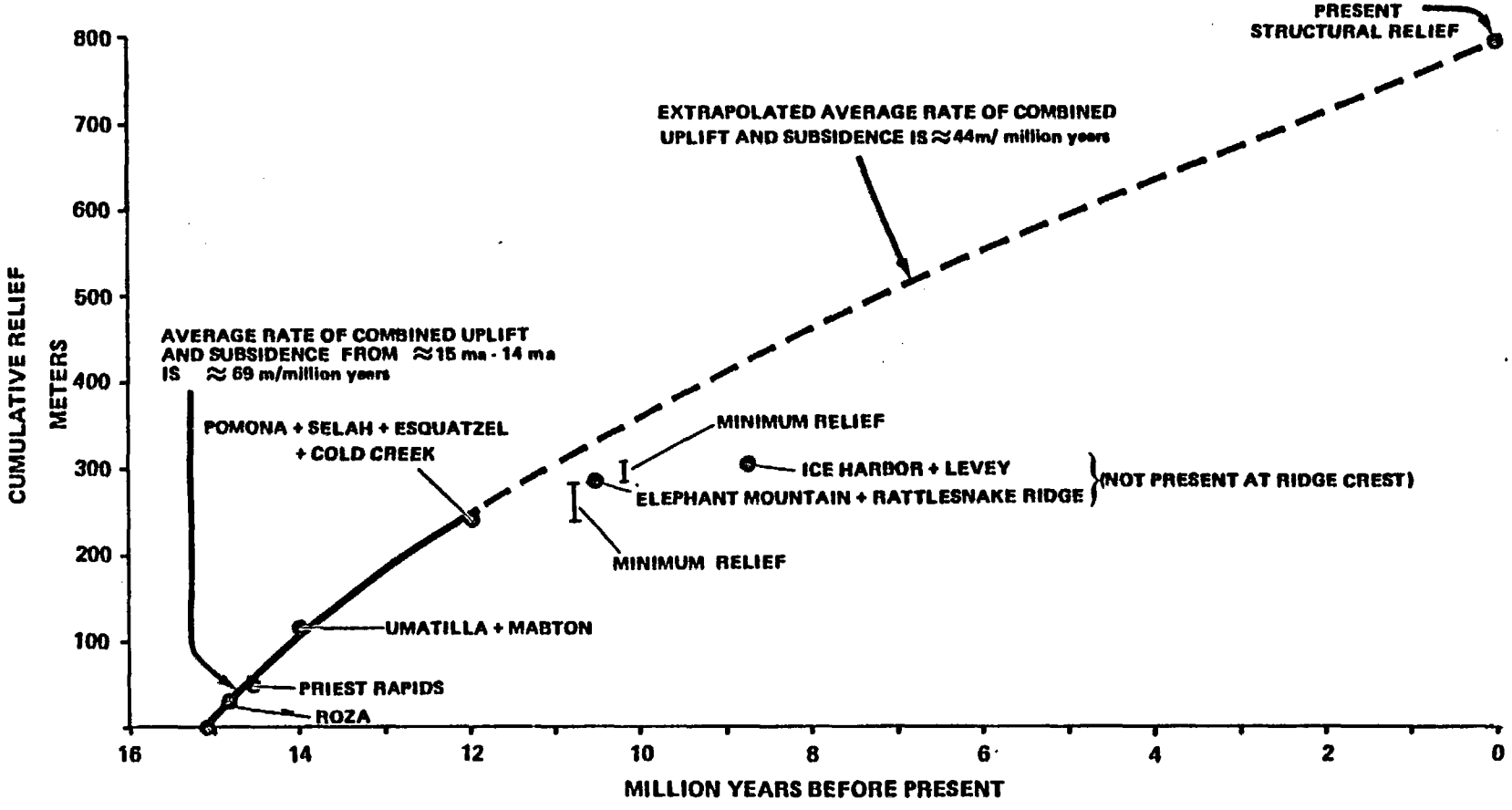

Figure 46. Curve showing the rate of relief development between the Kiona anticline and the lower Yakima Valley syncline during a portion of CRB time and extrapolation to the present. Age dates used in constructing the curves are subject to error ranges which could alter the shape of the curve locally, but not the general trend.

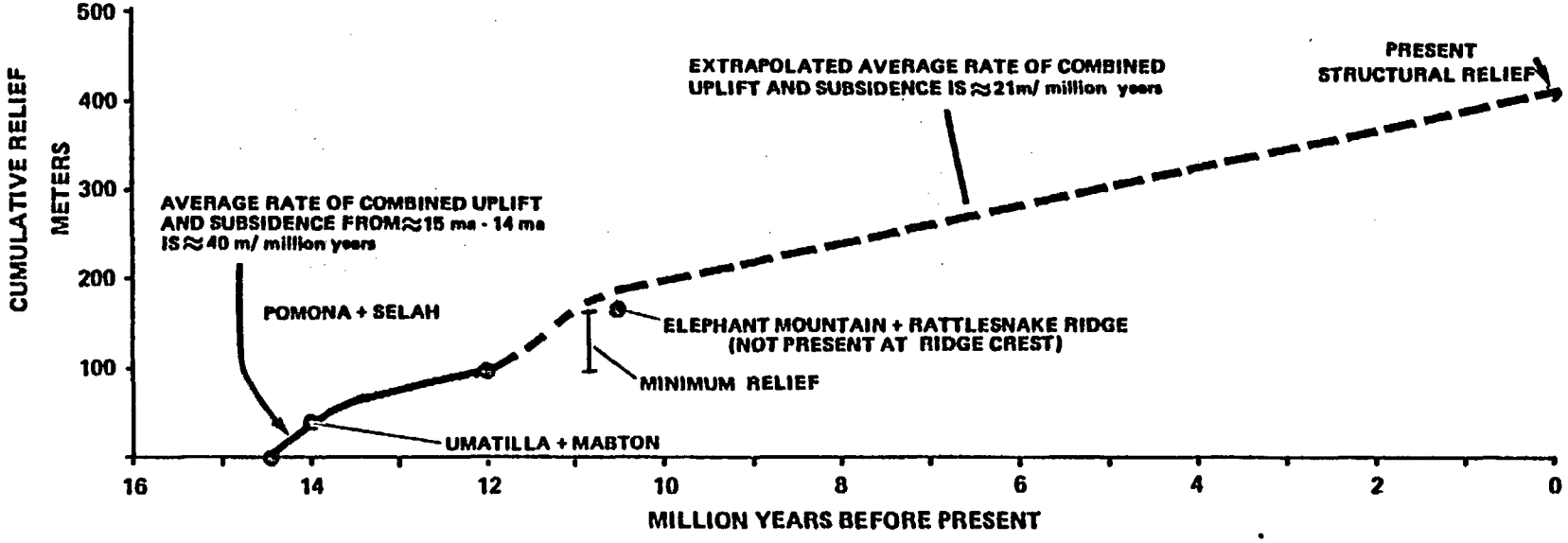

Figure 47. Curve showing the rate of relief development between the Kiona anticline and the Piening syncline during a portion of CRB time and extrapolation to the present. Age dates used in constructing the curves are subject to error ranges which could alter the shape of the curve locally, but not the general trend.

CONSTRAINTS ON TECTONIC MODELS FOR THE DEVELOPMENT OF THE HORSE HEAVEN HILLS UPLIFT

Many tectonic models have been published to date which address the genesis of the various east-west-trending and northwest-trending folds of the Yakima Fold Belt (Table XIV). These models also imply directly or indirectly an origin for the Horse Heaven Hills uplift. Choosing one of these tectonic models (or a new one) for the genesis of the Horse Heaven Hills uplift is beyond the scope of this study, however these tectonic models can be constrained by the findings of this study. This chapter contains a brief evaluation of these tectonic models as they apply to the Horse Heaven Hills uplift, followed by some suggested constraints. More detailed reviews of such tectonic models are also presented elsewhere (Davis 1981; Price 1981; Duncan 1983).

It is generally agreed that the Yakima folds developed under approximately north-south compression based on the orientations of surficial structures (e.g., folds, dikes) and that these folds are presently deforming under north-south compression (Campbell and Bentley 1981; Rohay and Davis 1983). However, the origin of the folding has been debated by most workers (Table XIV). Published tectonic models for the Yakima folds can be fit into several catagories (Fig. 48). These categories are: (1) differential horizontal displacement of a coupled CRBG layer and sub-basalt layer (includes wrench models), (2) horizontal contraction within a detached

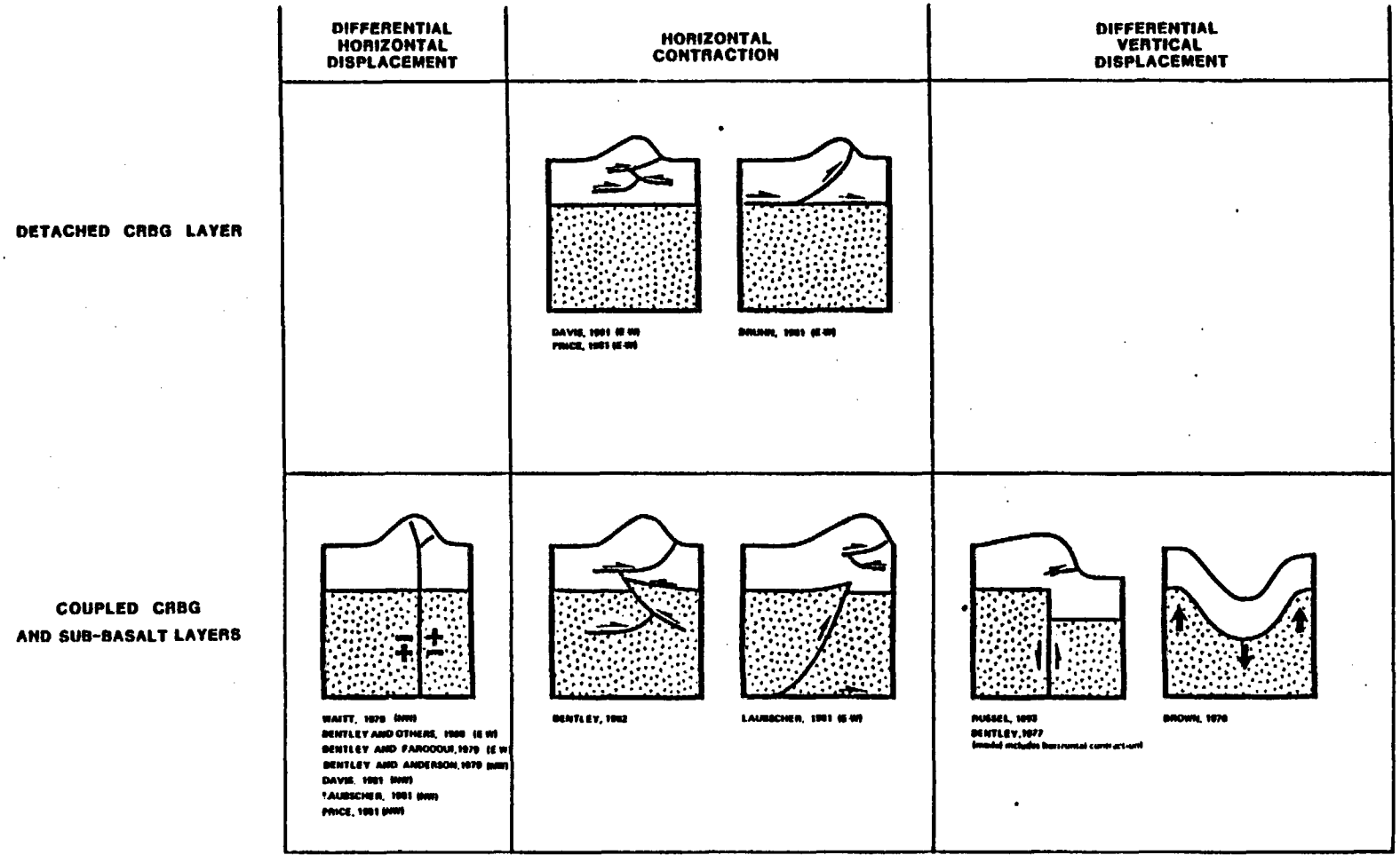

Figure 48. Tectonic model classification.

CRBG layer (includes decollement models), (3) horizontal contraction involving coupled CRBG and sub-basalt layers and, (4) differential vertical displacement (includes drape fold models).

An interpretation of recently collected magnetotelluric data suggests that the sub-basalt rock is composed of an upper sediment sequence and a lower crystalline rock layer (Mitchell and Bergstrom 1983). The rheological differences between these two sub-basalt layers may cause a different accommodation to stress, however for the purposes of this discussion these two layers are considered as a homogeneous sub-basalt medium, or basement.

East-West-Trending Folds

Formation of the Horse Heaven Hills uplift from horizontal contraction within a detached basalt layer (thin-skinned folds) is suggested by the uplift's long, linear trend; thrusting along its flanks; and the uplift's lack of structural deviation over a strong regional gravity gradient aligned with the 120° west longitude meridian (Konicek 1975, Finn and others 1984) thought by Konicek to represent an eastward increase in thickness of basalt. In addition, along a north-south transect the fold pattern of east-west-trending Yakima folds as a whole might suggest the presence of thin skinned tectonics. East-west-trending Yakima folds have also been thought to form over local detachments or ramps off of regional detachments (e.g., see Davis and Price, Table IV).

Data are also available that suggest coupling between the basalt and sub-basalt rock. Along the Rattlesnake Hills, the 3.2 km deep

RSH-1 well is interpreted by Reidel and others (1982) not to encounter such a fault. In addition, a thrust fault along the Columbia Hills (Swanson and others 1979a) is observed to steepen with depth similar to that interpreted for the Rattlesnake Hills area. Also, magnetotelluric data in the Pasco Basin area indicate high relief at the base of the basalt which has been interpreted to indicate a lack of decollement at the base of the basalt (Mitchell and Bergstrom 1983). Moreover, seismicity suggests that the basement and the basalt react as though coupled (Duncan 1983).

Differential horizontal displacement (left-lateral wrenching) involving a coupled CRBG layer and sub-basalt layer along the northeast trend of the Horse Heaven Hills uplift (as proposed for other east-west folds, Bentley and Farooqui 1979; Bentley and others 1980b) is suggested by the presence of left-stepping en echelon anticlines (e.g., Gibbon anticline and Chandler anticline). The importance of this en echelon relationship (in the absence of more concrete data) as a surficial indicator for wrenching is questionable when one observes that other east-west folds (e.g., the Simcoe Mountains, Alder Ridge, and Paterson Ridge) contain en echelon folds oriented in a right-stepping sense. In addition, clockwise rotation is found along: (1) the northeast trend of the Horse Heaven Hills uplift (see Appendix E), (2) the east-west-trending Saddle Mountains, (3) the Gable Mountain trend, and (4) the northwest-trending folds of the ARW and RAW (Reidel and others 1984).

Reidel and others (1984) use this consistent clockwise rotation along both east-west- and northwest-trending folds to dismiss models

which call for sinistral faulting (sinistral faulting would suggest counterclockwise rotations). Also, seismicity along east-west-and at trending folds indicates, that presently, reverse or thrust faults lie along these folds (Rohay and Davis 1983).

The asymmetric and near-monoclinal fold geometry, along with the presence of thrust and reverse faults along the folds of the northeast trend of the Horse Heaven Hills uplift (see Chapter 2) resembles folds originating from horizontal contraction and/or vertical displacement along faults in the basement (e.g., Rattlesnake Mountain, Wyoming, (Brown 1984)). This type of folding and faulting is consistent with seismic data (Rohay and Davis 1983), and what is known of the angle of faulting as constrained by RSH-1 and the thrust fault along the Columbia Hills, mentioned previously. Overturned limbs, the possible migration of ridge crests with time (see Chapter 3), and the hypothesized north-south oriented compression during the Miocene and Pliocene indicate that uplift may not be caused strictly by vertical displacement.

Northwest-Trending Folds

It is proposed here that based on their proximity, parallel nature, similar lengths, similar structural forms, and timing of development, the structures along the ARW (includes the northwest trend of the Horse Heaven Hills uplift) and portions of the RAW are genetically related, and thus, tectonic models concerned with the

origin of the RAW (aswell as structures coincident with the OWL) are applicable to the northwest trend of the Horse Heaven Hills uplift.

The development of the aligned and en echelon brachyanticlines along the RAW has been attributed to dextral wrenching (differential horizontal displacement involving both sub-basalt and CRBG layers) based on their similarities to other wrench-produced folds (e.g., see Davis 1981). There is a similar alignment along the ARW (Fig. 12), however a "sense of step" for the en echelon folds is not clearly indicated. Paleomagnetic data, which indicate clockwise rotation has occurred along folds of both the ARW and RAW, can be explained by dextral shear along these two structural trends (Reidel and others 1984). In addition, the Wallula Gap fault which lies along the RAW has been suggested by several workers to be a dextral fault, although Gardner and others (1981) indicate that the fault is predominantly dipslip with minor strike-slip movement. According to Rohay and Davis (1983) earthquake hypocenters and focal mechanisms in the vicinity of the RAW do not support contemporary right lateral movement along the RAW. Thus although several workers have proposed strike-slip faults along the RAW, evidence is not demanding that this is the case.

Constraints

Data from this study provide further constraints for the tectonic models discussed above. Both the northwest and northeast trends of the Horse Heaven Hills uplift were developing simultaneously

and at similar rates (at least in Wanapum and Saddle Mountains time) under generally north-south compression. In addition, structural forms along both trends are very similar (see Chapter 2). Based on these observations, I propose that folding along the northwest and northeast trends of the Horse Heaven Hills uplift formed by the same tectonic process. These data would require reconsideration of models which attribute different tectonic conditions to the formation of the east-west trends and the northwest trends (e.g., detached deformation along one trend and basement involved deformation along the other trend).

My hypothesis does not consider the structural implications of the numerous northwest-trending dextral faults and folds mapped along the southwestern portion of the Yakima fold belt (Swanson and others 1979a). There is no apparent relationship between the northwest-trending faults and folds and the RAW and ARW based upon available data. In support of this difference, there is a change in orientation of the axis of least compression from vertical in the central Columbia Plateau (study area) to a east-west orientation of the axis in the western portion of the Columbia Plateau, suggesting that present deformation at the western margin is predominantly produced by strike-slip movement on northwest-southeast oriented fault planes (Rohay and Davis 1983).

Similarities of structural forms and timing of deformation between the Horse Heaven Hills uplift and other folds such as Umtanum

Ridge (described in detail by Price 1981) the Saddle Mountains (Reidel 1984), and Rattlesnake Mountain (Reidel 1984, unpub. map) may also imply that these folds had a similar mechanical development.

Another structural feature which must be accommodated within a tectonic model for the Horse Heaven Hills uplift (and other Yakima folds) is the simultaneous growth of the Hog Ranch-Naneum Ridge anticline with the Horse Heaven Hills uplift during at least Saddle Mountains time. Other studies have inferred pre-CRBG ages for the Hog Ranch-Naneum Ridge anticline to the north (see Table XIII). Tabor and others (1982) have indicated that the Hog Ranch-Naneum Ridge anticline is related to basement structure along the northern margin of the Columbia Plateau. Campbell (1984) proposed that the "Naneum High" (a pre-CRB high coincident with the Hog Ranch-Naneum Ridge anticline) to the north of the study area limited the eastward extent of the Cascade volcaniclastic sediments. The extension of the Hog Ranch-Naneum Ridge anticline in the lower Yakima Valley may have limited the westward progression of much of the Columbia River basalts, such as found in the northern Pasco Basin (Reidel and Fecht 1981). The north-south gravity gradient paralleling the 120° west longitude meridian is thought by Konicek (1975) to represent a progressive west to east thickening of the basalt. The projection of the Hog Ranch-Naneum Ridge anticline into the lower Yakima Valley roughly parallels this gravity gradient and may be related to this increase in thickening of the basalt.

The structural and tectonic relationship between the north-northwest-trending Hog Ranch-Naneum Ridge anticline, and the east-west- and northwest-trending Yakima folds remains unclear, and further work is needed to ascertain their relationship.

CONCLUSIONS

Basalt flows of the Grande Ronde, Wanapum, and Saddle Mountains Basalts of the CRBG were mapped along and in the immediate vicinity of the Horse Heaven Hills uplift. Borehole data provided additional information away from principal exposures. The Grande Ronde Basalt consists of flows of the Sentinel Bluffs sequence; the Wanapum Basalt consists principally of flows of the Frenchman Springs, Roza, and the Priest Rapids Members; the Saddle Mountains Basalt consists of flows of the Umatilla, Esquatzel, Pomona, Elephant Mountain, and Ice Harbor Members. Several sedimentary interbeds of the Ellensburg Formation are intercalated with these flows in the study area. Additional sedimentary units of the Ellensburg Formation, the Snipes Mountain conglomerate, McBee conglomerate, or undifferentiated Ellensburg sediments occur above the CRB. A depositional hiatus occurs within the study area between the late Miocene and Pleistocene epochs.

Within the study area, the Horse Heaven Hills uplift consists of two distinct intersecting trends, a northwest (N50°-55°W) and northeast (N60°-70°E) structural trend. The northwest-trending portion forms a part of the ARW which parallels the RAW (part of the OWL). Each trend consists of aligned or en echelon anticlines and monoclines. At the intersection of the northwest and northeast trends, two major anticlines, the Chandler anticline (part of the

northeast trend) and the Kiona anticline (part of the northwest trend) merge. As the northwest-trending Kiona anticline is traced into the intersection, the trace of its axis gradually changes to a more westerly direction and is accompanied by tear faults in the northern flank of the anticline. This portion of the Kiona anticline could represent: (1) the northwest-plunging nose of the anticline, or (2) change in trend of the anticline as a result of local differential stresses caused by the interference of folding along the northwest and northeast trends.

Along the crest of the Horse Heaven Hills uplift a series of asymmetric (north vergence) eroded, usually double-hinged anticlines or monoclines occur. Some of these anticlines or monoclines are paralleled to the immediate north by a lower-relief anticline or monocline. All folds either are, or approach monoclines in geometry. Also, along certain folds there is a transition between the monoclinal and anticlinal geometries.

Surface faults along the uplift generally represent strain caused by folding. Reverse faults parallel the folds and are commonly found or inferred along (1) the base of the northern limb of anticlines or monoclines and (2) in the hinge zone of monoclines or in the northern hinge zone of the double-hinged anticlines. Reverse faults are rarely observed along the southern hinge or the interhinge limb of a double-hinged anticline. Tear faults are coincident with marked changes in fold wavelength and/or changes in strike of fold axes. Layer-parallel faults are common in steeply dipping strata along stratigraphic contacts or zones of preferred weakness in the

intraflow structures, but are also locally found along stratigraphic contacts of low dip. Observations indicate that much of the landsliding along northern fronts of the folds was enhanced by the presence of fault-shattered basalt and interbeds situated along steeply dipping limbs.

The geometry is strikingly similar between the northwest and northeast trends of the Horse Heaven Hills uplift. In addition, the magnitude of relief between the major folds (those that compose the ridge crest of the uplift) of the two trends and between the minor folds of the two trends are similar.

Uplift along the Horse Heaven Hills during portions of the middle and late Miocene was concentrated on the major folds which are now present. Growth occurred simultaneously along folds of both the northwest and northeast trends. Local structural lows occurred between certain major folds of each trend and also between the northwest and northeast trends themselves. Other structures such as the lower Yakima Valley syncline, the Piening syncline, and the Hog Ranch-Naneum Ridge anticline were also developing simultaneously with the Horse Heaven Hills uplift. Because of a lack of a depositional geologic record between the late Miocene and the Pleistocene, it is not possible to determine the details of the growth of these structures during this time. However, it is apparent that the Horse Heaven Hills uplift continued to grow to its present-day relief either uniformily or intermittently. Also, the lower Yakima Valley syncline appears to have structurally "risen" in relation to the Pasco and Toppenish Basins after the Miocene. The uplift of the Hog Ranch-

Naneum Ridge anticline within the study area may have slowed after Elephant Mountain time and/or is related to the relative rise of the lower Yakima Valley syncline.

Combined uplift and subsidence rates between the Horse Heaven Hills uplift and the lower Yakima Valley syncline for Wanapum and Saddle Mountains time is less than 70 m/m.y. and between the Horse Heaven Hills uplift and the Piening syncline less than 40 m/m.y. Growth rates appear to decrease during Wanapum to Saddle Mountains time. Extrapolation of growth rates to the present approximates the cumulative relief developed since at least Wanapum time and supports the possibility that the folds developed at a uniform or nearly uniform rate from CRB time to the present. However, this does not preclude intermittent growth (thus higher or lower rates of growth).

An evaluation of the diverse group of published tectonic models proposed for the Yakima folds indicates that choosing a tectonic model for the Horse Heaven Hills uplift is not possible with the available data. However constraints can be placed on such models from data gathered in this study. These models must consider (1) the monoclinal or near-monoclinal fold geometry and associated reverse faults, (2) development of the folds along both trends of the Horse Heaven Hills uplift occurred simultaneously and at similar rates (at least during Wanapum and Saddle Mountains time), (3) folds along the northwest trend of the Horse Heaven Hills uplift are genetically related and formed simultaneously with at least portions of the RAW, (4) the uplift was developing simultaneously with the north-northwest-trending Hog Ranch-Naneum Ridge anticline as well as other Yakima

folds, and (5) preliminary results indicate that clockwise rotation is found at sites along folds of both the northwest and northeast trends of the Horse Heaven Hills uplift. From these constraints it is proposed that the northeast and northwest trend of the Horse Heaven Hills uplift was generated by the same tectonic process.

Further work of this type, elsewhere in the Yakima fold belt, will help determine if these constraints are applicable to other Yakima folds. Present studies suggest they are. Future subsurface data, as it becomes available, in coordination with this type of work will further constrain tectonic models for the Columbia Plateau.

REFERENCES CITED

Anderson, J. V., Bush, J. H., Crosby, J. W., III, Kiesler, J. P., Siems, B. A., 1973. Correlation of Columbia River basalt and geophysical techniques [abs.]: Geological Society of America, Abstracts and Programs, v. 5, no. 1.

Anderson, J. L., 1980. Deformation and canyon cutting in post-Grande Ronde, pre-Frenchman Springs time, Grayback Mountain, south-central Washington: Geological Society of America Abstracts with Programs, v. 12, n. 8, p. 93.

ARHCO, 1976. Preliminary feasibility study on storage of radioactive waste in Columbia River basalts: ARH-ST-137, Richland, Washington, Atlantic Richfield Hanford Company, v. 1, 169 p.

Baker, V. R., Nummendal, D., eds., 1978. The channeled scabland. A guide to the geomorphology of the Columbia Basin, Washington, prepared for the Comparative Planetary Geology Field Conference held in the Columbia Basin, June 5-8, 1978: Washington, D.C., National Aeronautics and Space Administration, 186 p.

Barrash, W. P., Bond, J. G., and Vankatakrishnan, R., 1983. Structural evolution of the Columbia Plateau in Washington and Oregon: American Journal of Science, v. 283, pp. 897-935.

Beeson, M. H., Fecht, K. R., Reidel, S. P., and Tolan, T. L., in preparation, Stratigraphy of the Frenchman Springs Member of the Wanapum Basalt of the Columbia River Basalt Group.

Bentley, R. D., 1977. Stratigraphy of the Yakima Basalts and structural evolution of the Yakima ridges in the western Columbia Plateau, in Brown, E. H., and Ellis, R. C., eds., Geological Excursions in the Pacific Northwest: Western Washington University Press, Bellingham, pp. 339-389.

Bentley, R. D., 1979. Right lateral strike-slip faults in the western Columbia Plateau Washington [abs.]: EOS, American Geophysical Union Transactions, v. 60, p. 961.

Bentley, R. D., 1980a. Wrench tectonic model for the late Cenozoic evolution of Oregon and Washington [abs.]: Geological Society of America Abstracts and Programs, v. 12, p. 385.

Bentley, R. D., 1980b. Angular unconformity and thrust fault in the Umtanum anticlinal uplift near Priest Rapids Dam, Central Washington: EOS, American Geophysical Union Transactions, v. 61, n. 46, p. 1108.

Bentley, R. D., 1982. Late Tertiary thin-skin deformation of the Columbia River basalt in the western Columbia Plateau, Washington-Oregon [abs]: EOS Transactions of the American Geophysical Union, v. 63, p. 173.

Bentley, R. D., Anderson, J. L., 1979. Right lateral strike-slip faults in the western Columbia Plateau [abs.]: Rockwell Hanford Operations, Richland, Washington, RHO-BWI-SA-28A.

Bentley, R. D., and Farooqui, S. M., 1979. Left-lateral, strike-slip Riedel shears in the Yakima ridges, Columbia Plateau, Washington and Oregon [abs.]: Rockwell Hanford Operations, Richland, Washington, RHO-BWI-SA-40-A.

Bentley, R. D., Anderson, J. L., Campbell, N. P., and Swanson, D. A., 1980a. Stratigraphy and structure of the Yakima Indian Reservation with emphasis on the Columbia River Basalt Group: U.S. Geological Survey Open-File Report 80-200, 73 p.

Bentley, R. D., Powell, J., Anderson, J. L., and Farooqui, S. M., 1980b. Geometry and tectonic evolution of the Columbia Hills anticline, Washington and Oregon [abs.]: Geological Society of America Abstracts with Programs, v. 12, n. 3, p. 97.

Bentley, R. D., Campbell, N. P., and Powell, J., in press, Geologic map of the Blue Light Quadrangle, south-central Washington: Washington Department of Natural Resources, Div. of Geology and Earth Resources, scale 1:48,000.

Biggane, J., 1982. The low-temperature geothermal resource and stratigraphy of portions of Yakima County, Washington: Washington Department of Natural Resources Division of Geology and Earth Resources, Open-File Report 82-6, 128 p.

Bingham, J. W., Londquist, C. J., and Baltz, E. H., 1970. Geologic investigation of faulting in the Hanford region, Washington: U.S. Geological Survey Open-File Report, Tacoma, Washington, 104 p.

Bond, J. G., Kauffman, J. D., Miller, D. A., and Barrash, W., 1978. Geology of the southwest Pasco Basin: Geoscience Research Consultants for Rockwell Hanford Operations, Richland, Washington, RHO-BWI-C-25, 217 p.

Brown, J. C., 1978. Discussion of geology and groundwater hydroloqy of the Columbia Plateau, with specific analysis of the Horse Heaven, Sagebrush Flat, and Odessa-Lind areas, Washington: Washington State University, College of Engineering, Research Report 78/15-23, 49 p.

Brown, R. E., 1970. Some suggested rates of deformation of the basalts in the Pasco Basin, and their implications, in Gilmour, E. H., and Stradling, D., eds.: Proceedings of the Second Columbia River Basalt Symposium, pp. 179-189.

Brown, R. E., 1979. A review of water-well data from the unconfined aquifer in the eastern and southern parts of the Pasco Basin: Rockwell Hanford Operations, Richland, Washington, RHO-BWI-C-56, 17 p.

Brown, W. G., 1984. Basement Involved Tectonics Foreland Areas: Association of American Petroleum Geologists, Continuing Education Course Note Series #26, 92 p.

Caggiano, J. A., Fecht, K. R., Price, S. M., Reidel, S. P, and Tallman, A. M., 1980. A preliminary assessment of the relative rate of deformation in the Pasco Basin, south-central Washington [abs.]: Geological Society of America Abstracts with Programs, v. 12, n. 7, p. 297.

Campbell, N. P. 1977. Geology of the Snipes Mountain area, Yakima County, Washington: Washington Department of Natural Resources, Division of Geology and Earth Resources, Open-File Report 77-8, scale 1:24,000,

Campbell, N. P., 1983. Correlation of Late Cenozoic gravel deposits along the Yakima River Drainage from Ellensburg to Richland, Washington: Northwest Science, v. 57, n. 3, p. 179-193.

Campbell, N. P., 1984. Stratigraphy and hydrocarbon potential of the northwestern Columbia Basin based on recent drilling activities: Rockwell Hanford Operations, Richland, Washington, data package SD-BWI-TI-265, 41 p.

Campbell, N. P. and Bentley, R. D., 1981. Late Quaternary deformation of the Toppenish Ridge uplift in south-central Washington: Geology, v. 9, pp. 519-524.

Choniere, S. R., and Swanson, D. A., 1979. Magnetostratigraphy and Correlation of Miocene basalts of the northern Oregon Coast and Columbia Plateau, southeast Washington: American Journal of Science, v. 279, p. 755-777.

Crosby, J. W., III and Anderson, J. V., 1971. Some applications of geophysical well logging to basalt hydrogeology: Ground Water, v. 9, p. 13-20.

Crosby, J. W., III, Anderson, J. V., and Kiesler, J. P., 1972. Geophysical investigation of wells in the Horse Heaven Hills area: Washington State University, College of Engineering, Research Report, 72/11-24.

Davis, G. A., 1981. Late Cenozoic tectonics of the Pacific Northwest with special reference to the Columbia Plateau in Final Safety Analysis Report, WNP-2, Amendment 18, Appendix 25 N: Washington Public Power Supply System, Richland, Washington, 49 p.

Dennis, T. E., 1938. The structure of the Horse Heaven Hills of Washington: Washington State College, Pullman, M.S. thesis.

Duncan, D. W., 1983. A review of tectonic models of the Columbia Plateau and Pasco Basin, in Caggiano, J. A., and Duncan, D. W., eds., Preliminary interpretation of the tectonic stability of the reference repository location, Cold Creek syncline, Hanford Site: Rockwell Hanford Operations, Richland, Washington, RHO-BWI-ST-19, pp. 7-1 to 7-22.

Farooqui, S. M., Bunker, R. C., Thoms, R. E., Clayton, D. C., Bela, J. L., 1981. Post-Columbia River Basalt Group stratigraphy and map compilation of the Columbia Plateau, Oregon: Oregon Department of Geology and Mineral Resources Open-File Report O-81-10, 77 p.

Fecht, K. R., Reidel, S. P., and Tallman, A. M., 1982. Evolution of the Columbia River system in the central Columbia Plateau of Washington from the Miocene to the present [abs.]: Geological Society of America Abstracts with Programs, v. 14, n. 4, p. 163.

Fecht, K. R., Reidel, S. P., and Tallman, A. M., in press, Paleodrainage of the Columbia River system on the Columbia Plateau of Washington State: Geology of Washington Symposium Volume, Washington Department of Natural Resources, Division of Geology.

Finn, C., Phillips, W. M., Williams, D. L., 1984. Gravity maps of the State of Washington and adjacent areas: U.S. Geological Survey Open-File Report 84-416, scale 1:250,000.

Gardner, J. N., Snow, M. G., and Fecht, K. R., 1981. Geology of the Wallula Gap Area, Washington: Rockwell Hanford Operations, Richland, Washington, RHO-BWI-LD-9, 67 p.

Goff, F. E., and Myers, C. W., 1978. Structural evolution of east Umtanum and Yakima Ridges, south-central Washington [abs.]: Geological Society of America Abstracts with Programs, v. 10, n. 7, p. 408.

Grolier, M. J., and Bingham, J. W., 1966. Geology of parts of Grant, Adams, and Franklin Counties, east-central Washington: Washington Department of Natural Resources Division of Geology and Earth Resources, Bulletin 71, 91 p.

Hagood, M. C., in prep., Geologic map of the Mabton East, Prosser, Whitstran, Whitstran NE, Webber, 71/2' quadrangles and the south half of the Corral Canyon 71/2 quadrangle: Washington Department of Natural Resources, Division of Geology and Earth Resources, scale 1:48,000.

Jones, M. G., and Landon, R. D., 1978. Geology of the Nine Canyon Map Area: Rockwell Hanford Operations, Richland, Washington, RHO-BWI-LD-6.

Kienle, C. F., Jr., 1980. Geologic reconnaissance of parts of the Walla Walla and Pullman, Washington and Pendleton, Oregon 1° x 2° AMS quadrangles: Foundation Sciences, Inc., report to U.S. Army Corps of Engineers, Seattle District, Seattle, Washington, 76 p.

Kienle, C. F., Jr., Bentley, R. D., and Anderson, J. L., 1977. Geologic reconnaissance of the Cle Elum-Wallula lineament and related structures: Shannon and Wilson, Inc., Report to Washington Public Power Supply System, 33 p.

Kienle, C. F., Jr., Bentley, R. D., Farooqui, S. M., Anderson, J. L., Thomas, R. E., and Couch, R. C., 1978. The Yakima Ridges--an indication of an anomalous Plio-Pleistocene stress field [abs.]: Geological Society of America Abstracts with Programs, v. 10, n. 3, p. 111.

Konicek, D. L., 1975. Geophysical survey in south-central Washington: Northwest Science, v. 49, n. 2, pp. 106-117.

Landon, R. D., Long, P. E., and Reidel, S. P., 1982. Stratigraphy and flow distribution of Grande Ronde Basalt--evidence for early tectonic deformation in the central Columbia Plateau [abs.]: Geological Society of America Abstracts with Programs, v. 14, n. 6, p. 318.

Laubscher, H. P., 1981. Models of the development of Yakima deformation, in Final safety analysis report, WNP-2, Amendment 18, Appendix 250: Washington Public Power Supply System, Richland, Washington, 69 p.

Laval, W. N., 1956. Stratigraphy and structural geology of portions of south-central Washington: University of Washington, Seattle, Ph.D. dissertation, 208 p.

Lobdel, G. T., and Brown, J. C., 1977. Geophysical investigation of Washington's ground-water resources: Annual Report 1976/77: Washington State University, College of Engineering, Research Report 77/15-76, 17 p.

Long, P. E., and Duncan, R. A., 1982. $^{40}Ar/^{40}Ar$ ages of Columbia River basalt from deep boreholes in south-central Washington [abs.]: Proceedings of the 33rd Alaska Science Conference, Fairbanks, Alaska, p. 119, also, Rockwell Hanford Operations, Richland, Washington, RHO-BW-SA-233P.

Long, P. E., and Landon, R. D., 1981. Stratigraphy of the Grande Ronde Basalt, in Price, S. M., eds., Subsurface geology of the Cold Creek syncline: Rockwell Hanford Operations, Richland, Washington, RHO-BWI-ST-14.

Mackin, J. H., 1961. A stratigraphic section in the Yakima Basalt and Ellensburg Formations in south-central Washington: Washington Department of Conservation Division of Mines and Geology Report of Investigations 19, 45 p.

Mason, G. W., 1953. Interbasalt sediments of south-central Washington: Washington State University, Pullman, M.S. thesis, 116 p.

McKee, E. H., Swanson, D. A., and Wright, T. L., 1977. Duration and volume of Columbia River basalt volcanism, Washington, Oregon and Idaho [abs.]: Geological Society of America Abstracts with Programs, v. 9, n. 4, p. 463-464.

Mitchell, T. H. and Bergstrom, K. A., 1983. Pre-Columbia River Basalt Group stratigraphy and structure in the central Pasco Basin in Caggiano, J. A. and Duncan, D. W., eds., Preliminary interpretation of the tectonic stability of the reference repository location, Cold Creek syncline, Hanford Site: Rockwell Hanford Operations, Richland, Washington, RHO-BWI-ST-19, pp. 4-1 to 4-18.

Myers, C. W., 1973. Yakima basalt flows near Vantage, and from Coreholes in the Pasco Basin, Washington: University of California, Santa Cruz, Ph.D. dissertation, 147 p.

Myers, C. W., 1981. Bedrock structure of the Cold Creek syncline area, in Myers, C. W., Price, S, M., eds., Subsurface geology of the Cold Creek syncline: Rockwell Hanford Operations, Richland, Washington, RHO-BWI-ST-14.

Myers, C. W., Price, S, M., Caggiano, J. A., Cochran, M. P., Czimer, W. J., Davidson, N. J., Edwards, R. C., Fecht, K. R., Holmes, G. E., Jones, M. G., Kunk, J. R., Price, E. H., Reidel, S. P., and Tallman, A. M., 1979. Geologic studies of the Columbia Plateau: a status report: Rockwell Hanford Operations, Richland, Washington, RHO-BWI-ST-4.

Newcomb, R. C., 1970. Tectonic structure of the main part of the basalt of the Columbia River Group, Washington, Oregon, and Idaho: U.S. Geological Survey Miscellaneous Geological Investigations Map I-587, scale 1:500,000.

Newcomb, R. C., 1971. Geologic map of the proposed Paterson Ridge pumped-storage reservoir, south-central Washington: U.S. Geological Survey Water Investigations Map I-653.

Pearson, H. E., 1973. Test-observation well near Paterson, Washington: Description and preliminary results: U.S. Geological Survey Water Resources Investigation 9-73, 23 p.

Powell, VanDiver-, L., 1978. The structure, stratigraphy, and correlation of the Grande Ronde Basalts on Tygh Ridge, Wasco County, Oregon, University of Idaho, Moscow, M.S. thesis, 57 p.

Price, E. H., 1981. Structural geometry, strain distribution, and mechanical evolution of eastern Umtanum Ridge at Priest Rapids, and a comparison with other selected localities within Yakima folds structures, south-central Washington: Rockwell Hanford Operations, Richland, Washington, RHO-BWI-SA-138, 199 p.

Price, S. M., 1977. An evaluation of dike-flow correlations indicated by geochemistry, Chief Joseph swarm, Columbia River basalt: Rockwell Hanford Operations, Richland, Washington, RHO-SA-59, 322 p.

Raisz, E., 1945. The Olympic-Wallowa lineament: American Journal of Science, v. 243-A, pp. 479-485.

Reidel, S. P., 1978. Geology of the Saddle Mountains between Sentinel Gap and 119° 30' longitude: Rockwell Hanford Operations, Richland, Washington, RHO-BWI-LD-4, 75 p.

Reidel, S. P., 1984. The Saddle Mountains: The evolution of an anticline in the Yakima Fold belt: American Journal of Science, v. 284, pp. 942-978.

Reidel, S. P. and Fecht, K. R., 1981. Wanapum and Saddle Mountains Basalts of the Cold Creek syncline area, in Myers, C. W., and Price, S. M., eds., Subsurface geology of the Cold Creek syncline: Rockwell Hanford Operations, Richland, Washington, RHO-BWI-ST-14, pp. 3-1 to 3-45.

Reidel, S. P. and Fecht, K. R., 1982. Uplift and subsidence rates in the central Columbia Plateau and their relation to siting a waste repository [abs.]: Geological Society of America Abstracts with Programs, v. 14, n. 6, p. 347.

Reidel, S. P., Ledgerwood, R. K., Myers, C. W., Jones, M. G., and Landon, R. J., 1980. Rate of deformation in the Pasco Basin during the Miocene as determined by distribution of Columbia River basalt flows [abs]: Geological Society of America Abstracts with Programs, v. 12, n. 3, p. 149; also Rockwell Hanford Operations, Richland, Washington, RHO-BWI-SA-29.

Reidel, S. P., Long, P. E., Myers, C. W., and Mase, J., 1982. New evidence for greater than 3.2 km of Columbia River basalt beneath the central Columbia Plateau [abs]: EOS, Transactions of the American Geophysical Union, v. 63, no. 8, p. 173; also Rockwell Hanford Operations, Richland, Washington, RHO-BWI-SA-162A.

Reidel, S. P., Fecht, K. R., and Cross, R. W., 1983a. Constraints of tectonic models for the Columbia Plateau from the age and growth rates of Yakima folds [abs.]: EOS, Transactions of the American Geophysical Union, v. 64, p. 87.

Reidel, S. P., Cross, R. W., and Fecht, K. R., 1983b. Constraints on tectonic models as provided from strain rates, in Caggiano, J. A., and Duncan, D. W., eds., Preliminary interpretation of the tectonic stability of the reference repository location, Cold Creek syncline, Hanford Site: Rockwell Hanford Operations, Richland, Washington, RHO-BWI-ST-19, pp. 5-1 to 5-19.

Reidel, S. P., Scott, G. R., Bazard, D. R., Cross, R. W., and Dick, B., 1984. Post 12 Ma clockwise rotation in the central Columbia Plateau, Washington: American Geophysical Union Tectonics, v. 3, n. 2, pp. 257-273.

Reitman, J. D., 1966. Remnant magnetism of the Late Yakima Basalt, Washington State: Stanford University, Stanford, Ph.D. dissertation, 114 p.

Rigby, J. G., and Othberg, Kathy, 1979. Reconnaissance surficial geologic mapping of the late Cenozoic sediments of the Columbia Basin, Washington: Washington State Department of Natural Resources, Division of Geology and Earth Resources, Open File Report 79-3, 88 p.

Robbins, S. L., Burt, R. J., and Gregg, D. O., 1975. Gravity and aeromagnetic study of part of the Yakima River basin, Washington: U.S. Geological Survey Professional Paper 726E, 7 p.

Rockwell Hanford Operations, 1984. unpublished borehole data, SD-BWI-DP-035 Rev. B-0.

Rohay, A. C. and Davis, J. D., 1983. Contemporary deformation in the Pasco Basin area of the central Columbia Plateau, in Caggiano, J. A. and Duncan, D. W., eds., Preliminary interpretation of the tectonic stability of the reference repository location, Cold Creek syncline, Pasco Basin: RHO-BWI-ST-19, Richland, Washington, Rockwell Hanford Operations, pp. 6-1 to 6-30.

Russell, I. G., 1893. Geologic reconnaissance in central Washington: U.S. Geological Survey Bulletin 108, 108 p.

Schmincke, H. U., 1964. Petrology, paleocurrents, and stratigraphy of the Ellensburg Formation and interbedded Yakima basalt flows, south-central Washington: John Hopkins University, Baltimore, Maryland, Ph.D. dissertation.

Schmincke, H. U., 1967a. Fused tuff and peperites in south-central Washington: Geological Society of America Bulletin, v. 78, pp. 319-330.

Schmincke, H. U., 1967b. Graded lahars in the type sections of the Ellensburg Formation, south-central Washington: Journal of Sedimentary Petrology, v. 37, n. 2, pp. 438-448.

Schmincke, H. U., 1967c. Stratigraphy and petrography of four upper Yakima Basalt flows in south-central Washington: Geological Society of America Bulletin, v. 78, pp. 1385-1422.

Schmincke, H. U., 1967d. Flow directions in Columbia River basalt flows and paleocurrents of interbedded sedimentary rocks, south-central Washington: Geologische Rundschaw, v. 56, pp. 992-1020.

Shannon and Wilson, 1973. Geologic studies of Columbia River basalt structures and age of deformation, the Dalles-Umatilla region, Washington and Oregon, Boardman Nuclear Project: Shannon and Wilson, Inc., for the Portland General Electric Company, Portland, Oregon.

Shaw, H. P. and Swanson, D. A., 1970. Eruption and flow rates of flood basalts, in Gilmour, E. H. and Stradling, D., eds., Proceedings of the Second Columbia River Basalt Symposium, Cheney, Washington, March 1969: Eastern Washington State College Press, Cheney, pp. 271-300.

Shedd, S., 1925. Geologic map of Pasco and Prosser quadrangles, Washington: Washington State Department of Conservation and Development, Bulletin 32, Plate 1, scale 1:125,000.

Sheriff, S. D., 1984. Paleomagnetic evidence for spatially distributed post-Miocene rotation of western Washington and Oregon: American Geophysical Union Tectonics, v. 3, n. 3, pp. 397-408.

Siems, B. A., Crosby, J. W., III, Anderson, J. V., Bush, J. H., and Weber, T. L., 1973. Final report 1972/73, Geophysical investigations of Washington's ground-water resources: Washington State University, College of Engineering, Research Report 73/1558.

Siems, B. A., Bush, J. H., and Crosby, J. W., III, 1974. TiO_2 a geophysical logging criteria for Yakima Basalt correlation, Columbia Plateau: Geological Society of America Bulletin, v. 85, n. 7, pp. 1061-1068.

Strait, S. R., 1978. Theoretical analysis of local ground-water flow in the Bickleton area, Washington: Washington State University, Pullman, M.S. thesis, 70 p.

Swanson, D. A. and Wright, T. L., 1976. Guide to field trip between Pasco, and Pullman, Washington emphasizing stratigraphy, vent areas, and intracanyon flows of Yakima Basalt: Geological Society of America, Cordilleran Section Meeting, Field Guide No. 1, 33 p.

Swanson, D. A. and Wright, T. L., 1978. Bedrock geology of the northern Columbia Plateau and adjacent area, in Baker, V. R., and Nummendal, D., eds., The channeled scabland, a guide to the geomorphology of the Columbia Basin, Washington: Planetary Geologic Program, Office of Space Science, National Aeronautics and Space Administration, Washington, D.C., pp. 37-57.

Swanson, D. A., Anderson, J. L., Bentley, R. D., Camp, V. W., Gardner, J. N., and Wright, T. L., 1979a. Reconnaissance geologic map of the Columbia River Basalt Group in Eastern Washington and Northern Idaho: U.S. Geological Survey Open-File Report 79-1363, scale 1:250,000.

Swanson, D. A., Brown, J. C., Anderson, J. L., Bentley, R. D., Byerly, G. R., Gardner, J. N., and Wright, T. L., 1979b. Preliminary structure contour maps on the top of the Grande Ronde and Wanapum Basalts, eastern Washington and northern Idaho: U.S. Geological Survey, Open-File Report 79-1364.

Swanson, D. A., Wright, T. L., Hooper, P. R., and Bentley, R. D., 1979c. Revision in stratigraphic nomenclature of the Columbia River Basalt Group: U.S. Geological Survey Bulletin 1457-G, 59 p.

Swanson, D. A., Wright, T. L., and Helz, R. T., 1975. Linear vent systems and estimated rates of magma production and eruption for the Yakima Basalt on the Columbia Plateau: American Journal of Science, v. 275, n. 8, pp. 877-905.

Sylvester, J. S., 1978. Geophysical investigations of the hydrogeology of the Goldendale-Centerville Areas, Washington: Washington State University, Pullman, M.S. thesis, 160 p.

Tabor, R. W. and Frizzel, V. A., Jr., 1979. Tertiary movement along the southern segment of the Straight Creek fault and its relation to the Olympic-Wallowa lineament in the central Cascades, Washington: Geological Society of America Abstracts with Programs, v. 11, n. 8, p. 131.

Tabor, R. W., Waitt, R. B., Jr., Frizzell, V. A., Jr., Swanson, D. A., Byerly, G. R., and Bentley, R. D., 1982. Geologic map of the Wenatchee 1:100,000 quadrangle, Washington: U.S. Geological Survey, Miscellaneous Investigations Series Map I-1311.

Taylor, T. L., 1976. The basalt stratigraphy and structure of the Saddle Mountains of south-central Washington: Washington State University, Pullman, M.S. thesis, 116 p.

Tallman, A. M., Lillie, J. T., and Fecht, K. R., 1981. Suprabasalt sediments of the Cold Creek Syncline area, in Myers, C. W. and Price, S. M., eds., Subsurface geology of the Cold Creek syncline: Rockwell Hanford Operations, Richland, Washington, RHO-BWI-ST-14, 28 p.

Taubeneck, W. H., 1970. Dikes of Columbia River basalt in northeastern Oregon, western Idaho, and southeastern Washington, in Gilmour, E. H., and Stradling, D., eds., Proceedings of the second Columbia River Basalt Symposium, Cheney, Washington, March 1969: Eastern Washington State College Press, Cheney, Washington, pp. 73-96.

Tolan, T. L., Beeson, M. A., and Vogt, B., 1984. Exploring the Neogene history of the Columbia River: Discussion and geologic field trip guide to the Columbia River: Oregon Geology, v. 46, n. 8, pp. 87-97.

Van Alstine, D. R. and Gillett, S. L., 1981. Magnetostratigraphy of the Columbia River basalt, Pasco Basin and vicinity, Washington: Rockwell Hanford Operations, RHO-BWI-C-110, 60 p.

Waitt, R. B., 1979. Late Cenozoic deposits, landforms, stratigraphy and tectonism in Kittitas Valley, Washington: U.S. Geological Survey Professional Paper 1127, 18 p.

Waring, G. A., 1913. Geology and water resources of a portion of south-central Washington: U.S. Geological Survey Water Supply Paper 316, 46 p.

Warren, C. R., 1941a. The Hood River Conglomerate in Washington: American Journal of Science, v. 239, p. 106-127.

Warren, C. R., 1941b. Course of the Columbia River in south-central Washington: American Journal of Science, v. 239, p. 209-232.

Waters, A. C., 1955. Geomorphology of south-central Washington, illustrated by the Yakima East quadrangle: Geological Society America Bulletin, v. 66, pp. 663-684.

Waters, A. C., 1961. Stratigraphic and lithologic variations in the Columbia River basalt: American Journal of Science, v. 274, pp. 583-611.

Watkins, N. O. and Baski, A. K., 1974. Magnetostratigraphy and oroclinal folding of the Columbia River, Steens and Owyhee basalt in Oregon, Washington and Idaho: American Journal of Science, 274, pp. 148-189.

WPPSS, 1977. Preliminary Safety Analysis Report: Amendment 23, v. 1 and 2, Washington Public Power Supply System, Richland, Washington.

Wright, T. I., Grolier, M. H., and Swanson, D. A., 1973. Chemical variation related to the stratigraphy of the Columbia River basalt: Geological Society of America Bulletin, v. 84, pp. 371-386.

APPENDIX A

CHEMICAL ANALYSES

Chemical analyses of CRB samples are shown in Table IV. Most of the analyses are for major oxide concentrations and were determined by the x-ray fluorescence method, completed at Washington State University under the direction of Dr. Peter Hooper under contract to the Rockwell Hanford Operations. Concentrations of the trace element Cr were taken from the unpublished data of Beeson, Fecht, Tolan, and Reidel, 1984.

TABLE IV

CHEMICAL ANALYSES OF COLUMBIA RIVER BASALT GROUP FLOWS IN THE STUDY AREA. (SHEET 1 OF 4)

SENTINEL BLUFFS SEQUENCE

Sample #	SiO_2	Al_2O_3	FeO[1]	MgO	CaO	Na_2O	K_2O	TiO_2	P_2O_5	MnO
SS158015	53.14	14.98	11.95	4.77	8.62	2.63	1.18	1.99	0.34	0.21
SS158816	52.79	15.63	11.77	5.05	8.66	2.56	1.01	1.83	0.30	0.20
C 8376	54.10	15.14	11.00	4.62	8.69	2.66	1.33	1.76	0.30	0.19

FRENCHMAN SPRINGS MEMBER

BASALT OF GINGKO

Sample #	SiO_2	Al_2O_3	FeO	MgO	CaO	Na_2O	K_2O	TiO_2	P_2O_5	MnO
SS144014	49.56	14.45	14.85	4.38	8.43	2.93	1.00	3.11	0.62	0.23
SS152015	50.85	14.22	14.25	4.38	8.04	2.85	1.30	3.06	0.61	0.24
C 8375	51.58	14.22	14.20	4.21	8.05	2.38	1.33	3.03	0.60	0.21

BASALT OF SILVER FALLS

Sample #	SiO_2	Al_2O_3	FeO*	MgO	CaO	Na_2O	K_2O	TiO_2	P_2O_5	MnO	Cr[2]
MH83SS132030	51.45	13.89	14.00	4.50	8.53	2.52	1.05	3.10	0.53	0.22	15.90
MH83SS138040	52.14	14.07	14.38	3.66	8.38	2.33	1.21	3.06	0.54	0.21	16.90

BASALT OF SAND HOLLOW

Sample #	SiO_2	Na_2O	FeO	MgO	CaO	Na_2O	K_2O	TiO_2	P_2O_5	MnO	Cr
MH82H206	51.26	14.77	13.69	4.51	8.05	2.48	1.51	2.82	0.50	0.21	
MH82H207	51.15	14.66	13.81	4.56	8.10	2.46	1.48	2.87	0.49	0.22	
MH82H220	51.55	14.65	13.67	4.38	7.93	2.84	1.19	2.90	0.50	0.20	
SS105010	50.23	14.69	13.93	4.52	8.60	2.69	1.00	3.04	0.53	0.24	
MH83SS124050	51.70	13.48	14.23	4.39	8.65	2.44	1.29	2.88	0.53	0.22	37.40
C 8373	52.53	14.73	12.74	4.04	8.59	2.32	1.27	2.86	0.48	0.18	
C 8374	51.51	14.42	13.85	4.63	8.20	2.37	1.30	2.84	0.48	0.20	

[1] $FeO = FeO + .9(Fe_2O_3)$

[2] All chrome data is from Beeson, Fecht, Reidel, and Tolan, 1984. All values in ppm.

* All values in wt. %

TABLE IV

CHEMICAL ANALYSES OF COLUMBIA RIVER BASALT GROUP FLOWS IN THE STUDY AREA. (SHEET 2 OF 4)

BASALT OF SENTINEL GAP

Sample #	SiO_2	Na_2O	FeO	MgO	CaO	Na_2O	K_2O	TiO_2	P_2O_5	MnO	Cr
MH81089	51.11	14.41	13.97	4.09	8.21	3.03	1.18	3.08	0.51	0.20	
MH82HH16	49.72	15.29	12.86	4.49	9.20	3.17	1.05	3.21	0.59	0.22	
MH82H205	51.53	14.96	13.27	4.10	8.03	2.52	1.50	3.11	0.56	0.22	
MH82H218	51.54	14.78	13.83	4.09	7.79	2.58	1.44	2.98	0.55	0.21	
MH82H219	51.80	15.46	12.06	4.18	8.73	2.69	1.09	3.10	0.52	0.17	
SS960970	51.44	14.28	13.89	4.17	8.11	2.76	1.44	2.92	0.56	0.23	
MH83SS810820	51.57	14.22	13.85	4.51	8.19	2.19	1.36	3.15	0.55	0.22	
SS960970	51.44	14.28	13.89	4.17	8.11	2.76	1.44	2.92	0.56	0.23	16.10
C 8371	51.66	14.06	14.17	4.24	8.02	2.49	1.39	3.03	0.53	0.20	
C 8372	51.90	14.09	14.15	4.07	7.76	2.72	1.42	2.91	0.57	0.21	

PRIEST RAPIDS MEMBER

ROSALIA FLOW

Sample #	SiO_2	Na_2O	FeO	MgO	CaO	Na_2O	K_2O	TiO_2	P_2O_5	MnO
MH81083	48.82	14.35	14.24	5.14	9.03	3.23	0.98	3.12	0.66	0.22
MH81087	49.80	15.21	13.08	4.40	9.28	3.07	0.89	3.22	0.55	0.20
MH82H179	49.38	14.44	14.01	5.12	9.02	2.56	1.12	3.22	0.70	0.23
MH82H185	50.34	14.89	13.12	4.96	8.95	2.53	0.94	3.19	0.65	0.23
SS620630	50.82	14.78	12.80	5.19	8.54	2.54	1.12	3.13	0.65	0.22
SS750760	50.59	14.34	14.61	4.63	7.68	2.71	1.27	3.06	0.68	0.23
C 8370	50.51	14.36	13.59	4.80	8.86	2.41	1.17	3.24	0.67	0.20

LOLO FLOW

Sample #	SiO_2	Na_2O	FeO	MgO	CaO	Na_2O	K_2O	TiO_2	P_2O_5	MnO
MH81086	49.68	14.14	13.23	4.15	9.67	3.26	0.81	3.92	0.72	0.20
MH82HH75	51.11	16.48	13.58	3.82	7.33	2.72	0.36	3.52	0.69	0.20
MH82H175	50.59	14.18	14.41	4.34	7.94	2.69	1.22	3.53	0.68	0.22
MH82180	50.18	14.72	14.09	4.27	8.42	2.60	0.99	3.63	0.65	0.24

TABLE IV

CHEMICAL ANALYSES OF COLUMBIA RIVER BASALT GROUP FLOWS IN THE STUDY AREA. (SHEET 3 OF 4)

UMATILLA MEMBER

UMATILLA FLOW

Sample #	SiO_2	Al_2O_3	FeO	MgO	CaO	Na_2O	K_2O	TiO_2	P_2O_5	MnO
MH82HH21	53.05	15.36	12.18	3.27	6.42	2.93	2.63	3.05	0.72	0.19
MH82HH67	51.59	14.74	12.94	3.36	7.74	2.32	2.97	3.20	0.72	0.22
MH82HH69	53.62	15.54	11.86	2.83	6.39	3.07	2.48	3.15	0.71	0.16
MH82H154	53.88	15.15	12.31	2.91	6.25	2.90	2.49	2.98	0.74	0.18
MH82H166	54.66	15.54	10.10	2.72	7.04	2.88	2.56	3.22	0.75	0.30
MH82H176	53.12	14.93	12.72	3.18	6.30	3.22	2.35	3.08	0.73	0.19
MH82H189	53.28	15.07	12.60	3.23	6.33	2.79	2.60	2.94	0.76	0.21
MH82H234	53.07	15.04	12.79	2.89	6.32	3.34	2.46	2.94	0.75	0.20
MH82H235	53.07	14.65	13.72	3.28	5.86	2.79	2.50	3.03	0.75	0.16
MH82H279	53.27	14.98	12.34	3.00	6.53	2.99	2.74	3.01	0.75	0.19
SS470480	53.07	15.40	12.76	3.30	6.10	2.83	2.49	2.92	0.73	0.20
C 8369	53.80	14.66	12.70	2.95	6.37	2.93	2.51	3.00	0.71	0.17

SILLUSI FLOW

Sample #	SiO_2	Al_2O_3	FeO	MgO	CaO	Na_2O	K_2O	TiO_2	P_2O_5	MnO
MH81062	53.73	15.13	12.55	2.87	6.01	3.23	2.60	2.71	0.78	0.19
MH82H159	53.87	15.32	12.56	2.72	5.75	3.19	2.70	2.64	0.85	0.20
MH82H174	53.88	15.19	12.37	2.66	5.92	2.88	3.11	2.61	0.98	0.21
MH82H182	54.45	15.21	12.37	2.63	5.87	2.79	2.77	2.64	0.88	0.18
MH82H183	54.31	15.65	11.35	2.80	6.18	2.53	3.22	2.66	0.89	0.20
SS350360	54.13	15.25	12.33	2.97	5.96	2.69	2.00	2.63	0.87	0.22

ESQUATZEL MEMBER

Sample #	SiO_2	Al_2O_3	FeO	MgO	CaO	Na_2O	K_2O	TiO_2	P_2O_5	MnO
MH81063	53.64	14.89	11.55	3.74	7.80	2.90	1.66	3.05	0.37	0.19
MH82HH38	51.85	15.23	12.72	3.65	7.97	2.73	1.66	3.34	0.47	0.18
MH82HH45	52.79	15.56	11.43	3.87	7.80	2.68	1.84	3.22	0.43	0.18
MH82HH56	51.65	14.76	13.70	3.78	7.56	2.62	1.92	3.22	0.41	0.20
MH82HH64	49.61	13.98	14.23	3.67	10.26	2.46	1.78	3.20	0.40	0.20
MH82HH65	51.67	14.29	13.41	4.03	7.59	2.87	2.09	3.17	0.42	0.25
MH82HH72	53.51	15.21	12.95	3.72	6.17	2.64	1.83	3.08	0.49	0.19
MH82HH87	48.44	15.29	14.29	3.80	10.59	2.15	1.04	3.55	0.48	0.18

TABLE IV

CHEMICAL ANALYSES OF COLUMBIA RIVER BASALT GROUP FLOWS IN THE STUDY AREA. (SHEET 4 OF 4)

POMONA MEMBER

Sample #	SiO_2	Al_2O_3	FeO	MgO	CaO	Na_2O	K_2O	TiO_2	P_2O_5	MnO
MH81035	51.66	15.32	10.45	6.68	10.43	2.83	0.41	1.60	0.24	0.18
MH81045	51.44	15.35	10.20	6.86	10.56	2.88	0.49	1.62	0.21	0.18
MH81055	51.56	15.76	9.79	6.64	11.01	2.90	0.21	1.62	0.22	0.18
MH81057	53.43	15.63	10.97	5.03	8.82	2.89	0.78	1.80	0.25	0.18
MH81064	51.74	16.23	11.73	6.38	10.74	2.75	0.17	1.66	0.23	0.17
MH81065	50.16	15.10	11.19	6.93	10.84	3.04	0.38	1.73	0.25	0.19
MH81071	51.20	15.49	10.75	6.81	10.35	2.83	0.40	1.59	0.21	0.18
MH81072	51.36	15.67	10.35	6.49	10.56	2.98	0.38	1.61	0.22	0.18
MH81092	51.37	15.32	10.27	6.57	10.72	3.01	0.53	1.62	0.22	0.18
MH81093	51.42	15.77	10.02	6.25	10.86	2.93	0.51	1.63	0.22	0.18
MH81100	51.54	15.52	10.30	6.72	10.37	2.84	0.55	1.57	0.21	0.18
MH81101	51.60	15.42	10.35	6.53	10.50	2.88	0.53	1.60	0.22	0.18
MH82HH34	51.22	15.90	10.08	6.68	10.91	2.29	0.56	1.72	0.27	0.17
MH82HH35	51.59	15.98	10.28	6.49	10.34	2.39	0.57	1.71	0.26	0.17
MH82HH37	50.99	15.98	10.10	6.55	10.93	2.49	0.45	1.85	0.29	0.18
MH82HH46	51.44	15.91	10.30	6.54	10.49	2.26	0.63	1.78	0.27	0.18
MH82HH49	51.01	15.78	10.08	6.76	10.77	2.70	0.46	1.82	0.27	0.17
MH82HH58	50.83	15.75	10.30	6.80	10.57	2.80	0.49	1.81	0.28	0.18
MH82HH60	52.37	16.26	10.27	6.42	9.60	2.14	0.56	1.73	0.27	0.17
MH82HH61	50.94	15.89	10.37	6.81	10.60	2.29	0.67	1.76	0.26	0.19
MH82HH76	53.05	16.57	9.72	6.62	9.00	2.46	0.37	1.60	0.26	0.16
MH82HH77	52.31	16.04	10.18	6.57	10.35	1.99	0.32	1.65	0.24	0.16
MH82H102	51.46	15.78	10.35	6.92	10.32	2.23	0.57	1.73	0.25	0.17
MH82H124	52.06	16.42	10.89	5.61	11.50	2.58	0.56	1.69	0.24	0.26
MH82H152	51.65	15.39	10.71	6.66	10.50	2.05	0.67	1.72	0.23	0.23
MH82H153	51.23	15.82	10.91	6.62	10.25	2.28	0.54	1.72	0.26	0.18
MH82H276	51.51	15.73	11.20	6.41	10.37	2.20	0.21	1.75	0.26	0.17
MH82H280	51.74	15.66	10.54	6.46	10.51	2.22	0.53	1.69	0.26	0.17
SS170180	51.59	15.73	10.69	6.90	10.08	2.17	0.55	1.69	0.23	0.18

ELEPHANT MOUNTAIN MEMBER

Sample #	SiO_2	Al_2O_3	FeO^*	MgO	CaO	Na_2O	K_2O	TiO_2	P_2O_5	MnO
MH82H100	49.62	14.24	14.83	4.45	8.52	2.45	1.38	3.58	0.51	0.21
MH82H101	51.01	15.01	13.17	4.41	8.60	2.31	1.00	3.63	0.48	0.20
MH82H252	50.30	14.38	14.19	4.46	8.31	2.79	1.19	3.49	0.48	0.21
MH82H253	50.03	14.23	14.67	4.10	8.58	2.58	1.24	3.64	0.52	0.21
MH82H278	50.62	14.41	14.11	4.43	8.39	2.43	1.09	3.61	0.48	0.22
MH82H283	50.65	14.28	15.10	3.89	8.10	2.38	1.18	3.51	0.51	0.21
SS8090	49.85	14.32	14.74	4.59	8.38	2.23	1.00	3.63	0.50	0.22

APPENDIX B

BOREHOLE LOGS

Borehole Geophysical Logs

Methods for identifying CRB flows and Ellensburg Formation interbeds from borehole geophysical logs in this study is based on a series of reports, theses, and articles prepared by the faculty, staff, and students of Washington State University, College of Engineering (Crosby and Anderson 1971; Crosby and others 1972; Anderson and others 1973; Siems and others 1973; Lobdell and Brown 1977; Brown 1978; Strait 1978; Sylvester 1978; Biggane 1982). Their work was concerned with characterizing the geohydrologic regime beneath portions of the Columbia Plateau.

The majority of borehole geophysical logs were gathered from the Washington State University College of Engineering, but also from the Washington State Department of Ecology, Rockwell Hanford Operations, and unpublished logs from the U.S. Geological Survey in Tacoma, Washington. In addition, at the request of the writer, Rockwell Hanford Operations conducted borehole geophysical logging of the Chandler well (Fig. 69).

Generally, the most useful logs in this study were the various radiation logs (gamma-gamma, neutron-gamma, neutron-epithermal, neutron, and natural gamma) which were used to pinpoint stratigraphic

specific borehole may consist from one to all of these radiation logs. Caliper and electric logs were also contained in certain suites of logs, but are not included in the appendix. If prior stratigraphic interpretations of pertinent logs had been done by other workers, they were checked and evaluated by the author.

The gamma-gamma, neutron-gamma, and neutron-epithermal neutron logs measure radioactive emissions reflected off the wall rock from a downhole probe source. These logs reflect the density (gamma-gamma) and porosity (moisture content; neutron-gamma, neutron-epithermal neutron) of the wall rock. For this study, the logs were used for locating stratigraphic contacts.

The natural gamma log is a recording of the natural radioactive (primarily ^{40}K) emission of the rock in the borehole. Since this emission is directly related to the concentration of total potassium in the wall rock, the natural gamma log can be used to identify individual basalt flows. Major variations in K_2O between individual basalt members (e.g., Umatilla and Pomona Members) are reflected in the natural gamma log (see Fig. 5). Sedimentary interbeds of the Ellensburg Formation often, but not always, contain K-rich clays which provide a high gamma "kick" in the natural gamma log.

Drillers' logs are available for many of the geophysically logged boreholes; geologists' logs are rare (e.g., Paterson Test Well, Pearson 1973). Both were consulted during interpretations of the borehole geophysical logs.

Drill cuttings of the CRB were collected from the Moon #1 well and were cursorily inspected to ascertain their identities. Cuttings from several intervals were then analyzed for their major oxide concentrations to confirm identities. XRF analyses of basalt were also available for the Horse Heaven Test well. Basalt samples extracted from Boreholes DC-15 and DDH-3, located in the Pasco Basin, have been chemically analyzed in detail to confirm basalt flow identities and serve as reference boreholes for correlating geophysical logs.

Although the Wanapum Basalt was frequently penetrated by boreholes, certain chemical and physical factors thwarted confident identification the Wanapum basalt flows. These factors were (1) immeasurable differences in K_2O content between the Priest Rapids, Roza, and Frenchman Springs Members; (2) multiple vesicular zones within an individual basalt flow; (3) variations in the total number of flows within a member; (4) the discontinuous nature of the interbedded sediments; (5) the nonuniform thickness of the basalt flows and sedimentary interbeds. However, in two boreholes (Grandview City, Prosser Experiment Station) this problem was overcome by correlating the borehole geophysical logs with those of boreholes DDH-3 and DC-15.

Driller's Logs

Driller's logs provided additional control for constructing isopach maps. Although driller's logs are one of the least reliable tools for identifying stratigraphic units, they can, with caution, be

most effective. Over 90 driller's logs were used for this study. Logs were obtained from both the Washington State Department of Ecology and from files of Rockwell Hanford Operations, Richland, Washington.

Successful identification of CRB flows or Ellensburg Formation sediments using Driller's logs is dependent primarily upon the driller's ability to differentiate sedimentary interbeds from the basalt flows, and secondarily, that person's ability to recognize variations in the physical properties of the sediments or basalt (e.g., vesicular flow top). The driller is able to do this by noting differences in the drilling rate and in drill cuttings. Identification of the stratigraphic units takes into account the local stratigraphy determined from field mapping from this and other studies and borehole geophysical logs. In addition, it is necessary to become acquainted with the diverse terminology used for describing drill cuttings. During an evaluation of these driller's logs many were discarded because of lack of credibility, a judgment made by the author.

Interpretations were complicated by: (1) inconsistencies in the quality and style of reporting found in the driller's logs, (2) proximity of well sites to complex or unknown structure, (3) lack of stratigraphic control nearby, (4) the discontinuous nature of sedimentary interbeds (e.g., Selah interbed), and (5) low-volume flows (e.g., Esquatzel Member). As is the case with the borehole geophysical logs, driller's logs are inadequate in delineating Wanapum Basalt flows and intercalated sedimentary interbeds.

TABLE V

BOREHOLE GEOPHYSICAL LOGS USED IN STUDY

LOCATION	BOTTOM-HOLE DEPTH (METERS)	WELL DESIGNATION	LOG SOURCE	PRIOR STRAT. INTERP.
7N/22E-23B	990.0	SHARPE	W.S.U.	4
7N/23E-36R	245.4	CHESLEY	W.S.U.	4
7N/24E-08D	329.5	HORRIGAN FARMS	W.S.U.	
7N/25E-23F	380.7	PALMER 2	W.S.U.	
7N/25E-35M	307.2	PALMER	W.S.U.	
7N/25E-36F	264.3	BARBER 2	W.S.U	
7N/25E-36N	256.0	PATERSON TEST WELL	W.S.U.	1
7N/26E-05B	327.7	MOON	W.S.U	1
7N/26E-30R	159.4	MOON 1	W.S.U.	
7N/27E-36A	368.5	HORSE HEAVEN TEST WELL	W.S.U.	6
8N/22E-11J	161.5	FLOWER	W.S.U.	5
8N/24E-01J	381.0	PROSSER MUNICIPAL WELL	W.S.U.	3
8N/24E-10N	188.1	LONG	U.S.G.S.	
8N/27N-29Q	221.0	SMITH	W.S.U.	
8N/28E-28N	508.4	MILLER	W.S.U.	
8N/28E-34C	197.2	CLODFELTER	W.S.U.	1
9N/23E-22J	429.5	GRANDVIEW CITY	W.S.U.	
9N/25E-06B	366.4	PROSSER EXPERIMENT STATION	W.S.U.	
9N/25E-07J	206.7	GOROCH	W.S.U.	
9N/26E-20A	209.4	BAUDER (CHANDLER)	R.H.O.	
9N/27E-25M	322.2	79-07	R.H.O.	
9N/28E-34H	271.0	BAUDER	R.H.O.	
10N/23E-04L	150.3	YAKIMA VALLEY COLLEGE	R.H.O.	2
10N/23E-17B	359.7	STOUT	R.H.O.	3
10N/23E-36A	401.1	EVANS	R.H.O.	3
10N/23E-36G	283.5	WHITE	R.H.O.	
10N/24E-24F	140.2	AARONS	U.S.G.S.	
10N/25E-25E	184.1	NAKAMURA	U.S.G.S.	
10N/25E-33N	275.5	J & R ORCHARDS	W.S.U.	
10N/26E-27Q	236.2	SHAW	W.S.U.	3
10N/28E-14F	1079.0	DDH-3	R.H.O.	7
11N/28E-35F	1293.2	DC-15	R.H.O.	7

1. Crosby and others, 1972
2. Brown, unpub. data, 1973
3. Lobdel and Brown, 1977
4. Brown, 1978
5. Washington State University, unpub. data, date unknown
6. Washington State Department of Ecology, unpub. data, date unknown
7. Rockwell Hanford Operations- document SD-BWI-DP-035 Rev. B-O

LEGEND

Stratigraphic contact

Water table

GG = Gamma Gamma Log
NN = Neutron-Epithermal Neutron Log
NATG = Natural Gamma Log
NG = Neutron Gamma Log

TI = Ice Harbor Member
TEM = Elephant Mountain Member
TER = Rattlesnake Ridge interbed
TP = Pomona Member
TES = Selah interbed
TE = Esquatzel Member
TECC = Cold Creek interbed
TU = Umatilla Member
TEMA = Mabton interbed
TPR = Priest Rapids Member
TSC = Squaw Creek interbed
TR = Roza Member
TF = Frenchman Springs Member
TGR = Grande Ronde Basalt

• Sampled for chemical analysis

Figure 49. Legend for borehole geophysical logs.

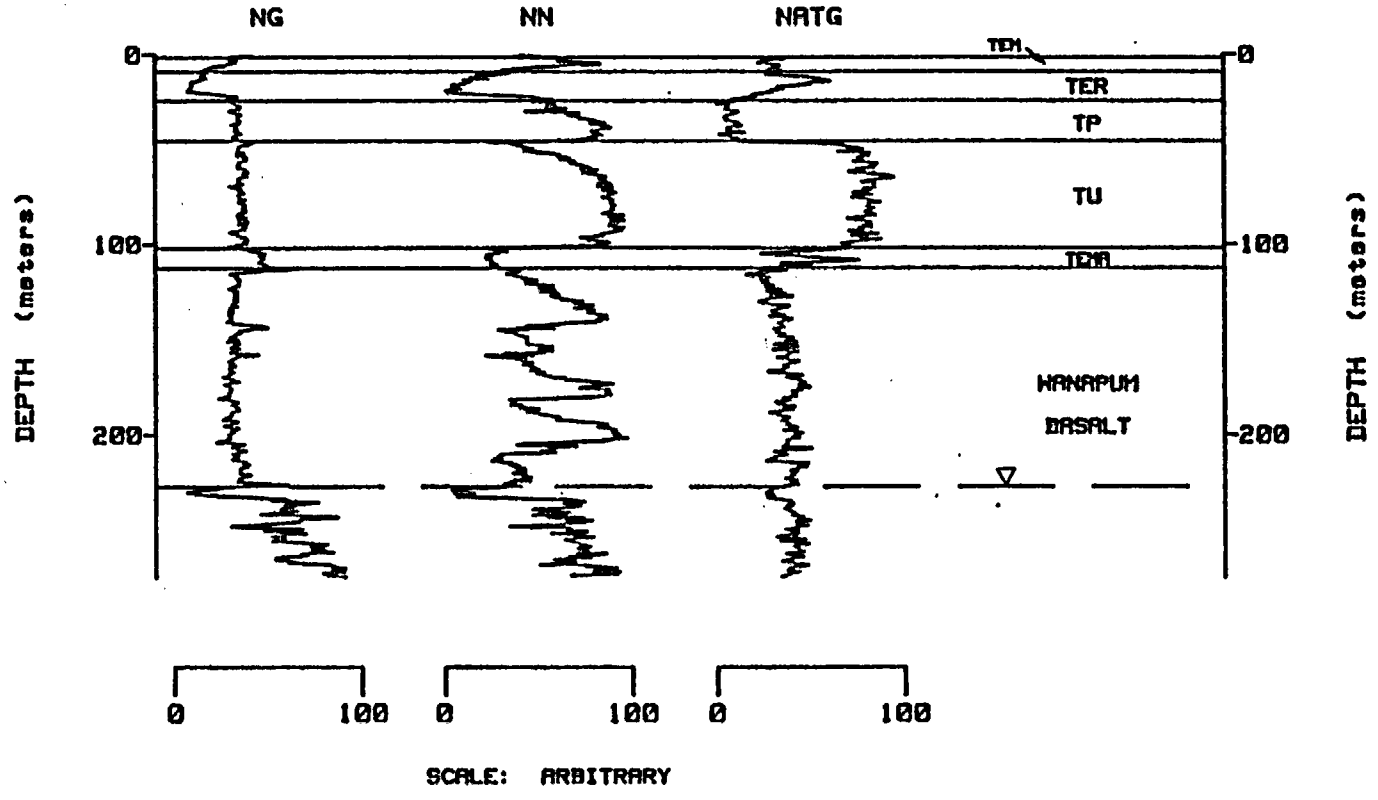

Figure 50. Borehole geophysical logs of the Sharpe well.

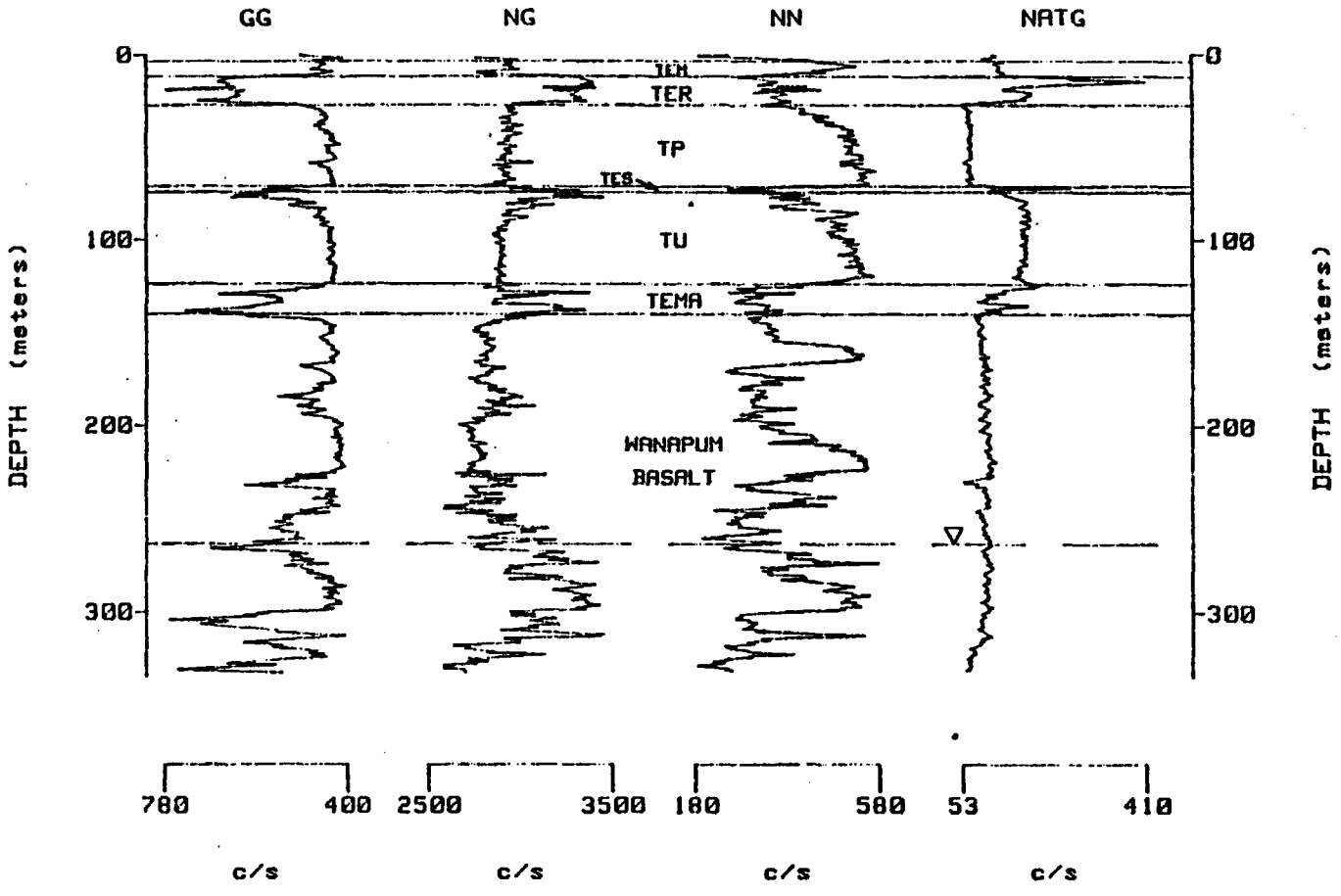

Figure 52. Borehole geophysical logs of the Horrigan Farms well.

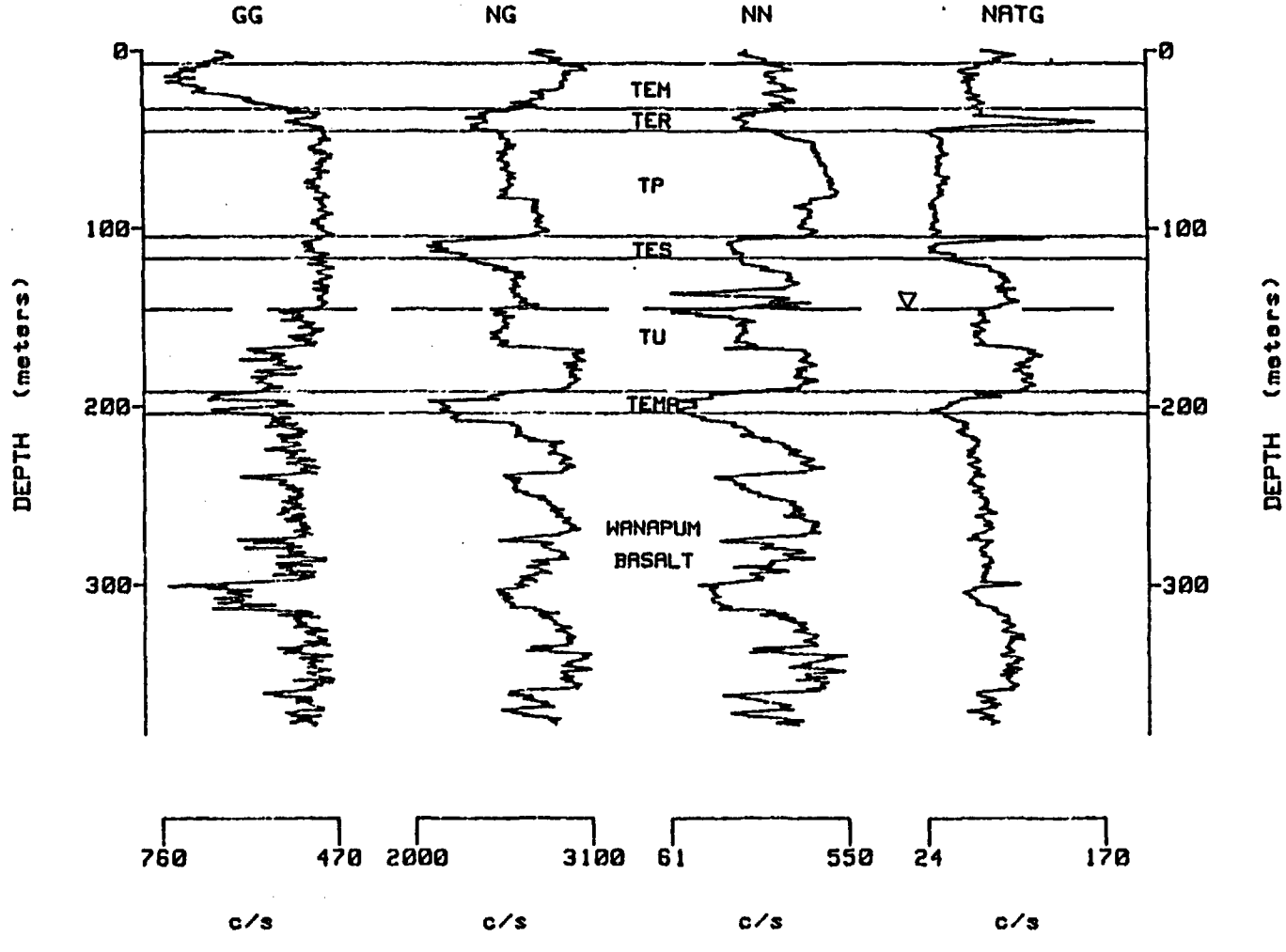

Figure 53. Borehole geophysical logs of the Palmer 2 well.

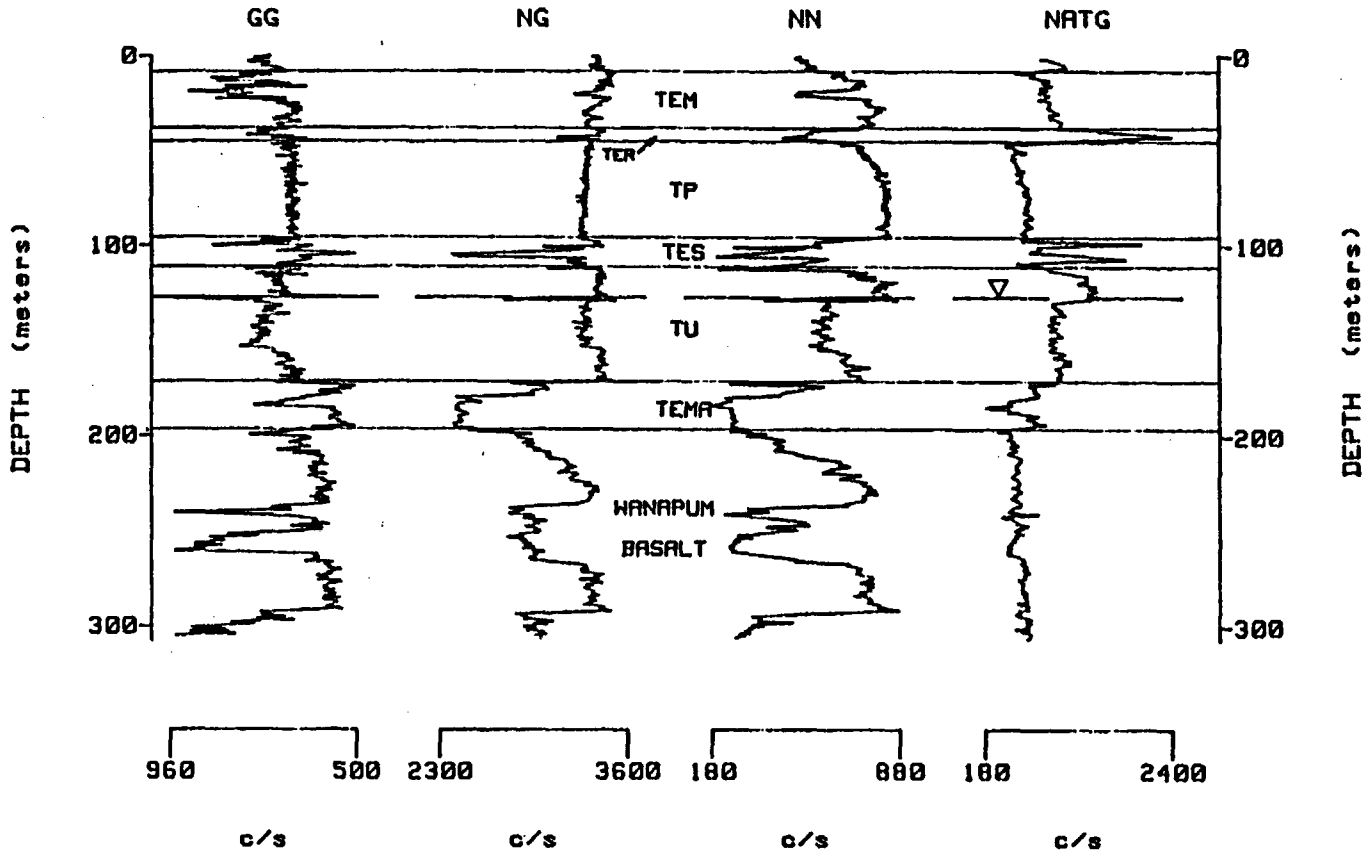

Figure 54. Borehole geophysical logs of the Palmer well.

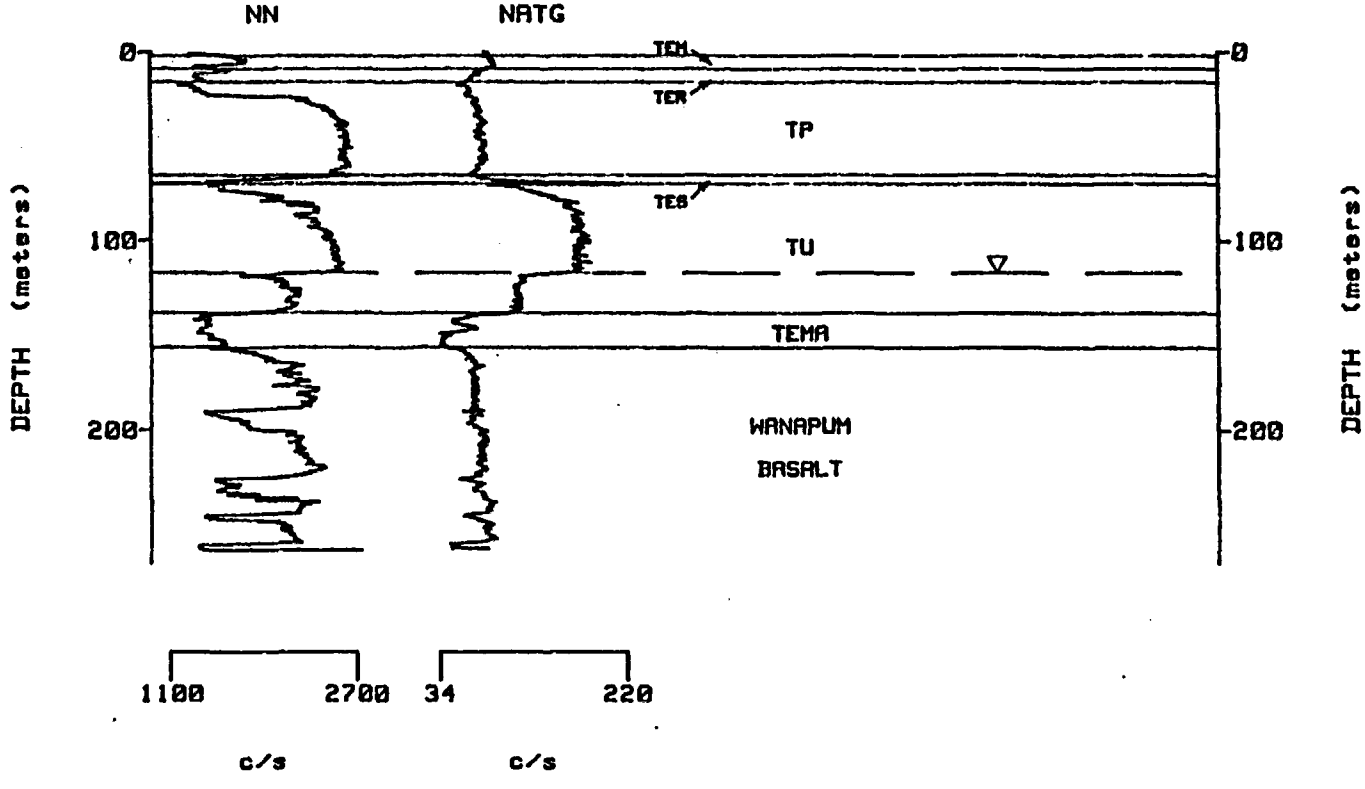

Figure 55. Borehole geophysical logs of the Barber 2 well.

Waitt, 1979

In the Kittital Valley "An hypothesis consistent with regional relations is that the ... southeast trend of dextral echelon pattern is due to right lateral couple across a southeast-trending structural zone that includes, but is not limited to the topographically defined Olympic-Wallowa lineament ..."

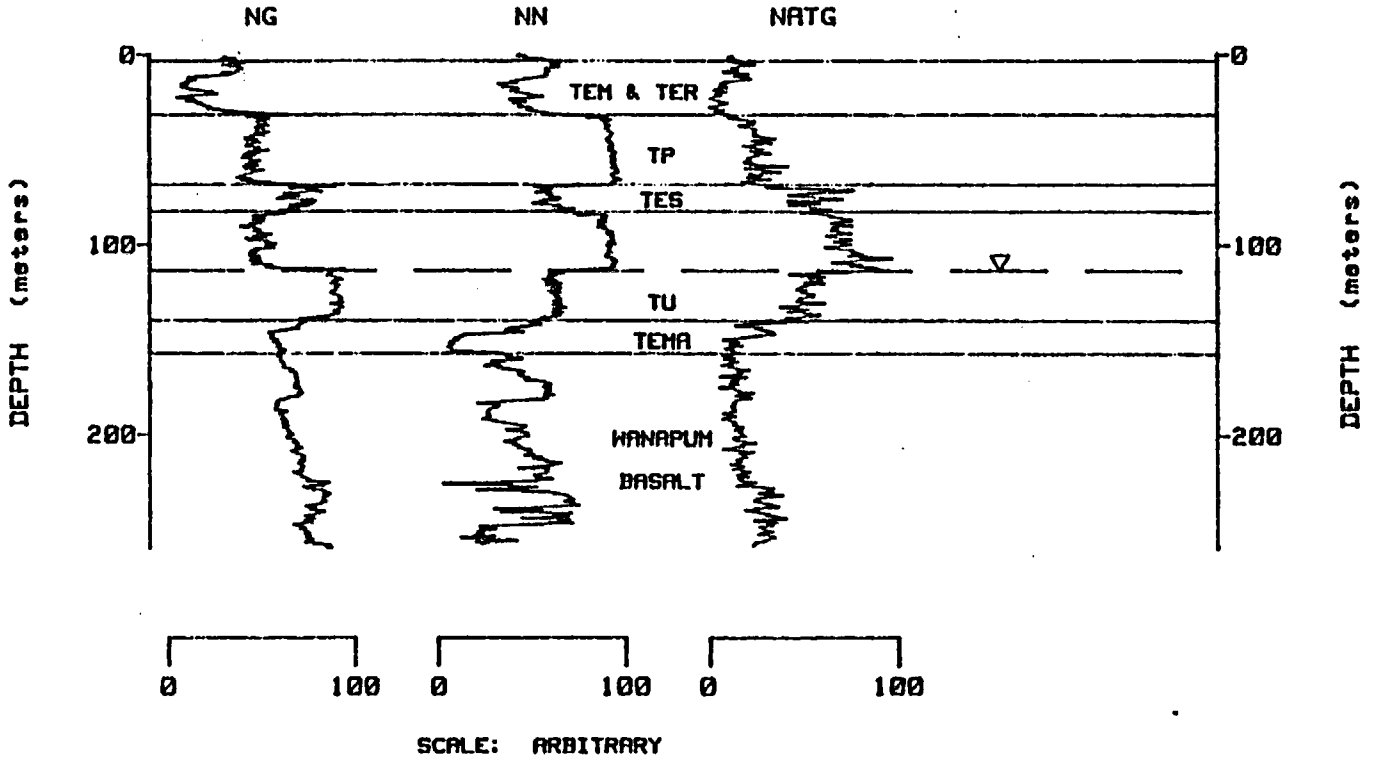

Figure 56. Borehole geophysical logs of the Paterson Test well.

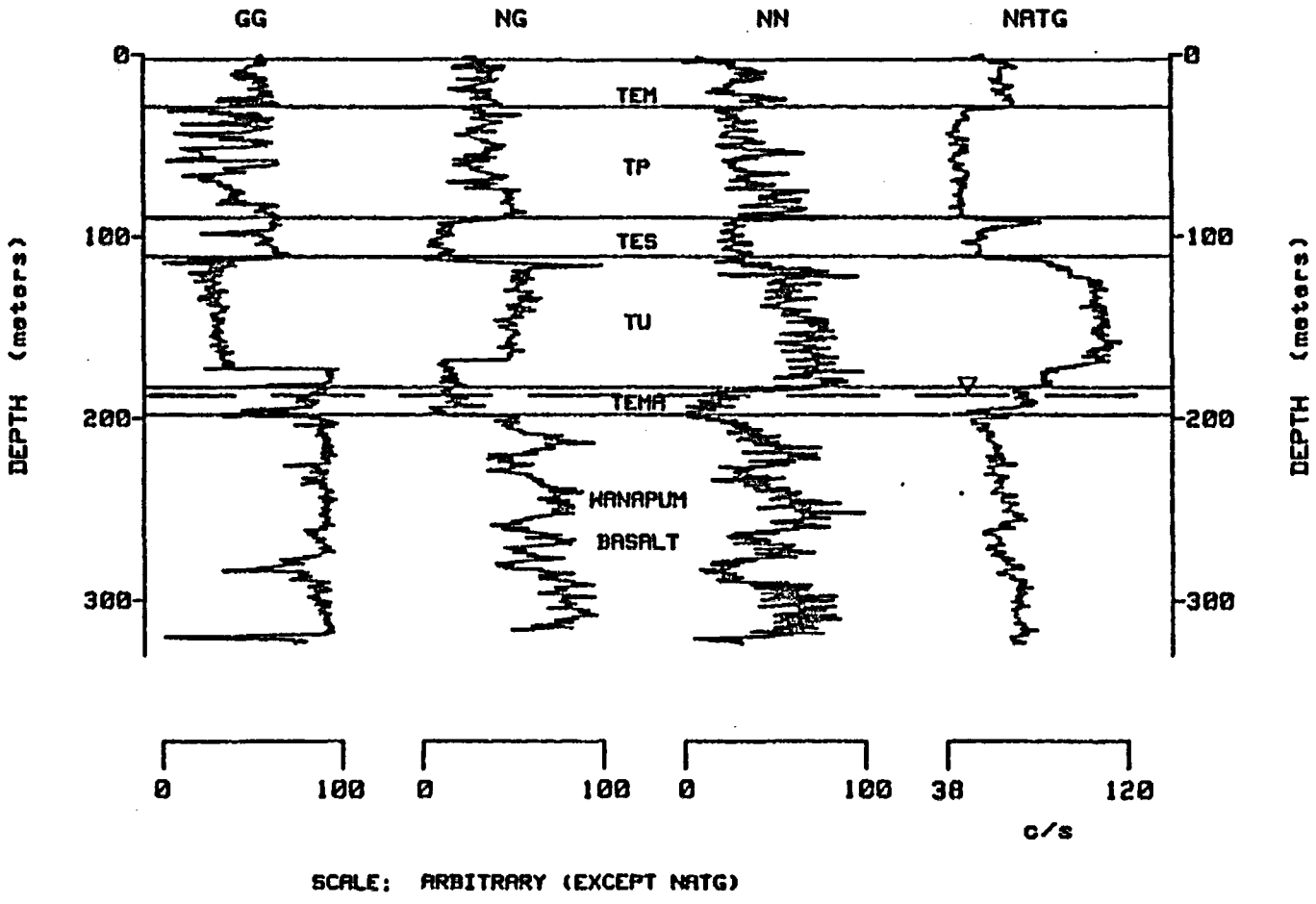

Figure 57. Borehole geophysical logs of the Moon well.

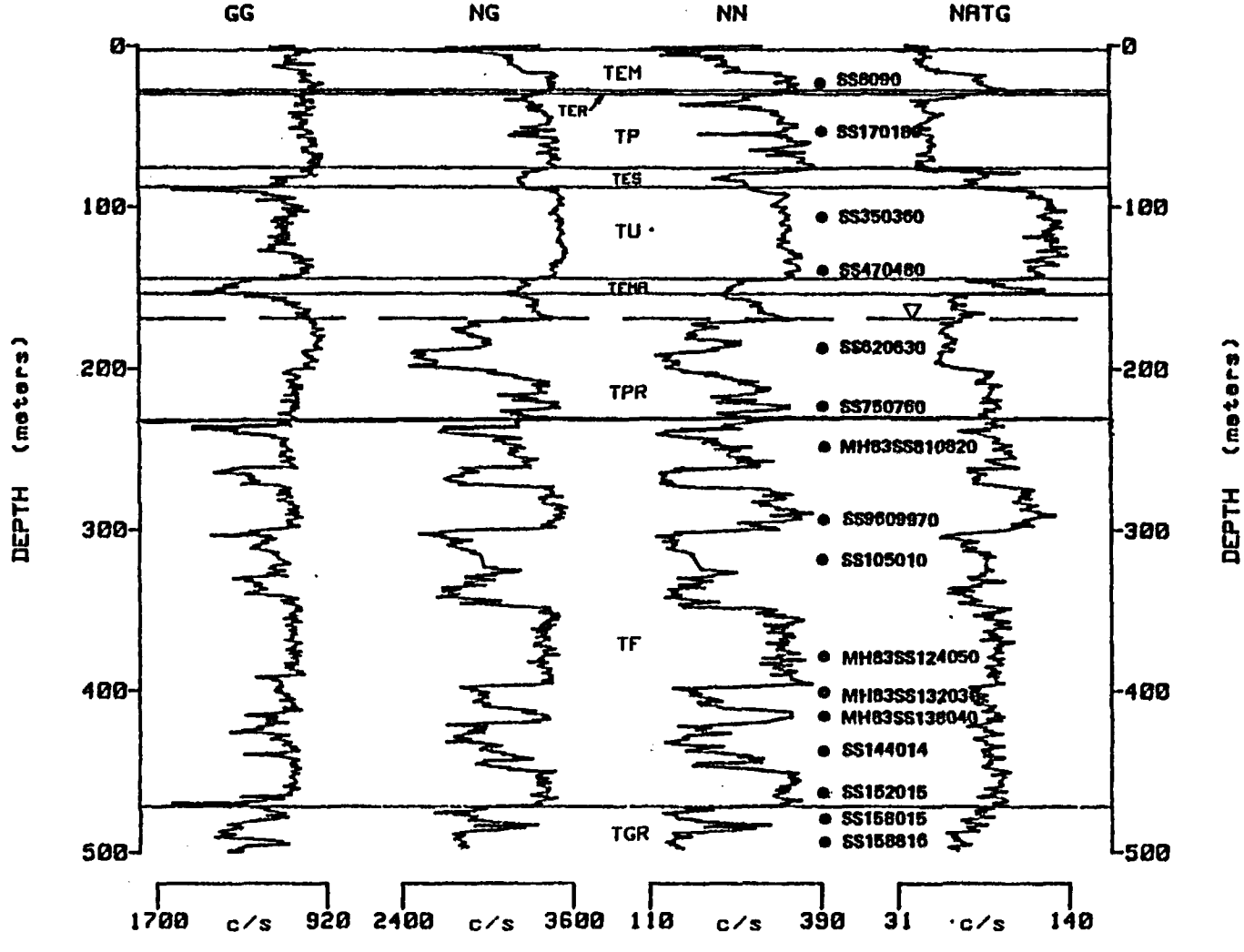

Figure 58. Borehole geophysical logs of the Moon 1 well.

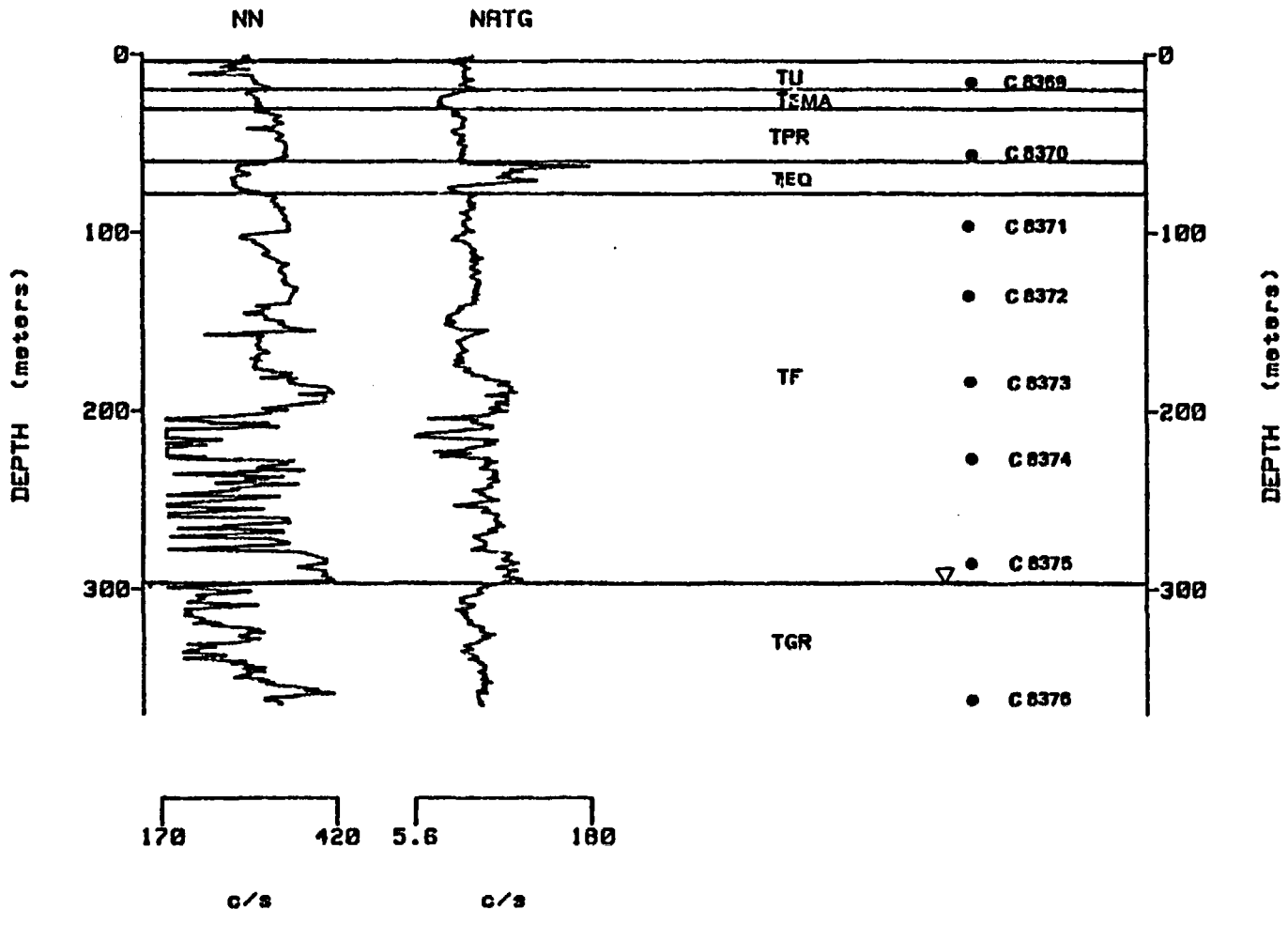

Figure 59. Borehole geophysical logs of the Horse Heaven Test well.

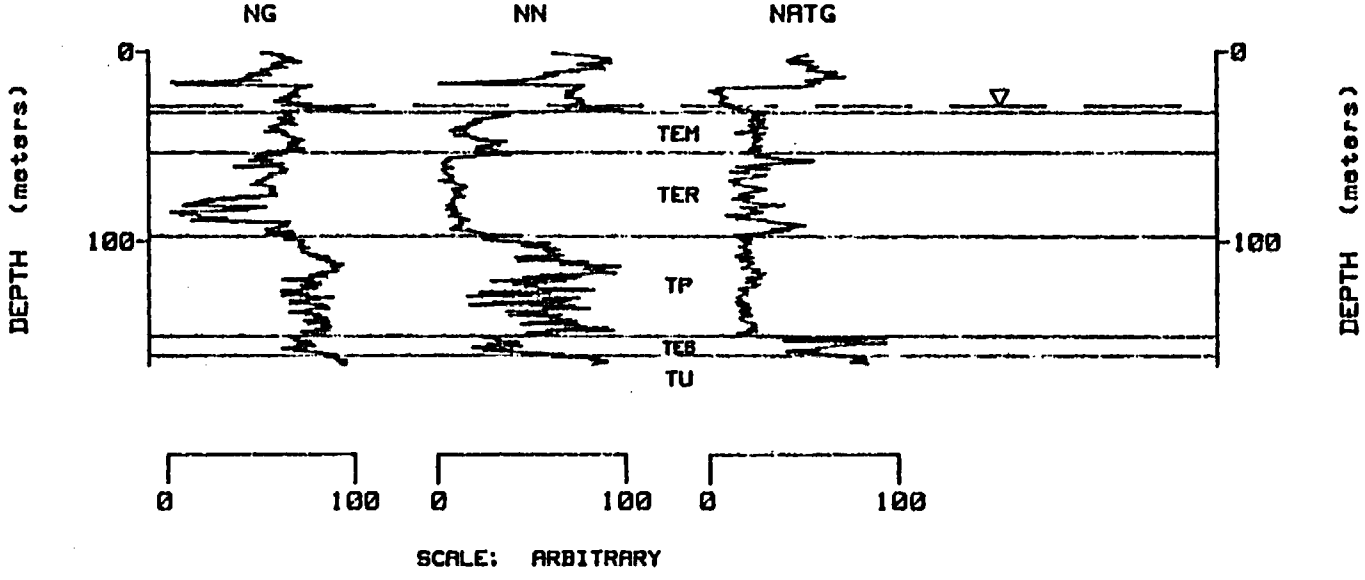

Figure 60. Borehole geophysical logs of the Flower well.

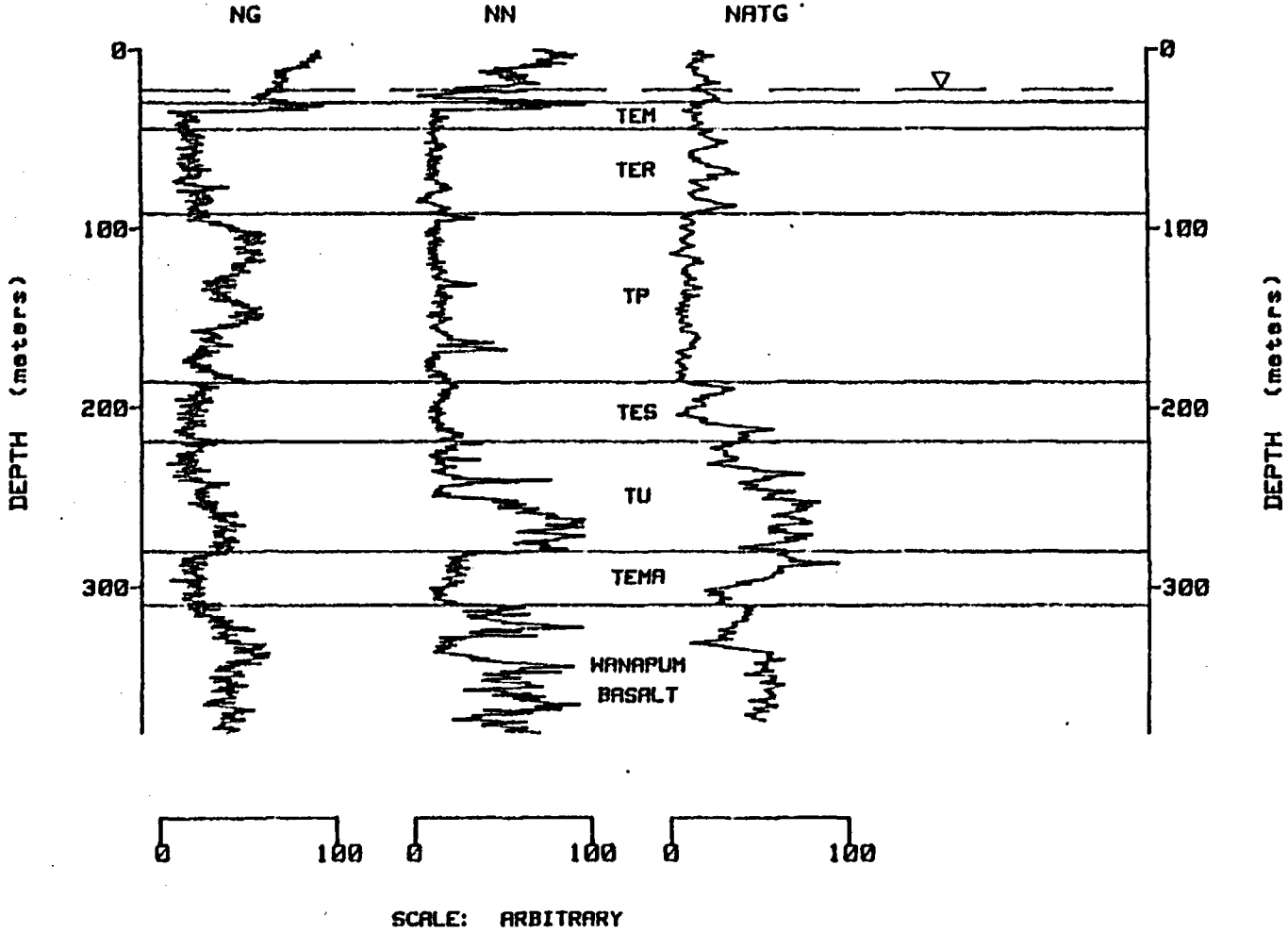

Figure 61. Borehole geophysical logs of the Prosser Municipal well.

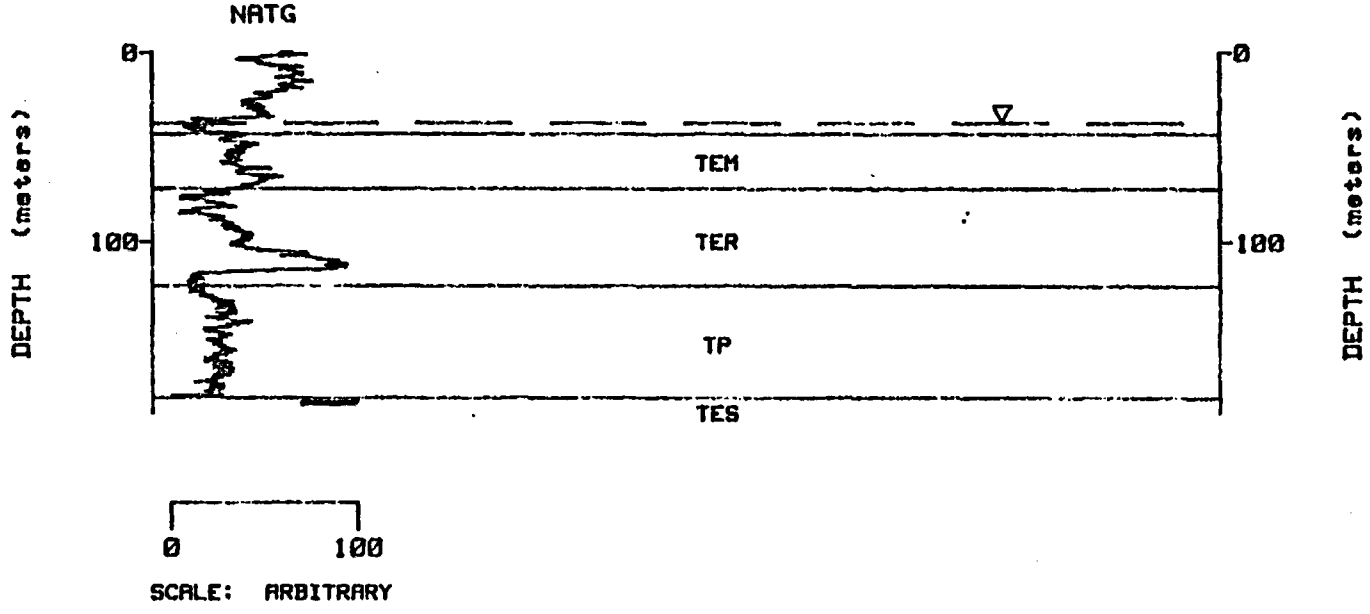

Figure 62. Borehole geophysical logs of the Long well.

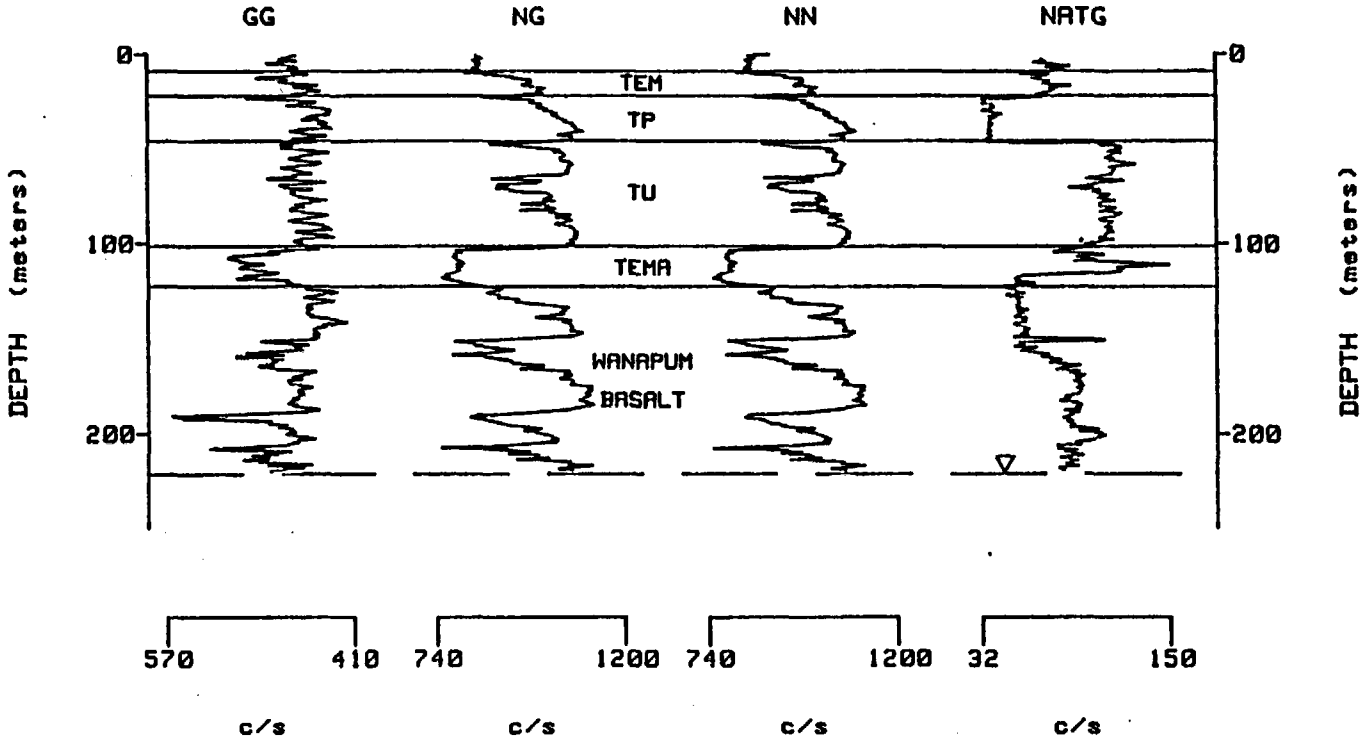

Figure 63. Borehole geophysical logs of the Smith well.

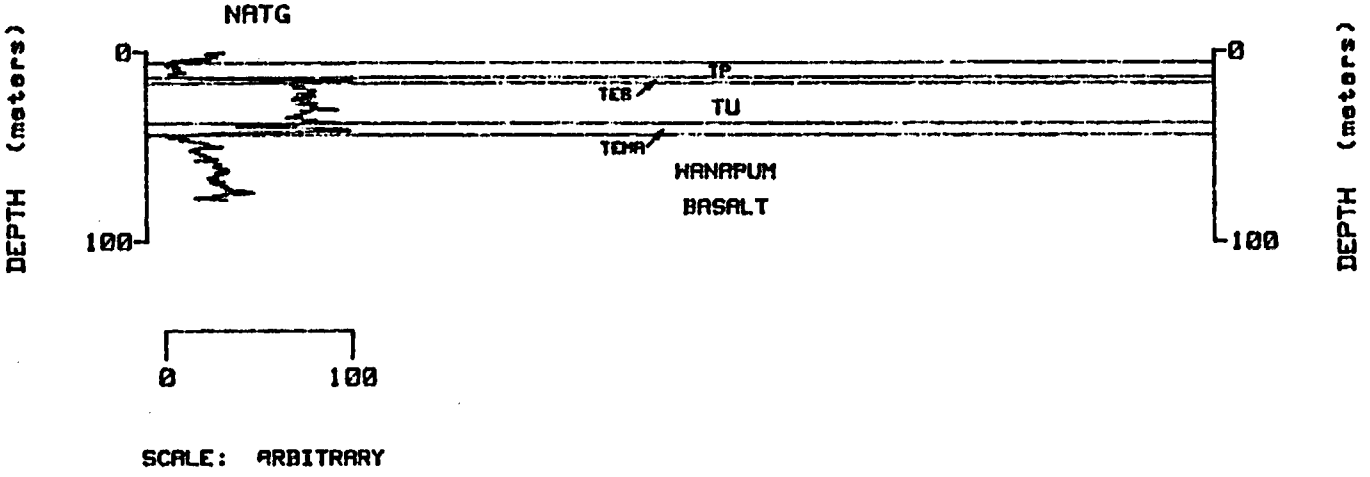

Figure 64. Borehole geophysical log of the Miller well.

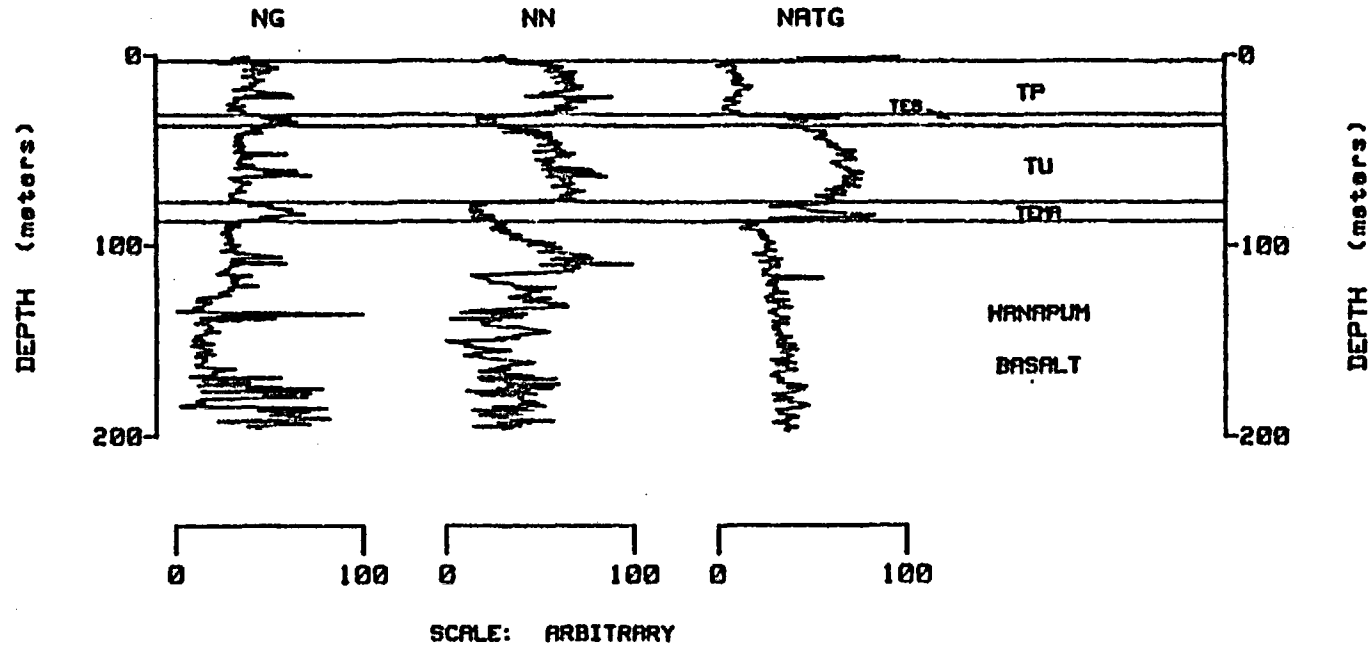

Figure 65. Borehole geophysical logs of the Clodfelter well.

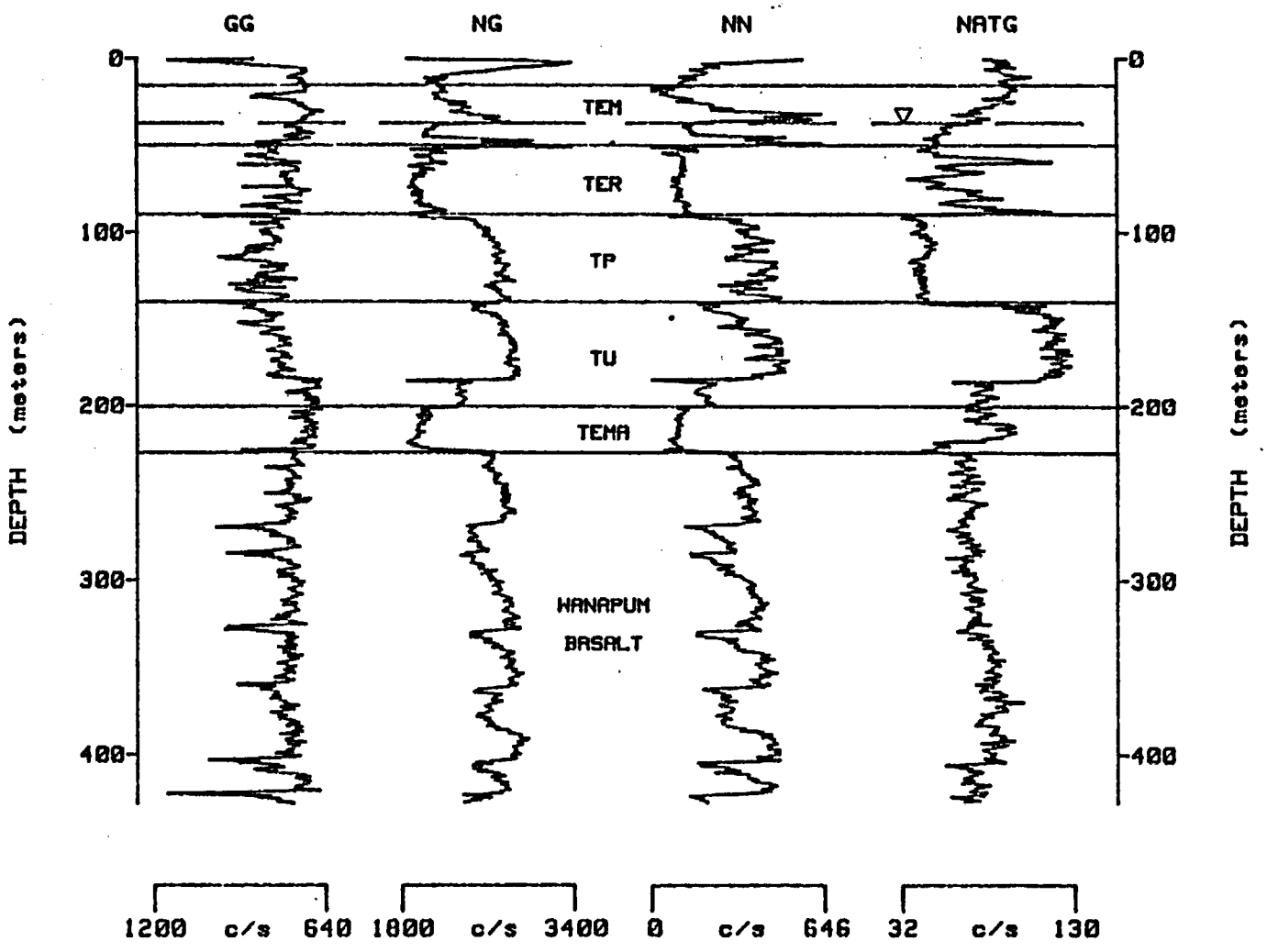

Figure 66. Borehole geophysical logs of the Grandview City well.

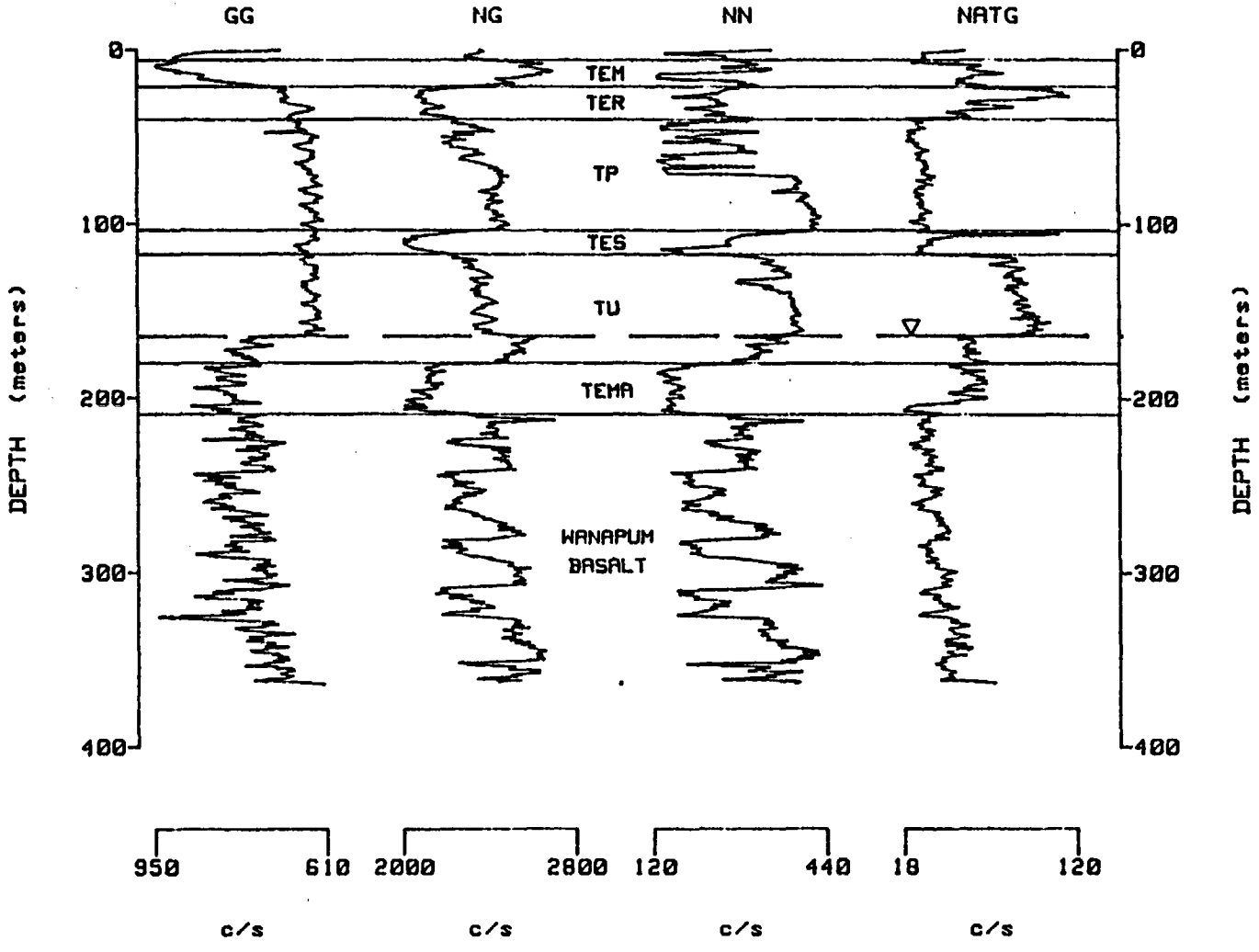

Figure 67. Borehole geophysical logs of the Prosser Experiment Station well.

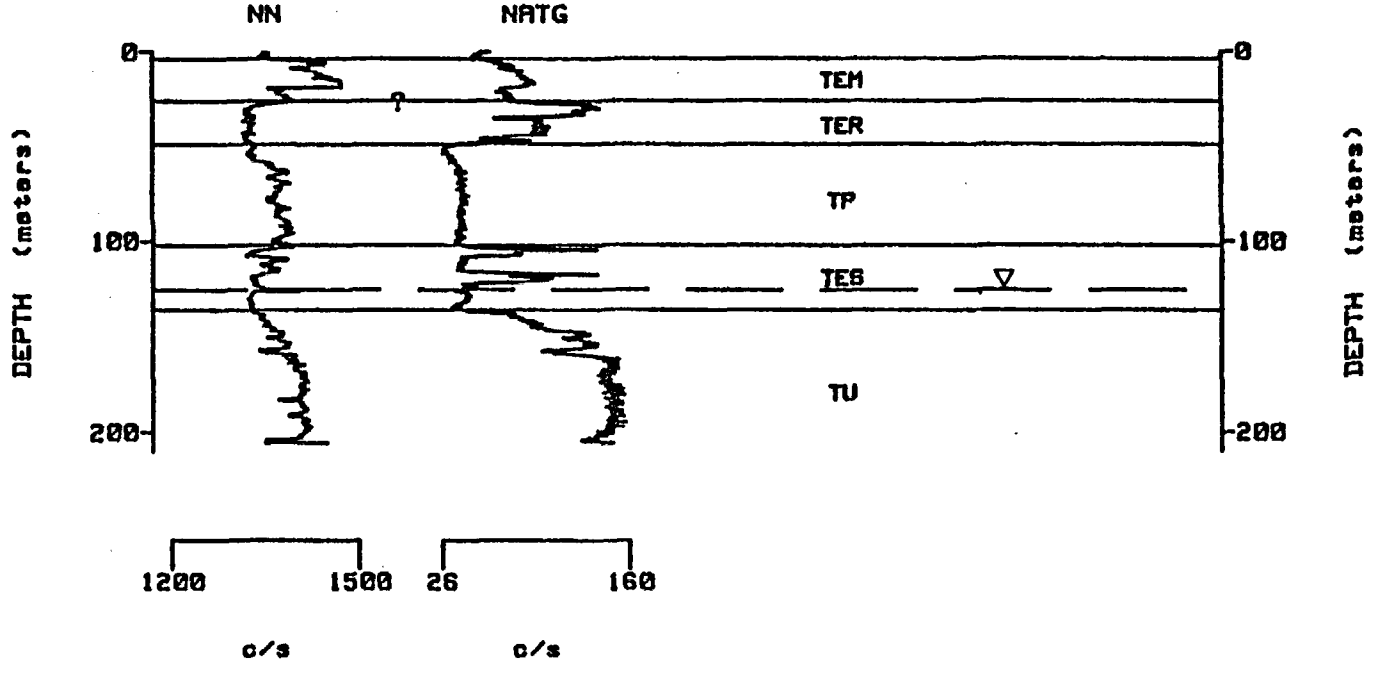

Figure 68. Borehole geophysical logs of the Goroch well.

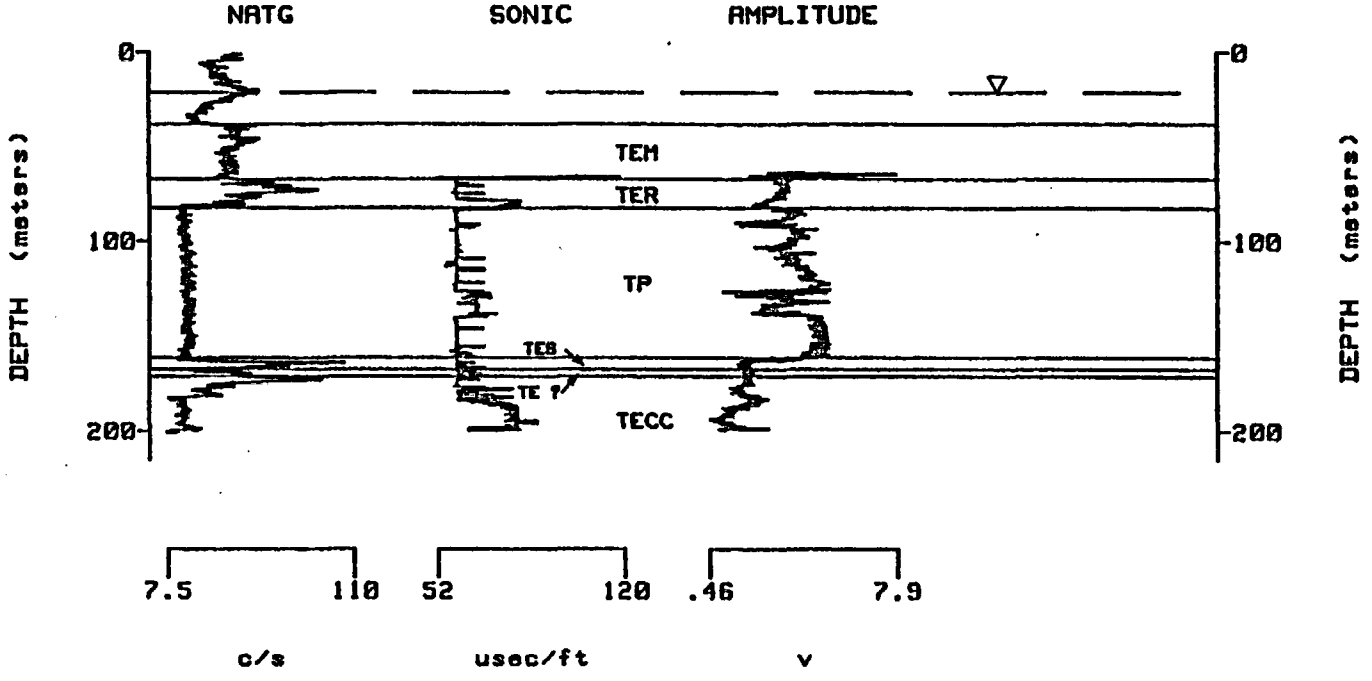

Figure 69. Borehole geophysical logs of the Chandler well.

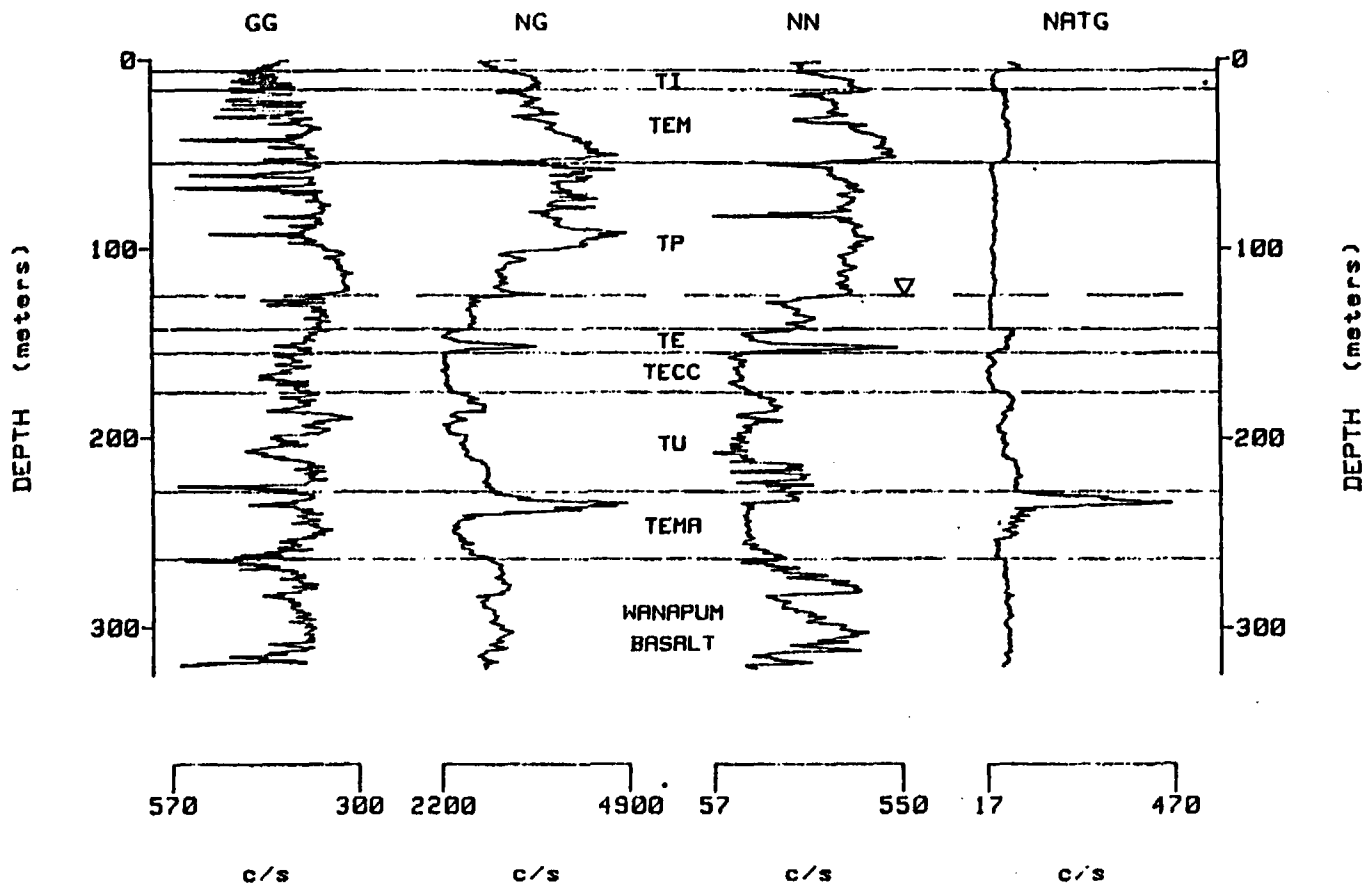

Figure 70. Borehole geophysical logs of the 79-07 well.

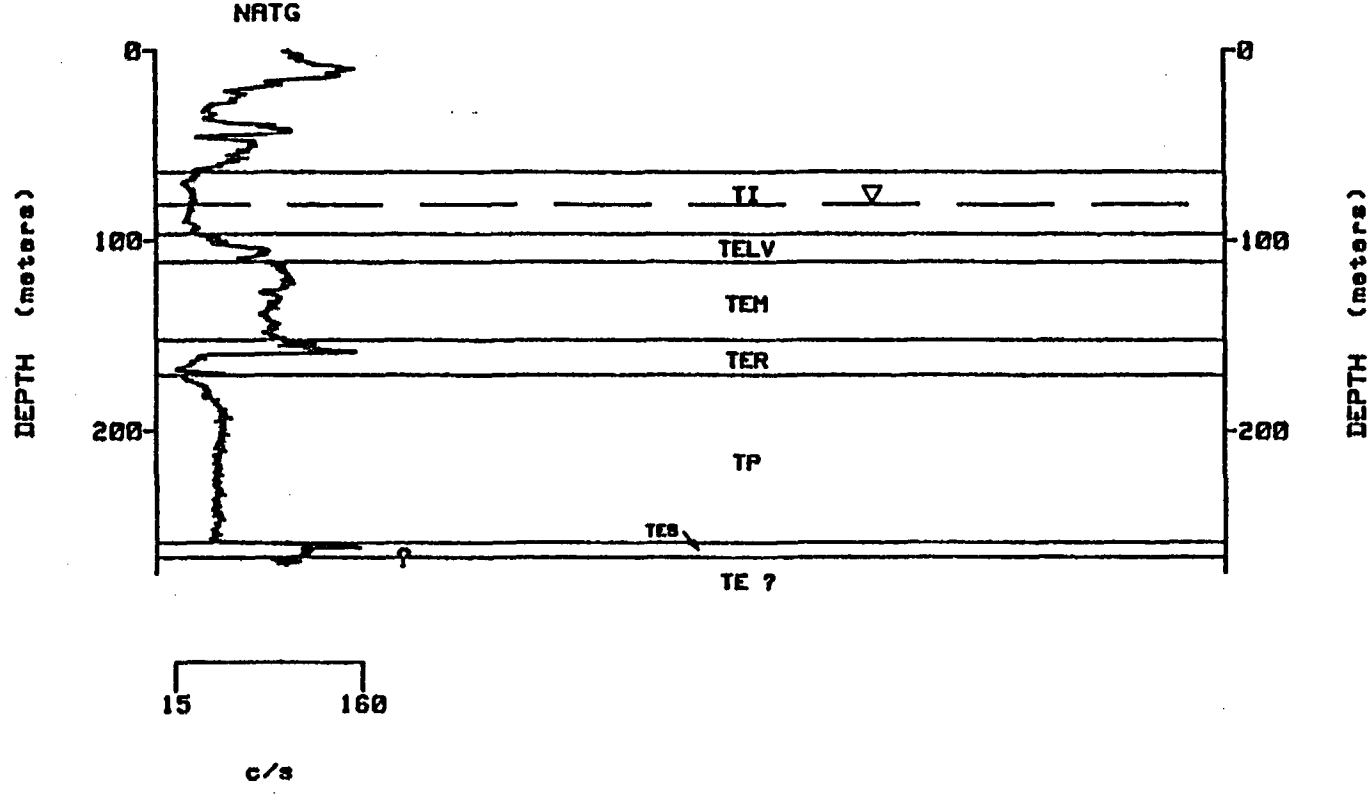

Figure 71. Borehole geophysical log of the Bauder well.

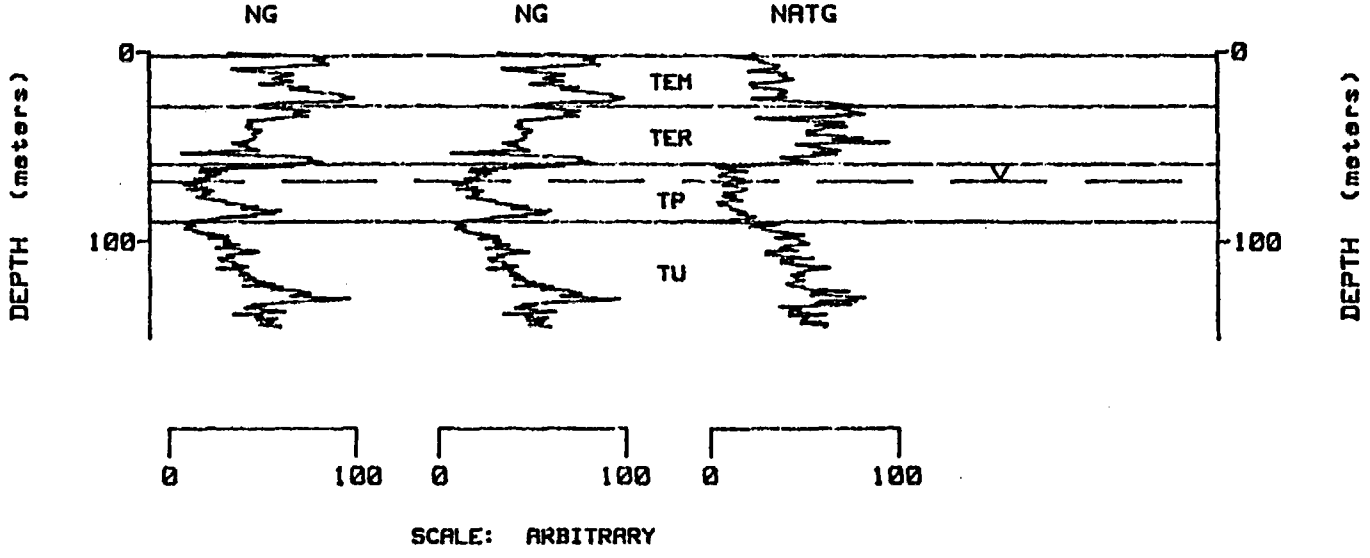

Figure 72. Borehole geophysical logs of the Yakima Valley College well.

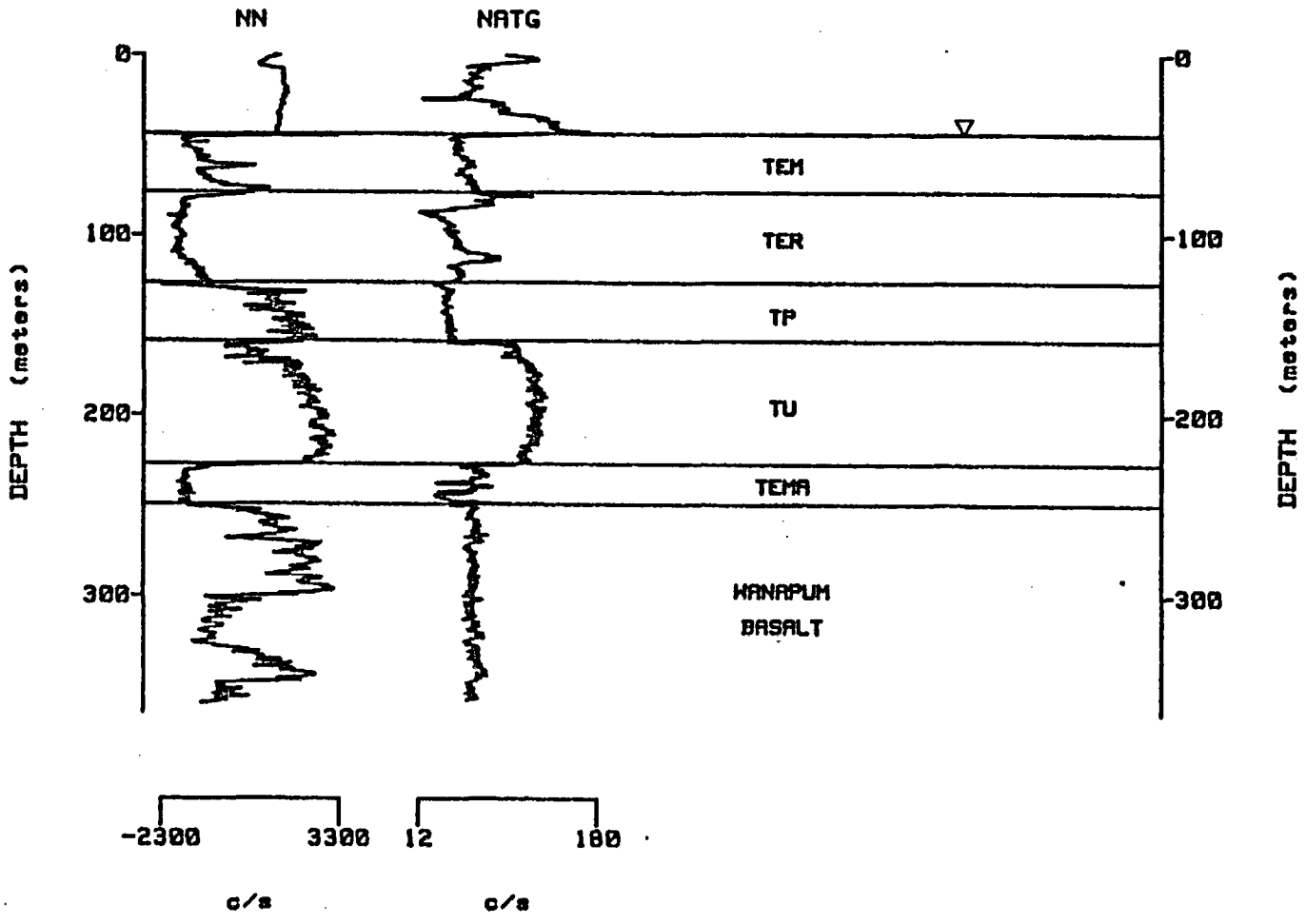

Figure 73. Borehole geophysical logs of the Stout well.

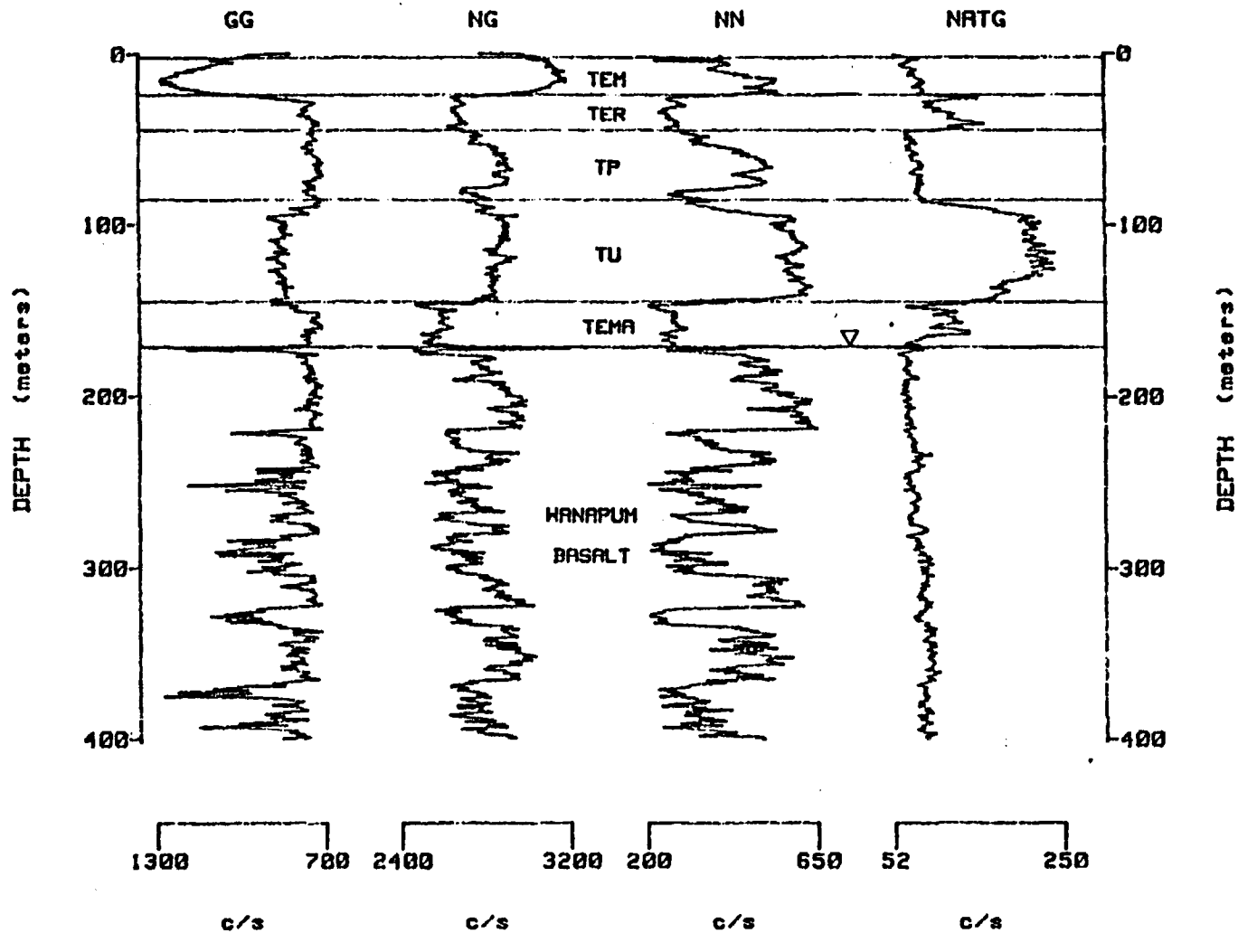

Figure 74. Borehole geophysical logs of the Evans well.

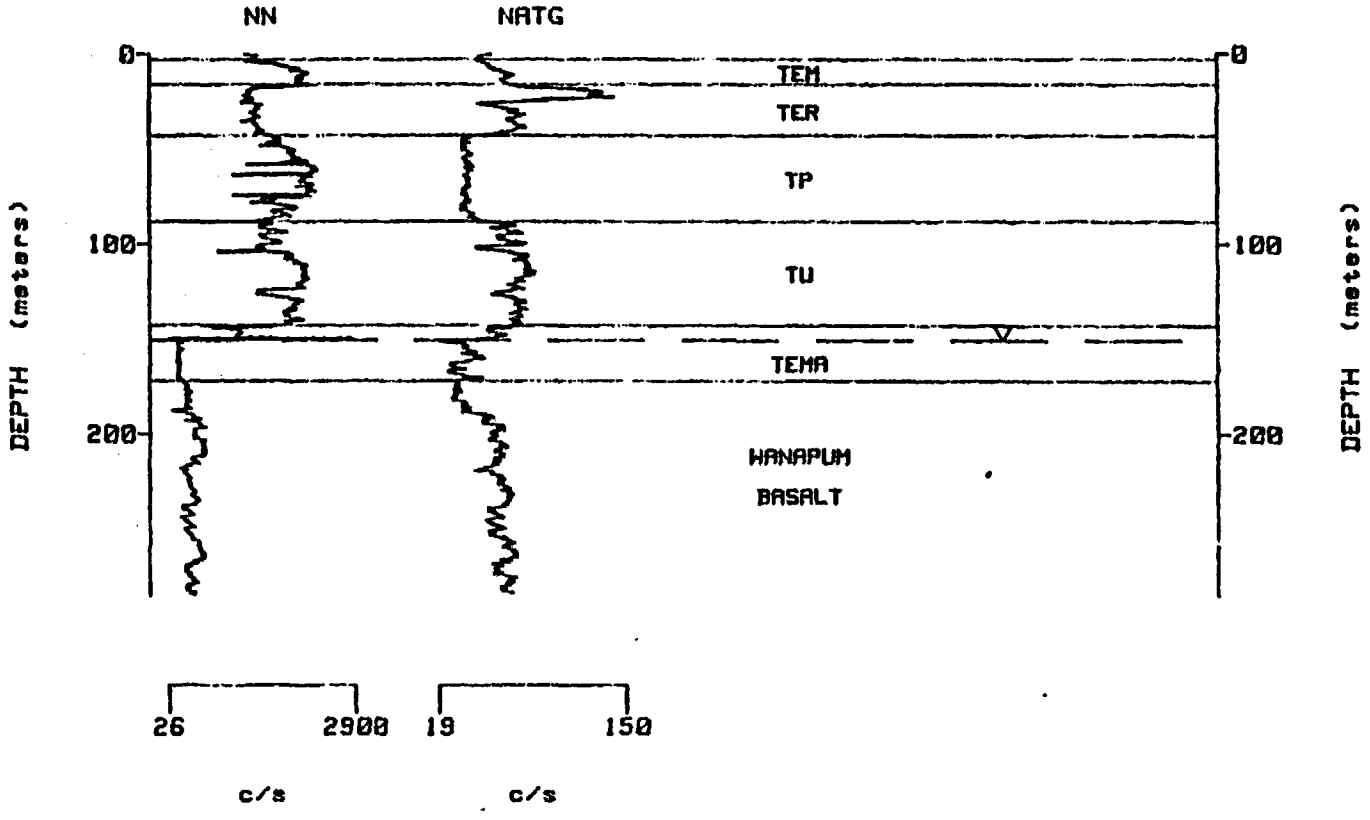

Figure 75. Borehole geophysical logs of the White well.

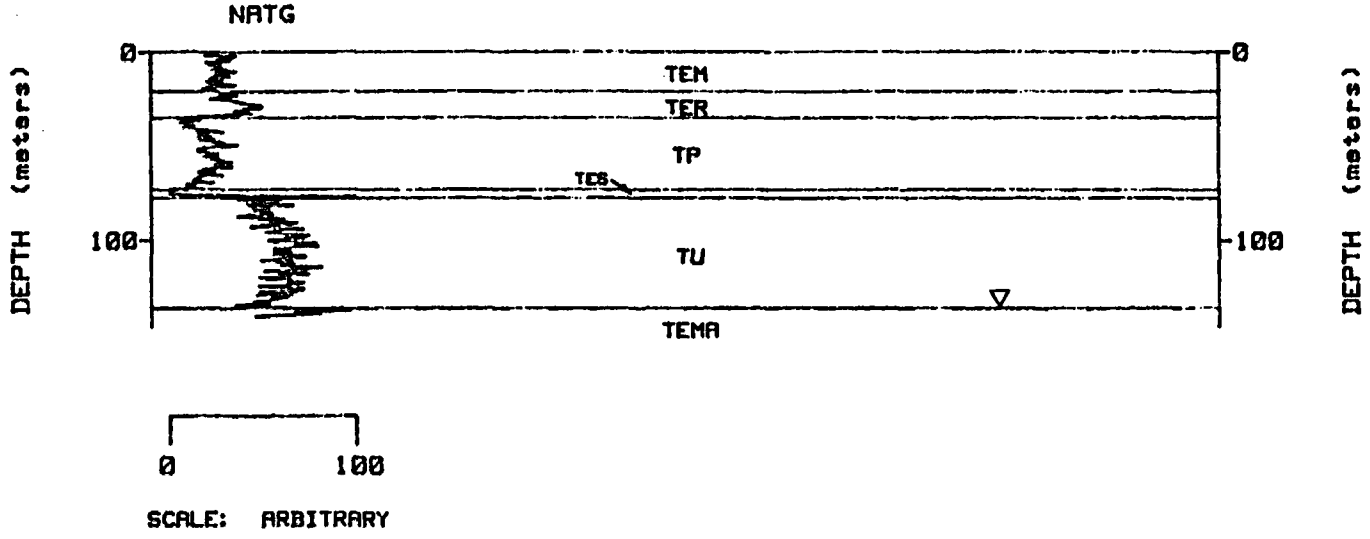

Figure 76. Borehole geophysical log of the Aarons well.

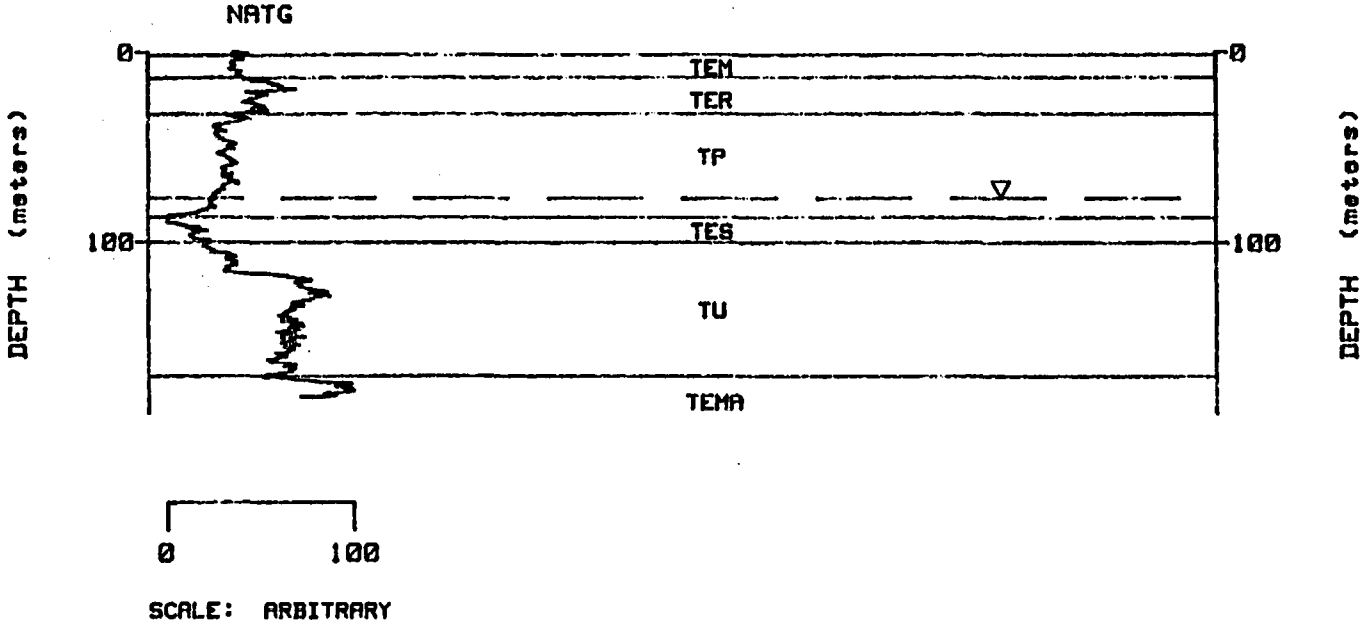

Figure 77. Borehole geophysical log of the Nakamura well.

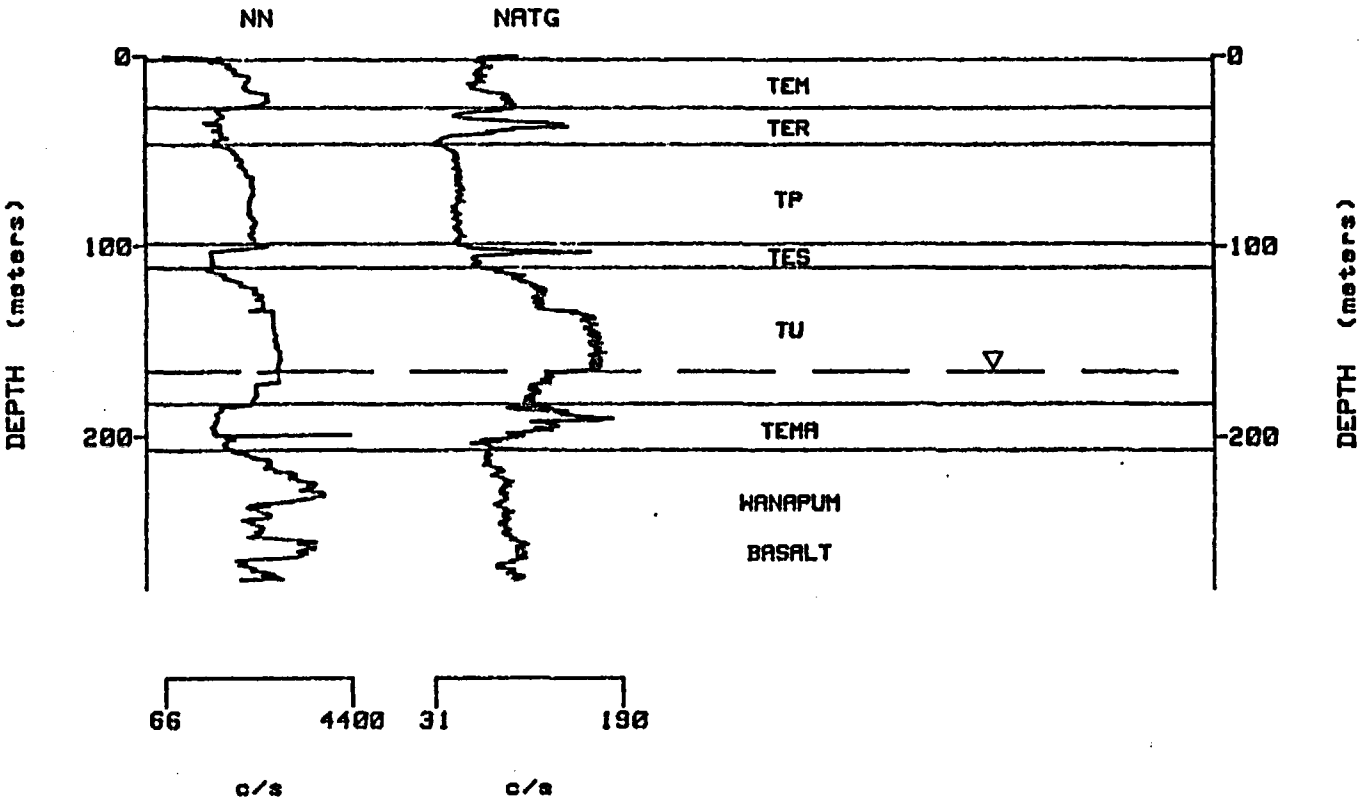

Figure 78. Borehole geophysical logs of the J & R Orchards well.

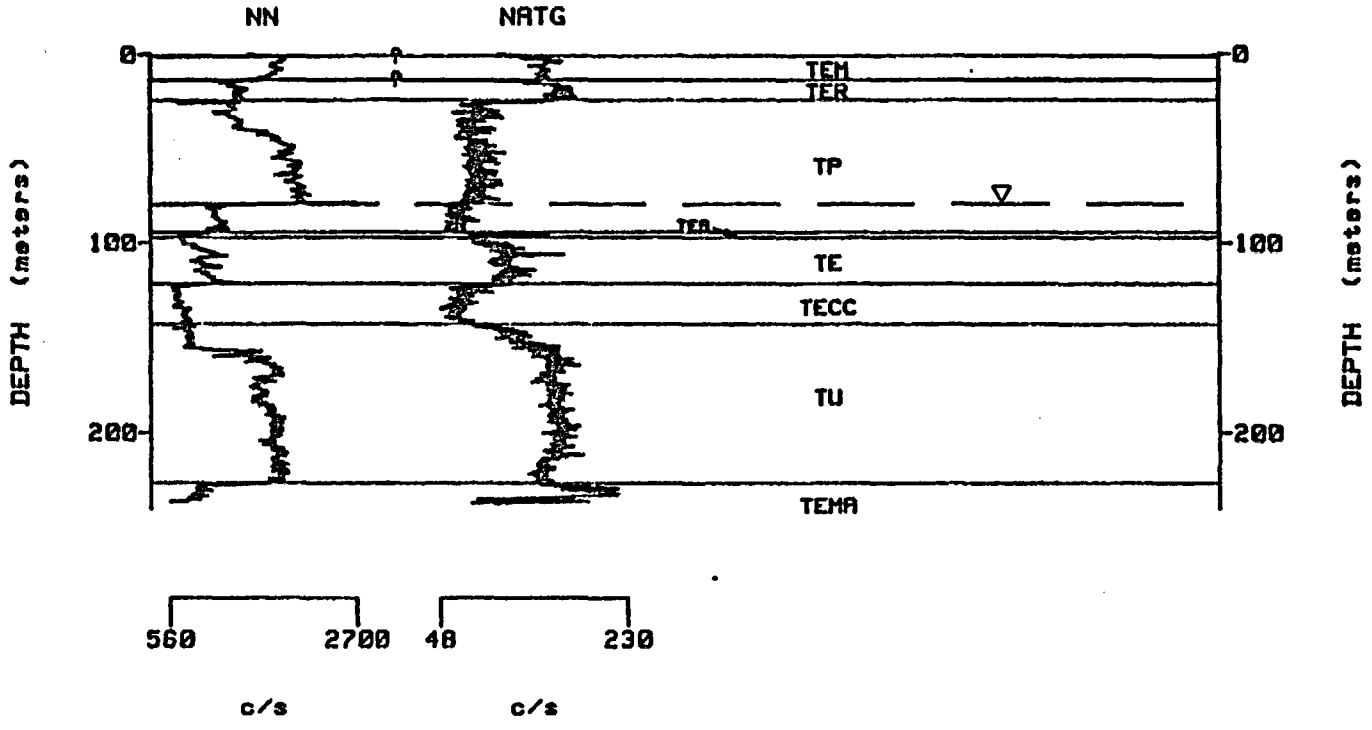

Figure 79. Borehole geophysical logs of the Shaw well.

APPENDIX C

DESCRIPTIVE GEOLOGIC CROSS SECTIONS

The cross sections shown in this appendix depict as clearly as possible the structure that can be observed in the field. These data were used to construct the cross sections interpreted within the Chapter Two.

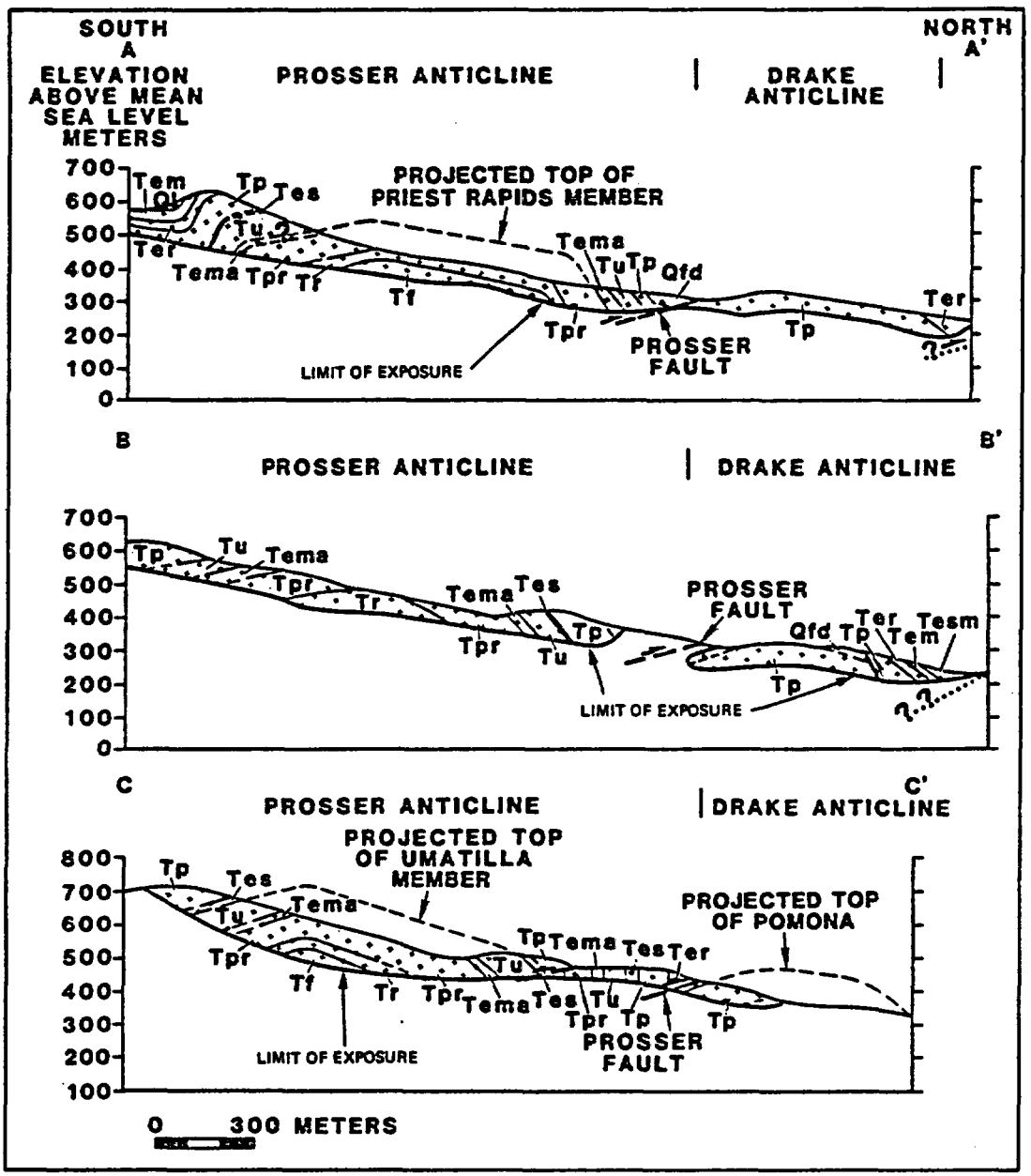

Figure 80. Descriptive geologic cross sections through the Horse Heaven Hills uplift within the Byron segment (see Fig. 15 for locations and Fig. 18 for legend).

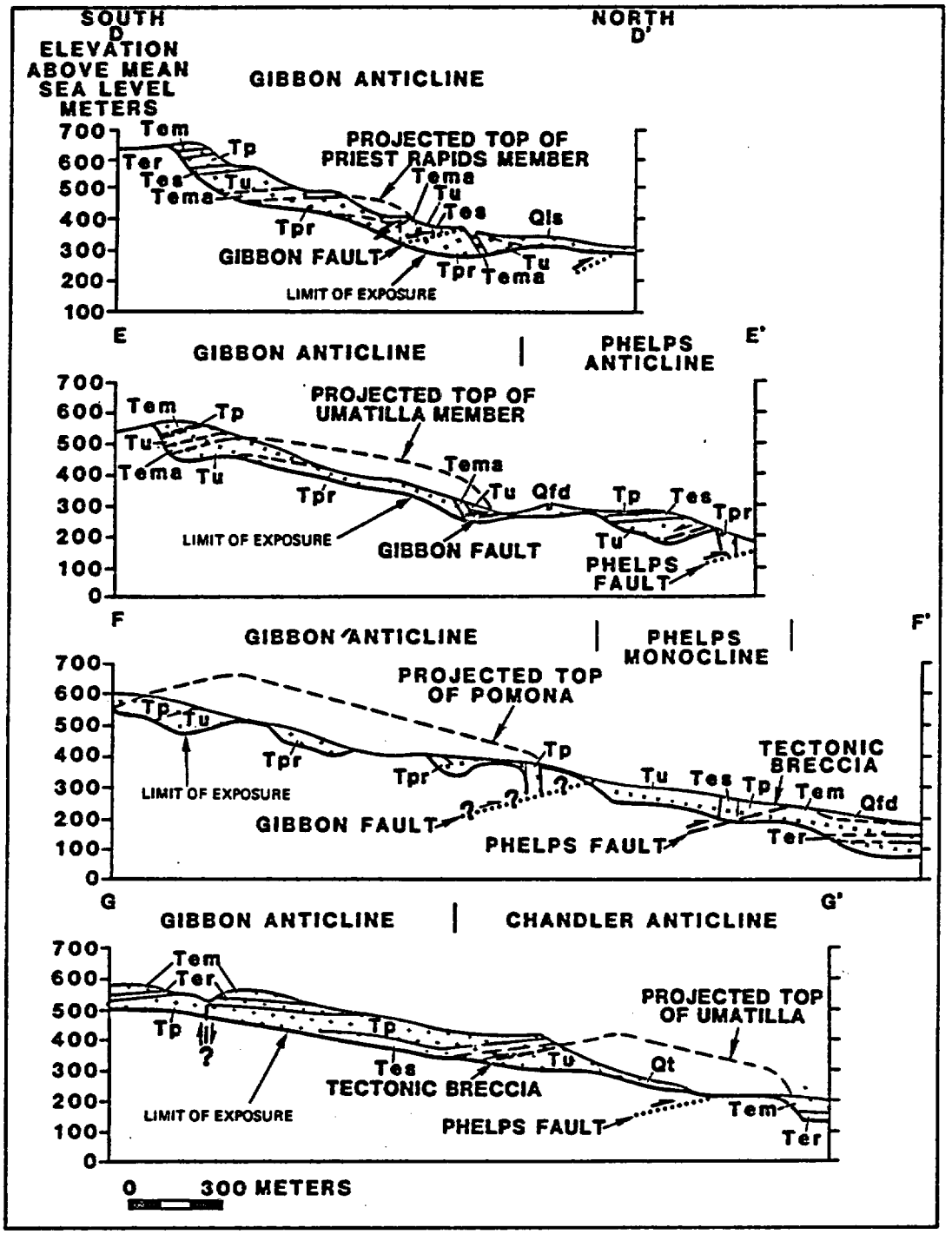

Figure 81. Descriptive geologic cross sections through the Horse Heaven Hills uplift within the Gibbon segment (see Fig. 15 for locations and Fig. 18 for legend).

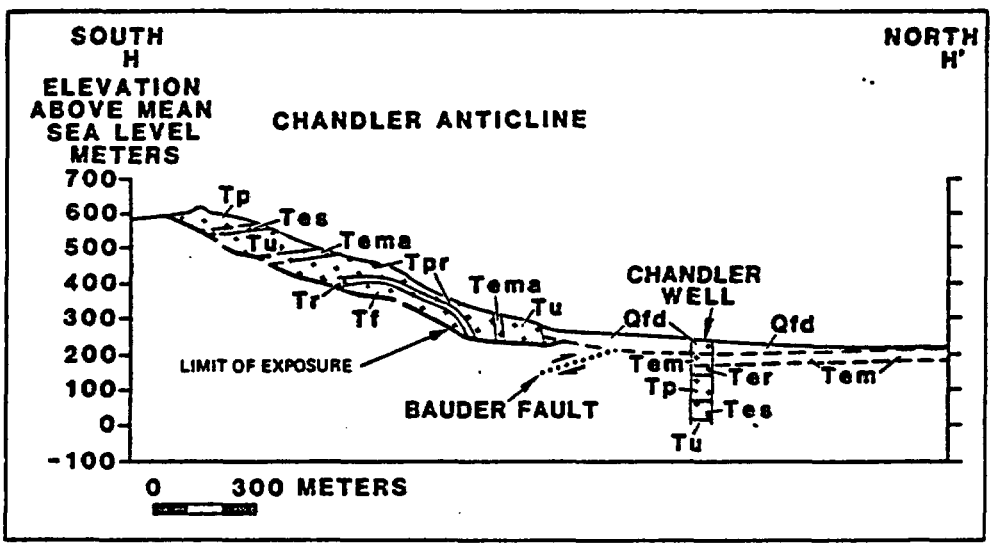

Figure 82. Descriptive geologic cross section through the Horse Heaven Hills uplift within the Chandler segment (see Fig. 15 for location and Fig. 18 for legend).

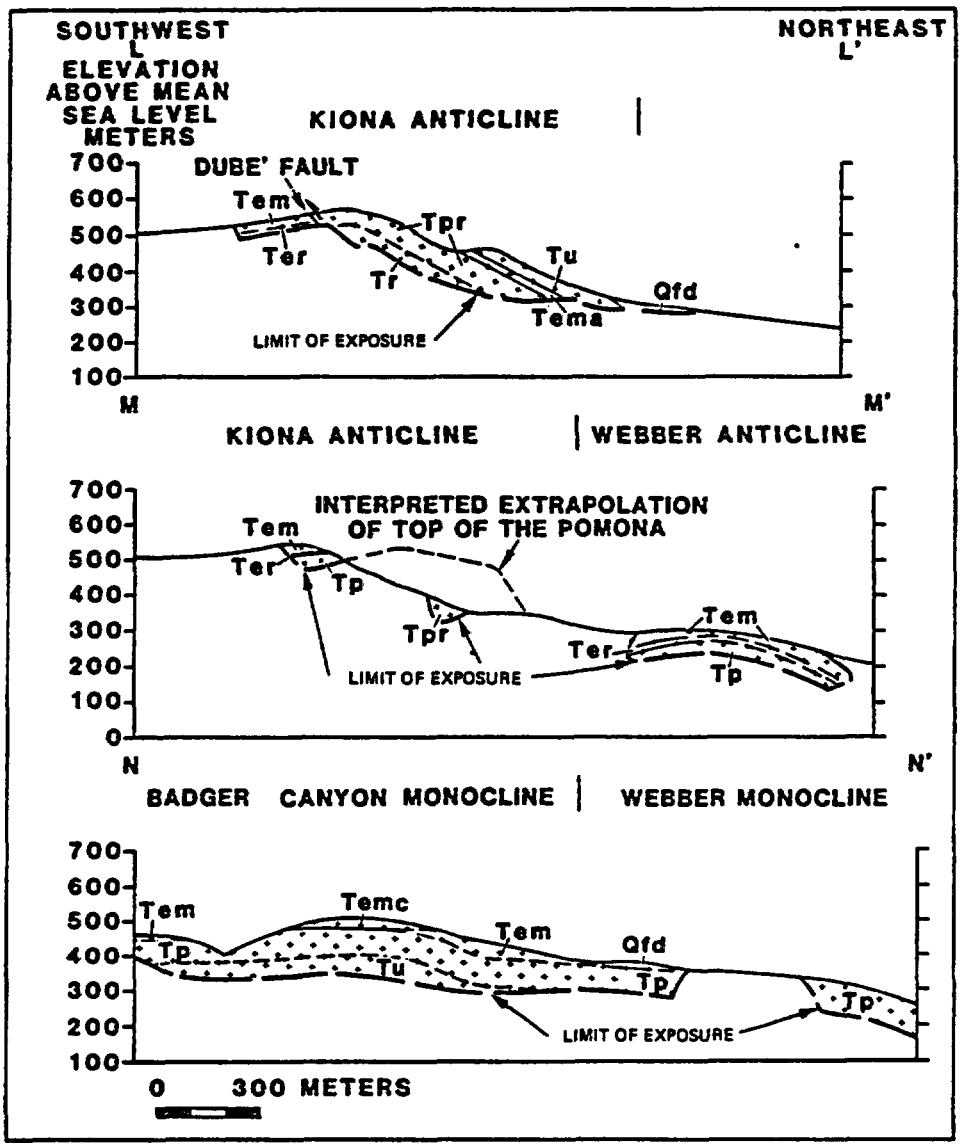

Figure 83. Descriptive geologic cross sections through the Horse Heaven Hills uplift within the Webber segment (see Fig. 15 for locations and Fig. 18 for legend).

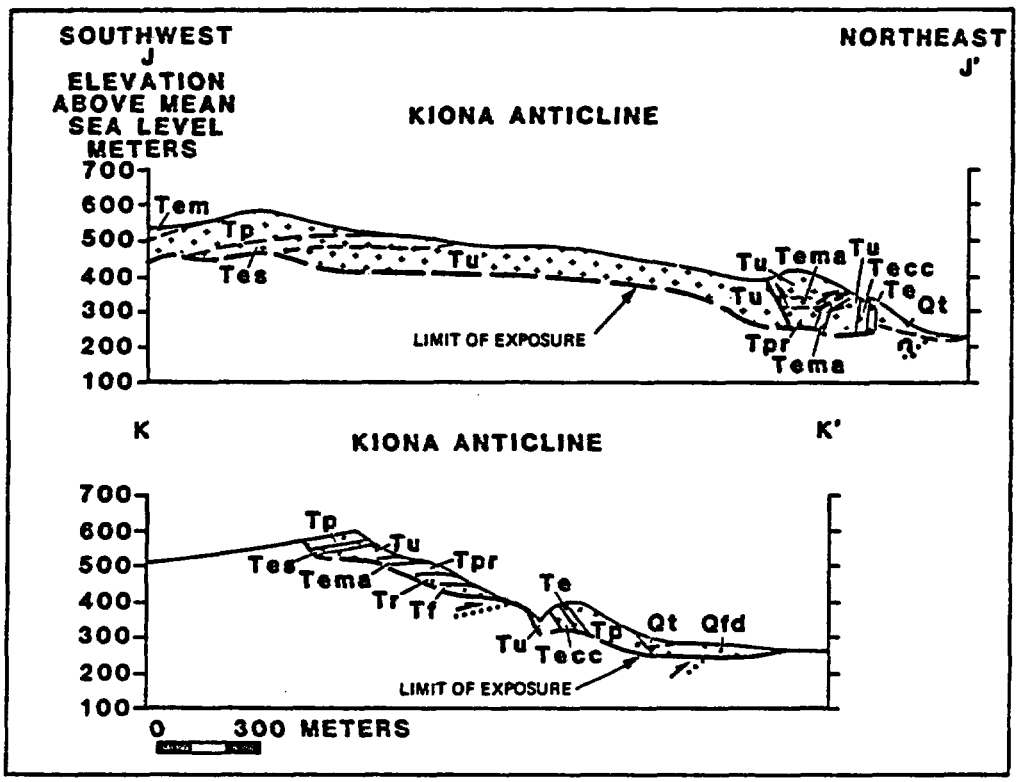

Figure 84. Descriptive geologic cross sections through the Horse Heaven Hills uplift within the Kiona segment (see Fig. 15 for locations and Fig. 18 for legend).

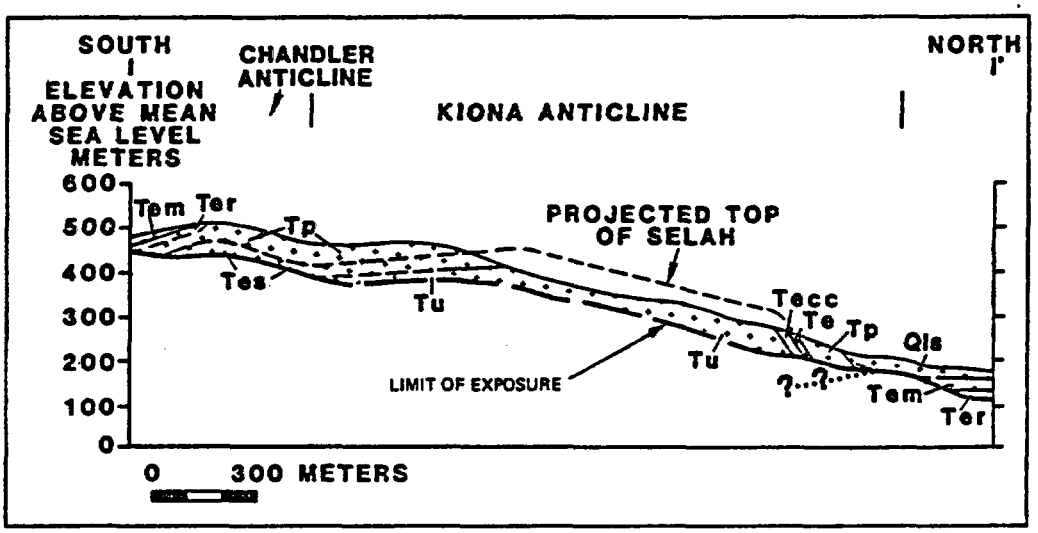

Figure 85. Descriptive geologic cross sections through the Horse Heaven Hills uplift within the Junction segment (see Fig. 15 for location and Fig. 18 for legend).

APPENDIX D

ASSUMPTIONS USED IN CALCULATING GROWTH RATES

Section Thicknesses

According to Reidel (1984) some assumptions must be made when using thicknesses of basalt flows to calculate rates of growth. These are: (1) CRBG flows had low viscosities (Waters 1961, Shaw and Swanson 1970) and their flow tops are an indicator of paleo-horizontality (Shaw and Swanson 1970); (2) the thickness variations in the CRBG flows record existing topography and structure and do not represent normal variations in the flow or erosion. It has been demonstrated by Reidel (1984) for the Pasco Basin, that such normal variations in individual CRBG members have a one standard deviation of approximately 4 meters or less for certain members of the Saddle Mountains or Wanapum Basalt; (3) folding or faulting has not altered the original flow thickness since the time of emplacement. That is, structural thickening can be recognized. Section thicknesses used in the calculations are shown in Tables VII-IX.

Section thicknesses of CRB flows and Ellensburg sedimentary interbeds were measured in the field, from borehole geophysical logs, and from driller's logs. In all cases measurements were made after delineating the stratigraphy and structure.

TABLE VI

THICKNESS DATA USED IN CALCULATING THE COMBINED RATE OF UPLIFT AND SUBSIDENCE FOR THE PROSSER ANTICLINE AND THE LOWER YAKIMA VALLEY SYNCLINE

UNIT	SYNCLINE			ANTICLINE			PALEO-RELIEF
	DATA TYPE	LOCATION	UNIT THICKNESS	DATA TYPE	LOCATION	UNIT THICKNESS	
ELEPHANT MOUNTAIN MEMBER	G.L.	EX*	34.0 m		8N/24E-14L	0.0 m	34.0 m
RATTLESNAKE RIDGE INTERBED	G.L.	8N/24E-01J	47.2 m		8N/24E-14L	0.0 m	47.2 m
POMONA MEMBER	G.L.	8N/24E-01J	93.9 m		8N/24E-14L	43.3 m	50.6 m
SELAH INTERBED	G.L.	8N/24E-01J	33.2 m		8N/24E-14L	1.5 m	31.5 m
UMATILLA MEMBER	G.L.	8N/24E-01J	61.3 m		8N/24E-14L	31.4 m	29.9 m
MABTON INTERBED	G.L.	8N/24E-01J	29.9 m		8N/24E-14L	15.8 m	14.1 m
PRIEST RAPIDS MEMBER	F.M.	8N/25E-07M	62.5 m		8N/24E-14L	3.0 m	27.5 m
ROZA MEMBER	F.M.	EX*	47.0 m		8N/25E-07M	3.0 m	45.0 m

Present structural relief = 393 m

* thickness extrapolated between geophysically logged Grandview City well and the Prosser well

** thickness extrapolated between the geophysically logged Grandview City well and the driller logged IAREC wells (9N/25E-19B, 9N/25E-19C), and the Heintz well (9N/25E-19D)

D. L. = data from driller's log
G. L. = data is from borehole geophysical logs
F. M. = data from field measurements

TABLE VII

THICKNESS DATA USED IN CALCULATING THE COMBINED RATE OF UPLIFT AND SUBSIDENCE FOR THE CHANDLER ANTICLINE AND THE LOWER YAKIMA VALLEY SYNCLINE

UNIT	SYNCLINE			ANTICLINE			PALEO-RELIEF
	DATA TYPE	LOCATION	UNIT THICKNESS	DATA TYPE	LOCATION	UNIT THICKNESS	
ELEPHANT MOUNTAIN MEMBER	G.L.	9N/26E-20A	29.0 m	F.M.	9N/26E-20R	0.0 m	29.0 m
RATTLESNAKE RIDGE INTERBED	G.L.	10N/25E-26E	19.2 m	F.M.	9N/26E-20R	0.0 m	19.2 m
POMONA MEMBER	G.L.	9N/26E-20A	79.2 m	F.M.	9N/26E-20R	29.6 m	49.6 m
SELAH INTERBED	G.L.	9N/26E-20A	45.7 m	F.M.	9N/26E-20R	18.5 m	27.2 m
UMATILLA MEMBER	F.M.	9N/26E-20G	107.3 m	F.M.	9N/26E-20P	77.7 m	29.6 m
MABTON INTERBED	F.M.	9N/26E-20H		F.M.	9N/26E-20P	7.6 m	21.1 m
PRIEST RAPIDS MEMBER	F.M.	9N/26E-20G	61.6 m	F.M.	9N/26E-20P	50.9 m	10.7 m
ROZA MEMBER	G.L.	EX*	48.8 m	F.M.	9N/26E-20P	12.2 m	36.6 m

Present structural relief = 406 m

* thickness extrapolated between DC-15/DDH-3 and the Prosser Experimental Station wells

D. L. = data is from driller's log
G. L. = data from borehole geophysical logs
F. M. = data from field measurements

TABLE VIII

THICKNESS DATA USED IN CALCULATING THE COMBINED RATE OF UPLIFT AND SUBSIDENCE FOR THE KIONA ANTICLINE AND THE LOWER YAKIMA VALLEY SYNCLINE

UNIT	SYNCLINE			ANTICLINE			PALEO-RELIEF
	DATA TYPE	LOCATION	UNIT THICKNESS	DATA TYPE	LOCATION	UNIT THICKNESS	
ICE HARBOR MEMBER	D.L.	10N/26E-26J	3.7 m	F.M.	9N/26E-23E	0.0 m	3.7 m
LEVEY INTERBED	D.L.	10N/26E-26J	5.8 m	F.M.	9N/26E-23E	0.0 m	5.8 m
ELEPHANT MOUNTAIN MEMBER	D.L.	10N/26E-33F	23.5 m	F.M.	9N/26E-23E	0.0 m	23.5 m
RATTLESNAKE RIDGE INTERBED	D.L.	10N/26E-33F	21.3 m	F.M.	9N/26E-23E	24.4 m	21.3 m
POMONA MEMBER	G.L.	10N/26E-27Q		F.M.	9N/26E-23F	4.6 m	81.4 m
SELAH INTERBED	G.L.	10N/26E-27Q	3.0 m	F.M.	9N/26E-23F	4.6 m	-1.6 m
ESQUATZEL MEMBER	G.L.	10N/26E-27Q	24.4 m	F.M.	9N/26E-23F	0.0 m	24.4 m
COLD CREEK INTERBED	G.L.	10N/26E-27Q	21.3 m	F.M.	9N/26E-23F	0.0 m	21.3 m
UMATILLA MEMBER	G.L.	10N/26E-27Q	83.2 m	F.M	9N/26E-23G	33.0 m	50.2 m
MABTON INTERBED	D.L.	EX**	19.0 m	F.M.	9N/26E-23G	2.4 m	16.6 m
PRIEST RAPIDS MEMBER	G.L.	EX*	52.0 m	F.M.	9N/26E-23Q	30.5 m	21.5 m
ROZA MEMBER	G.L.	EX*	48.0 m	F.M.	9N/26E-23F	19.8 m	28.2 m

Present structural relief = 408

* thickness extrapolated between geophysically logged DC-15/DDH-3 and the Prosser Experiment Station wells

** thickness averaged from driller-logged well located at 10N/26E-33D and 10N/26E-33F

D. L. = data is from driller's log
G. L. = data is from borehole geophysical logs
F. M. = data from field measurements

TABLE IX

THICKNESS DATA USED IN CALCULATING THE COMBINED RATE OF UPLIFT AND SUBSIDENCE FOR THE PROSSER ANTICLINE AND THE PIENING SYNCLINE

UNIT	SYNCLINE			ANTICLINE			PALEO-RELIEF
	DATA TYPE	LOCATION	UNIT THICKNESS	DATA TYPE	LOCATION	UNIT THICKNESS	
ELEPHANT MOUNTAIN MEMBER	D.L.	8N/25E-36B	42.7 m	F.M.	8N/24E-14L	0.0 m	42.7 m
RATTLESNAKE RIDGE INTERBED	D.L.	8N/25E-36B	19.8 m	F.M.	8N/24E-14L	0.0 m	19.8 m
POMONA MEMBER	G.L.	7N/26E-05B	61.0 m	F.M.	8N/24E-14L	43.3 m	10.0 m
SELAH INTERBED	D.L.	8N/25E-36B	38.1 m	F.M.	8N/24E-14L	1.5 m	36.6 m
UMATILLA MEMBER	G.L.	7N/26E-05B	71.6 m	F.M.	8N/24E-14L	31.4 m	40.2 m
MABTON INTERBED	G.L.	7N/26E-05B	15.2 m	F.M.	8N/24E-14L	15.8 m	-0.4 m

Present structural relief = 253 m

D. L. = data from driller's log
G. L. = data from borehole geophysical logs
F. M. = data from field measurements

Field measurements of basalt flows and sedimentary interbeds were gathered using a surveying tape, Paulin altimeter, or in some cases a Brunton compass. Measurements were made where both the upper and lower contacts could be delineated (except where flows comprise the top of the section). The presence or absence of erosion in the basalt was determined by the observation of primary physical features (e.g., vesicular flow top). Where the exact location of the stratigraphic contact could not be pinpointed, it was sometimes possible to measure a maximum or minimum thickness. Measurements were corrected for structural tilt where necessary. Caution was exercised in determining whether section thicknesses were "increased" by invasive flows.

Thickness data interpreted from borehole geophysical logs are deemed quite accurate as the senstive radiation logs make accurate picks of the stratigraphic contacts.

Radiometric Age Dates

Two methods of radiometric age dating have been used to determine absolute ages for CRBG flows: potassium-argon and argon-argon. Argon loss in the older CRBG flows gives abnormally young potassium-argon age estimates (Long and Duncan 1982). Argon-argon dating techniques achieve better age dates for these older CRBG flows Long and Duncan (1982). The two dating techniques give similar age dates for the younger basalts, but different ages for the older basalts (Wanapum and Grande Ronde flows). In this study, the argon-argon technique was used for the older basalts.

Table X shows the age dates used in the construction of the growth curves. Age dates from certain flows must be estimated since there are no available radiometric dates.

TABLE X

AGE DATES USED IN CALCULATING DEVELOPMENT RATES OF THE HORSE HEAVEN HILLS UPLIFT

CRB MEMBER or STRATIGRAPHIC BOUNDARY	AGE (m.y.B.P.)	DATING METHOD	SOURCE
Ice Harbor	8.5	K-Ar	McKee and others, 1977
Elephant Mountain	10.5	K-Ar	McKee and others, 1977
Pomona	12.0	K-Ar	McKee and others, 1977
Umatilla	14.0	Ex*	
Priest Rapids	14.5	^{40}Ar-^{39}Ar	Rockwell Hanford Oper. and Duncan, unpub. data, 1982
Roza	14.8	Ex**	
Frenchman Springs	15.1	Ex**	
Wanapum/Grande Ronde Contact	15.6+.2	^{40}Ar-^{39}Ar	Long and Duncan, 1982

Ex* Age calculated by averaging eruption times of flows between the Pomona and Priest Rapids Members

Ex** Age calculated by averaging eruption times of flows between the Priest Rapids Member and the Wanapum/Grande Ronde contact.

1 error range given for the dates of Long and Duncan, 1982 only

APPENDIX E

PALEOMAGNETIC VECTOR ROTATION-PRELIMINARY RESULTS

A recent study (Reidel and others 1984) in the Pasco Basin area evaluated vector rotation from the Pomona Member along Yakima folds. One of the findings of the study was that clockwise rotation occurred at sites along both east-west-trending folds and northwest-trending folds. This finding has important tectonic significance. It is the purpose of this section to compile both published and unpublished paleomagnetic results for the Pomona Member at sites located along folds of both trends of the Horse Heaven Hills to see if a similar clockwise rotation occurs.

A reference Pomona direction reported by Reidel and others (1984; inclination = -52.2°, declination = 189.7°, $\alpha 95$ = 1.6°) was used as the stable magnetic vector direction to calculate mean rotational values (Table XI; Fig. 86). All but one of the sites record a clockwise rotation. Although the declination uncertainty for some of these sites is great, clockwise rotation along both trends of the Horse Heaven Hills uplift (including other folds of the ARW) is preliminarily indicated.

TABLE XI

COMPILATION OF AVAILABLE PALEOMAGNETIC DATA FOR THE POMONA MEMBER WITHIN THE STUDY AREA

SITE	LOCATION			α 95	STRATIGRAPHIC DIRECTION			SOURCE
	TOWNSHIP	RANGE	SECTION		DECLINATION (DEG.)	INCLINATION (DEG.)	ΔD (DEG.)	
IW 59	9N	26E	NW NW 23	2.3	189.2	-56.4	4.2	1
IW 60	9N	26E	NW NW 23	2.9	192.5	-54.7	5.0	1
IW 61	9N	26E	SE SW 9	2.4	198.0	-56.5	4.4	1
IW 62	9N	26E	SE SW 9	2.4	190.7	-54.4	4.1	1
PO-4	9N	26E	SW NW 17	5.6	193.3	-50.1	8.8	2
PO-7	8N	22E	NW 35	10.9	192.9	-46.7	16.0	2
P1D1	9N	26E	SE SE 8	1.6	198.5	-51.0	2.5	3
F1	8N	28E	NW NW 35	3.0	203.0	-52.7	4.7	4
H1	8N	27E	NE SE 8	1.6	198.5	-50.6	2.6	4
K1	10N	24E	NW NE 2	2.1	196.6	-51.0	3.3	4
L1	10N	25E	NW SW 23	3.2	198.3	-50.6	5.0	4
HH1	8N	24E	SW NE 20	9.1	227.3	-65.8	22.8	5

1. Simpson, Wells, and Bentley (unpublished data, 1981)
2. Rietman (1966)
3. Van Astine and Gillett (1981)
4. Reidel and others (1984)
5. Reidel and Scott (unpublished data, 1984)

α95 = radius of 95% confidence
stratigraphic direction = declination and inclination relative to paleohorizontal (rotated about strike line)
ΔD = declination uncertainty ($\Delta D = \sin^{-1}(\sin \alpha 95 / \cos I)$).

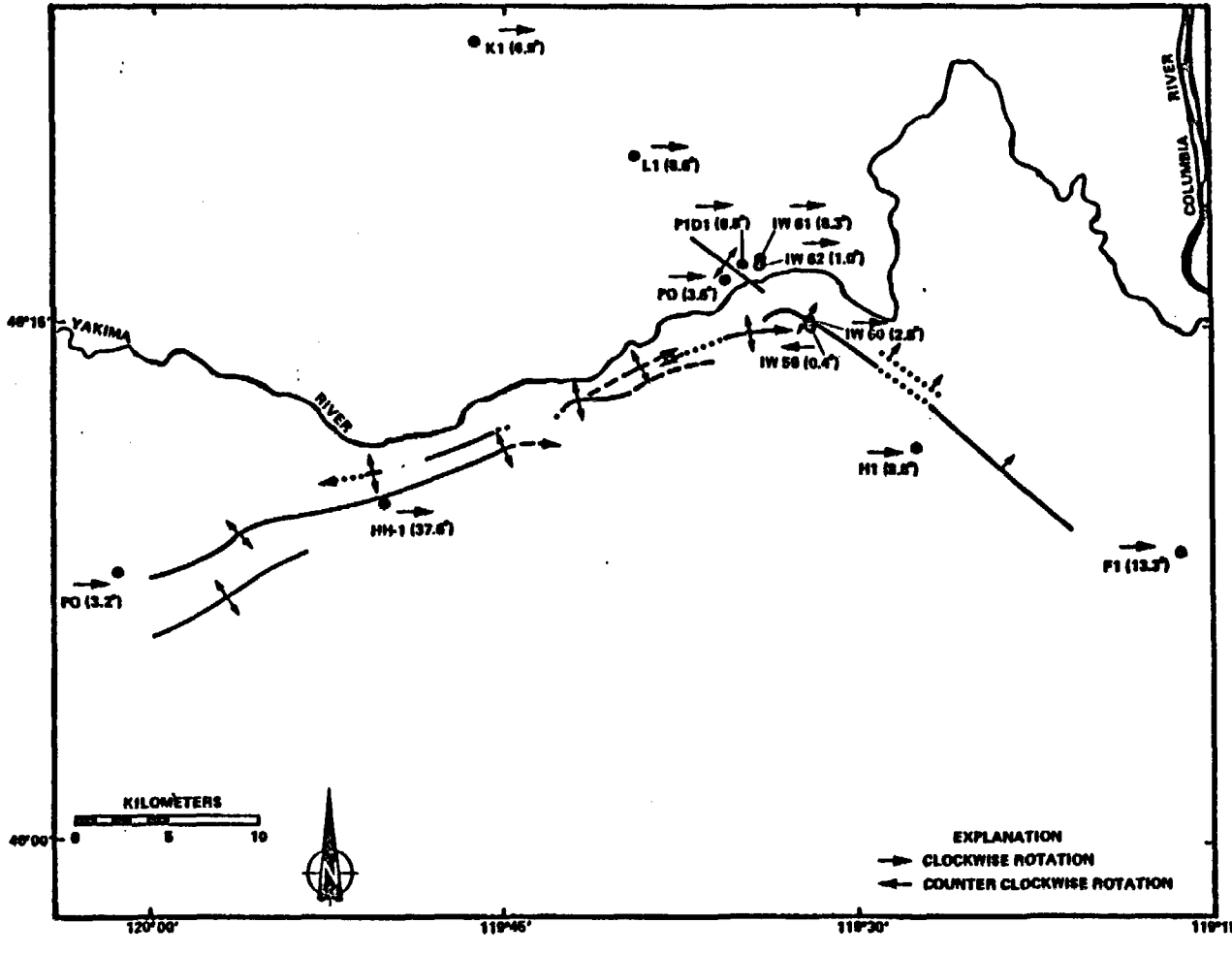

Figure 86. Map of paleomagnetic sites and the mean vector rotation of the sites relative to the reference Pomona direction of Reidel and others (1984).

APPENDIX F

TECTONIC MODELS

A summary of published tectonic models that deal with the timing of growth, rate of growth, and origin of Yakima folds is presented in the following pages in table form (Tables XII-XIV).

TABLE XII

SUMMARY OF MODELS FOR THE TIMING OF DEVELOPMENT OF YAKIMA FOLDS

Anderson, 1980. Simcoe-Horse Heaven Hills, Deformation and associated faulting during Vantage horizon time.

Barrash and others, 1983
Yakima Folds. Mild, episodic anticlinal folding localized in the Yakima Ridges area (17-10 + 2 m.y.B.P.). Present structural relief is dominantly post basalt (10 + 2 - 4 m.y.B.P.). Minor folding since 4 m.y.B.P. Simultaneous deformation of east-west folds and CLEW structures.
Horse Heaven Hills Uplift. Developed after 10.5 m.y.B.P. Eastern segment (northwest trend) developed after 8.5 m.y.B.P.

Bentley, 1977
Yakima Folds. Local substantial deformation occurred between 14-12 m.y.B.P., but majority of folds developed between 6-1.5 m.y.B.P.

Bentley, 1980b
CLEW. Pre-Umatilla regional deformation north of Yakima Ridge in the CLEW.
Umtanum uplift. Two phases of deformation; post Wanapum and post Saddle Mountains time. Minor folding in post basalt time.

Bentley and others, 1980b
Columbia Hills. Thrusting along the fold during Grande Ronde time and subsequently post 10 m.y.B.P.

Biggane, 1982
Hog Ranch Fault Axis. Thinning and pinching out of the Pomona Member towards the Hog Ranch Fault Axis which separates the Moxee and Black Rock Valleys.

Bond and others, 1978
Pasco Basin Area. Most folds in southwestern Pasco Basin developed since Saddle Mountains time (minor uplift indicated in Umatilla time Rattlesnake Mountain uplift).
Horse Heaven Hills Uplift. Possible development in post-Pomona time.

Brown, J., 1978
Horse Heaven Plateau. Possibly tectonically active during late Wanapum time.

Brown, R., 1970
Pasco Basin Area. Anticlinal uplift in Pasco Basin began in earliest Pliocene time-near the close of emission of the basalts and continuous to present. Uplift progressive roughly from north to south with the Horse Heaven Hills rising slower, later or both than the northerly anticlines. Variations in rate and time of rise also occurred along a single anticline.

Campbell, 1984
Hog Ranch-Naneum Anticline. The "Naneum high" is a prebasalt structure and lies below the 1-29 Bissa well.

Campbell and Bentley, 1979
Toppenish Ridge. Late Quaternary and Holocene faulting is found along the crest.

Davis, 1981
Yakima Folds. Contemporaneous deformation along east-west folds and CLEW structures beginning about 14 m.y.B.P. and continuous to the present. Most deformation is post Pomona in age.

Fecht and others, in press
Hog Ranch-Naneum Anticline. Uplift of the "Hog Ranch structure" diverted the ancestral Columbia River to a more southerly course across the emerging Rattlesnake Hills.

Gardner and others, 1981
Horse Heaven Hills. Structural uplift began prior to extrusion of the Pomona flow.

Goff and Myers, 1978
Umtanum and Yakima Ridges. Anticlines began folding before extrusion of the Umatilla Member.
Hog Ranch-Naneum Anticline. Southward growth of the Hog Ranch anticline cuts off an ancient stream channel during Saddle Mountains time.

Jones and Landon, 1978
Horse Heaven Hills. Structural uplift began prior to extrusion of the Pomona and Elephant Mountain flows but possibly even as early as Priest Rapids time.
RAW. The RAW is younger than the Horse Heaven Hills structure and folding probably began in post-Elephant Mountain time and continued through Ice Harbor time.

Kienle and others, 1978
Yakima Folds. Greatest amount of uplift on most structures took place after Elephant Mountain time.

Kienle, 1980
Horse Heaven Hills and Columbia Hills. Formed largely between 3.5 and 4.5 m.y.B.P.

Landon and others, 1982
Hog Ranch-Naneum Anticline. Hog Ranch anticline, west of the Pasco Basin was in existence by late Grande Ronde time.

Laubscher, 1981
Yakima Folds. "The main part of the Yakima basalt deformation north of Yakima took place between about 3-1 m.y.B.P. with some deformation continuing into the younger Pleistocene and present. Yakima deformation began at the south and proceeded north."

Laval, 1956
Yakima Folds. Mild local warping during the accumulation of the "upper Yakima basalt formation. Intensified bedload warping and folding culminated during the early Pleistocene.

Mackin, 1961
Yakima Folds. Uplift in part of Wanapum time.

Myers and others, 1979
Yakima Folds. "Most folding is probably of late Miocene and Pliocene age."

Powell, 1978
Tygh Ridge. "Uplift along the Tygh Ridge structure appears to have occurred sporadically throughout the time of the extrusion of the Grande Ronde Basalt."

Price, 1981
Hog Ranch-Naneum Ridge Anticline. Hog Ranch possibly present in Grande Ronde time in the Priest Rapids area.

Reidel, 1984
Saddle Mountains Uplift. Growing continuously from at least Grande Ronde time to at least 3.5 m.y.B.P. and probably into present.
Hog Ranch-Naneum Anticline. Hog Ranch present in Grande Ronde time.

Reidel and others, 1980
Saddle Mountains Uplift and other Yakima Folds. The Saddle Mountains uplift was forming in early Wanapum time and most of the other Yakima folds in the Pasco Basin were active by late Wanapum/early Saddle Mountains time.

Reidel and Fecht, 1981

Yakima Folds in the Cold Creek Syncline Area, Pasco Basin. Relief was present by at least Wanapum time. "... any structural relief present during Grande Ronde time would have been obscured by the large volume of lava which was erupted over a short period of time."

Reidel and others, 1983

Yakima Folds. Folds were growing in Grande Ronde time and were actually growing through much of Miocene time along anticlinal axes.

Schmincke, 1964

Saddle Mountains Area. Deformation began in two synclines along the north scarp of the Saddle Mountains at least by Priest Rapids time. "Cross folding along north-south axes was slightly earlier than, or contemporaneous with, the more prominent east-west warping shown by the Saddle Mountains anticline."

Shannon and Wilson, 1973

Northwest-Southeast Trending Structures in the Arlington, Oregon Area. These structures are interpreted to be at least pre-Roza in age.

Columbia Hills, Blue Mountains, and Horse Heaven Anticline. These structures as well as their related synclines were last deformed prior to middle Pleistocene time. The best bracket on the time of the major deformation of the region places it between 3.5 and 4.5 m.y.B.P."

Swanson and Wright, 1978

Yakima Folds. Forming during Saddle Mountains time.

Hog Ranch-Naneum Anticline. Naneum Ridge anticline in the Wenatchee Mountains was probably active as early as Grande Ronde time.

Sylvester, 1978

East-West-Trending Structures. The Mosier syncline, the Horseshoe Bend anticline, and the Swale Creek syncline were initiated in the post-Priest Rapids time.

Northwest-Southeast-Trending Folds. Developed in the late Miocene to early Pliocene (Warwick, Snipes Butte, and Goldendale anticlines) and transect the east-west structures.

Tabor and others, 1977

Hog Ranch-Naneum Anticline. Naneum Ridge anticline causes thinning of Vantage Member.

Tolan and Beeson, 1984

Yakima Folds. Yakima folds which extend through the Cascade Range control the course of the ancestral Columbia River as early as Frenchman Springs time.

Waters, 1955

Yakima Folds. Folding grew intensely during early Pliocene time.

TABLE XIII

SUMMARY OF GROWTH RATE MODELS FOR YAKIMA FOLDS

Barrash, 1983
: Uplift of the Saddle Mountains occurred at an average rate of between "0.1 mm/yr. (assuming deformation occurred between 10.5 and 4 m.y.B.P.) and 0.14 mm/yr. (for the period of 8.5-4 m.y.B.P.). "Estimated average uplift rate for Rattlesnake Hills between 10.5 and 4 m.y.B.P. to be 0.14-0.20 mm/yr."

Brown, 1970
: Anticlinal Ridges grew at the rate of 0.1 mm/yr.

Caggiano and others, 1980
: Basalt deformation progressed at less than 1 mm/yr.

Kienle and others, 1978
: Yakima folds developed at 0.75-1.5 mm/yr for the period between 8 or 6 m.y.B.P. to 4 m.y.B.P.

Reidel, 1984
: Saddle Mountains uplift was undergoing a vertical rate of uplift of approximately 250 m/m.y. in late Grande Ronde time but slowed to approximately 40 m/m.y. by Elephant Mountain time. Extrapolation of these rates to the present structural relief indicates a rate of approximately 40 m/m.y. for post CRB time.

Reidel and others, 1980
: A minimum rate of uplift for the Saddle Mountains during Wanapum and Saddle Mountains time is approximately 39 m/m.y. A maximum rate of uplift for Rattlesnake Mountain during this same time interval is approximately 70 m/m.y.

Reidel and others, 1983
: Between Rattlesnake Mountain and the Cold Creek syncline, the combined rate of uplift and subsidence was found not to exceed 150 m/m.y. over the timer interval of 14.5 to 10.5 m.y.B.P. During this same time interval the combined uplift and subsidence of the Saddle Mountains and Wahluke syncline decreased to approximately 80 m/m.y. by 10.5 m.y.

TABLE XIV

SUMMARY OF MODELS FOR THE ORIGIN OF YAKIMA FOLDS

East-West Folds and Faults

Bentley, 1977

"Brittle basalts can fold only under a combined horizontal compression and vertical movement along basement weakness zones. Each anticlinal structure has a weakness zone in basement rocks that has localized the horizontal stresses and caused the vertical uplift of the ridges at successive times. In gross character, anticlines are "drape" folds caused by vertical breakup of basement blocks."

"The "ridges" are faulted monoclinal anticlines formed as drape folds above rotated basement blocks. The narrow ridges were uplifted as adjacent broad synclinal basins subsided."

Bentley, 1982a

"These faulted anticlines (east-west folds) may be part of an extensive decollement system that has approximately 1% north-south horizontal shortening across the system."

Bentley, 1982b

Yakima folds reflect drag on ramps from sub-basalt and interbasalt decollements.

Bentley and others, 1980b

The Columbia Hills formed over "deep-seated left lateral strike-slip faulting (N70 E) localized mobile zone."

Bentley and Farooqui, 1979

"East-west Yakima folds mark the position of fundamental Reidel shears that formed in early Miocene time by left-lateral-strike-slip zones in later deformation, localizing most thrusting and folding, and subsequent minor, left lateral movement.

Brown, 1970

"Anticlinal ridges, sometimes uplifted plateaus, are in part at least related to the vertical forces of basining. Evidence of major compression or tension with the formation of major thrust faults or normal faults respectively, appear absent."

Bruhn, 1981
Long gentle limbs indicate fault ramp-flexure model with decollement of group of localized detachments at 3-5 km deep near the base of the basalts.

Davis, 1981
East-west trending fold-fault structures formed by buckling and local detachment.

Laubscher, 1981
East-west folds were formed over ramps which emanate from a decollement at the base of the crust.

Laval, 1956
"... two modes of structural genesis are suggested: folding free of the basement, or folding directly related to deformation of the basement. The first is suggested in the similarity of Snipes Mountain and Toppenish Ridge to some of the simpler of Jura Mountains folds, and the second is suggested in the similarity of Saddle Mountains and the Horse Heaven Plateau to the Pryor Mountains of Montana. Neither type of folding can be proved because the base of the Yakima basalt is not exposed in the areas mapped."

Price, 1982
Major thrusts cannot underlie the Yakima anticlinal folds due to the lack of associated strain features. Folds probably overlie local detachments. Basalt was rotated clockwise into the folds from the southeast around the Palouse slope which acted as a rigid buttress.

Reidel and others, 1984
East-west directed sinistral shear along the major anticlinal ridges is not supported by paleomagnetic data. Direct relationship between amount of rotation and amount of deformation and position of fold.

Russel, 1893
"An example of the upturned edge of an orographic block is furnished by the northern escarpment of the sloping table land known as Horse-heaven, which is well exposed in the neighborhood of Kiona and Prosser. This long line of cliffs is a fault scarp from which the strata slope gently southeast toward the Columbia."
"Narrow ridges were formed by an arching of the strata without breaking. The arches were raised by a force acting from below upward, and not by lateral pressure which forced the strata into ridges and troughs, as is common especially in the Appalachian Mountains."

Waitt, 1979
"An hypothesis consistent with regional relations is that the individual east-trending scarps in Kittitas Valley evince reverse faults caused by north-south compression ..."

Northwest-Trending Folds and Faults

Barrash, 1983
"The Warps and folds may reflect local responses to rapid crustal loading over pre existing northwest-trending structural grains. Alternately, or in addition, northwest compression may have induced limited dextral shear on pre-existing, northwest-trending basement structure(s) beneath the OWL and thereby influenced the orientation of surface folds as in Reidel-type deformation (Laubscher, ms and 1981, Konde and Bhattacharji, 1977, fig. 3F)."
"We suggest that a buttressing effect at depth across steeply dipping structures along the Rattlesnake Lineament (Bond and others, 1978; Davis, 1981) influenced the initial deformation pattern at the surface, and that the lateral continuity of the basalt flows allowed HHH area to respond as a continuous unit with similar volumes of rock displaced east and west of the symmetry plane."

Bentley, 1977
The OWL is a crustal weakness zone, old basement structures localized the later vertical movement along the line. "All structures are formed by vertical movement and are rooted in basement weakness zones and most structures are monoclinal faults at the surface.

Bentley, 1980a
The OWL marks a Mesozoic Benioff zone formed from dextral translation abutted against a more rigid zone.

Bentley, 1980b
"The geometry of the Umtanum thrust fault zone is consistent with a model of north-south (horizontal) compression with decollement in several sedimentary interbeds within the Grande Ronde and Wanapum Basalt."

Bentley and Anderson, 1979
The OWL formed as result of dextral shear along an incompetent compressive zone, as much of the translation abutted against the more rigid North American Plate."

Price, 1982
Rattlesnake Mountain and the Northwest-trending portion of the Horse Heaven Hills are associated with dextral shear.